

**THE ROLE OF DISTRIBUTED ENERGY RESOURCES (DERs) IN  
SMART GRID STABILITY**

**by**

**Mkhutazi Mditshwa**

**Thesis submitted in fulfilment of the requirements for the degree**

**Master of Engineering: Electrical Engineering**

**in the Faculty of Engineering & the Built Environment**

**at the Cape Peninsula University of Technology**

**Supervisor:** Dr. M.E.S. Mnguni

**Co-supervisor:** Mr. M. Ratshitanga

**Bellville Campus**

Date submitted: June 2021

**CPUT copyright information**

The dissertation/thesis may not be published either in part (in scholarly, scientific or technical journals), or as a whole (as a monograph), unless permission has been obtained from the University.

## DECLARATION

I, **Mkhutazi Mditshwa**, declare that this dissertation/thesis's contents represent my own unaided work and that the dissertation/thesis has not previously been submitted for academic examination towards any qualification. Furthermore, it represents my own opinions and not necessarily those of the Cape Peninsula University of Technology.



**Signed**

**Date**

23/06/2021

## **ABSTRACT**

The power system grid is designed to be flexible and dynamic. Its flexibility is helping to re-adjust when the system operating conditions are changing. The conventional power systems are heavily dependent on fossil fuels such as coal as the energy source. Due to the global warming effect, traditional power generation through coal is becoming a significant concern, and policies have been put in place to mitigate air pollution. Most African countries have subscribed to those international policies, and South Africa is one of them. The only option to achieve an environmentally friendly power generation system is to integrate renewable energy resources. The integration of these energy resources can be done at the distribution level, with the benefit of minimizing transmission power losses.

However, integrating the distributed energy resources into the conventional power system can result in a complex power grid. The energy management system will need to be improved. The other challenge about the distributed energy resources is that they quickly respond to system dynamic events. Lack of primary resources such as wind or sun can also be challenging. However, when the resources are available, these energy sources can be adequately utilized in various applications.

The thesis explores utilizing the wind power generation system as an active power compensator following load demand increase in the power system to stabilize the system frequency. As the load demand increases, the frequency is declining. In the conventional generation system, the governing system is utilized as the primary control to release an additional active power to the grid following a load demand increase event. However, the governing system fails to restore the system frequency to its nominal value. A load reduction is the only viable solution for other control systems for the system frequency to recover and go back to its nominal state.

The implementation of secondary control, which utilizes a decentralized automatic generation control, was developed and implemented to restore the system frequency when the governing system failed. When the load demand kept increasing, the wind power plant was integrated into the grid to improve frequency stability. Both decentralized automatic generation control and wind power active power compensator control loops were developed on DIgSILENT Power factory simulation software. The simulations were performed on the DIgSILENT software and were verified on the Real-Time Digital Simulator (RTDS) simulation platform.

In the conventional system, Programmable Logic Controllers (PLC) are used for the control system, this requires a large number of separated control cards, and

there is too much wiring involved. The complexity of the PLC control system makes troubleshooting to be difficult when there is a fault. The information to the control center is made through telemetry, and there is often a delay in obtaining the data due to signal transmission traffic. The utilization of the IEC 61850 standard has advanced communication and the mitigation of using too much wiring to achieve a working control system.

The developed frequency control system was practically implemented using an IEC 61850 standard protocol. The control logic was developed using SEL-3555 Real-Time automatic Controller (RTAC) intelligent electronic device (IED).

**Keywords:** Power system stability, frequency control, Automatic Generation Control (AGC), control loop, IEC 61850 standard, integration, primary control, secondary control. Area, Tie-line power interchange, active power, protection.

## ACKNOWLEDGEMENTS

### **I wish to thank:**

- The God of heavens and earth, the almighty for the strength courage.
- My wife for the support and the time to focus on this project
- My mother and my entire family for the support and prayers throughout the journey.
- Exceptionally my supervisor Dr. M.E.S Mnguni for all the support and guidance. My gratitude also goes to my co-supervisor, Mr. Ratshitanga, and the entire Center for Substation automation and Energy Management systems (CSAEMS)

The financial assistance of CPUT Postgraduate Bursary towards this research is acknowledged. Opinions expressed in this thesis and the conclusions arrived at, are those of the author, and are not necessarily to be attributed to CPUT Postgraduate Bursary.

## **DEDICATION**

This thesis is dedicated to my mother, **Thembeke Mditshwa (MaBhedla)**, my child **Lingwele Mditshwa**, and my friend **Inga Ngxamngxa**. Moreover, this thesis is dedicated to my entire family for their immense contribution and support.

## GLOSSARY

**Distributed Energy Resources (DER's)** – They are any energy resources that can produce electrical energy and be integrated into the distribution network system.

**Protection system** - It is a system that safeguards electrical power plant equipment in the event of fault by isolating the faulted part from the standard system.

**Frequency stability** – A power system frequency can remain stable during regular operation and restore frequency to its predefined nominal level after a disturbance occurred between load and generation.

**Rotor angle stability** – It is the ability of synchronous generators in an interconnected power system to continue running at the same time after disturbances.

**Power system stability** - The power system's ability to recover and remain stable after the power system was exposed to disturbance.

**Microgrid** integrates loads and distributed energy resources connected in a distribution system, working in isolation from the power system grid and centrally controlled. It can have the option of being integrated into the power grid or operate in island mode.

**An islanded mode** is a unit system integration mode that allows micro-grid to operate independently and supply electrical power to end users based on the power demand.

**Voltage control** – It is a voltage monitoring function at the common point of coupling (PCC) / point of connection (POC).

**Frequency control** – Refers to frequency monitoring function at the point of common coupling to maintain it at an acceptable operating range

**Power system reliability** refers to the probability of a power system's ability to function as per the expected specific operating condition.

**Power system security** – The power grid can resist changes in the power system without interrupting the system function. It relates system strength to contingencies.

## LIST OF ABBREVIATIONS

<b>IEDs</b>	-	Intelligent Electronic Devices.
<b>RES</b>	-	Renewable Energy Systems.
<b>DER</b>	-	Distributed Energy Resources.
<b>AGC</b>	-	Automatic Generation Control
<b>DG</b>	-	Distributed Generators.
<b>AVR</b>	-	Automatic Voltage regulator.
<b>MG</b>	-	Microgrid.
<b>AC</b>	-	Alternating Current.
<b>DC</b>	-	Direct Current.
<b>RPPs</b>	-	Renewable Power Plants.
<b>PLL</b>	-	Phase-Locked-Loop.
<b>CHP</b>	-	Combined Heat and Power.
<b>IEC</b>	-	International Electrotechnical Commission.
<b>POC</b>	-	Point Of Connection.
<b>ECP</b>	-	Electrical Connection Point.
<b>N-1</b>	-	Single contingency event on the network.
<b>DMS</b>	-	Distribution Management System
<b>EMS</b>	-	Energy Management System
<b>SCADA</b>	-	Supervisory Control and Data Acquisition
<b>ROCOF</b>	-	Rate of change of frequency
<b>RTDS</b>	-	Real-Time Digital Simulator
<b>WTG</b>	-	Wind Turbine Generator
<b>IEEE</b>	-	Institute of Electrical and Electronics Engineers



## TABLE OF CONTENTS

DECLARATION.....	i
ABSTRACT.....	ii
ACKNOWLEDGEMENTS.....	iv
DEDICATION.....	v
GLOSSARY.....	vi
CHAPTER ONE.....	1
INTRODUCTION.....	1
1.1 Introduction.....	1
1.2 Awareness of the problem.....	4
1.3 Problem statement.....	4
1.4 Research aim and objectives.....	4
1.4.1 Objectives.....	5
1.5 Hypothesis.....	5
1.6 Delimitation of research.....	6
1.7 The motivation of the research project.....	6
1.8 Assumptions.....	7
1.9 Research Design and Methodology.....	7
1.9.1 Literature review.....	7
1.9.2 Methods for the power system frequency control.....	7
1.9.3 Simulations.....	8
1.9.4 Data collection.....	8
1.10 Thesis chapters.....	8
1.10.1 Chapter One.....	8
1.10.2 Chapter Two.....	8
1.10.3 Chapter Three.....	9
1.10.4 Chapter Four.....	9
1.10.5 Chapter Five.....	9
1.10.6 Chapter Six.....	9
1.10.7 Chapter Seven.....	9
1.10.8 Chapter Eight.....	10

1.10.9 Chapter Nine.....	10
1.10.10 Appendix A.....	10
1.10.11 Appendix B.....	10
1.10.12 Appendix C .....	10
<b>CHAPTER TWO.....</b>	<b>11</b>
LITERATURE REVIEW .....	11
2.1 Introduction .....	11
2.2 Overview of power system stability.....	12
2.2.1 Rotor angle stability.....	13
2.2.1.1 Transient stability .....	14
2.2.1.2 Small-signal stability.....	15
2.2.2 Voltage stability .....	17
2.3 Frequency stability .....	20
2.3.1 Impact of load demand increase to frequency stability .....	20
2.3.2 The frequency stability recovery process .....	21
2.3.3 Frequency control system .....	22
2.3.3.1 The primary frequency control system.....	25
2.3.3.2 Secondary frequency control.....	26
2.3.3.3 Tertiary frequency control.....	26
2.3.3.4 Emergency frequency control.....	27
2.3.3.4.1 The frequency protection system configuration .....	27
2.3.4 The integration of distributed energy resource for frequency control systems.....	29
2.3.5 Communication system.....	31
2.3.5.1 Application of the IEC 61850 standard .....	32
2.3.5.2 Requirements for standard implementation .....	32
2.3.5.3 IEC 61850 standard benefits.....	34
2.3.5.4 The implementation of hardware-in-loop (RTDS) .....	35
2.4 Literature review of the existing papers for load frequency control. ....	35
2.4.1 Findings from the existing literature .....	35
2.5 Discussion.....	46
2.6 Conclusion .....	47
<b>CHAPTER THREE .....</b>	<b>48</b>
THE POWER SYSTEM OPERATION, CONTROL, AND PROTECTION ANALYSIS.....	48

3.1	Introduction .....	48
3.2	Steady-state modeling approach.....	49
3.3	Power flow analysis.....	66
3.4	Dynamic power system analysis and modeling approach.....	72
<b>CHAPTER FOUR.....</b>		<b>107</b>
MODIFIED IEEE 14 BUS NETWORK MODELLING AND ANALYSIS .....		107
4.1	Introduction .....	107
4.2	Modeling of the modified IEEE14 bus system and its associated control systems. ....	111
4.3	Steady-state analysis and results analysis .....	117
4.4	Dynamic state analysis.....	129
4.6	Discussion of results .....	138
4.7	Conclusion .....	138
<b>CHAPTER FIVE.....</b>		<b>139</b>
MODELING OF AUTOMATIC GENERATION CONTROL AND PERFORMANCE ANALYSIS USING DIgSILENT SIMULATION SOFTWARE. ....		139
5.1	Introduction. ....	139
5.2	The implementation of Automatic Generation Control (AGC). ....	139
5.3	Modeling of a decentralized AGC in DIgSILENT power factory software..	144
5.4	Decentralized AGC performance assessment and results.....	148
5.5	Discussion of results .....	155
5.6	Conclusion .....	155
<b>CHAPTER SIX.....</b>		<b>157</b>
MODELING OF AN AGGREGATED WIND FARM AND THE DEVELOPMENT OF WIND ACTIVE POWER COMPENSATOR ON DIgSILENT.....		157
6.1	Introduction .....	157
6.2	The role of the wind active power compensation in frequency control .....	165
6.3	Simulations and results discussion .....	167
6.4	Conclusion .....	177
<b>CHAPTER SEVEN.....</b>		<b>178</b>
MODIFIED IEEE 14 BUS NETWORK AND IMPLEMENTATION OF THE DEVELOPED CONTROL SCHEME IN REAL-TIME DIGITAL SIMULATOR (RTDS).....		178
7.1	Introduction .....	178

7.2	Modeling of modified IEEE 14 bus power system network in RSCAD .....	178
7.2.1	Steady-state simulation and results analysis .....	181
7.2.2	Dynamic state simulation and results analysis .....	181
7.3	Modeling of decentralized automatic generation control (AGC) .....	187
7.4	The modeling and integration of the wind turbine generator active power compensator.....	193
7.4.1	Wind Turbine generator active power supplementary control loop .....	193
7.5	Contingency application and results .....	194
7.6	Conclusion .....	200
<b>CHAPTER EIGHT .....</b>		<b>201</b>
IEC 61850 STANDARD IMPLEMENTATION ON THE DEVELOPED FREQUENCY CONTROL AND PROTECTION SCHEME FOR SMART STABILITY.....		201
8.1	Introduction .....	201
8.2	Development of a test bed for Hardware-In-The- Loop (HIL) implementation.....	201
8.3	IEC 61850 standard communication configuration .....	203
8.4	Development of Automatic Generation Control (AGC) and wind active ....	209
8.5	The application of contingencies to validate the effectiveness of the developed control scheme.....	217
8.6	Conclusion .....	229
<b>CHAPTER NINE .....</b>		<b>231</b>
CONCLUSION AND RECOMMENDATIONS .....		231
9.1	Introduction .....	231
9.2	Thesis deliverables .....	232
9.3	Academic and industrial application .....	234
9.4	Future work .....	234
9.5	Publication .....	235
<b>BIBLIOGRAPHY/REFERENCES .....</b>		<b>236</b>
<b>APPENDIX A.....</b>		<b>245</b>
DlgSILENT PARAMETERS.....		245
<b>APPENDIX B.....</b>		<b>259</b>
REAL-TIME DIGITAL SIMULATOR PARAMETERS AND CONFIGURATION.....		259
<b>APPENDIX C .....</b>		<b>268</b>
RTAC SEL-3555 DEVELOPED AGC AND WTG ACTIVE POWER COMPENSATION CONTROLLER.....		268

Figure 1.1: Typical integrated Grid system operates in AC (Ghafouri et al., 2015).....	2
Figure 1.2: The smart grid and active Distributed System (Ahmad et al., 2018).....	3
Figure 2.1: Power system stability classification (Kundur et al., 2004).....	13
Figure 2.2: Transient stability analysis of rotor or power angle (Sallam & Malik, 2015).....	15
Figure 2.3: Single line diagram (Kundur, 1994) .....	15
Figure 2.4: Ideal single line model (Kundur, 1994) .....	16
Figure 2.5: Power angle oscillation curve for small signal stability (Sallam & Malik, 2015).	16
Figure 2.6: Voltage instability radial single line diagram representation (Kundur, 1994) ....	17
Figure 2.7: The relationship between voltage, current, and power at the receiving end (Kundur, 1994) .....	19
Figure 2.8: The relationship between the receiving end voltage and power (Kundur, 1994) .....	19
Figure 2.9: The process of restoring system frequency (Wazeer et al., 2019) .....	22
Figure 2.10: Hierarchical control process (Luna et al., 2016).....	24
Figure 2.11: Frequency control requirement (NERSA, 2016).....	24
Figure 2.12: Frequency control stages block diagram (Hassan Bevrani, 2014) .....	25
Figure 2.13: Operation of over/under-frequency relays (Mohamed et al., 2018) .....	28
Figure 2.14: Frequency control and protection coordination algorithm (Mohamed et al., 2018).....	28
Figure 2.15: Under/over frequency relay logic diagram (Vieira et al., 2008).....	29
Figure 2.16: Consolidated frequency control and protection integrated diagram (E. A. Mohamed et al., 2018) .....	30
Figure 2.17: The conventional SCADA system communication to RTU (Tomsovic et al., 2005).....	31
Figure 2.18: Generic IEC 61850 DERs application architecture (Ustun et al., 2011).....	33
Figure 3.1: Power system grid (Bragantini, 2019).....	48
Figure 3.2: Magnetic flux flowing through the core (Venkatasubramanian & Tomsovic, 2005) .....	50

Figure 3.3: Magnetic flux linkage (between primary and secondary windings) (Venkatasubramanian & Tomsovic, 2005).....	51
Figure 3.4: Equivalent circuit of a two winding transformer(Jan et al., 2005) .....	52
Figure 3.5: Equivalent circuit with secondary and the primary (Jan et al., 2005).....	52
Figure 3.6: Transmission line from Ingula Eskom Power Station (Chris, 2020).....	54
Figure 3.7: Equivalent circuit for transmission line representation (Jan et al., 2005).....	55
Figure 3.8: The transmission line nominal $\pi$ -equivalent circuit (Jan et al., 2005) .....	56
Figure 3.9: The rotor of the generator with an electromagnetic coil (Beukman et al., 2011)	58
Figure 3.10: Illustration of three-phase winding positions in the stator and sinusoidal waveforms of 50Hz three-phase system displaced at $120^\circ$ (Beukman et al., 2011) .....	59
Figure 3.11: Illustration of rotor configurations (a) Salient pole rotor, and (b) Nonsalient pole rotor (Philip, 2004).....	59
Figure 3.12: (a) Difference between two and four-pole rotor. (a) Two-pole rotor, and (b) A four-pole rotor (Beukman et al., 2011).....	60
Figure 3.13: Synchronous generator and load model (Venkatasubramanian & Tomsovic, 2005).....	61
Figure 3.14: Voltage sensitivity of the load (Jan et al., 2005).....	62
Figure 3.15: Voltage characteristic of (a) Conventional light bulb, and (b) Discharge light (Jan et al., 2005) .....	63
Figure 3.16: Induction motor equivalent circuit (Jan et al., 2005).....	63
Figure 3.17: Voltage characteristic (a) Combination of industrial loads such as induction motors and discharge lights, and (b) Residential and commercial loads such as conventional lighting and heating (Jan et al., 2005).....	64
Figure 3.18: Tap-change contribution to voltage characteristics (Jan et al., 2005).....	65
Figure 3.19: The objectives of power system analysis (Bergen & Vittal, 2007).. .....	66
Figure 3.20: The relationship between power and speed of the turbine generation units (Jan et al., 2005) .....	74
Figure 3.21: The relationship between change in power demand and frequency (Jan et al., 2005).....	75
Figure 3.22: Frequency control stages (Laghari et al., 2013).....	77
Figure 3.23: Modified frequency recovery process (Anca Daniela et al., 2016).....	77

Figure 3.24: Load and generation power characteristics (Jan et al., 2005) .....	79
Figure 3.25: Speed - Droop characteristic (Jan et al., 2005).....	81
Figure 3.26: Turbine speed–droop characteristics for various settings of <i>Pref</i> (Jan et al., 2005).....	82
Figure 3.27: Supplementary control added to the turbine governing system. (Jan et al., 2005).....	83
Figure 3.28: Power balance of a control area (Jan et al., 2005).....	84
Figure 3.29: Functional block diagram of a central regulator (Jan et al., 2005).....	85
Figure 3.30: Proportional controller block diagram (Grobler, 2011).....	89
Figure 3.31: Integral controller block diagram (Grobler, 2011).....	91
Figure 3.32: Derivative controller block model (Grobler, 2011) .....	92
Figure 3.33: The full PID controller block diagram (Grobler, 2011) .....	93
Figure 3.34: Changes in power interchange (Jan et al., 2005).....	93
Figure 3.35: The application of automatic generator controller in an integrated control system (Jan et al., 2005) .....	95
Figure 3.36: A typical configuration between the primary plant and the control center (Van Der Walt et al., 2011). .....	98
Figure 3.37: Cellular radio communication configuration system (Yousuf, 2018). .....	99
Figure 3.38: Packet-switched network configuration (Yousuf, 2018).....	100
Figure 3.39: Substation communication network configuration (Yousuf, 2018). .....	101
Figure 3.40: Modbus implementation configuration (Mohagheghi et al., 2009). .....	102
Figure 3.41: IEC 61850 standard communication architecture (Mohagheghi et al., 2009). .....	104
Figure 3.42: IEC 61850 standard logical node representation (Mohagheghi et al., 2009). .....	105
Figure 3.43: The practical IEC 61850 standard communication structure (Mohagheghi et al., 2009).....	106
Figure 4.1 Workflow stages .....	108
Figure 4.2: Modified IEEE 14 bus power system network .....	109
Figure 4.3: Synchronous generator parameters .....	112
Figure 4.4: Generation system model frame structure (Zhao et al., 2013). .....	112

Figure 4.5: Transmission line data (line 1-5).....	113
Figure 4.6: Transformer parameters.....	114
Figure 4.7: Frequency-dependent load model parameters .....	115
Figure 4.8: Modified IEEE 14 bus network in a de-energized state.....	116
Figure 4.9: Selected load flow method.....	117
Figure 4.10: Modified IEEE 14 bus network during load flow. ....	122
Figure 4.11: Steady-state simulation flowchart .....	126
Figure 4.12: Power system grid frequency during steady-state. ....	127
Figure 4.13: Network bus bar voltages .....	128
Figure 4.14: (a) Scheduled tie-line active power interchange in area 2, (b) Scheduled tie-line active power interchange in area 3, and (c) Scheduled tie-line active power interchange in area 4.....	129
Figure 4.15: Power system grid frequency on GOV response .....	132
Figure 4.16: Power system load demand on GOV response. ....	133
Figure 4.17: Total Generation supply on GOV response. ....	133
Figure 4.18: Net Power Interchange in Area 2 on GOV response.....	134
Figure 4.19: Net Power Interchange in Area 3 on GOV response.....	135
Figure 4.20: Net Power Interchange in Area 4 on GOV response.....	135
Figure 4.21: Voltage response to 15% load demand increase. ....	136
Figure 5.1: A simplified diagram of a four area interconnected power system .....	140
Figure 5.2: Coordination of a decentralized frequency controller in the power system block diagram (Gjengedal, 2002).....	142
Figure 5.3: Decentralised AGC block diagram without considering tie-line power interchange (Pavlovsky & Steliuk, 2014) .....	143
Figure 5.4: Decentralised AGC block diagram considering tie-line power interchange (Pavlovsky & Steliuk, 2014).....	143
Figure 5.5: Area 1 decentralized AGC block diagram .....	144
Figure 5.6: Area 2 decentralized AGC block diagram .....	144
Figure 5.7: Area 3 decentralized AGC block diagram .....	145
Figure 5.8: Area 4 decentralized frequency controller.....	145



Figure 5.9: Total Load Demand before and after AGC implementation.....	148
Figure 5.10: Total Generation Supply before and after AGC implementation following load demand increase.....	149
Figure 5.11: System frequency before and after AGC implementation following load demand increase.....	150
Figure 5.12: Area 2 Net Tie-line Power Interchange before and after the implementation of AGC.....	151
Figure 5.13: Area 3 Net Tie-line Power Interchange before and after the implementation of AGC.....	151
Figure 5.14: Area 4 Net Tie-line Power Interchange before and after the implementation of AGC.....	152
Figure 5.15: Bus voltages when AGC is activated during 15% load demand increase.....	153
Figure 6.1: Modified IEEE 14 bus network illustrated in four controlled areas with wind farm integrated.....	157
Figure 6.2: Type 3 wind turbine generator frame structure diagram (Motta et al., 2019) ..	158
Figure 6.3: Aerodynamic model for Type 3 wind turbine generator.....	160
Figure 6.4: Drive-train model for type 3 wind turbine generator .....	160
Figure 6.5: Pitch control model for type 3 wind turbine generator model.....	161
Figure 6.6: Torque control model for type 3 wind turbine generator .....	162
Figure 6.7: The modified IEEE 14 bus network with wind power plant integration .....	164
Figure 6.8: Wind turbine generator primary frequency supplementary control loop .....	166
Figure 6.9: Consolidated power system frequency and power interchange control scheme algorithm .....	167
Figure 6.10: System frequency before and after the AGC and WTG implementation following a 15% load demand increase. ....	170
Figure 6.11: Active power contribution of the wind turbine generator following load demand increase. ....	171
Figure 6.12: Area 2 Net Tie-line Power Interchange before and after the implementation of AGC and the WTG active power compensator.....	172
Figure 6.13: Area 3 Net Tie-line Power Interchange before and after the implementation of AGC and the WTG active power compensator.....	173

Figure 6.14: Area 4 Net Tie-line Power Interchange before and after the implementation of AGC and the WTG active power compensator. ....	174
Figure 6.15: System bus voltage after 15% load demand increase when all control functions are activated.....	175
Figure 7.1: Modified IEEE 14 bus power system network model in RSCAD .....	180
Figure 7.2: Steady-state generation supply, bus voltages, load demand, and system frequency .....	181
Figure 7.3: Load scheduler.....	182
Figure 7.4: System monitored variables after a 15% load demand increase contingency	183
Figure 7.5: Total load demand after 15% load demand increase (1% incremental steps)	183
Figure 7.6: Total generation supply after 15% load demand increase contingency (1% incremental steps).....	184
Figure 7.7: System frequency during speed governing system response .....	185
Figure 7.8: Area 2 Net tie-line power interchange during the speed governing system response .....	185
Figure 7.9: Area 3 Net tie-line power interchange during the speed governing system response .....	186
Figure 7.10: Area 3 Net tie-line power interchange during the speed governing system response .....	187
Figure 7.11: Area 1 Automatic Generation Control (AGC) .....	188
Figure 7.12: Area 2 Automatic Generation Control (AGC) .....	188
Figure 7.13: Area 3 Automatic Generation Control (AGC) .....	189
Figure 7.14: Area 4 Automatic Generation Control (AGC) .....	189
Figure 7.15: System grid meters results after the implementation of AGC following a 15% load demand increase. ....	190
Figure 7.16: System frequency response after the implementation of AGC following a 15% load demand increase. ....	190
Figure 7.17: Area 2 Net tie-line power interchange after the implementation of AGC following a 15% load demand increase. ....	191
Figure 7.18: Area 3 Net tie-line power interchange after the implementation of AGC following a 15% load demand increase. ....	192

Figure 7.19: Area 4 Net tie-line power interchange after the implementation of AGC following a 15% load demand increase. ....	192
Figure 7.20: Wind power plant active power scaling control .....	194
Figure 7.21: System frequency when the governing system, AGC and WTG were active after the 15% load demand increase .....	195
Figure 7.22: Active power delivered by the wind power plant measured at the sending-end. ....	196
Figure 7.23: Area 2 net tie-line power interchange when the wind power plant was activated.....	197
Figure 7.24: Area 3 net tie-line power interchange when the wind power plant was activated.....	198
Figure 7.25: Area 4 net tie-line power interchange when the wind power plant was activated.....	199
Figure 7.26: Bus voltage results recorded after the load demand increase contingency..	199
Figure 8.1: Modified IEEE 14 fully integrated with SEL-3555 RTAC in hardware in the closed-loop configuration.....	202
Figure 8.2: GNET-GSE Communication configuration.....	203
Figure 8.3: IED name tab .....	203
Figure 8.4: Define datasets and signal type to be published.....	204
Figure 8.5: Output signals mapping published through GTNET-GSE .....	204
Figure 8.6: Data published from RSCAD is displayed using GOOSE inspector .....	205
Figure 8.7: IEC 61850 GOOSE messaging configuration on AcSelerator Architect .....	206
Figure 8.8: IEC 61850 GOOSE Receive messaging subscription configuration on AcSelerator Architect.....	207
Figure 8.9: Dataset configuration for analog signal transmission from the SEL-3555 RTAC to RSCAD .....	208
Figure 8.10: Dataset type and arrangement configuration for analog signals transmission the SEL-3555 RTAC to RSCAD .....	208
Figure 8.11: IEC 61850 GOOSE transmission analog signals the SEL-3555 RTAC to RSCAD .....	209
Figure 8.12: IEC 61850 configuration file upload on AcSelerator RTAC platform .....	210

Figure 8.13: Area 1 logic development using IEC 61131-3 language (CFC).....	211
Figure 8.14: Area 1 automatic generation control configuration.....	211
Figure 8.15: Area 2 automatic generation control configuration.....	212
Figure 8.16: Area 3 automatic generation control configuration.....	212
Figure 8.17: Area 4 automatic generation control configuration.....	212
Figure 8.18: Wind active power compensation scaling logic.....	212
Figure 8.19: Uploading the configured control logics and settings to the SEL-3555 RTAC device.....	213
Figure 8.20: Control signal data from GTNET received by SEL-3555 RTAC via GOOSE messaging.....	214
Figure 8.21: Output control signal published by SEL-3555 RTAC to GTNET.....	214
Figure 8.22: Mapping the IEC 61850 GOOSE messaging signals transmitted by SEL-3555 RTAC to GTNET .....	215
Figure 8.23: Control signals signal from SEL-3555 RTAC to GNET arrangement on GNET-GSE communication module .....	216
Figure 8.24: Data published from SEL-3555 RTAC via GOOSE messaging to GTNET is viewed using GOOSE Inspector .....	216
Figure 8.25: Control signal from SEL-3555 RTAC to RSCAD generator governing system and WTG active power compensator scaling captured on RSCAD RUNTIME.....	217
Figure 8.26: System frequency during speed governing system response and SEL-3555 RTAC on manual mode.....	218
Figure 8.27: Area 2 Net tie-line power interchange during the speed governing system response and SEL-3555 RTAC on manual mode.....	219
Figure 8.28: Area 3 Net tie-line power interchange during the speed governing system response and SEL-3555 RTAC on manual mode.....	220
Figure 8.29: Area 4 Net tie-line power interchange during the speed governing system response and SEL-3555 RTAC on manual mode.....	220
Figure 8.30: Bus voltages during speed governing system response and SEL-3555 RTAC on manual mode .....	221
Figure 8.31: System frequency response after the implementation of AGC on SEL-3555 RTAC .....	222

Figure 8.32: Area 2 Net tie-line power interchange after the implementation of AGC on SEL-3555 RTAC .....	223
Figure 8.33: Area 3 Net tie-line power interchange after the implementation of AGC on SEL-3555 RTAC .....	223
Figure 8.34: Area 4 Net tie-line power interchange after the implementation of AGC on SEL-3555 RTAC .....	224
Figure 8.35: Bus voltages after the implementation of AGC on SEL-3555 RTAC .....	224
Figure 8.36: System frequency when the governing system, AGC and WTG were active on SEL-3555 RTAC .....	226
Figure 8.37: Active power delivered by the wind power plant measured at the sending-end controlled through SEL-3555 RTAC .....	226
Figure 8.38: Area 2 net tie-line power interchange when the wind power plant was activated through SEL-3555 RTAC.....	227
Figure 8.39: Area 3 net tie-line power interchange when the wind power plant was activated through SEL-3555 RTAC.....	228
Figure 8.40: Area 4 net tie-line power interchange when the wind power plant was activated through SEL-3555 RTAC.....	228
Figure 8.41: Bus voltage results recorded when the wind power plant was activated through SEL-3555 RTAC. ....	229
Table 2.1: Different system types of inertia constants (Musau et al., 2017) .....	22
Table 2.2: Frequency operation and control/protection actions ((Emad A Mohamed et al., 2018).....	23
Table 2.3: Logical nodes description as per the IEC 61850 standard (Ustun et al., 2011) .	34
Table 2.4: Review overview of the power system frequency control. ....	39
Table 3.1: System elements data expression to indicate the given data and unknown data (Bergen & Vittal, 2007) .....	68
Table 3.2: Power system frequency defense plan (Jan et al., 2005).....	96
Table 4.1: Bus, generator, and load data.....	109
Table 4.2: Transmission and distribution lines data .....	110
Table 4.3: Transformer data .....	111

Table 4.4: Load model sensitivity coefficients(Jan et al., 2005) .....	114
Table 4.5: Network bus voltage profile in steady-state.....	119
Table 4.6: Network grid summary .....	124
Table 4.7: Case study 1 .....	131
Table 4.8: Case study 1 results .....	137
Table 5.1: Comparison between the centralized and decentralized controller .....	141
Table 5.2: Case study 2 .....	147
Table 5.3: Case study 2 results .....	154
Table 6.1: Case study 3 – Assessment of the effectiveness of wind turbine generator active power compensation control loop .....	168
Table 6.2: Case study 3 results– Assessment of the effectiveness of wind turbine generator active power compensation control loop.....	176

# CHAPTER ONE

## INTRODUCTION

### 1.1 Introduction

The power system network is expected to operate normally, be stable, reliable, and secure to ensure the customer's continuity and supply quality. A comprehensive study and monitoring of the power system are necessary to ensure that any disturbance that may occur to it does not leave customers without supply. Such disruption is anticipated; there should be preliminary measures to avoid such disturbance. The power system network is exposed to different disturbances based on their severance of occurrence and duration (Kundur et al., 2004).

If the power system network is not constantly monitored and maintained according to its specification, there are high chances that it can operate abnormally. Severe disturbances and maloperation can even result in a complete system collapse and lead to a blackout. Several blackouts had occurred in the power systems network, of which some were claimed to be due to frequency instability. The frequency instability is caused by a discrepancy between the electrical load demand and generation capacity available at a given time, and this means if the load demand varies and the generation remains unchanged, the frequency will also change (Kundur, 2004).

There was a blackout that took place in India on the 30<sup>th</sup> of July 2012. In the investigation that was conducted, it was revealed that the incident occurred due to overloading. The 400kV transmission system from Gwalior to Bina is a double circuit. During this blackout, one of its lines was out due to maintenance, and there was only one line feeding Bina. Overloading occurred on the line feeding Bina and caused a cascade of tripping through the network, resulting in approximately 32 GW of generation shortage to supply the area. It was also discovered that there was no adequate control and protection system to respond to the problem. Since there were no mitigation measures in place, the incident occurred again on the 31st of July 2012. One of the reasons that cause the blackouts include inadequate control and monitoring of voltage and frequency (Wu et al., 2017).

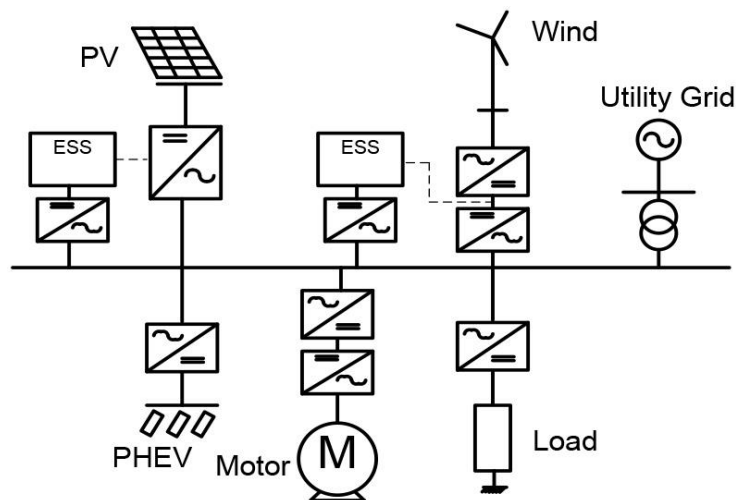
It was clear that there were no resources in place to provide a backup supply in the distribution power system grid. The protection system was also not adequately coordinated. It did not only isolate the faulted part of the system, but a

cascade tripping was observed, leaving many customers without a power supply (Wu et al., 2017).

In the conventional distribution power system grid, the integration of Distributed Energy Resources (DERs) can strengthen the power system stability. However, there is a risk in the frequency and voltage stability due to their intermittency and the small-time constant (E. A. Mohamed et al., 2018).

Figure 1.1 below illustrates the single line configuration of micro-grid with DERs incorporated into the network grid. The different DERs, such as wind and solar systems, are connected to the power grid utilizing an electronic interface. Solar and Wind system does not have a built-in capacity to store the generated electrical energy; hence the energy generated through these DERs is stored in Energy Storage System (ESS). The wind energy system generates power in AC mode, and this energy is then converted to DC for storage (as batteries operate in DC). It gets converted to AC again to be connected to the grid.

In contrast, energy generated through solar is directly stored in the ESS and later converted to AC for the grid interface. Figure 1.1 below shows that an electric vehicle can be utilized and re-use the energy stored to supply the grid. The voltage on the point of a connection must be the same between the micro-grid and the whole network grid. Hence, this system's voltage gets transformed to be suitable for the grid where it will be applied (Ghafouri et al., 2015).



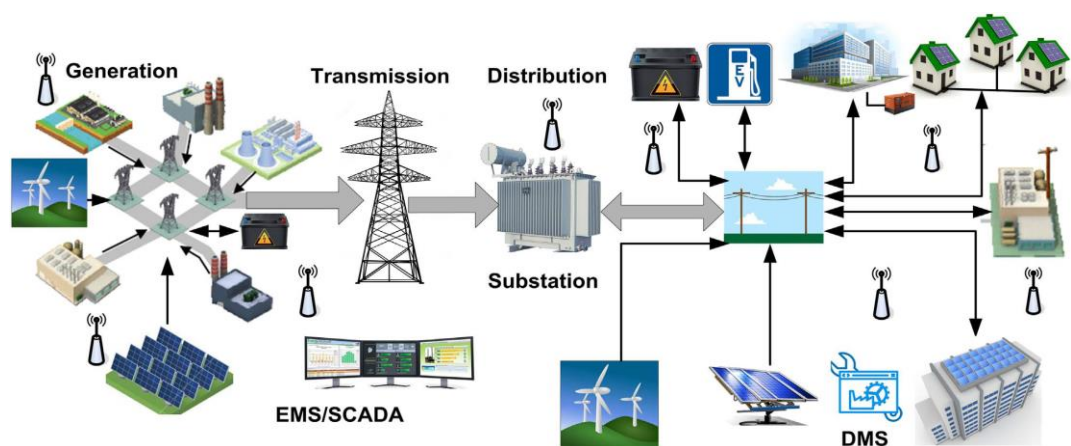
**Figure 1.1: Typical integrated Grid system operates in AC (Ghafouri et al., 2015).**

Figure 1.2 is the graphical representation of the power system divided into three primary components generation, transmission, and distribution system. In the



generation system, the orientation of DERs is demonstrated. These three components are connected in the following manner: The generation system is where mechanical energy is converted to electrical energy. The power generated is then transformed to a high voltage level to minimize any power losses and transmitted using pylon structures and high voltage conductors across long distances. The electrical energy is then stepped down and distributed to the customers, for example, commercial, residential and industrial areas. The main essential control centers, such as an Energy Management System (EMS), optimize the power system performance and Distribution Management System (DMS) to ensure the power system reliability. EMS deals with control and monitoring of Conventional Power Plants (CPPs) while DMS monitors the distribution system, which is integrated with DERs; this includes maintenance scheduling and fault diagnostics systems of DERs in service (Ahmad et al., 2018).

The illustration of Figures 1.1 and 1.2 shows how the DERs can be integrated into the power grid and all the components found in the power grid.



**Figure 1.2: The smart grid and active Distributed System (Ahmad et al., 2018)**

Protection and control are critical aspects to consider in dealing with the frequency uncertainty problems in the power grids (E. A. Mohamed et al., 2018). The power grid's control and protection need to be continuously and significantly improved as there is consistent advancement in technology. Therefore, it is required that power system control plant designers consider an application of advanced intelligent electronic devices (IEDs) to maintain the power system complexity adequately.

## 1.2 Awareness of the problem

The variable power generated through DERs is causing power system instability through frequency and voltage changes affecting the power flow and causing more system operational issues. With the high penetration rate of the DERs to the power system grid, the concern is that they will make the power grid more inferior due to their low inertia and small-time constant; consequently producing frequency and voltage instability affecting the entire grid stability and resiliency (Zhang et al., 2011).

The load power demand changes affect the system frequency, the generation system voltage, and active and reactive power. The frequency variations resulting from power generation fluctuation of DERs have the potential impact on the control and protection performance if there is no adequate coordination, which may lead to the operation of under/over-frequency protection relay (Vieira et al., 2006). The frequency protection relay operation might cause the disconnection of some loads and generation units of the DER's system. Therefore, the grid system frequency control and protection coordination issues need to be critically investigated (Ghafouri et al., 2015).

## 1.3 Problem statement

The power system grid is becoming modernized and strengthened through the integration of different energy resources. These power grids integrated energy resources create a risk on the conventional power system due to their variable power generations, leading to a complete system collapse/blackout if they are not carefully monitored and controlled (Hill, 2004). The power variation caused by the DER's can also create voltage and frequency instability because of the generation's variation.

**Problem statement:** To develop IEC 61850 standard-based control and improved protection schemes for integrating the DERs to the power grid, focusing on conditions of system frequency instability events.

## 1.4 Research aim and objectives

This project aims to develop an IEC 61850 standard-based control and protection schemes for integrating the DERs (Distributed Energy Resources) to the power grid in the conditions of frequency instability events. Such a control and

protection scheme will improve the protection response time during abnormal system conditions, enhancing power grid stability, reliability, and quality of supply. This scope of work will be accomplished through an IEC 61850 standard implementation for communication and automation.

#### **1.4.1 Objectives**

The aim indicated above will be attained through the following objectives:

- Literature review of the methods for the solution of the smart grid's problems for stability.
- IEC 61850 standard-based protection schemes are used to improve frequency stability.
- Modeling and controlling a wind power plant for intelligent grid integration (types, controllers, and protection)
- Modeling and simulation of the case study network in the power factory's software environment (DIgSILENT) and RTDS
- Stability and contingency analysis and design of control and protection schemes for a selected case study network
- Design of the logic algorithm for the integration of wind power plant to the grid.
- Programming the algorithm in the software environment of RTDS. Investigation of the performance of the algorithm for various conditions of operation in smart grids
- Development of a test-bed for Hardware-In-the-Loop (HIL) real-time simulation of the developed system. Investigation of the performance of the algorithm for various types of operating conditions.

#### **1.5 Hypothesis**

The development of a control and protection scheme will improve power system stability and reliability. It will also improve the quality of supply to endusers as it will provide a real-time power system control and monitoring. This system's application will be generic and relevant to any types of DER's that could be integrated into the grid.

## **1.6 Delimitation of research**

The research project concentrate on control and protection of power system grid integrated with Distributed Energy Resources, focusing on system frequency and through IEC 61850 standard implementation.

The research will analyze conventional power system stability in detail and evaluate it when integrated with DERs. A control and protection scheme will be developed and tested using the DIgSILENT Power factory and RDTs.

The simulation will be based on the analysis of the following:

- Case study for the existing network under normal and abnormal conditions focusing on voltage and frequency behavior.
- Power system response to the incorporation of DERs emphasizing more on the voltage and frequency performance.
- Compare the existing control and protection schemes response and performance against the proposed control and protections IEC 61850 standard-based scheme.

## **1.7 The motivation of the research project**

A power system network is one of the essential systems serving electricity to customers loads at the desired quality with minimal supply disruptions. Since the power system is subjected to disturbances during operation, its reliability is prioritized at the planning and design stage. The power system is expected to be stable and reliable, secured in the event of disturbance and post-fault periods (Sallam & Malik, 2015). The integration of Renewable Energy Systems (RESs) and DERs are expected to improve the power system grid's reliability. These systems are quick to respond to power system changes between generation and load. Their poor coordination has a significant contribution to frequency and voltage instability, causing the weakening of grid resiliency

This research project will benefit the power utility such as Electricity Supply Commission (ESKOM) and other independent power utilities. It is intended to identify and investigate the potential impacts of the DERs on the power system network and their influence on voltage and frequency stability. Introduce an improved control and protection scheme for frequency stability. It will also help the utilities to identify some system modifications that will enable a smooth integration of those energy resources without the uncertainty of possibilities of power system collapse.

IEC 61850 standard is being implemented internationally with its benefits on improving substation communication and operation. The control and protection scheme to be developed will be based on the application of an IEC 61850 standard using advanced Intelligent Electronic Devices (IEDs) that have such capability.

## **1.8 Assumptions**

This project will be based on the steady-state IEEE 14 bus power system network, which will be used as a generic network. Modifications/alterations will be made to accommodate the purpose of fulfilling the objectives of this research. DlgSILENT power factory software will be used as it has the required simulation functions. Real-Time Digital Simulator (RTDS) will be used for real-time simulation to validate the proposed algorithms.

## **1.9 Research Design and Methodology**

This project focuses on improving control and protection scheme used to maintain frequency stability in the power system network. Improve the current algorithms and technologies in service by implementing the IEC 61850 control scheme. The IEC 61850 standard-based control scheme will improve both hardwiring and communication between the power station and the control center. The research objectives will be achieved through the following:

### **1.9.1 Literature review**

There are various control schemes currently in services, and this thesis focuses on developing the control scheme to use wind power plants as active power compensators. This is because the conventional generation system can no longer contribute an additional active power flowing load demand increase event. The information collected through reading related books, journals, and the internet enables the path to achieve the desired outcomes.

### **1.9.2 Methods for the power system frequency control**

Several control schemes could be possible applied in the power system frequency control. A decentralized automatic generation control was selected for the conventional system based on the following benefits:

- In an interconnected system, each has its dedicated control scheme.
- When one area control scheme fails, the other area control scheme automatically becomes the backup and controls the frequency in the entire system.

### **1.9.3 Simulations**

Simulation software is used to develop a function control scheme for system frequency instability and implemented on a modified IEEE 14 bus network. The modified network is modeled using the DIgSILENT power factory simulation platform. The validation of the proposed control scheme operating principles is implemented in the real-time digital simulation (RTDS) platform. The aim of using this platform is to assess the operation of the developed scheme in real-time. The practical implementation of the hardware control scheme is made possible using the SEL-3555 RTAC from Schweitzer Engineering Laboratories (SEL). The control scheme logic is developed using RTAC architect software.

### **1.9.4 Data collection**

The developed control scheme's results and parameters using DIgSILENT are collected for further control scheme development using a different simulation platform. The functionality of the control scheme in these different simulation platforms is being compared to one another. Comparing the developed control in different platforms will have to adequately assess the control scheme's behavior for effective and efficient implementation in real-time.

## **1.10 Thesis chapters**

This thesis is composed of eight chapters and three appendixes. The description of what these chapters and appendixes contain is as follows:

### **1.10.1 Chapter One**

This chapter outlines the research background, the aim, objectives, awareness of the problem, motivation of the research, problem statement, subproblems, hypothesis, delimitation of research, project assumptions, research design, and research design and methodology, thesis chapter breakdown, and conclusion.

### **1.10.2 Chapter Two**

The literature on basic power system frequency stability, significant causes of instability, methods used in frequency control, and the impact of integrating distributed energy resources in frequency stability are covered in this chapter. Communication system and protocols used in power system environment are covered. The benefits of the application of an IEC 61850 to advance the frequency control scheme are also outlined. Various articles related to power system frequency stability were reviewed.

### **1.10.3 Chapter Three**

In this chapter, a detailed theory regarding power system frequency control and protection is outlined. The methodologies applied in the conventional power system grids to ensure frequency stability are also defined.

### **1.10.4 Chapter Four**

This chapter defines the modeling of the modified IEEE 14 bus network. The network frequency stability is investigated based on incremental load contingency. DIgSILENT simulation software is used to model the modified IEEE 14 bus network and analyze the primary control performance through the governing system as the load demand increases. The interarea power interchange is also monitored. It has been noted that the governing system can only bring the system to a steady state; therefore, an additional control measure is required to restore the frequency to its nominal. This additional control system is described in chapter five.

### **1.10.5 Chapter Five**

This chapter describes the modeling of a decentralized automatic generation control. The utilization of an automatic generation came into effect as the governing system failed to maintain the frequency to its nominal state following an incremental load contingency, as analyzed in chapter four. This chapter seeks to improve the system frequency as analyzed in chapter four by utilization a secondary control strategy through decentralized automatic generation control.

### **1.10.6 Chapter Six**

The secondary control system, the automatic generation control, can recover the system frequency when there are enough generation reserves. When the reserves are depleted, the automatic generation control can no longer sustain the ever-increasing load contingency. The wind power plant is integrated into the power system grid to assist with active power compensation to maintain the system frequency to its nominal value. These analyses are performed using a DIgSILENT power factory.

### **1.10.7 Chapter Seven**

In this chapter, DIgSILENT simulation results obtained in chapters four, five, and six are verified and validated using the Real-Time Digital Simulation (RTDS) platform. The incremental load contingency case studies applied in chapters four, five, and six are repeated. The developed control scheme in DigSielnt is also developed using RTDS. This verification and validation enable implementing the

control scheme in hardware-in-the-loop and IEC 61850 standard implementation, as described in chapter eight.

#### **1.10.8 Chapter Eight**

This chapter describes the practical implementation of the developed frequency control scheme. Hardware-in-the-loop system, as well as IEC 61850 standard implementation, is also covered in this chapter. SEL-3555 RTAC is used as the hardware control system IEDs. The control logic was developed and configured using this device in the practical

#### **1.10.9 Chapter Nine**

The comparison of the developed frequency control scheme on DlgSILENT is made against the one developed on RTDS. The result was obtained from DlgSILENT, RTDS, and when the IEC 61850 standard is implemented, the conclusion is drawn based on the results, and recommendations are made.

#### **1.10.10 Appendix A**

This appendix comprises of some additional Figures for the system developed control using DlgSILENT simulation software. The settings and the control loop function block diagrams are also included.

#### **1.10.11 Appendix B**

The additional function block diagram for the developed power system network and control loops in the RTDS simulation platform is contained in this appendix. System setting and additional Figures are also attached.

#### **1.10.12 Appendix C**

The additional information related to IEC 61850 standard implementation and the configuration settings of the SEL-3555 RTAC is attached. The function block diagrams that were configured on RTAC are also attached.



## **CHAPTER TWO**

### **LITERATURE REVIEW**

#### **2.1 Introduction**

Distributed energy resources (DERs) are essential in the power system as they strengthen the power system's reliability and improve supply quality. The distributed energy resources form part of the distribution grid. The energy generated through these systems can either be renewable or non-renewable. Renewable energy, often referred to as green or clean energy, is generated through natural sources such as wind and sunlight replenished continuously. Non-renewable energy sources such as bio-fuel, coal, and oil and gas are often referred to as dirty energy. Non-renewable energy sources are not available in every country, and they are limited; they take a long to replenish or are never replaced. The energy sources that form part of renewable systems are wind power plants and solar power plants, while non-renewable systems are coal-fired, gas-turbine, diesel generators, etc. These energy resources need constant control and monitoring when integrated into the power system grid. Failure to do so can lead to an unstable power grid.

The power system stability has been observed as one of the essential features to be considered, and this was due to blackouts that occurred due to the power system being unstable (Kundur et al., 2004). The conventional power system is highly dominated by synchronous generators, which are the main contributors to the electrical power generation system (Johnson et al., 2017). Generally, the main two causes of the power system becoming unstable are the disturbance due to fault in the system or a rapid change in the load being supplied (Basler et al., 2008).

The power system is being evolved, and this ongoing electric power industry transformation trend has led to high penetration of variable and distributed energy resources on electric grids across the globe (Johnson et al., 2017). These emerging integrations are now causing uncertainties on power system stability, power quality as well as security. The power system is also becoming more complex and comprehensive as new technologies are also being introduced. Control, protection, and system communication also form part of significant concerns within the power system industry (Ustun et al., 2012).

There is power system research underway focusing on power system stability, power quality, data quality, power system modeling, power system reliability,

reactive power management, power systems economics, etc. There are still limited studies on distributed energy resources, their impact on the conventional power system grid, the control and protection strategies to be used due to their nature and operation, etc. These limited studies motivated this research proposal to investigate the role of distributed energy resources (DERs) in smart grids.

## **2.2 Overview of power system stability**

The conventional interconnected power system relies on synchronous generators to ensure that the power grid is stable and is the primary source of electrical energy production. The synchronous generators are configured to allow their rotors to be electromechanically coupled so that they rotate at the same time under normal operating conditions. In synchronized stable conditions, the generator's shaft rotates at 50Hz frequency (Johnson et al., 2017). The classification of power system stability brought the critical understanding and the effects of its disturbances to understand the power system and its instabilities. The analysis and identification of the significant factors influencing the stability and methods to be used in improving the stability can also be achieved through classification (Kundur et al., 2004).

The power system behavior is influenced by three factors: rotor angle, frequency, and voltage. Either fault condition primarily causes these three factors in the power system grid or a change in load demand. The duration of the disturbance due to rotor angle can be a short-term base (3 to 5 seconds after the disturbance, and it can be 10 to 20 seconds for massive systems), while frequency and voltage can either be a short or long-term base. Figure 2.1 below illustrates the classification of power system stability. The variables that can contribute to power system instabilities, the size of disturbance are also shown. This classification will significantly assist in calculation methods as well as stability forecasting (Kundur et al., 2004). The impact of each stability category is further elaborated on in Figure 2.1 below.

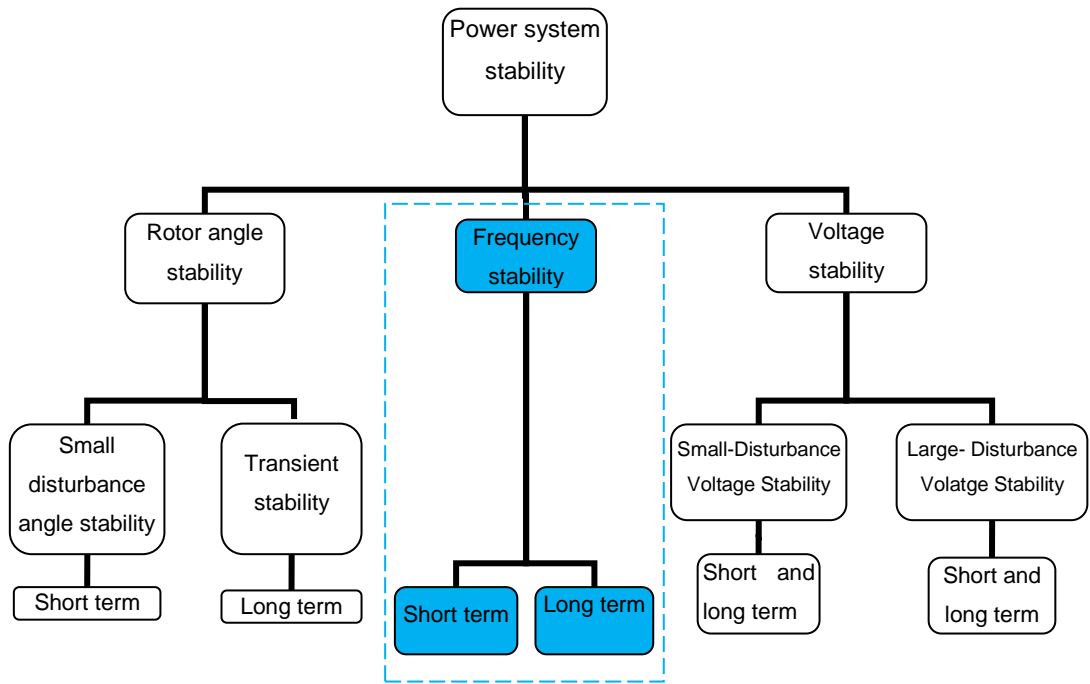


**Figure 2.1: Power system stability classification (Kundur et al., 2004).**

### 2.2.1 Rotor angle stability

Rotor angle stability is defined as the ability to maintain the interconnected generator's synchronism when the power system is disturbed, and this is to maintain both the mechanical torque and electromagnetic torque of interconnected generators. In the synchronous generator, the prime mover (turbine) uses mechanical power to turn the rotor. The mechanical torque will be in the direction of rotation, and the electrical torque opposes the rotation. In the fault, the electrical output power changes faster compared to its mechanical counterpart due to its excitation system response. There will be an imbalance between torques applied (mechanical and electrical), resulting in rotor speed which will cause the rotor angle to change the rotor angle shifts between rotor mmf magnetomotive force and resultant of rotor mmf and stator mmf. The power system is expected to withstand such events of disturbance and bring the system to its regular operation (Sallam & Malik, 2015).

Rotor angle stability is one of the three main contributors to power system stability. The rotor angle stability can be further divided into two types such as transient and small-signal stability, and these disturbances happen at a short duration period (Kundur et al., 2004):

### 2.2.1.1 Transient stability

Transient Stability is defined as the power system's ability to regain its normal operating condition when subjected to a significant disturbance in a short period. This can be a result of transmission line faults. This type of disturbance on electrical torque can be fixed by categorizing its components into two aspects: the synchronizing torque and the damping torque. The exciter system is the one that can regulate any changes in the system. If the torque is not enough to oppose the rotor angle changes, the exciter needs to provide more magnetic flux to resist such changes. If the mechanical torque is more than the electrical torque, the exciter system should immediately apply a more positive voltage to the generator field. On the other hand, when the electrical torque is high than the mechanical torque, the exciter should apply a more negative voltage to the field generator and suppress any changes that might lead to instability (Sallam & Malik, 2015).

Considering Figure 2.2 below, the grid-connected generator is expected to operate at O, whereby normally  $P_m$  (mechanical power) is equal to  $P_e$  (electrical power). A grid disturbance happening next to the generator will cause electrical output power to drop to zero, resulting in rotor angle or power angle shift from  $\delta_0$  to  $\delta_1$  where the disturbance is cleared. At point one, the electrical output power is returned to its normal level in correspondence to the power angle curve post-fault. The new curve is lower than the one before the fault, and the protection system might have isolated the faulted part of the system. At point 3, the electrical power is more than the mechanical power resulting in rotor momentum drop, and the exciter system will suppress the discrepancy in both powers. The generator will then return to its normal operating region. This will only be true if the exciter system can respond quickly to the system's changes (Sallam & Malik, 2015).

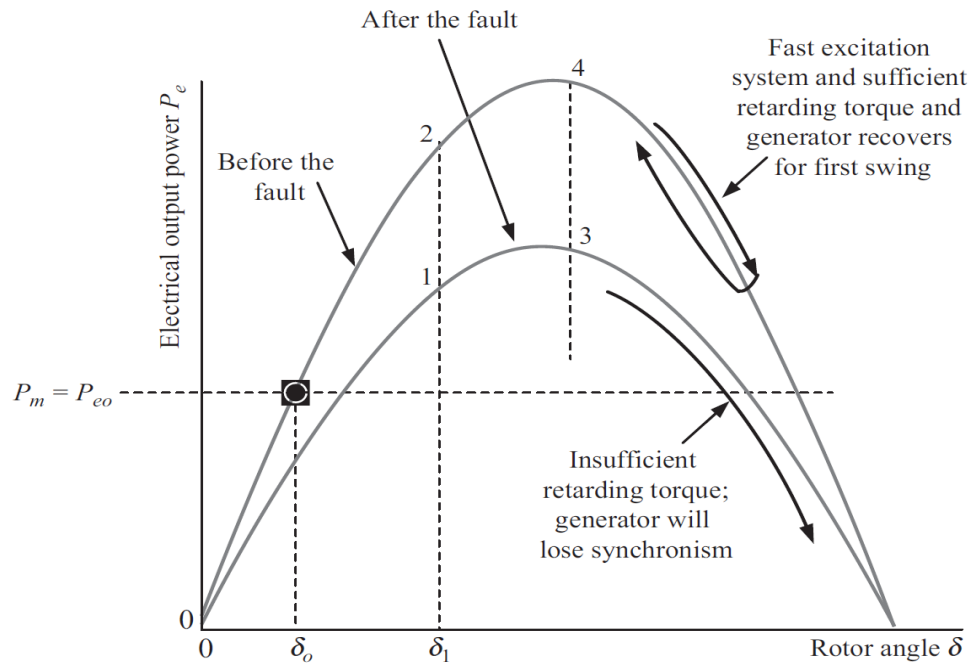


**Figure 2.2:** Transient stability analysis of rotor or power angle (Sallam & Malik, 2015)

### 2.2.1.2 Small-signal stability

Small-signal stability, which can also be called small-disturbance stability, is the power grid's capability to function in a stable condition after it was affected by a small disturbance. This type of disturbance is small, such that its equation can be linear to analyze its impact on the power system (Gu et al., 2018). The mathematical expression of small-signal disturbance can be presented as follows (Kundur, 1994):

$$P_e = P_{max} \sin \delta = \frac{E_G E_M}{X_T} \sin \delta \quad 2.1.$$

$$X_T = X_G + X_L + X_M \quad 2.2.$$

This interconnected system can be illustrated in a single line diagram below in Figure 2.3.

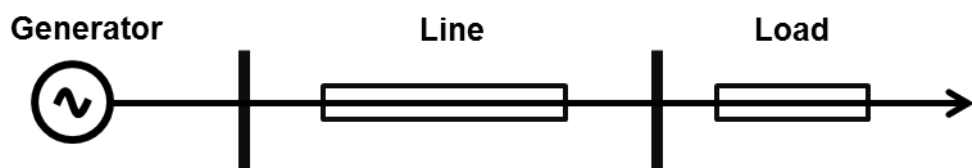


**Figure 2.3:** Single line diagram (Kundur, 1994)

In this representation  $P_e$  is the electrical output power,  $E_G$  is the source voltage,  $X_G$  (source reactance),  $X_L$  (line reactance),  $X_M$  (load reactance) whilst  $X_T$  is the sum of all reactance. When  $P_{max} = \frac{E_G E_M}{X_T}$  Moreover,  $\delta = 90^\circ$  it is said that the system has reached its steady-state limitation.

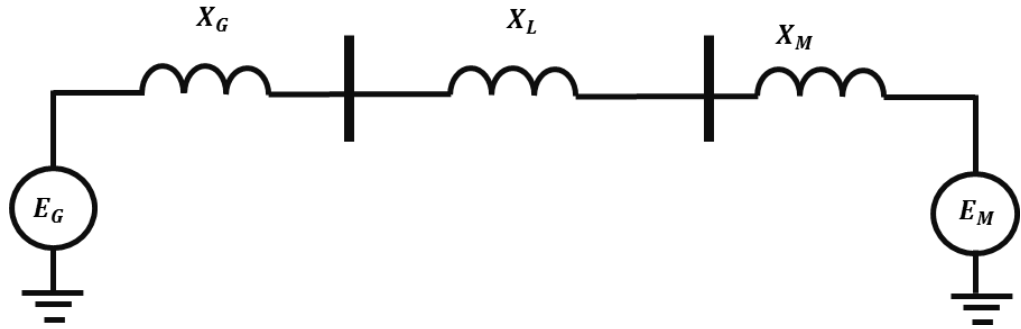


**Figure 2.4: Ideal single line model (Kundur, 1994)**

Considering Figure 2.5 below, at O, the mechanical power is equal to the electrical output power where the is power angle  $\delta_0$ . In the event of a minor disturbance, the electrical output power  $P_{e1}$  at point 1 will drop, causing the rotor to accelerate more, trying to move back point O. At this instances, the mechanical power  $P_m$  will be more than the electrical output power. At point 2, electrical power is more than the electrical output power. Therefore the rotor will decelerate to move back to operating point O. Hence the power system becomes stable again due to damping oscillation (Sallam & Malik, 2015).

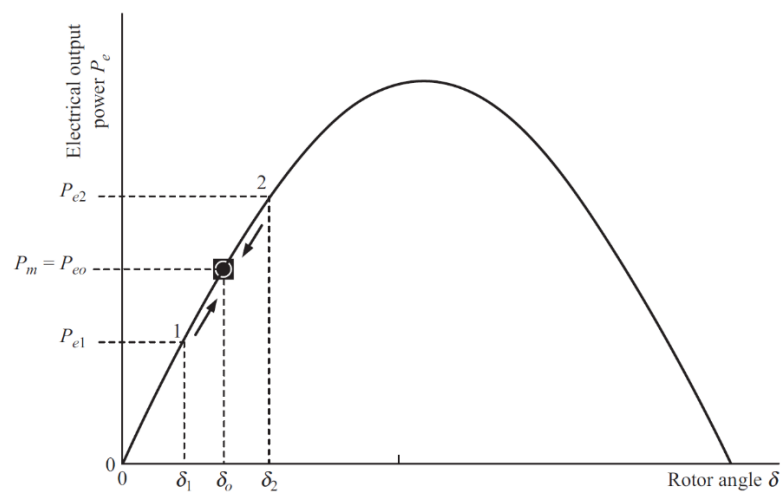


**Figure 2.5: Power angle oscillation curve for small signal stability (Sallam & Malik, 2015)**

## 2.2.2 Voltage stability

Voltage stability is the power system's ability to maintain the voltage levels within its tolerances at all buses after the power system was disturbed. This will help prevent power outages or power system grid collapse (Johnson et al., 2017).

Voltage instability can be caused by system fault disturbance, increased load demand, or operational changes in the system. When the power flows through inductive reactive in a transmission system, there will be a voltage drop. If the reactive power is not adequately maintained, voltage instability can occur. A system is declared unstable when one of the buses' voltage magnitude decreases when there is a rise in reactive power. The system is unstable when the sensitivity of voltage and reactive power is harmful, and it is stable when the sensitivity of voltage and reactive power is positive. This means that the buses' voltage must also increase (positive sensitivity). Rotor angle can cause voltage instability when it loses synchronism between the generators and becomes out of step over  $180^\circ$  (Kundur, 1994).

Various factors are resulting in voltage instability. A single line diagram representation of a radial system is shown in Figure 2.6 below to analyze and understand how voltage instability occurs.

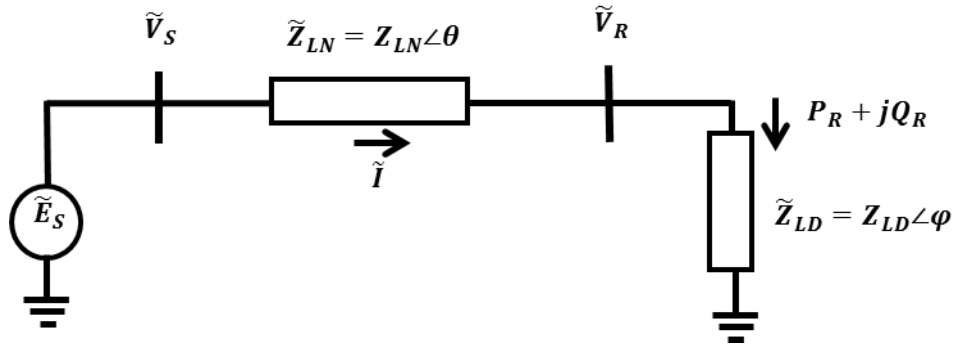


**Figure 2.6: Voltage instability radial single line diagram representation (Kundur, 1994)**

The current flow through this network can be calculated using equation 2.3.

$$\tilde{I} = \frac{\tilde{E}_S}{\tilde{Z}_{LN} + \tilde{Z}_{LD}} \text{ and } I = \frac{E_S}{\sqrt{F} \times Z_{LN}} \quad 2.3$$

Where

$$\begin{aligned}
F &= \sqrt{(Z_{LN}\cos\theta + Z_{LD}\cos\varphi)^2 + (Z_{LN}\sin\theta + Z_{LD}\sin\varphi)^2} \\
&= 1 + \left(\frac{Z_{LD}}{Z_{LN}}\right)^2 + 2\left(\frac{Z_{LD}}{Z_{LN}}\right)\cos(\theta - \varphi)
\end{aligned} \tag{2.4}$$

The receiving end voltage can be calculated as:

$$V_R = Z_{LD}I = \frac{Z_{LD} \times E_S}{\sqrt{F} \times Z_{LN}} \tag{2.5}$$

The receiving end power is calculated as follows:

$$P_R = V_R I \cos\varphi = \frac{Z_{LD}}{\sqrt{F}} \left(\frac{E_S}{Z_{LN}}\right)^2 \cos\varphi$$

The relationship between  $P_R$ ,  $V_R$  and  $I$  is graphically illustrated in Figure 2.7 below as a function of line impedance overload impedance focusing on the receiving end.

Considering Figure 2.7 below, when the load demand is increased by dropping the value of  $Z_{LD}$ , the receiving end power increases and lowers before it reached saturation, hence there is maximum power transferred, and at this point, the power factor is at unity ( $\cos\varphi = 1$ ). The current also increases while the voltage is decreasing. This happens under regular operation, that is, before the line impedance equates with load impedance. It should be noted that before line impedance is equal to the load impedance, the current is increasing at a high rate compared to the rate of voltage reduction. This results in an increase in power transfer at the receiving end. As the reduction in load impedance is more bringing it closer to the line impedance, the voltage reduction is more than the current rise resulting in load power decreasing (Kundur, 1994).

When the voltage and current reach the critical operation point where the line impedance is equal to the load impedance, the system will decide to regulate voltage and use all the available mechanism such as an automatic underload tap changer in case there is a transformer used to raise the load impedance to be more than the line impedance to maintain the voltage. If the voltage at the buses is lower than the accepted level, then the system unstable due to voltage (Kundur, 1994).



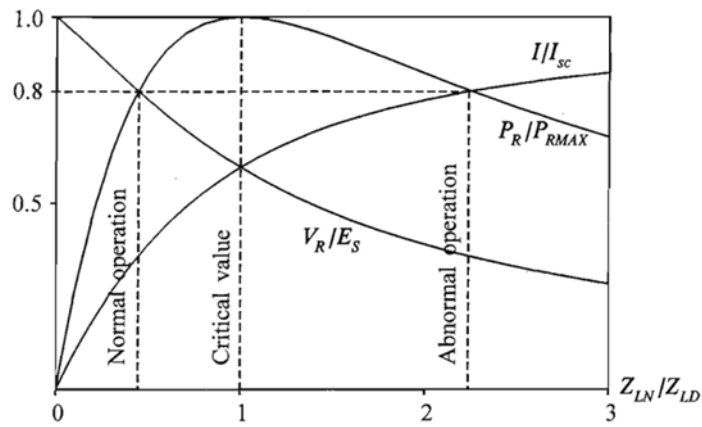


**Figure 2.7: The relationship between voltage, current, and power at the receiving end (Kundur, 1994)**

Figure 2.8 below illustrates the relationship between the power at the receiving end voltage. In this diagram, it can be seen that any changes in the power factor might affect the stability of the system. If the power factor is reduced, the reactive power will increase, and the system's operation condition can become unstable. The dotted line represents the locus critical operating point, and any point below the locus operating point is regarded unstable operating condition. Therefore the system must continuously operate above the critical operating point (Kundur, 1994).

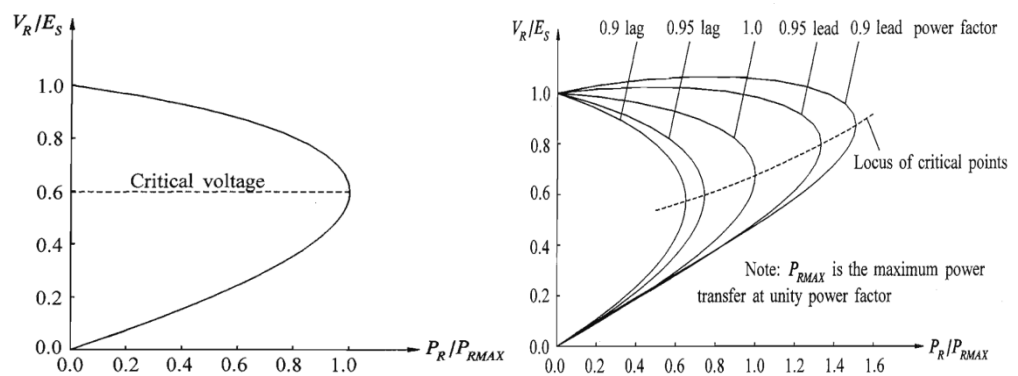


**Figure 2.8: The relationship between the receiving end voltage and power (Kundur, 1994)**

Voltage stability can be due to small or large disturbances. To bring a better understanding of the analysis, they need to be considered separately. This means that the impact of minor disturbance needs to be studied separately from significant system disturbance. In the convention system, voltage stability can be improved using tap changing transformers, which change the transformer, booster transformer, series & shunt capacitor, and synchronous phase modifiers.

Voltage and frequency are directly proportional; changes to system bus voltages also affected the system frequency stability point.

## **2.3 Frequency stability**

Frequency stability is regarded as a power system's ability to sustain steady frequency in the event of system upset, leading to the power imbalance between load and generation. The power system should restore or maintain equal power between the generation and load without interrupting the power supply (Kundur et al., 2004).

Instability is occurring due to sustained frequency fluctuation resulting in the tripping of generation units or loads. These frequency fluctuations can result from increased load demand, loss of synchronism between generation units, and transmission line faults. The frequency stability can be impacted by equipment failure to respond to system changes when there are no adequate control and protection systems (Kundur et al., 2004).

Frequency stability can be further categorized into three forms: short-term or transient, mid-term, and long-term frequency stability due to the dynamic behavior of the power system in disturbances. Short-term frequency stability is the system's recovery within a few seconds (10 seconds maximum) after being subjected to a disturbance. Mid-term stability is the system restoration time from a few seconds to a few minutes (typically, about 10 seconds to less than 10 minutes). The long-term stability takes to a maximum of 10 minutes for the system to regain its normal operating condition after being subject to a significant disturbance. However, in most cases, mid-term and long-term stability analyses are considered as one aspect as their analysis involves the same considerations with power system stability studies (Kundur, 1994).

### **2.3.1 Impact of load demand increase to frequency stability**

When there is a power imbalance between the generation and the load demand, the synchronous generators do not immediately become activated to supply the load's additional power. This concept is expressed by equation 2.6 below about a single line diagram in Figure 2.3 above.

$$ROCOF = \frac{\partial f}{\partial t} = \frac{f_0 \Delta P}{2H_{sys}} \quad 2.6$$

From equation 2.6, the rate of change of frequency (ROCOF) is the magnitude of the rate of change of frequency,  $\Delta P$  is the magnitude of power imbalance,  $f_0$  is

the rated system frequency, and  $H_{sys}$  is the system inertia after disturbance. There will be changes in the frequency; the synchronous generator's governor will start after some time due to its inertia. In that period, the power imbalance, system inertia, and frequency change rate impact the system frequency stability. When the frequency increases and the power imbalance is significant, the frequency will rapidly decrease; this is also true for when there is small inertia in the system, the frequency will decrease faster (Rahmann et al., 2018).

Another factor that also contributes to frequency stability is the frequency nadir. This happens when the frequency drops below the minimum threshold frequency level, activating under frequency load shedding scheme isolating part of the load to recover the system frequency. This effect is can then be analyzed using equation 2.7 (Rahmann et al., 2018).

$$\Delta f = a \cdot e^{b(ROCOF)} + c \quad 2.7$$

And

$$\Delta f = f_0 - f_{min} \quad 2.8$$

In equation 2.8,  $f_{min}$  is the nadir minimum frequency after the imbalance. The constant parameters  $a, b, \text{ and } c$  are extracted from generator disconnection historical data. Equation 2.8 is mostly used in the most severe frequency nadir (Rahmann et al., 2018).

### 2.3.2 The frequency stability recovery process

When there is an extended power outage due to fault or regular system maintenance, there will be a discrepancy between the generation and load demanded power in the process of restoration. The process to be followed is elaborated in point form below. The inertial response immediately opposes the frequency deviation. After the inertia response, the primary frequency control will be activated, whereby the governor will adjust the output power of the synchronous generator (typically between 5-30s). Secondary frequency control activates an automatic generation controller to mitigate the error between the nominal system frequency and the generation frequency (usually between 30s-15min). The last step will be to adjust the generator's operation points to rebalance the power generated and the load demand. This stage typically takes place after 15 min (Wazeer et al., 2019).

Given the rapid change of frequency due to low inertia, Table 2.1 below shows the expected range of inertia magnitudes in the various generation unit's power

systems. Inertia is when a machine can take to supply its related output power concerning its kinetic energy. The inertia is directly proportional to the machine's energy when it rotates and is inversely proportional to its rated apparent power.

**Table 2.1: Different system types of inertia constants (Musau et al., 2017)**

System type (turbine)	Inertia ( $H_{sys}$ )
Steam	4-9
Gas	3-4
Hydro	2-4
Wind	2-5
Solar PV	0

The frequency recovery process's demonstration is shown in Figure 2.9 below after the system was subjected to a disturbance, as explained above.

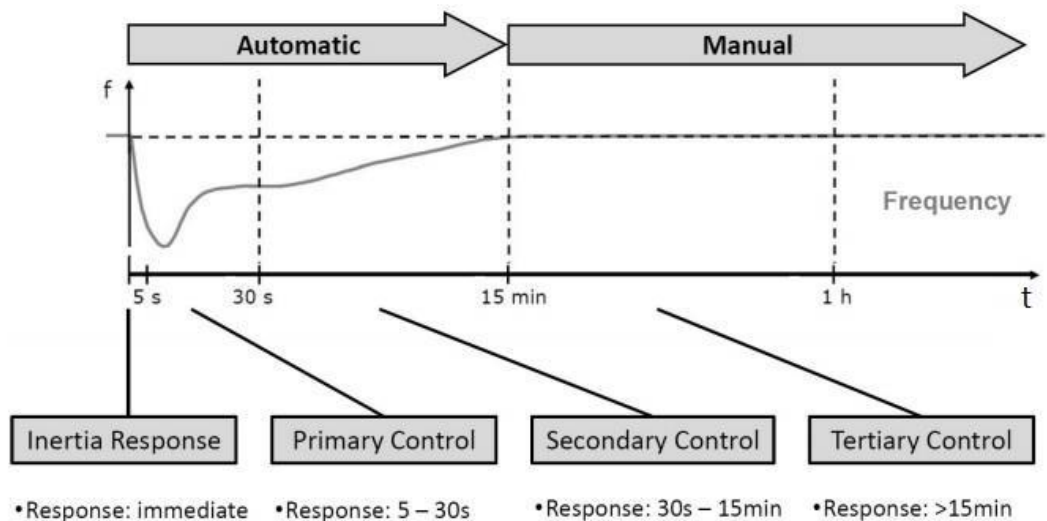


**Figure 2.9: The process of restoring system frequency (Wazeer et al., 2019)**

### 2.3.3 Frequency control system

When a bulk of the load is lost in the power system grid, there will be a power imbalance between the generator and load. The frequency will also change due to the power imbalance. The speed of the synchronous generator will increase. The governor is used to regulate the generator's speed in the conventional power system, which acts as the synchronous generator's central controller. The governor regulates the turbine's speed by varying the prime mover position and effectively regulating the output power of the synchronous generator. The governor is equipped with frequency dips regulation features and it should

maintain the output power deviation between 4-9% (Endegnanew & Uhlen, 2016).

In Table 2 below, the normal frequency is up to  $\Delta f_1$ , this type of power deviation that led to frequency changes is balanced by reducing these deviations through the governor's application. The governor performs the power system's primary control by regulating the generator's speed and the frequency is then normalized. If the frequency changes are more than  $\Delta f_1$  up to  $\Delta f_2$ , the secondary control, a load frequency control, must recover the system frequency to its normal operating condition and activate the automatic generation system to maintain the load demand. In the case of significant frequency deviations such as  $\Delta f_3$ , such a condition might result from a disturbance due to fault or load changes, then the tertiary control (protection scheme operation) must be activated. In such events, the protection devices such as the frequency relays may be activated and trip generators. This action will interrupt power system supply and cause strain to the power system. There must be proper coordination of control system and protection scheme ((Emad A Mohamed et al., 2018).

**Table 2.2: Frequency operation and control/protection actions** ((Emad A Mohamed et al., 2018)

Frequency Deviation	Condition	Control Action
$\Delta f_1$ (0.3Hz)	no contingency/load event	Primary control
$\Delta f_2$ (1<2 Hz)	generation/load event	secondary control
$\Delta f_3$ (>2Hz)	large difference event	Protection operation

The control process is configured in a hierarchical form. The primary control is concentrating on the power generated, system voltage, and current. The secondary control process ensures the power quality. The power quality entails frequency and voltage stability control. The third control process is tertiary, which focuses on the power flow, and these control processes are shown in Figure 2.10 below (Luna et al., 2016).

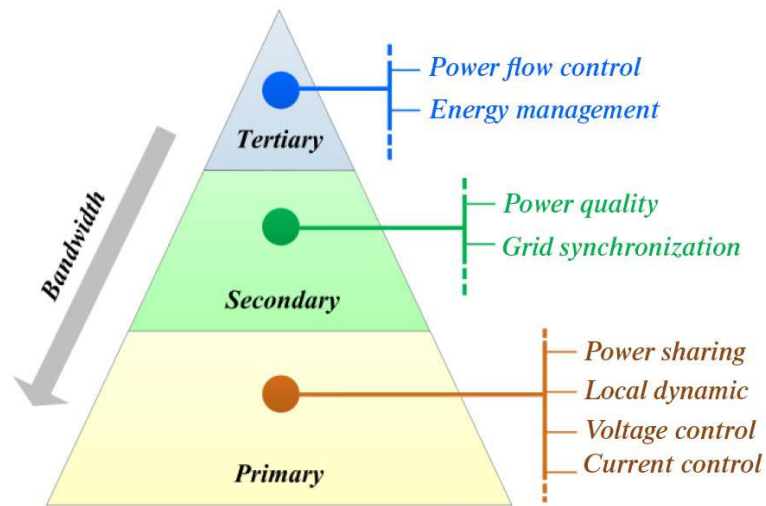


**Figure 2.10: Hierarchical control process** (Luna et al., 2016)

The frequency limit maintenance is graphically presented in Figure 2.11 below. The frequencies  $f_2$  to  $f_6$  form a dead band whereby the frequency deviation discussed in Table 2.2 is less than 0.3Hz. When the power system is subjected to a disturbance (load demand increased), the power deviation between load and generation will result in frequency deviation that might even be less 49.5Hz (droop 1), leading to power increase due to generator speeding up, droop controller will be activated to regulate the system changes. When the frequency deviates more than  $f_1$ , then the protection system should be triggered on Underfrequency Load Shedding (UFLS). The frequency band can be controlled in control, but under/over-frequency protection needs to occur beyond the control band. Figure 2.11 below illustrates the South African Distribution Grid Code requirement (NERSA, 2016).

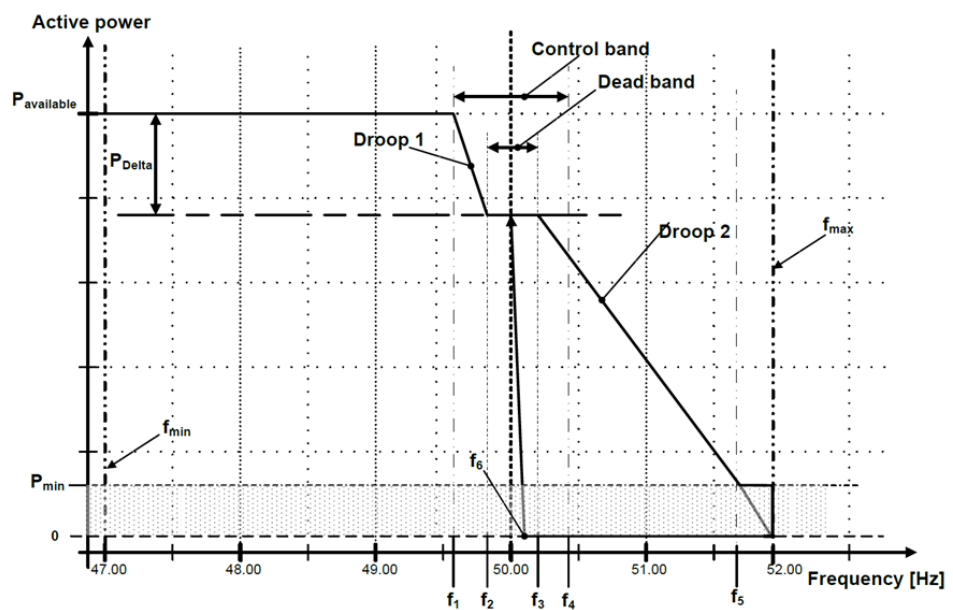


**Figure 2.11: Frequency control requirement** (NERSA, 2016)

Frequency control in the power system follows different stages. These control stages are time base as well as considering the severance of the disturbance. The frequency control stages are shown in the block diagram, as illustrated in Figure 2.12 below. These control stages include the primary, secondary, tertiary, and emergency frequency control.

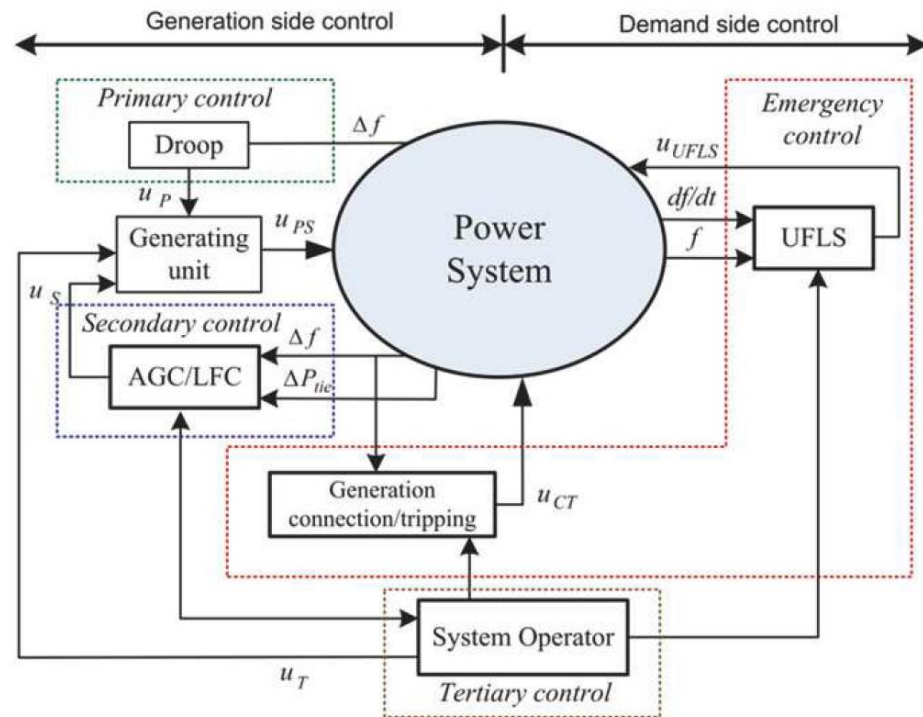


**Figure 2.12: Frequency control stages block diagram (Hassan Bevrani, 2014)**

The power system frequency is proportional to the synchronous generator's speed connected in the grid; therefore, the control of speed results in direct control of the system frequency. The frequency control function stages are elaborated below (Hassan Bevrani, 2014):

### 2.3.3.1 The primary frequency control system

The primary frequency control is the initial regulation process performed by the governing system on minor frequency deviations. The governing system mechanism measures the generator's speed and adjusts the inlet valve to set the mechanical power output based on load changes to restore the system frequency to its nominal value. The primary control is performed locally at the power station; therefore, no control signal is transmitted to the control center (Tomsovic et al., 2005).

### **2.3.3.2 Secondary frequency control**

When the system frequency deviations are severe, the secondary control is initiated, provided that there are enough spinning reserves. This function is also known as the load frequency control (LFC) and is performed by automatic generation control (AGC). The primary function of the AGC is to restore the system frequency while maintaining the power interchange between the interconnected areas. To maintain the system frequency and the power interchange during secondary control, an area control error is determined by measuring the system frequency with respect to the reference frequency and the network power interchange with respect to the scheduled power interchange. The error signal is fed to the proportional integrating controller (PI), which filters the error, and the control signal is sent to the generators participating in the secondary control. According to (Gjengedal, 2002), the AGC has to meet the following principles:

- To keep the frequency close to its nominal value
- To keep the power interchange close to its schedule value
- Run the generation units at their economic state.

The above requirements can be adequately achieved when there are enough generation reserves.

Secondary control is performed at the control center. The information is gathered using a remote terminal unit (RTU) which is locally based at the power station. Each power station has its dedicated RTU for information retrieval and transmission to the control center (Tomsovic et al., 2005).

### **2.3.3.3 Tertiary frequency control**

When the system frequency keeps on decaying while the secondary control is active, the tertiary control is initiated. This control action includes manually adjusting the dispatched power output of the generation units. This action also replaces the spinning reserves utilized in secondary control and consequently leads to power interchange adjustment as well (Schneider et al., 2019). The tertiary control is performed at the control center (Schneider et al., 2019) and (Tomsovic et al., 2005). The integration of generation units that can be online within 15min is performed. These generation are integration to the grid to provide stability when the secondary control fails. These generation units' connection is made based on market pricing merit order system (Machowski et al., 2008).

The rescheduling of the dispatched power on the generation can lead to overloading to the generation units. The overload can damage the generation,



also reducing its lifespan and efficiency. The economic scheduling can be compromised when the load keeps on increasing. When the generators are no longer able to supply active power demanded by the load after reschedule or operating at the maximum capacity, the emergency control is initiated.

#### **2.3.3.4 Emergency frequency control**

The emergency control is the last control function in power system stability, including the protection scheme's activation, such as under frequency load-shedding (UFLS). The frequency drop happens simultaneously as the system voltage drop. The UFLS configuration is made so that the load to be shed is categorized based on priority. This is implemented to avoid shedding critical loads such as hospitals and other essential services before other non-critical loads (Hassan Bevrani, 2014) and (Mnguni & Darcy, 2020).

When the power system operates at its emergency state, many risks of a complete collapse of the grid are very high. This operational state needs to be avoided. The power system operating in an emergency state can be avoided by considering the utilization of the distributed energy resources to enhance the power system stability.

Frequency protection is one of the power system tools to be used to protect the system to avoid instability or power system collapse due to disturbances that occur in the power system. The power system needs to be protected against over-frequency and under-frequency due to load changes. The frequency protection system does not become activated if the power system frequency is between 49.5-50.5Hz. If the frequency is beyond more than 50.5Hz due to power system disturbance, over-frequency protection needs to be activated and on the other side. If the system frequency is less than 49.5, then UFLS protection needs to be activated to shed the power system's load to maintain its normal operating normalize (Marchesan et al., 2016).

##### **2.3.3.4.1 The frequency protection system configuration**

The frequency protection's operational principle is that the frequency gets measured by the frequency relay, where an analog signal will be converted to a digital signal. The measured frequency is then compared against the over/under-frequency setpoint ( $f_{min} < f < f_{max}$ ). If the frequency is beyond the limits, the integrator will receive a time-discrete signal compared to the time set value. If the time-discrete signal is larger than the set value, the relay will initiate a trip signal to open the breaker. The frequency relay settings should conform with the tertiary

control limits, whereby the protection will only activate when the frequency deviates from 49Hz and below and deviates from 51Hz and above. Figure 2.13 below shows the over/under-frequency relays configuration (E. A. Mohamed et al., 2018).

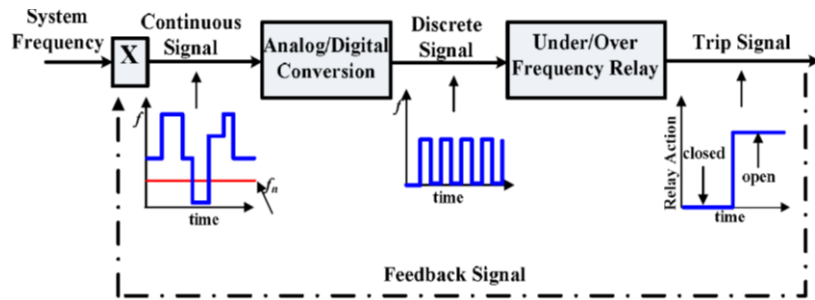


**Figure 2.13: Operation of over/under-frequency relays** (Mohamed et al., 2018)

How the over/under-frequency protection relays functions are explained using the flowchart diagram in Figure 2.14 developed by (Magdy et al., 2019) and (Mohamed et al., 2018).

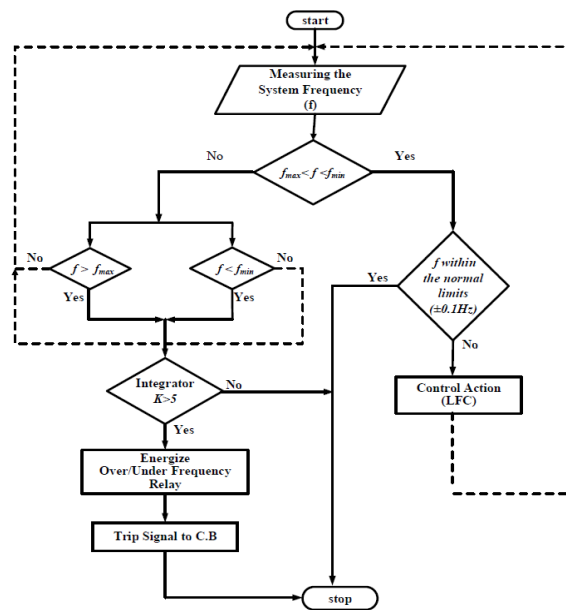


**Figure 2.14: Frequency control and protection coordination algorithm** (Mohamed et al., 2018)

However, the logic diagram that supports the functionality of these digital relays is shown in Figure 2.15 below. To answer when the relay should operate, it depends on the relay's predefined settings. The logic diagram show below is necessary, and it is shown to highlight the functionality of the frequency relays. In this case, there are distributed generators present in the power system. The frequency is measured about the angular speed of

the generator. Considering over-frequency protection, if the signal is more than the predefined setting and the terminal voltage is more than the preset minimum voltage, the relay will send a trip signal to open the breaker. In an event whereby the frequency is also less than the predefined under-frequency setting, and the terminal voltage is more than the minimum set voltage, again, the trip signal will be initiated by the relay to open the breaker. This operation is presented in Figure 2.15 below (Vieira et al., 2008).

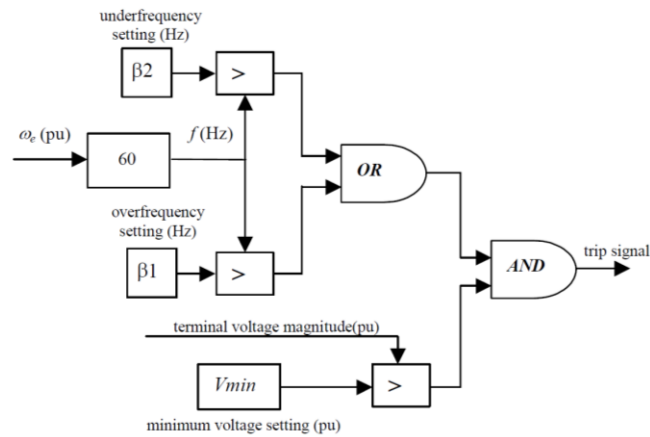


**Figure 2.15: Under/over frequency relay logic diagram** (Vieira et al., 2008)

### 2.3.4 The integration of distributed energy resource for frequency control systems

Integrating the distributed energy resources such as wind power plants and solar energy systems in the conventional power system is concerning due to their short time constant. These distributed energy resources are heavily dependent on intermittent resources such as wind and the sun. The varying wind and sun can lead to the protection scheme's activation and isolate some loads from the grid (Hassan Bevrani, 2014).

The integration of a wind power plan in an existing automatic generation control was explored by (Daniela et al., 2014). This approach was developed by (Gjengedal, 2002). To properly coordinate the wind power plant to secondary control, the active power produced by individual wind turbine generators should be summated together. Determining the total average active power produced by the wind turbine generator helps to smooth the total output power variations as indicated by (Gjengedal, 2002). Proper coordination of the wind power plant's control scheme can reduce the risks of causing more frequency variations (Hassan Bevrani, 2014).

When the microgrid's control and protection system are integrated together, the orientation of the over/under-frequency relay plays an important role. The frequency control system for wind and solar PV is presented, including the frequency protection system. It is also recommended that the coordination of such a system needs to be adequately applied. When the system is subjected to disturbance resulting in high-frequency deviations that a load frequency control cannot regulate, then protection needs to be activated. The isolation of a distributed generator needs to be coordinated in such a way that it starts from the generator that produces the least power (Mohamed et al., 2018).

In Figure 2.16, the power that is generated through a thermal power plant and the renewable energy resources is delivered to a common bus-bar where these resources are connected together, including the connection to the load. When the load demand changes, the power system frequency will also change. The system's primary control is configured as a closed-loop system whereby the generation system's output signal is feedback for accurate control and regulation input. If the primary and secondary control loops cannot regulate or normalize the frequency deviation and the system, the integrator is high, and a tertiary control loop will be triggered to send a trip signal to isolate the energy resource or the load that is contributing to the frequency deviation. The power system will maintain its stability (Magdy et al., 2019).

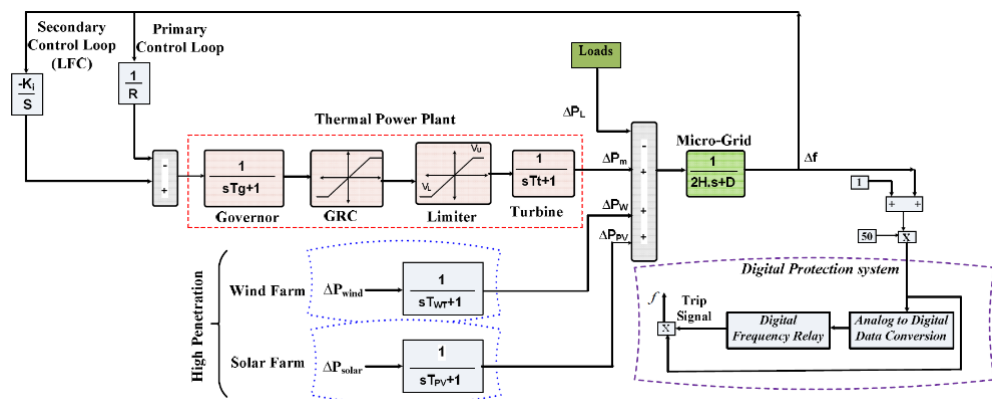


**Figure 2.16: Consolidated frequency control and protection integrated diagram (E. A. Mohamed et al., 2018)**

The communication between the power station and the control center is very crucial. This the communication that enables sends control data from the power station the AGC orientated at the control center. The control signal from the AGC to the generation units participating in secondary is also transmitted through the same communication system. The configuration of this communication is eblorated below under communication systems

### 2.3.5 Communication system

A remote terminal unit is used as the communication system based at each power station in the conventional system. Its function is to ensure communication between the power station and the control center is established. The Supervisory control And Data Acquisition (SCADA) system makes it possible to view the power system's state through a sophisticated management system. The image shown in Figure 2.17 below is the typical SCADA system configuration. This is the image that is used by the power system control and transmission system operators. The SCADA system communicates directly with the RTU orientated locally at the power station, as shown in Figure 2.17 below (Tomsovic et al., 2005).

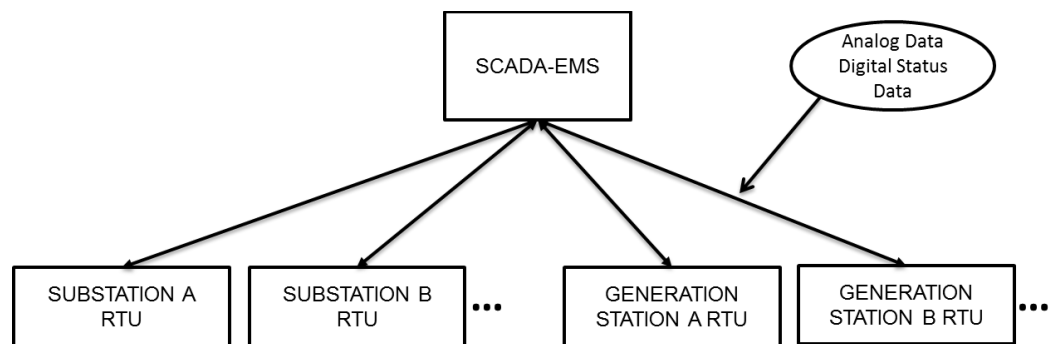


**Figure 2.17: The conventional SCADA system communication to RTU (Tomsovic et al., 2005)**

The information from the power station to the control center is typically gathered sequentially between 2-10s. The information is being updated between 2-10s as the communication will keep on polling. The fastest communication time would be between 2-4s (Tomsovic et al., 2005). The integration of distributed in this system with this communication setup could be problematic. The detection of the generation system state could delay. These energy resources react rapidly to changing conditions.

The SCADA system between the intelligent electronic devices (IEDs) and the remote terminal unit (RTU) to the control center uses Modbus or DNP 3.0. However, the information exchange and the interoperability between those protocols and the different vendors was impossible (Gu et al., 2019). Therefore when considering the integration of distributed energy resources, the communication system needed to be improved to cater to the fast-changing resources. This resulted in developing an IEC 61850 communication standard that addresses all the communication issues addressed above (Gu et al., 2019).

### **2.3.5.1 Application of the IEC 61850 standard**

An IEC 61850 is a communication standard that was developed for automated substations. Automation in power systems is the ability to acquire data and the capability to control the power system remotely. IEC 61850 standards allow the communication of substation intelligent electronic devices to be unique irrespective of the manufacturer to minimize the complexity and improve operating time and maintenance (Ustun et al., 2011).

Throughout the development of this communication standard, the issue of interoperability and control and monitoring of DERs were addressed through the extended focus of the standard; IEC 61850-7-420 was developed, which addresses these concerns (Ozansoy, 2016).

### **2.3.5.2 Requirements for standard implementation**

Implementing the IEC 61850-7-420 standard to support the integration of DERs requires a clear control hierarchy to be defined to control voltage, minimize the losses, support protection power balancing between the load and the generation. This control system will improve the system's operation integrated with DERs under the normal operating condition and when the system is disturbed. It must support the DER paramount protection function such as overcurrent, voltage, and frequency protection. Modeling of the power system with DERs integrated, the principle and models needs to follow, the abstract communication service interface (ACSI), standard data classes (CDC), and logical nodes classes (LN and data classes) needs to be defined. Notably, the modeling hierarchy such as the first level (ACSI), the second level (CDC), and the third level (LN and the Data classes) (Apostolov, 2009).

The DER system modeling in Figure 2.18 is the guide for the modeling and implementing IEC 61850-7-420. The protection devices (IEDs) that support IEC 61850 standard based are pre-programmed with these logical nodes. In Figure 2.18 below, the logical nodes with blue text represent IEC 61850-7-4, while the red text represents the new logical nodes developed in IEC 61850-7-420 (Ustun et al., 2011).

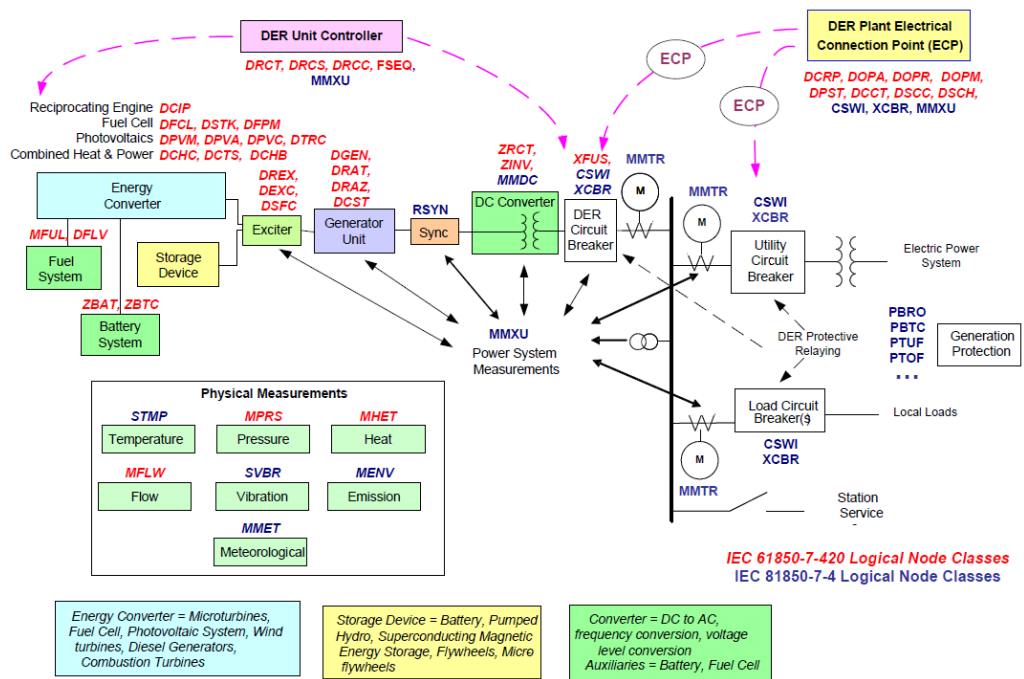


**Figure 2.18: Generic IEC 61850 DERs application architecture** (Ustun et al., 2011)

The DER control unit's logical nodes provide the information to the control unit of the DER. The DER controller characteristic (DRCT) governs the number of connected DERs in the power system grid. DER control status (DRCS) ensures that the information regarding the status of the controller is delivered. DER unit control actions (DRCC) is the supervisory control of DER for various remote operations. Sequencer (FSEQ) provides guidelines on the pattern to be followed when livening up of switching of the DER. The logical nodes for energy conversion differ at the generation, and they are based on a certain type of DER. The logical nodes predefined in IEC 61850 standard such as CSWI for switch controller while XCBR is for utility circuit breaker serve the function of power interruption by opening when there is a fault or planned maintenance MMTU is for current measurements (Ustun et al., 2011).

Table 2.3 below illustrates the power plant equipment's logical nodes and names as per the IEC 61850-7-420 standard.

**Table 2.3: Logical nodes description as per the IEC 61850 standard (Ustun et al., 2011)**

<b>Names</b>	<b>Logical nodes</b>	<b>Names</b>	<b>Logical nodes</b>
Circuit Breaker	XCBR	DER unit control actions	
Circuit switch	XSWI	Battery systems	ZBAT
Switch controller	CSWI	Meteorological conditions	MMET
Ground detector	PHIZ	Time overcurrent	PTOC
Overvoltage	PTOV	Thermal overload	PTTR
Measurement	MMXU	DC (Direct Current) measurement	MMDC
Metering	MMTR	Inverter	ZINV
Rectifier	ZRCT	Photovoltaic module characteristics	DVPM
Photovoltaic array controller	DPVC	Photovoltaic array characteristics	DPVA
Tracking controller	DTRC	Temperature measurements	STMP
DER controller characteristics	DRCT	Sequencer	FSEQ
DER controller status	DRCS	Battery charger	ZBTC
Synchronism-check	RSYN	Heat measured values Name	MHET

### 2.3.5.3 IEC 61850 standard benefits.

The IEC 61850 standard integrates different types of devices or vendors more accessible and compatible in communication. This standard also contributed to a common communication protocol such as DNP3 and other communication protocols whereby the IED devices can exchange the information and make use of the shared information in operation. There is improved communication between substation and master through the implementation of the IEC 61850 standard. The reduction in wiring and complexity of the protection schemes is made possible through the application effectiveness of the IEC 61850 standard, and it also results in reduced installation time, installation cost, and maintenance cost (Apostolov, 2009).



#### **2.3.5.4 The implementation of hardware-in-loop (RTDS)**

The DER integration to the power system grid needs to be evaluated and tested before an actual integration occurs. A test-bed needs to be developed using the simulation technologies available. RTDS technologies make it easy to assess the design of the control system for specific physical power equipment. It does not only assist in simulation but also validates the system design control and protection system. DERs can be modeled using power hardware in the loop, such as RTDS in the real-time base. The behavior of the protection system can also be assessed using the RTDS.

The RSCAD is a software of RTDS that allows the pictorial merging of an external interfaced system to be tested. In RSCAD, a draft module is used to map-up the system to be modeled, and already its library is equipped with various illustrative devices. When the system to be tested is compiled, there is a RunTime function of RSCAD software, leading to the software to communicate to the system through a workstation interface (WIF) card that is Ethernet processed. (Forsyth & Kuffel, 2007).

RTDS simulator can also be used to model and test an IEC 61850 standard-based control scheme for DERs and test the behavior of control and protection IEDs incorporated in the power system in the event of a stable and abnormal condition of the power system. The functionality of the protection relays can be tested in a similar fashion to the standard power system testing; this kind of test within RTDS is based on real-time scenarios (Forsyth & Kuffel, 2007) and (Kuffel et al., 2010).

### **2.4 Literature review of the existing papers for load frequency control.**

The conduction of the literature review is focusing on the work that has been done concerning load frequency control. The literature review conducted is based on the modern power system where renewable energy resources are utilized for the enhancement of system stability. Issues associated with the integration of distributed energy resources in the power system are also addressed. The control methodologies developed are also reviewed. Their strength, weakness, and limitations are also considered

#### **2.4.1 Findings from the existing literature**

A number of research projects have been conducted in regard to load frequency control. Different techniques are proposed for frequency control. (Umrao et al., 2012) reviewed the work that has been done around this topic, conventional and

intelligent techniques are reviewed. This work aimed to explore different techniques and strategies for load frequency control in assisting the researchers for future work in load frequency control. (Umrao et al., 2012)

Several research types were conducted concerning the control and frequency protection of DERs connected to the grid. Some of the researches and developments are stipulated below.

(Kundur et al., 2004) address the need for power system stability classification. This helps to understand the behavior and the functionality of the power system. The definition and classification help to understand particular disturbances that might influence the operation of the power system. It also defined the remedial actions to be done to stabilize the power system grid when it was disturbed due to fault or load changes.

(Hassan Bevrani, 2014), and (Machowski et al., 2008) highlight the power system control overview. The control overview highlights the rotor angle control, voltage control as well as frequency control loops. As the study focuses on the implementation of distributed energy resources to improve the power system stability, (H Bevrani, 2014) also highlights the frequency control strategy starting from primary control, secondary control, tertiary control, and emergency frequency control.

(Daniela et al., 2014) and (Gjengedal, 2002) illustrates how a large-scale wind power plant can be integrated into the conventional power system. The control block diagram on how its active power can be control and integrated into the automatic generation control loop was also developed. (Daniela et al., 2014) illustrated the simulation results to indicate the power system's response when the wind power plant was integrated.

(Ghafouri et al., 2015) investigate the impact of the high penetration rate of DERs on the power system frequency. Synchronous generator dominates the conventional power system grid, and when the system is disturbed, there will be frequency fluctuation which might result in complete grid collapse. The possible methods to control the frequency of the DERs were also developed and assessed. The simulation results show that when the DERs have a proper control system implemented, the power system's frequency stability can be maintained.

(Liu et al., 2017) developed a frequency control system for wind turbine generation as well as for the PV system. The development of these control systems is to deal with the low inertia of the DER, especially the PV system and

the governor. An implementation guideline of this control system is also included to integrate DERs in the enormous power system.

(Darussalam & Garniwa, 2019) Investigate the impact of varying power generated through the PV system on the grid code requirements' frequency. The impact is assessed using Matlab simulation for different values load levels at constant power. PV system operates in isolation of a storage system. The results show that if the PV's power is integrated into the system at 20% of the peak, the frequency can deviate to 48Hz.

(Wazeer et al., 2019) developed a proportional integrator-based controller to ensure frequency stability when the power system is subjected to a disturbance. The PID controller was found to have improved the frequency deviations. The conventional generator emulation system was also developed to deal with frequency deviation around the conventional generation system. The functionality of the developed systems was tested using Matlab/Simulink.

(Duymaz et al., 2018) Design an emulation system for the power plant to deal with the frequency instabilities. Different energy resources were integrated in order to assess the power system properties due to its dynamic behavior. A plant simulator was developed in cooperation field excitor and speed governor with buck converter integrated to it. A test rig was also developed, and simulations were done using DlgSILENT. The frequency response was controlled through DlgSILENT. This study was motivated by the high penetration of renewable energies, and power system frequency was improved.

(Mohamed et al., 2018) developed a coordinated control and frequency protection for over/under frequency protection. The analysis was made based on a micro-grid. The control and protection system was assessed in different scenarios, such as load changes and a high DER integration rate. The microgrid was investigated using MATLAB simulation. The results showed that the frequency stability was maintained, and the protection coordination also functioned as expected.

(Ozansoy, 2016) demonstrates how the protection system of the DER integrated to power system can be modeled. This development of the protection is following the implementation of an IEC 61850-7-420 standard.

(Apostolov, 2009) Demonstrated the modeling and configuration of DER based on the IEC 61850 standard. The description of logical nodes of the modeled system is also included.

(NERSA, 2010) outlines the power system grid requirements in South Africa. These requirements are there to ensure a smooth operation of the power system also to ensure the supply security to the end-users. (NERSA, 2016) outlines the grid requirement for the integration of the renewable energy resources. The aim of regulating the integration of the renewable energy resources is to ensure that the power system is safeguarded from any possible disturbances due to the integration of those energy resources. The acceptable tolerance or operating range for for voltage and frequency are outlined.

A summary of the reviewed paper pertaining to frequency control in power system are outlines in Table 2.4 below. The aim of the paper and the methods used are also covered.

**Table 2.4: Review overview of the power system frequency control.**

<b>Paper author and year</b>	<b>The aim of the paper/chapter</b>	<b>Method of the control strategy</b>	<b>The structure of the system considered</b>	<b>Used hardware/s software</b>	<b>Advantages / Drawbacks</b>	<b>Achievements</b>
(Kundur et al., 2004)	The power system stability definition, as well as its classification, are fundamentally outlined	None	None	None	The defined power system stability phenomena were not proven through a simulation platform. The defined disturbance classes need to be validated for the associated phenomena	The theoretical definition and classification of the power system stability phenomena were established. This enables the power system researchers to adequately analyze the types of disturbance during fault analysis practices critically.
(Gjengedal, 2002)	Discusses the implementation of the control scheme of automatic generation control in power system integrated with wind power farms	Conventional automatic generation control	Not defined	None	No simulations were conducted to prove the AGC's effectiveness in the presence of Wind Farms integrated into the power grid. The control logic to the wind farm control system is not defined.	The control scheme is defined and discussed.
(Machowski et al., 2008)	The frequency stability and control are discussed in chapter 9 of the book section. The theoretical fundamentals are considered and discussed.	The PI control strategy is adopted and discussed.	None	Not defined	The simulation to prove the working principle of the control system using different hardware or software is not defined. The theoretical analysis does not consider the integration of renewable energy systems.	The theory in applying the frequency control principle has been discussed. The theory discussed is starting from the primary to emergency frequency control.
(Hassan Bevrani, 2014)	Chapter 2 and 3 outline s the active power and frequency control and detailing the control concepts and definitions. Frequency control loops from primary, secondary, tertiary, and emergency control are discussed below.	The PI control strategy is adopted and discussed.	Three-control area power system	Not defined	The conventional AGC through active power control is utilized. The integration of the variability of the renewable energy system is not included in the control strategy.	The conventional frequency control strategies are defined.

Paper author and year	The aim of the paper/chapter	Method of the control strategy	The structure of the system considered	Used hardware/s software	Advantages / Drawbacks	Achievements
(Daniela et al., 2014)	The coordinated control strategy for AGC between the combined heat and power plants (CHPs) and wind power plants (WPPs) is proposed.	The PI control strategy is adopted and discussed.	Danish power system.	Power factory DigSILENT	The modeling and simulation have been performed on the software tool. The real-time validation is lacking.	The coordinated AGC control scheme considering the integration of WPPs was developed. Its effectiveness was tested using DigSILENT simulation software.
(Ghafouri et al., 2015)	The DER's high penetration impact on load frequency control is assessed, and the control strategy has been proposed.	Fuzzy logic control has been proposed for decentralized control implementation. This fuzzy logic is based on the neural network, and it is considered as Adaptive Network Fuzzy Inference System (ANFIS)	IEEE 34-Bus microgrid	PSCAD/MTdc software was used for simulation.	The developed ANFIS scheme was compared with the existing centralized and decentralized controller. It has been noted that its inertial response is low compared to the two other controllers.	The frequency stability point is reached quicker than the conventional controllers (centralized and decentralized controllers)
(Liu et al., 2017)	The frequency control of wind and PV system in the US Eastern and Texas interconnection network was studied to simplify the control approach	The active power control scheme for both wind and PV systems is used.	US Eastern and Texas interconnection network	Not specified	The penetration rate of renewable energy resources was assessed under three different rates (20%, 40%, and 60%). The higher the penetration rate, the lower the inertial response becomes.	The emulated governing and inertial response allow the wind and PV system to be flexible and responsive to power system dynamics.
(Darussalam & Garniwa, 2019)	The impact of photovoltaic fluctuations on the power system frequency is investigated	No control system proposed	20kV distribution grid	Matlab/Simulink	The assessment is done purely on the PV system integrated into the grid. There is no storage system. This was done to study the effects of irradiation on the power system frequency stability.	If there is no control and storage system in the power system where PV is integrated, the power system stability can be experienced quicker.

Paper author and year	The aim of the paper/chapter	Method of the control strategy	The structure of the system considered	Used hardware/s software	Advantages / Drawbacks	Achievements
(Wazeer et al., 2019)	A proper controller to support short-term frequency stability is investigated considering the penetration of the wind power plants to the grid.	PI, PID, and non-linear PID controller are used	No specified	MATLAB/SI MULINK is used	The PID has the shortest settling time. The NLPID has the shortest rising time, and the PID has a slight overshoot difference.	The penetration of wind power plants has a massive impact on frequency stability. The recommendation made is that the wind power plant should be integrated with the energy storage system.
(Duymaz et al., 2018)	Development of a test bench for power system studies to assess the response of an inertial emulator in the power system frequency.	PI regulator	A small circuit which consists of an AC synchronous generator, a DC motor, and a flywheel	DlgSILENT power factory	It is simple and low-cost for experimental learning.	The developed model emulates the similar dynamics of the power system. The experimental results in comparison with DlgSILENT simulation results show a similar response.
(Mohamed et al., 2018)	Developed a coordinated control scheme for load frequency control with under/over frequency protection relay.	Digital coordination of load frequency control and under/over frequency protection system.	Microgrid consist of WTG, solar PV, thermal generator, two bus bars, and a single load	MATLAB/Simulink	The modeled over/under frequency relay has improved the system stability due to its accuracy and quick response to disturbances.	Implementing the developed over/under frequency protection relay has improved the power system security and stability.
(Ozansoy, 2016)	Design of an IEC 61850-7-420 standard based adaptive protection system for distributed energy resources in Microgrids	Adaptive overcurrent protection scheme	22kV Medium voltage and 415V low voltage distribution system.	MATLAB/Simulink	The proposed control scheme was not tested; therefore, it lacks evidence of its operation	The concept is under construction. The author seeks to develop a windows based simulation. The IEC 61850-7-420 concept has been analyzed.
(Apostolov, 2009)	Describes the IEC 61850 modeling hierarchy considering the penetration of the distributed energy resources and the new logical nodes.	Not applicable	Not specified	None	The modeling hierarchy is described, which will help in industrial applications.	The description is made such that an applicator understands the logical devices and respective logical nodes in terms of the IEC 61850 standard.

Paper author and year	The aim of the paper/chapter	Method of the control strategy	The structure of the system considered	Used hardware/s software	Advantages / Drawbacks	Achievements
(Li et al., 2020)	Development of the continuous under frequency load-shedding (UFLS) scheme based on frequency deviation	Under frequency load shedding scheme	39-bus New England model	Not specified	The continuous load-shedding scheme helps to shed a specific load due to its control techniques.	The proposed scheme shed the frequency deviation. It is also adaptive to the power imbalance between the generation and the load demand. This becomes an advantage over the traditional UFLS scheme.
(Ding et al., 2020)	The load control scheme developed is aimed at providing reserve generation capacity through regulating the active power consumption	Load control scheme	East China Power Grid	Real-time digital simulator (RTDS)	The load control scheme is seen to be better than the emergency control scheme (UFLS) in cutting the load to stabilize the system to avoid possibly blackouts.	The proposed scheme seems to be effective in the improvement of the system frequency stability.
(Obaid et al., 2019)	The impacts of the current frequency control methods on the demand side in future power system grids with integration of DERs is reviewed.	Great Britain frequency control model with additional control loops considering the integration of distributed energy resources (DERs)	Great Britain power system and the 14-machine South-East Australian power system	MATLAB PowerSim	The inertial response and frequency nadir are supported by h integration of the DERs.	The integration of the large battery energy storage system (BESS) as the type of DER was seen to have improved the frequency response following a large disturbance.
(Yang-Wu et al., 2019)	Development of the load frequency control based on wind power forecast using Kalman filtering algorithm	PID controller and wind power forecast module	Four area interconnected power system	MATLAB/ Simulink,	The propose control scheme using the Khalma algorithm compensates phase lag through its inverted signal to deal with the frequency fluctuation due to the integrated wind power plant, consequently affecting the system frequency.	The result obtained from MATLAB indicates that the proposed control strategy is effective.
(Kumar & Anwar, 2019)	The fractional order proportion-integral-derivative controller (FOPID) organised in a parallel control structure is proposed for power system frequency control.	Fractional order proportional-integral-derivative controller.	Single area power system, and a two area power system	Not specified	The proposed scheme's settling time is quicker than Anwar and Pan,Tan, and Saxena and Hote strategies.	The proposed control scheme improved the the frequency nadir.



Paper author and year	The aim of the paper/chapter	Method of the control strategy	The structure of the system considered	Used hardware/s software	Advantages / Drawbacks	Achievements
(Ortega & Milano, 2018)	Investigation of the contribution of DERs integrated in distribution to transmission frequency regulation	Primary frequency controllers of DERs configured in centralised, decentralised and average	Modified Western System Coordinating Council (WSCC) 9-bus, 3-machine system where the load at bus 6 has been substituted with a 8-bus, 38 kV distribution system.	Not specified	The performance of the centralised control is seen to be better than other control strategies. The disadvantage of the centralised control over the other is its heavy dependence on communication.	The assessment of the control strategies performed highlight the effectiveness of the developed control strategies ranging from the one that outperforms to the least performing. The centralized control outperforms all the other strategies.
(Kumar & Anwar, 2019)	Determine the effect of tuning the two-degree-of-freedom internal model control (TDF-IMC) for the load frequency control in the power system stability	Two-degree-of-freedom internal model control (TDF-IMC)	Not specified	Not specified	The model order reduction scheme assessed includes Pade approximation, Routh and SOPDT. It was discovered that SOPDT can mitigate the b-parametric variation	It was discovered that, out of all the parameter tuning methods, SOPDT is the better performer as it responds quickly to disturbance and reduces the oscillations.
(Patel, 2017)	Development of an optimal PID controller with derivative filter (PIDF) to tune the controller of the automatic generation control	Hybrid differential evolution technique with particle swarm optimization algorithm are used	Three-area thermal system	MATLAB software	The differential evolution with particle swarm algorithm (DEPSO) was compared with bacteria foraging tuned conventional integral controller (BFO). The results show that the DEPSO improved the frequency control and its settling time is quicker than of BFO.	The proposed control scheme remains stable irrespective of the abnormalities applied.

Paper author and year	The aim of the paper/chapter	Method of the control strategy	The structure of the system considered	Used hardware/s software	Advantages / Drawbacks	Achievements
(Alhejji, 2017)	Proposed an adaptive load frequency control scheme to recover the system frequency to zero deviation	L <sub>1</sub> adaptive control technique	Not specified	MATLAB/Simulink.	The proposed scheme response was compared to linear quadratic regulator, and the results show that the proposed scheme regulates the frequency to its nominal state following a disturbance. While the LQR is brought to a new steady-state.	The proposed control scheme shows a convergence of the frequency to zero deviation following a system disturbance
(Umrao et al., 2012)	Review different load frequency control techniques and control strategies to assist researchers in future work were conducted.	None	None	None	Theoretical review with no simulations conducted to assess their effectiveness	Different LFC are theoretically reviewed
(El-Hawary & Ali, 2020)	Proposes augmented load frequency control for robust frequency regulation considering changing system parameters due to DERs integration	Augmented load frequency control (ALFC)	Five-area Great-Britain power system with	MATLAB Simulink	Software-based simulation. No practical implementation of the proposed control scheme.	Adaptability in changing system parameters. It has simplified system integration due to its flexibility. Frequency stability achieved.
(Nayak et al., 2019)	Proposes the utilization of PDF (1+PI) using a genetic algorithm to control micro-grid frequency. The control strategy is compared to PID and PI control algorithm.	Genetic algorithm	Two-area interconnected hybrid microgrid system	No specified	Assessment of the control scheme does not cover the interconnected grid system. It only focuses on islanded micro-grid.	The control settling time is improved compared to one of the PID and PI controllers.
(De Carne et al., 2018)	An intelligent transformer load power control to assist in primary frequency regulation in an interconnected power system with power electronics interfaced distributed energy resources was proposed.	Real-time frequency regulation.	Modified CIGRE European LV Distribution network	RTDS – RSCAD simulation software	The implementation can be costly.	The developed smart-transformer controller improved the frequency deviation. The voltage stability is also improved following a disturbance.

<b>Paper author and year</b>	<b>The aim of the paper/chapter</b>	<b>Method of the control strategy</b>	<b>The structure of the system considered</b>	<b>Used hardware/s software</b>	<b>Advantages / Drawbacks</b>	<b>Achievements</b>
(Zhang et al., 2020)	Proposed a fault-tolerant control scheme for the load frequency control in an interconnected power system	Integral based control algorithm	A three-area interconnected grid are presented	MATLAB Simulink	The setback to the developed control could be the communication between the power plant and the control scheme. A time delay could result in a dire instability situation	The observer-based fault-tolerant control scheme to track fault in the system was developed. The simulation indicates that the developed control scheme is quick in tracking the fault in the system.
(NERSA, 2010)	Outlines the South African Grid Code	None	None	None	The power system requirement as the grid code is outlined. This enables power system planners and system operators to understand to acceptable operating conditions of the power system.	The power system requirements are outlined. The compliance is enforced
(NERSA, 2016)	Outline grid connection code in South African Power system network for Renewable power.	None	None	None	The requirements for the grid integration of renewable energy sources are discussed. This includes the operating conditions of the Renewable energy resources and control stages.	Guide to the system operator and the independent power producers to be aware of the requirement and compliance to the grid code before integrating renewable energy resources can occur. This document also enforces the compliances.

## 2.5 Discussion

The literature review conducted on various system frequency control techniques is analyzed. The frequency control is performed to ensure that the power system remains stable when the system is subject to a disturbance. The proposed frequency control schemes developed by the previous researchers are mainly focusing on new strategies; there is little research work on improving the current implemented control techniques.

There are various methods of control power system frequency. The approach to these control strategies also differs. Three control stages are used in conventional power system frequency control: primary, secondary, and tertiary control. The primary control function is performed by the governing system of the synchronous generator to control the mechanical power based on the load demand. The secondary control is an additional control loop to the governing system; this function is known as automatic generation control (AGC). The supplementary control loop enables the governing system to optimally adjust its mechanical power based on the system frequency to meet the load demand. However, the power system is evolving, and various load types are integrated, and the load demand is increasing.

The heavy dependence on fossil fuel-based generation supply is still a concern on the environmental impacts. Considering the energy mix in South Africa, (Alan S & Hall, 2019) indicates that in 2018, 89% of the electrical energy was from fossil fuel. Electrical energy through fossil fuels is expected to decrease in order to reduce the impact on the environment. In order to meet the growing load demand, the integration of renewable energy resources is the only solution.

The growing interest in integrating renewable energy resources to enhance the power system stability comes with some concerns of instabilities. These renewable energy resources require an adequate control scheme that allows smooth integration.

Communication in the power system is also vital, and the proposed control schemes lack the implementation of the latest power system communication protocols such as the IEC 61850 standard protocol. This means that if these control strategies are remotely orientated, they need to be hardwired. For example, Eskom automatic generation control is centralized, and the controller at the load desk monitors it (Alan S & Hall, 2019). The primary role of the loading desk is to ensure that the frequency is monitored between 49.85Hz and 50.15Hz. If the frequency is high, then a generator trip will be initiated, and if the frequency

is low, then under-frequency load shedding will be implemented. Therefore, an advanced control scheme that will enable a smooth integration of the DERs and advanced control and communication system is needed.

## **2.6 Conclusion**

In this chapter, an overview of power system stability and phenomena that influences the stability was covered. A literature review on previous work covered by various researchers of power system frequency control is also included. The focus of the previous researcher was on developing new techniques in power system frequency control. The current control techniques still applicable, and they require an improvement such that the evolution of the power system to enable the integration of the renewable energy resources are addressed. The control scheme needs to be flexible to accommodate the current control system utilized in the power system.

This thesis focuses on developing a control scheme that will address power system frequency instabilities and enable a smooth integration of the renewable energy resource to assist the conventional generation in frequency regulation. This is also to assist the utilities to advance their control system, such as automatic generation control, which is currently implemented using programmable logic controls (PLC). These PLCs required many control cards and components for their implementation, and troubleshooting when there is a fault becomes difficult.

Chapter three covers the theoretical aspect of the power system frequency control. Various frequency control stages used in the power system are covered.

## CHAPTER THREE

### THE POWER SYSTEM OPERATION, CONTROL, AND PROTECTION ANALYSIS.

#### 3.1 Introduction

The power system grid comprises electrical components such as generators, transformers, power lines, circuit breakers, etc, which are interconnected to form a power system network. This power system is divided into three categories such as generation, transmission, and distribution system. The power system diagram illustrated in Figure 3.1 highlights the power system components which are integrated to form a network grid. The color codes within the diagram signifying the parts of the system, for example, generation is marked in brown, transmission in blue, and distribution in green

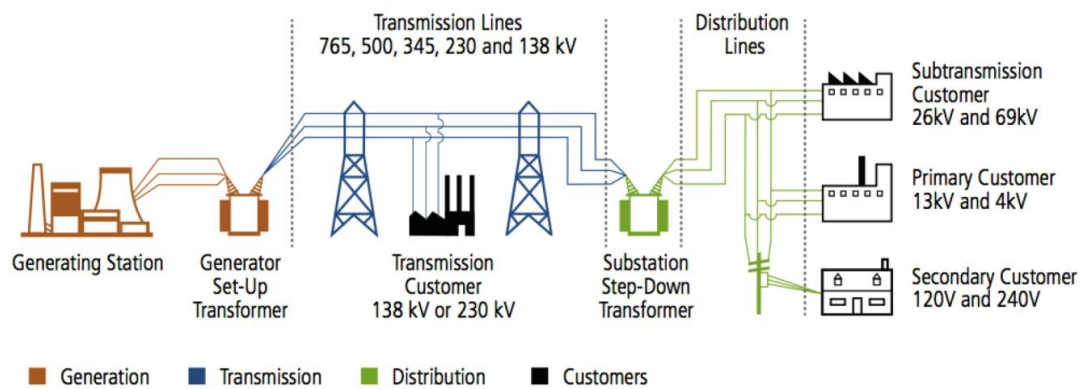


**Figure 3.1: Power system grid** (Bragantini, 2019)

The generation system's primary role is where the energy conversion from one form to another takes place, such as the conversion of mechanical power to electrical power. Transmission is responsible for power transportation from generation to distribution through high voltage transmission lines. The distribution level is where the electrical power is distributed to various loads such as industrial, residential, and commercial loads.

The power system is dynamically, hence one of its fundamental and critical characteristics is its flexibility in operation conditions due to the variability of the load demand. This characteristic is important so that the period in which the load demand can vary is predictable (Jan et al., 2005). The power system is expected to remain stable after it was subjected to a disturbance. Understanding the power system behavior is through analysis of its operation on steady-state and dynamic mode. To simplify the analysis, the three-phase power system is assumed to be balanced. This means the AC voltage magnitudes are equal and apart by  $120^\circ$ .

The is the same with three-phase currents, and the summation is equal to zero. The steady-state and dynamic power system model analysis is based on a balanced three-phase system(Venkatasubramanian & Tomsovic, 2005).

### **3.2 Steady-state modeling approach.**

In a steady-state the system is assumed to be stable, it can be before or after the disturbance. In a steady-state, the power generated is equal to the summation of power losses and load power demand, and the power system frequency is stable (In South African Grid  $f=50\text{Hz}$ ). The steady-state analysis deals with economic and reliability analysis which are critical in the power system. To analyze the system's steady-state operation, power flow analysis is performed to determine voltages and real and reactive powers in the system. This is the approach that is used for planning and operating the analysis of the network (Venkatasubramanian & Tomsovic, 2005).

Since the power system is categorized into three stages such as generation, transmission, and distribution. At each level, there are several components used to complete the system. On the generation side, synchronous generators are present, which are the main contributors to power generation. The transmission network consists of power transformers, transmission lines, cables, capacitors, reactors. Distribution networks also consist of power transformers, distribution lines, and a variety of loads, ranging from residential, commercial, and industrial loads. The residential loads can be lighting and heating loads, industrial and commercial loads can be machinery load such as induction motors, etc. It is these different types of components that influence the nature in which the power system operates. The modeling approach is to analyze these components individually (Venkatasubramanian & Tomsovic, 2005).

#### **3.2.1 Transformer modeling**

Transformers are widely used in the power system to step up or down the voltage to the desired level. The voltage conversion from low to a high level is used for power transmission at low current to minimize power losses in long transmission lines. This concept also improves the active power efficiency between generation and distribution area. At the distribution level, the voltage needs to be stepped down for electricity's economical and safe use. Another application of transformers is in instrumentation in more sensitive applications for isolating the electrical equipment from high voltages and current, as well as in real power flow control through changing phase shift (Venkatasubramanian & Tomsovic, 2005).

The transformer operates by linking the flux from the primary windings to the secondary windings through a core of ferromagnetic material. The windings are coiled around the ferromagnetic core as expressed in Figure 3.2 below. When the current  $I$  is injected into the primary windings, a magnetic field  $H$  will be generated and the magnetic flux  $\phi$  will flow in the core.

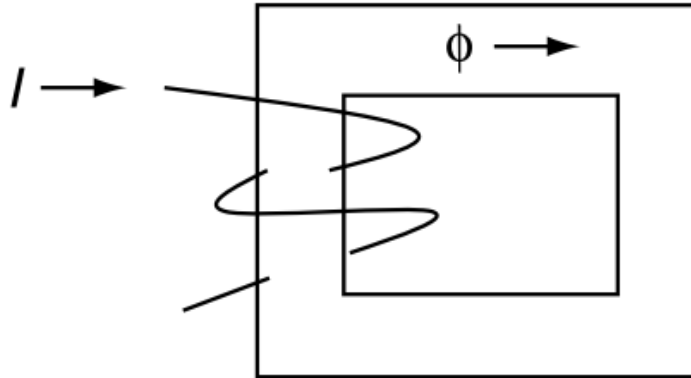


**Figure 3.2: Magnetic flux flowing through the core** (Venkatasubramanian & Tomsovic, 2005)

If the magnetic flux is constant throughout the core, then the product of the magnetic field  $H$  and the path length  $l$  will result in the generation of electromotive force (mmf) which is the product of current  $I$  and the number of turns  $N$  of the windings, as expressed in equation 3.1 below.

$$Hl = NI \quad 3.1$$

The relationship between the magnetic field and the magnetic flux is permeability. This relationship is expressed in equation 3.2, provided that the hysteresis and saturation effects are ignored. The flux  $\phi$  and flux density  $B$  are expressed.

$$\phi = \mu A \frac{NI}{l} \text{ and } B = \mu H = \mu \frac{NI}{l} \quad 3.2$$

In the above equation,  $A$  is the cross-sectional area of the core. The link between the flux flow and the electromotive force which is called Reluctance ( $R$ ) of the core, is expressed in equation 3.3 below

$$R\phi = NI \quad 3.3$$



The above expressions are based on the first set of windings which is the primary winding in the context of the transformer. When the secondary winding is introduced as illustrated in Figure 3.3 below, the magnetic induction linked the two currents. The primary and the secondary winding will notice the same magnetic flux, reluctance as well as electromotive force.

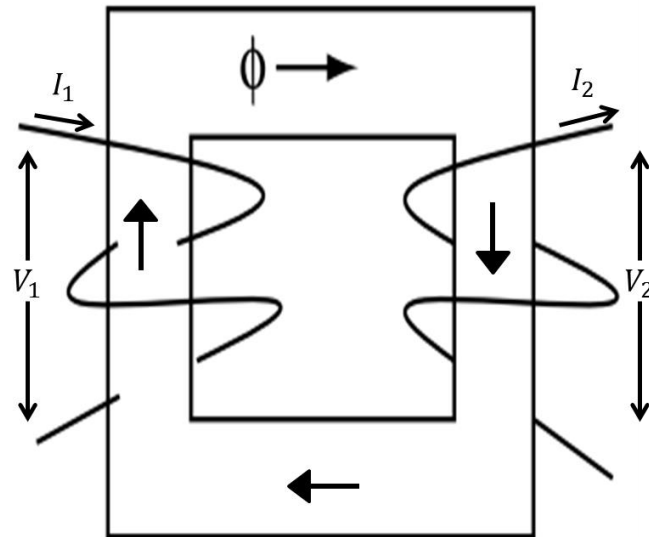


**Figure 3.3: Magnetic flux linkage (between primary and secondary windings)** (Venkatasubramanian & Tomsovic, 2005)

This relationship between the primary and the secondary windings of the transformer through the flux linkage is expressed in equation 3.4 below. Where  $N_1$  and  $I_1$  is the number of turns and current in the primary of the transformer while  $N_2$  and  $I_2$  is the number of turns and current on the secondary side of the transformer.

$$N_1 I_1 = N_2 I_2 \quad 3.4$$

According to faraday's law, when flux or current changes, then the voltage will be induced. Considering an ideal lossless transformer, the input power will be the same as the output power resulting in the formulation of equation 3.5 below where  $V_1$  and  $V_2$  is the primary and secondary voltage of the transformer.

$$V_1 I_1 = V_2 I_2 \quad 3.5$$

Equation 3.4 and 3.5 can be expressed in terms of the number of turns and the voltage as shown in equation 3.6 below.

$$\frac{V_2}{V_1} = \frac{N_2}{N_1}$$

In an ideal transformer as illustrated in Figure 3.3 above, the voltage gain is influenced by the turns ratio of the primary and secondary windings. In practice, transformers will have some effects such as eddy currents that might flow in the core, winding resistance, the permeability of the core, hysteresis, and magnetic saturation. These effects are presented as impedance configured in series and parallel as presented in Figure 3.4 below.

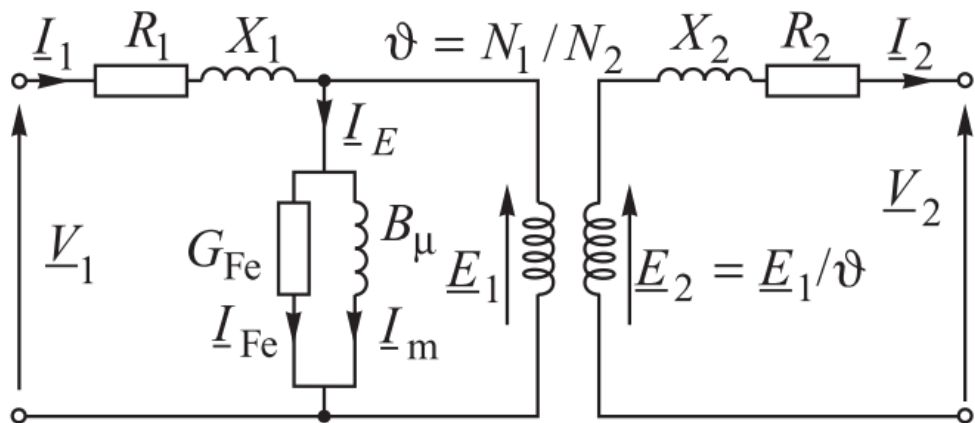


**Figure 3.4: Equivalent circuit of a two winding transformer**(Jan et al., 2005)

The series impedance in the transformer is due to the finite permeability inside the core, which causes the magnetic flux to flow even outside the core. This flux leakage creates a voltage drop across the terminals. The above diagram can be illustrated further as indicated in Figure 3.5 below whereby the secondary is presented concerning the primary side of the transformer.

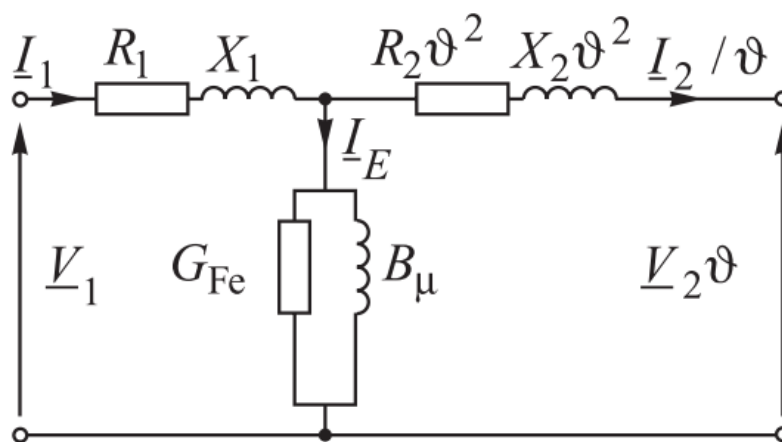


**Figure 3.5: Equivalent circuit with secondary and the primary** (Jan et al., 2005)

As for the shunt impedance, when the current flow in the windings of the transformer, the core will be magnetized and a magnetic flux will then flow in the core creating electromotive force (mmf). The difference between the primary and the secondary mmf is presented as the shunt inductances. The losses such as eddy currents and hysteresis can be modeled as a shunt resistor (G). The saturation can cause other losses in the transformers and create some harmonics in the voltage and current signal. In the steady-state analysis, the voltage and current components that are modeled are for 50Hz, hence the saturation effects are ignored.

The total primary and secondary impedances ( $Z_1$  and  $Z_2$ ) can be determined using equation 3.7.

$$\begin{aligned} Z_1 &= R_1 + jX_1 & 3.7 \\ Z_2 &= R_2\theta^2 + jX_2\theta^2 \end{aligned}$$

Total impedance is the summation of the primary and secondary impedances is presented in equation 3.8.

$$Z_T = R + jX \quad 3.8$$

To carry out calculation and computation of the transformer model, per unit system is used for simplicity. In the per-unit system, base quantities need to be established of which all the variables to be computed will be relative to the base values. The base value for current and impedance is determined in equation 3.9 and 3.10 below.

$$I_B = \frac{S_B}{V_B} \quad 3.9$$

$$Z_B = \frac{V_B}{I_B} = \frac{V_B^2}{S_B} \quad 3.10$$

The per-unit system is not only applied to the transformer modeling, but it is also applied throughout the network, where all the quantities need to be converted expressed to per-unit quantities. This conversion makes power flow and network faults calculation to be easy to calculate to avoid and minimize calculation errors.

### 3.2.2 Transmission line modeling

These are power lines used in the power system to transport electrical energy generation to distribution. The transmission line voltage varies from 138kV to 765kV. The power generation system is often located in an area where energy resources are available, for example, the coal power generation system is normally positioned next to coal mines. The use of transmission lines becomes vital to transport the larger power from the remote generation station to the local loads. This is done to maintain less power loss and operational costs (Jan et al., 2005).

One quality of the transmission is to have fewer losses in the process of electric power transportation. Configuration of the structure is designed to carry even two circuits in one structure. The electric conductors are stranded configured to meet the mechanical and electrical properties of the line. If the current that will flow on the line, then the conductors need to be bundle up. The other advantage of bundling the conductors is that the conductors can be easily cooled down unlike using a single conductor (Venkatasubramanian & Tomsovic, 2005). In Figure 3.6 below is the single circuit transmission line with the bundled conductor. The bundle conductor consists of four sub-conductors making one phase as indicated in the diagram.

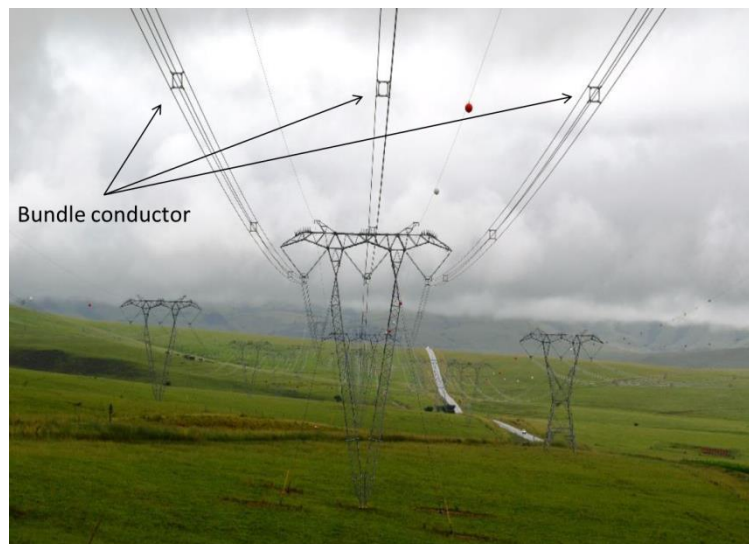


**Figure 3.6: Transmission line from Ingula Eskom Power Station** (Chris, 2020)

As the current flow in the conductor, a magnetic flow is developed and the voltage is induced on the adjacent line through mutual induction.

Transmission lines have distinctive parameters that determine their quality and properties.

- $r$  - series resistance per unit length ( $\Omega/\text{km}$ ) per phase
- $x = \omega L$  - series reactance per unit length ( $\Omega/\text{km}$ ) per phase and  $L$  is the series inductance per unit length ( $\text{H}/\text{km}$ ) per phase and  $\omega = 2\pi f$ , where  $f$  is the system frequency.
- $g$  - Shunt conductance per unit length ( $\text{S}/\text{km}$ ) per phase
- $b = \omega C$  - Shunt susceptance per unit length ( $\text{S}/\text{km}$ ) per phase and the  $C$  is the capacitance ( $\text{F}/\text{km}$ ) per phase

A single-phase representation of an equivalent circuit diagram of the transmission line with its parameters mentioned above is illustrated in Figure 3.7 below. The diagram is split into two sections such as the sending end and hence the parameter representation is seemed to be duplicated.

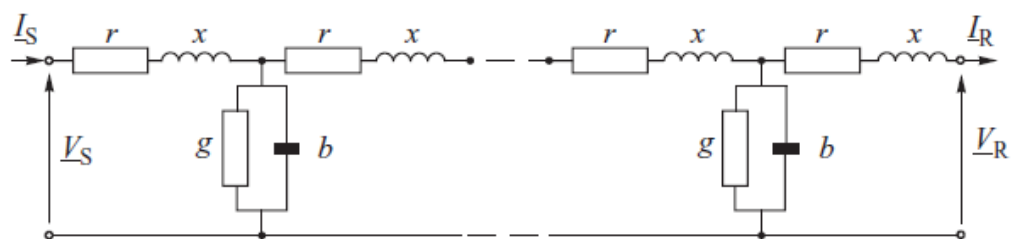


**Figure 3.7: Equivalent circuit for transmission line representation** (Jan et al., 2005)

From the diagram above, the series impedance ( $z$ ) and the shunt admittance ( $y$ ) can be determined as follows:  $z = r + jx$  and  $y = g + jb$ . The transmission line behavior is influenced by all the parameters that are specified on the equivalent circuit diagram above. When the current is flowing in the transmission line, power losses are incurred. The heating losses (series resistance  $r$ ) of the line depends on the type of the conductor used its diameter as well as its construction configuration. The flux linkage of the conductor influences the series inductance  $L$  of the line through cross-section and other fluxes of the nearby conductors. While the corona losses are caused by the shunt conductances  $g$  and the

leakage current on the insulators. The corona losses cannot be unique since the dirtiness of the insulator and the air humidity also plays their role influencing in increasing the magnitude of losses. The shunt conductance is normally neglected due to its small value. The potential difference between the line creates the shunt capacitance  $C$ . The charging and discharging of the shunt capacitance creating a line charging current which is caused by the alternating current voltage.

### 3.2.2.1 Transmission line equations formulation and nominal $\pi$ equivalent circuit representation.

The focus of the theory is on steady-state analysis, therefore only the variables of interest will be considered which is the voltage and the current. The formulation of the equations will be based on the equivalent circuit demonstrated in Figure 3.8 below. In the diagram the subscript R, S, and L represent the receiving end, sending end, and line.

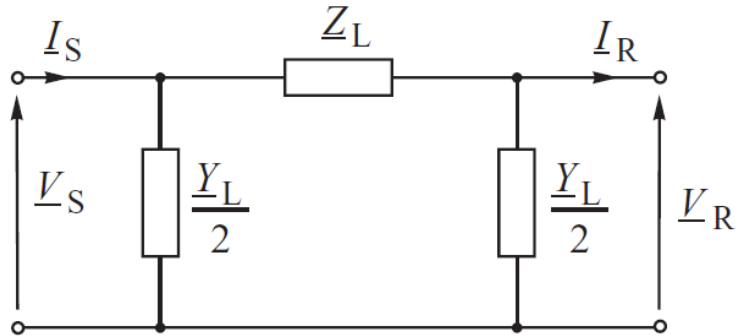


**Figure 3.8:** The transmission line nominal  $\pi$ -equivalent circuit (Jan et al., 2005)

To determine the voltages and current at both sending and receiving end, the equation is formed through the application of the two-by-two matrix as expressed below.

3.11

$$\begin{bmatrix} V_S \\ I_S \end{bmatrix} = \begin{bmatrix} A & B \\ C & D \end{bmatrix} \begin{bmatrix} V_R \\ I_R \end{bmatrix},$$

$$\begin{bmatrix} V_S \\ I_S \end{bmatrix} = \begin{bmatrix} \cosh \gamma l & Z_C \sinh \gamma l \\ \sinh \gamma l / Z_C & \cosh \gamma l \end{bmatrix} \begin{bmatrix} V_R \\ I_R \end{bmatrix}$$

The characteristic impedance of the line is  $Z_C = \sqrt{z/y}$ , the propagation constant is  $\gamma = \sqrt{zy}$ . The propagation constant and the impedance characteristics are both complex quantities, therefore the propagation constant is further expressed  $\gamma = \alpha + j\beta$  where  $\alpha$  is known as attenuation constant while  $\beta$  is the phase constant. ABCD in equation 3.2 is the four matrix elements that are linking the sending end and the receiving end. From the equation,  $A=D=\cosh \gamma l$ ,  $B=Z_C \sinh \gamma l$  and  $C= \sinh \gamma l / Z_C$ . The line impedance  $Z_L$  admittance  $Y_L$  can be determined as follows (Jan et al., 2005).

$$Z_L = Z \frac{\sinh(\gamma l)}{\gamma l}, Y_L = Y \frac{\tanh(\gamma l/2)}{\gamma l/2} \quad 3.12$$

$Z = zl$  is the series impedance of line per phase while  $Y = yl$  is the total shunt admittance of the per phase. For a medium-length line with a length between 80km to 200km, the parameters or the equivalent circuit can be equal to the parameters of the line.

$$Z_L = Z, \text{ and } Y_L = Y \quad 3.13$$

For a line length that is less than 80km, then the shunt admittance can be ignored, resulting in equation 3.5 below.

$$Z_L = Z, \text{ and } Y_L = 0 \quad 3.14$$

Transmission line structures can be configured to carry a single or double circuit. A single circuit consists of three powers line (red, white, and blue phase) while the double circuit consists of six power lines

### 3.2.3 Underground cables

The modeling of an underground cable system resembles the transmission line system modeling. The only difference can be the parameters. When it comes to the cable system, there is no specific type of construction, hence the parameters cable from one cable to another. For example, the shunt capacitance of the cable depends on the types of cable configuration whether the three-phase cable is single-core or 3 core. Another factor is that the per-unit-length series reactance of

an overhead line is two times the cable reactance. The cable charging current is time is exceeding the overhead line by more than 30 times (Jan et al., 2005).

### 3.2.4 Generator modeling

The term synchronous or alternating generator is given to a specific type of generator that is capable of converting mechanical energy into alternating current electrical energy. The operation principle of the synchronous generator is as follows: An exciting current (DC) is applied to the winding terminals of the rotor to produce a magnetic field. A primer mover turns the turbine which creating a rotating magnetic field of the rotor. This DC supply to create the magnetic field on the rotor wings can be through slip rings and brushes or through a unique design for DC power supply which would be mounted on the shaft of the rotor as indicated in Figure 3.9(a) below. A rotor is the large rotating electromagnetic inside the stator of the synchronous generator, as illustrated in Figure 3.9(b).

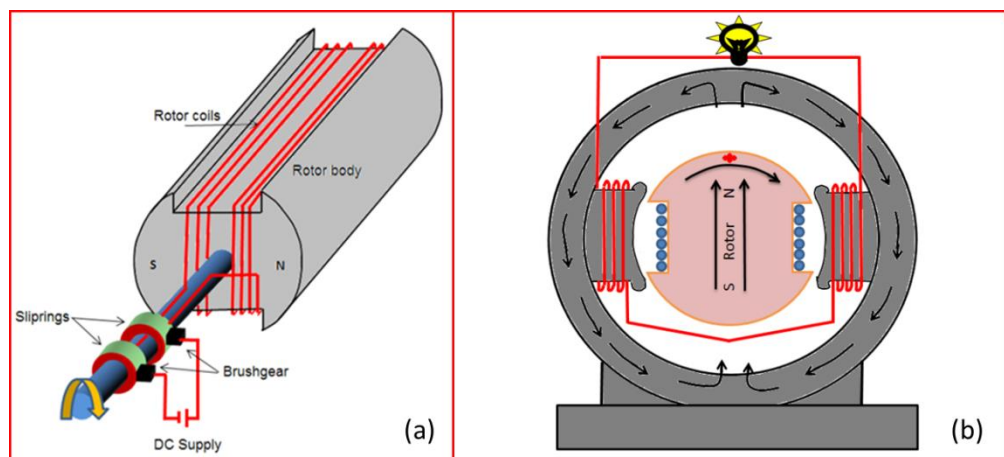


**Figure 3.9: The rotor of the generator with an electromagnetic coil**  
(Beukman et al., 2011)

The rotating magnetic field of the rotor induces three-phase voltages Red phase, B-White phase, and C-Blue phase in the stator windings, which are being displaced at  $120^\circ$  apart. Figure 3.10 below illustrates an ideal configuration of a synchronous generator. The rotor in the diagram is colored in blue, and the stator is the round grey part. The three phases are also indicated as three coils labeled as U1-U2, V1-V2, and W1-W2 which are phase to phase voltages (red, white, and blue phase). The developed 3-phase waveform is demonstrated on the left part of the diagram with a red, white, and blue wave.



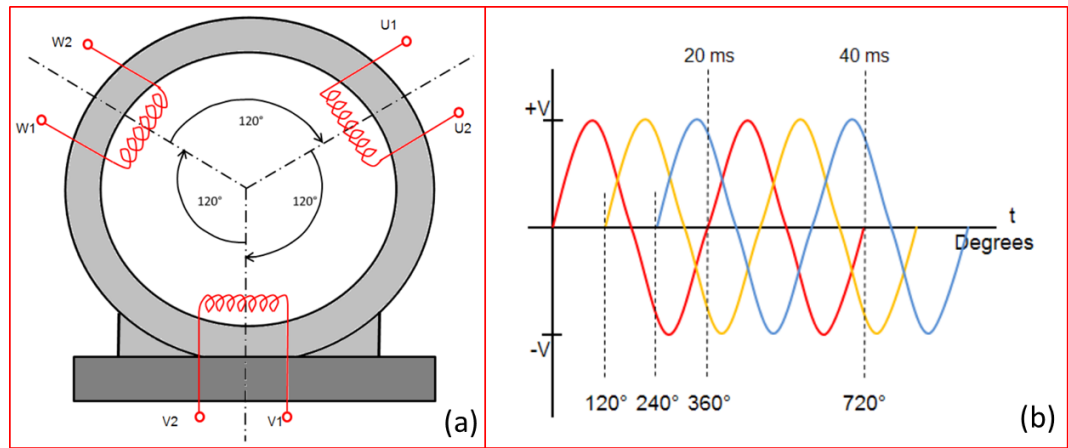


**Figure 3.10: Illustration of three-phase winding positions in the stator and sinusoidal waveforms of 50Hz three-phase system displaced at 120°**  
(Beukman et al., 2011)

There are two design configurations of the rotor, it can be salient or non-salient pole type. The difference between the salient pole rotor and the non-salient pole rotor is that it has teeth opening and it usually has two and, or four poles, unlike the non-salient which is just smooth on its surface. The poles for non-salient are usually more than four. Figure 3.11 below illustrates the two configurations of the rotor.

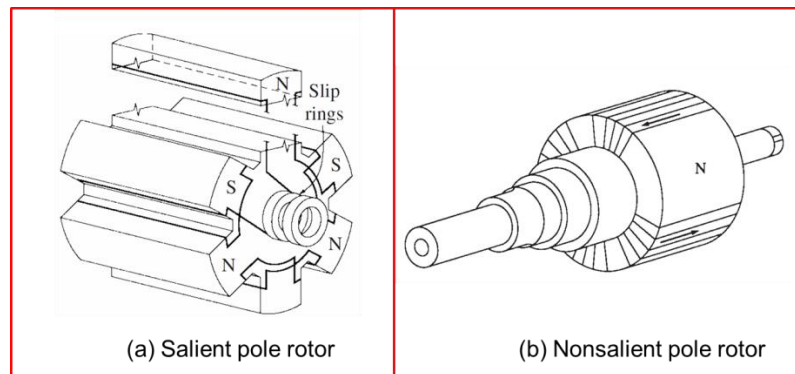


**Figure 3.11: Illustration of rotor configurations (a) Salient pole rotor, and (b) Nonsalient pole rotor** (Philip, 2004)

Magnetic flux is produced which changes as the rotor rotates, then the voltage is produced at the armature windings. The flux per phase is determined using equation 3.15 below

$$\lambda = K_f I_f \sin \theta_m \quad 3.15$$

In the above equation  $I_f$  is the field current,  $\theta_m$  is the rotor angle in respect to the armature, and  $K_f$  is the constant which depends on the generator properties as well as the number of windings.

The synchronous generator rotor can be two or four-pole. For example, the four pole machine is seen to be two times faster than a two-pole machine when observing on the armature side, this is due to the number of poles. The illustration of two and four pole rotor is illustrated in Figure 3.12 below.

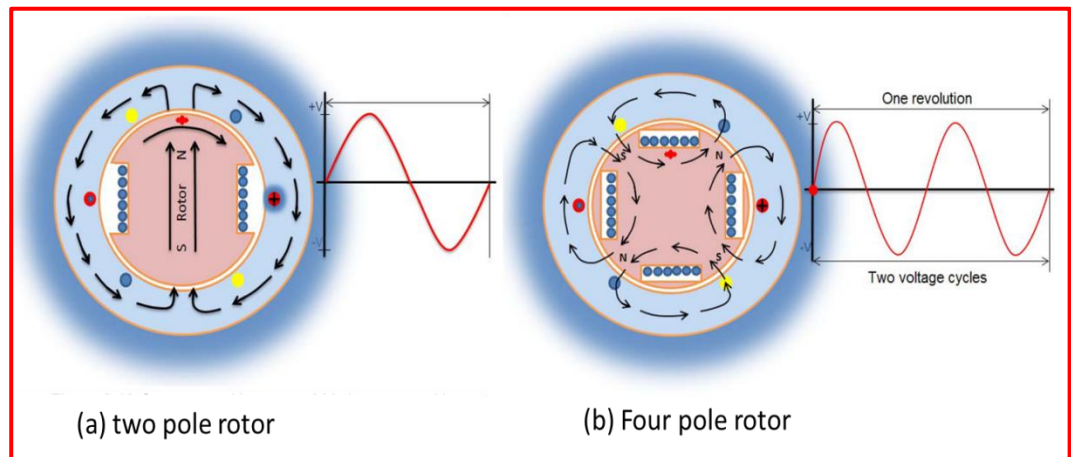


**Figure 3.12: (a) Difference between two and four-pole rotor. (a) Two-pole rotor, and (b) A four-pole rotor (Beukman et al., 2011)**

The other difference between the two types of rotor poles is the distribution of magnetic flux

To determine the frequency of the machine, equation 3.16 is used whereby  $\omega_m$  is the speed of the machine in radians,  $\omega_s$  is the synchronous frequency and  $p$  is the number of poles.

$$\omega_s = \omega_m \frac{p}{2} \quad 3.16$$

If the synchronous generator is rotating at a constant speed, the induced voltage of the armature winding terminals can be determine using equation 3.17 below which is following faraday's law.

$$V = \frac{d\lambda}{dt} = \omega_s K_f I_f \sin(\omega_s t + \theta_0) \quad 3.17$$

Consider the single line diagram illustrated in Figure 3.13 below, representing the synchronous generator and load model. As the load is connected to the armature windings, then a current will flow. This will result in the armature flux being linked with the magnetic field. This consequently leads to mechanical load on the rotor

and the power generated to be balanced with the load demand hence resulting in constant frequency

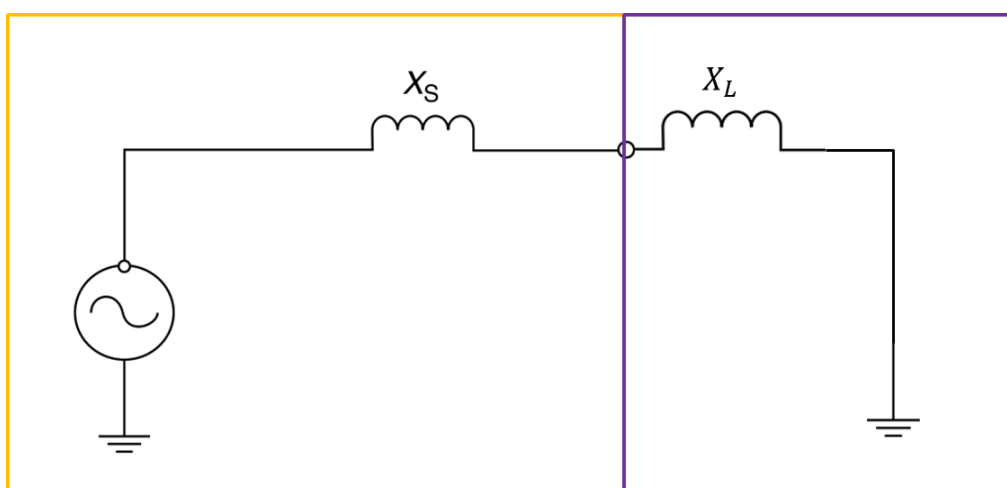


**Figure 3.13: Synchronous generator and load model** (Venkatasubramanian & Tomsovic, 2005).

.There will be some armature flux leaks that do not link with the field and power losses in the winding, which are ignored. The above single line model represents the synchronous generator in a steady state. Some generators are being operated at fixed voltage and constant power output, this results in the terminals to be referred to as PV bus(Venkatasubramanian & Tomsovic, 2005).

### 3.2.5 Power system load modeling

The definition of load in the large power system can be regarded as a portion of the power system that is generalized and that is treated as a single power-consuming device. The large power system analysis normally demonstrates generation, transmission, and sub-transmission system. The distribution systems are illustrated as equivalent loads or composite loads. The composite loads can represent a large portion of a low and medium voltage distribution system including power sources integrated at the distribution level (Munoz-Hernandez et al., 2013).

In steady-state, the bus voltage and the system frequency determine the response to the demand of the composite loads. Voltage and frequency are the function of real and reactive power  $P(V,f)$  and  $Q(V,f)$  and are characterized as a static load. Voltage is the function of real and reactive power  $P(V)$  and  $Q(V)$  when the frequency is kept constant and is known as voltage characteristic. When the voltage is kept constant, frequency becomes the function of active and reactive power  $P(f)$  and  $Q(f)$  called frequency characteristics. The slope of the

characteristics presented in Figure 3.14 below illustrates the voltage sensitivity of the load while the frequency sensitivity is also demonstrated in a similar fashion (Jan et al., 2005).

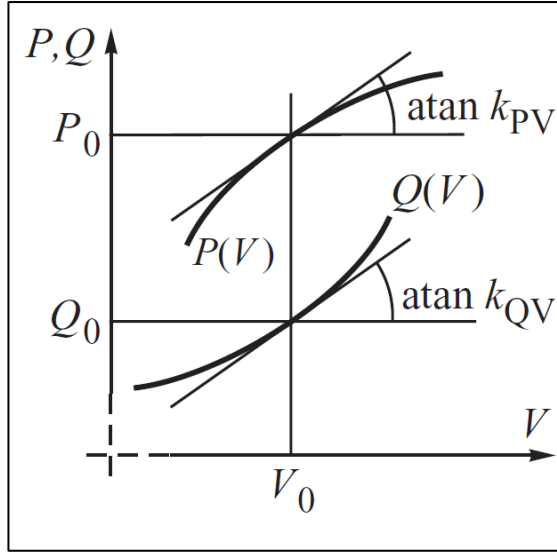


**Figure 3.14: Voltage sensitivity of the load** (Jan et al., 2005)

Equation 3.1 below demonstrates the process that determines the sensitivity of both frequency and voltage.

$$k_{PV} = \frac{\Delta P/P_0}{\Delta V/V_0}, k_{QV} = \frac{\Delta Q/Q_0}{\Delta V/V_0}, k_{Pf} = \frac{\Delta P/P_0}{\Delta f/f_0}, k_{Qf} = \frac{\Delta Q/Q_0}{\Delta f/f_0}, \quad 3.18$$

In the above equation,  $P_0$  is the real power,  $Q_0$  is the reactive power,  $V_0$  is the voltage and  $f_0$  is frequency are operation point at a given time.

The load can be regarded as stiff or entirely in an event where its voltage sensitivities are very small or equal to zero, and in that case, the load demand will not depend on the voltage. The load can be regarded as voltage-sensitive when its voltage sensitivities are significantly, and any slight deviation in voltage will result in high load demand deviations. In most cases  $k_{PV} < k_{QV}$ .

The behavior of the composite load is mostly dependant on each load type. It is therefore very crucial to analyze the behavior of each component.

### 3.2.5.1 Lighting and heating loads

The traditional light bulb is considered as resistive loads as they are not consuming any reactive power. The filament of these light bulbs depends on the voltage and cannot be treated as an ideal constant impedance. However, there is also another type called discharge lights, such as fluorescent, sodium vapor, and

mercury vapor. The discharge lights are voltage dependant and consume both real and reactive power. Figure 3.15 below illustrates the voltage characteristics of both types of lights. Conventional light bulbs are primarily used in residential areas, while discharge lights are used in industrial and commercial areas.

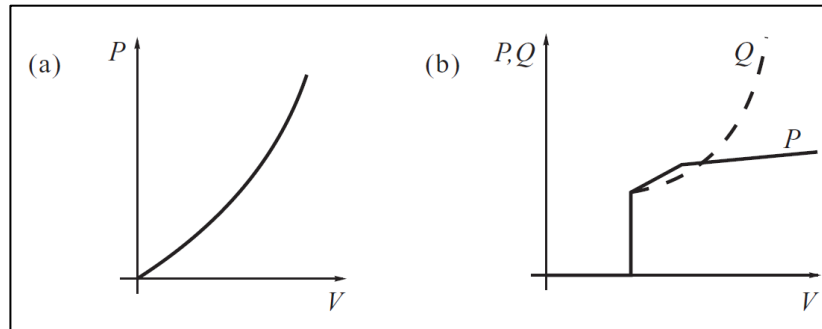


**Figure 3.15: Voltage characteristic of (a) Conventional light bulb, and (b) Discharge light** (Jan et al., 2005)

### 3.2.5.2 Induction motors

Induction motors are the most consuming loads of electrical energy. These are the types of loads that are primarily used in industrial areas than in commercial and residential. The equivalent circuit of the induction motor is presented in Figure 3.16 below, where  $x$  is the reactance of the stator,  $R$  is the rotor resistance,  $X_m$  is the magnetizing reactance and  $s$  is the motor slip which is equated as  $s = (\omega_s - \omega) / \omega_s$ .

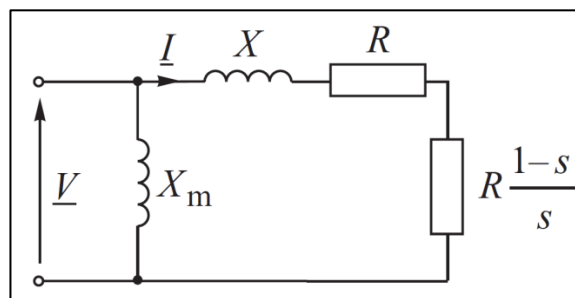


**Figure 3.16: Induction motor equivalent circuit** (Jan et al., 2005)

The induction motor equivalent is ideal for the analysis of real and reactive power-voltage characteristics. These characteristics assist in the determination of the starter control as well as motor protection.

### 3.2.5.3 Static Characteristics of the Load

The static characteristic of the load is influenced by the summation of different load types. The load types influence the behavior of the load in the power system

due to their unique and different properties of the characteristic of the individual load. Figure 3.17 below represents the composition of the loads. At (a) is the voltage characteristic of the composite loads consisting of induction machines and discharge light and at (b) is the commercial and residential loads consisting of traditional lighting and heating. Considering (a) in Figure 3.17, it can be noted that at  $V_n$  the  $P(V)$  curve is getting flat while  $Q(V)$  was dropping before the point and when it reached the operating point it exponentially increases. Due to the drop in voltage  $P(V)$  becomes fatter and  $Q(V)$  increases due to the reactive power demand increase. At (b) the load is more resistive and hence the response or the characteristic curve is steeper.

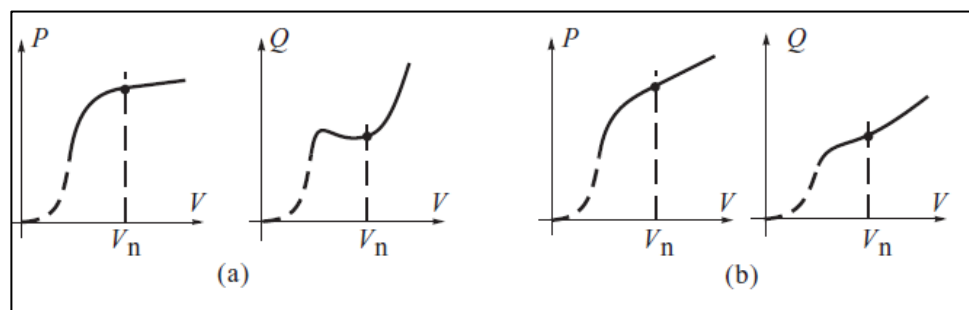


**Figure 3.17: Voltage characteristic (a) Combination of industrial loads such as induction motors and discharge lights, and (b) Residential and commercial loads such as conventional lighting and heating (Jan et al., 2005)**

Since the composite load also involves the transformers in the distribution level, which also have their power losses, the losses are also added to the net power demand. The transformers are equipped with an on-load tap changer voltage control unit which regulates the voltage when the demand changes. The influence of tap changer is a voltage control system in the voltage characteristic is illustrated in Figure 3.18 below. The bold dash line represents the nominal tap changer position. In the event of a tap changer operation, the voltage characteristic can either move left or to the right. The far left or right is the tap changer extreme limits. The tap changer is equipped with dead-zone, which helps avoid unnecessary operations when the transformer's voltage is within the limits.

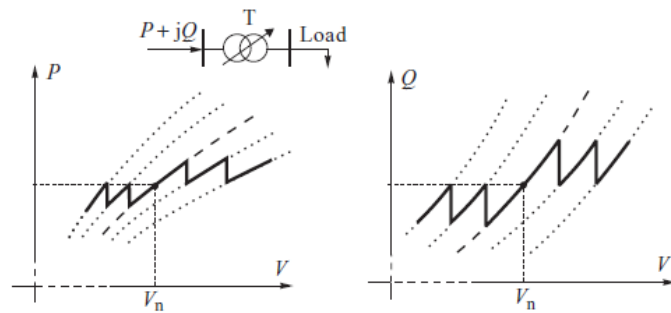


**Figure 3.18: Tap-change contribution to voltage characteristics** (Jan et al., 2005)

There are various models of power system loads which includes (Bergen & Vittal, 2007):

- Constant kVA: Such as running motor where the apparent power ( $S=P+jQ$ ) is kept constant
- Constant impedance load, this is typically used for the motor which is starting or static loads
- Constant power and current loads, these can be represented by static power conversion
- Generic loads, these are complex loads where the real power and reactive power are the functions of terminal voltage and frequency.

The most popular power system load models are constant power, current, and impedance. The constant power loads are known for being stiff meaning that they have small voltage sensitivity. This is the widely adopted model in load flow studies but it is not satisfactory due to its inadequate results when performing transient stability where large voltage deviations are experienced. The constant current model has a high voltage sensitivity, making it ideal for transient stability analysis and suitable in the analysis of dynamic network studies. The constant impedance is also regarded as having a high voltage sensitivity but is not adequate for stiff loads due to its dynamics. In order to obtain a general voltage characteristic, all three individual characteristics are combined to form the so-called polynomial constant impedance, constant current, and constant power (ZIP) model. The ZIP model is expressed in equation 3.19 below (Jan et al., 2005).

$$P = P_0 \left[ a_1 \left( \frac{V}{V_0} \right)^2 + a_2 \left( \frac{V}{V_0} \right) + a_3 \right]$$

$$Q = Q_0 \left[ a_4 \left( \frac{V}{V_0} \right)^2 + a_5 \left( \frac{V}{V_0} \right) + a_6 \right]$$

The initial conditions are represented ( $P_0$ ,  $V_0$ , and  $Q_0$ ). Various types of models such as exponential, piecewise approximation, and frequency dependant load models are derived from the polynomial ZIP model (Jan et al., 2005).

### 3.3 Power flow analysis.

Load flow, also called power flow, is the power system network analysis that helps to forecasts steady-state, focusing in all the branches' parameters. These parameters include voltages, currents, real and reactive power flows. Load-flow studies and simulations help analyze and predict the power system's operating conditions in the planning or operation phase. Some power system conditions may not be possible to analyze in real-time while the system is operational, and an incorrect operating approach may lead to complete system dysfunctioning. Power system analysis software tools such as power factory can perform system simulation without tempering the real power system, which helps mitigate the dangers of exposure of the system to maloperations. The aim and objective of the load flow studies are to gain an understanding of the behavior of the power system subjected to different operating conditions. This is critical for power system planning and operating. The flow chart diagram indicating the application of power system analysis as well as different conditions of operation in the analysis process is illustrated in Figure 3.19 below (Bergen & Vittal, 2007).

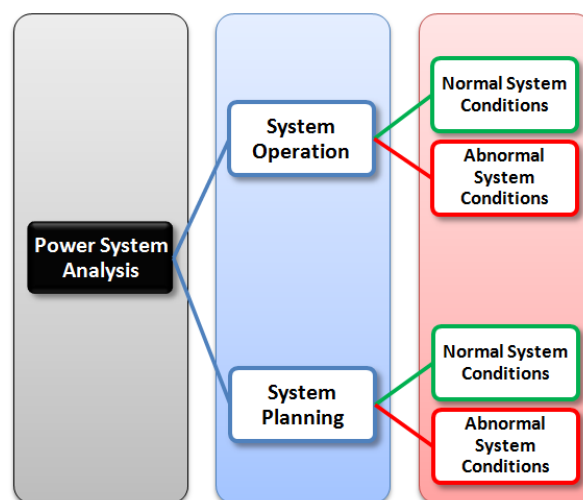


**Figure 3.19:** The objectives of power system analysis (Bergen & Vittal, 2007)..



The power flow equation is used to determine the bus voltages and angles as well as the amount of current flowing in the transmission line. These two parameters (voltage and current) need to be maintained and kept within the tolerance during operation to ensure the quality of supply, which will avoid overloading the transmission lines. However, the calculations of power flow can become complex due to the computation of nonlinear power flow equations as well as the power grid network size.

The power flow problem needs to be formulated in order to classify the power flow solution method that can be employed in the system. The methods that are used to solve power flow problems are Gauss-Seidel and Newton-Raphson. The Gauss-Seidel method is normally used in small networks where few iterations can be performed and Newton-Raphson is used in most power system industries.

The load flow calculations consist of solving a nonlinear equation, these solutions are regarded as impractical to achieve them manually but can be achieved on a small network where all the data is provided. In order to solve power flow problems, a meaningful guess is made for data not provided such as voltages and angles. In most applications, the 1pu voltage at angle zero degrees is used. The swing bus is set to angle of zero degrees as it is the point of reference which then results in a negative voltage angle at the load bus. Traditionally the use of 50 degrees at the swing bus was adopted which resulted in a positive angle at the load bus. Load flow, the power balance is achieved through the use of the voltage and angle values. It also solves the deviation in voltage magnitude and its angle. When all the iteration is made, the power flow calculations are terminated and the results such as voltage angle and its magnitude are recorded and updated (Bergen & Vittal, 2007)..

Conducting a load flow needs a problem formation, to identify the given data of each element as well as identifying the unknown data of such elements or components. Table 3.1 below illustrates the data that is commonly known and the unknown data for each element.

**Table 3.1: System elements data expression to indicate the given data and unknown data (Bergen & Vittal, 2007)**

Types of elements	Known variables	Unknown variables
Generator	Real power and voltage magnitude	Reactive power and voltage angle
Load and some generators	Real and reactive power	Voltage magnitude and voltage angle
Slack	Voltage magnitude and voltage angle	Real and reactive power

In order to determine the unknown values of the elements as specified in Table 3.1, equation formulation is key at each node and the use of the numerical equation to determine those quantities.

The network grid that is not large, its power flow can be computed through matrix admittance formulation. This method involves nodal equation formulation and this is achieved through the application of Kirchoff's laws which states that the current enters the node is equal to the summation of currents leaving the node

The matrix in equation 3.7 below represents the voltage and current in all the branches in the network. These calculations are performed in a per-unit form whereby the system impedances should first be converted into the per-unit network system impedances. The equation to find the base impedances is defines below.

$$Z_{base} = \frac{kV_{base}^2 (phase)}{MVA_{base}(1 - \phi)} \quad 3.20$$

Then the based admittance is given as:

$$Y_{base} = \frac{1}{Z_{base}} \quad 3.21$$

The admittance or Y matrix below is expressing the positive sequence voltages and currents in all the branches.

$$\begin{bmatrix} \bar{I}_1 \\ \bar{I}_2 \\ \dots \\ \bar{I}_n \end{bmatrix} = \begin{bmatrix} Y_{11} & Y_{12} & \dots & \dots & Y_{1n} \\ Y_{21} & Y_{22} & \dots & \dots & Y_{2n} \\ \dots & \dots & \dots & \dots & \dots \\ Y_{n1} & Y_{n2} & \dots & \dots & Y_{nn} \end{bmatrix} \begin{bmatrix} \bar{V}_1 \\ \bar{V}_2 \\ \dots \\ \bar{V}_n \end{bmatrix} \quad 3.22$$

In equation 3.22,  $I$  - is the positive sequence current that is flowing in the network,  $V$  - is the voltage at the nodal terminal while  $Y$  - is the nodal admittance matrix. The generator and the load are normally expressed in real and reactive power at their respective node. Therefore the current at a given node or bus  $k$  can be determined using equation 3.6 below.

$$I_k = \frac{(P_k + jQ_k)}{V_k} \quad 3.23$$

$P_k$  is the real power at the bus  $k$

$jQ_k$  is the imaginary reactive power at bus  $k$

while  $\bar{V}_k$  and  $I_k$  represent the phase voltage and phase conjugate current at bus  $k$

The current supplied to the system in respect to voltage is defined in equation 3.24.

$$\bar{I}_k = \bar{V}_k Y_{kG} + \sum_{m \neq k} \frac{\bar{V}_k - \bar{V}_m}{Z_{km}} \quad 3.24$$

$Y_{kG}$  - the sum of admittances connected to buses to the ground

$Z_{km}$  - is the series impedance of the two connected buses

Equation 3.24 can be expanded further as

$$\bar{I}_k = \bar{V}_k \left( Y_{kG} + \sum_{m \neq k} \frac{1}{Z_{km}} \right) - \sum_{m \neq k} \frac{\bar{V}_m}{Z_{km}} \quad 3.25$$

The part within the brackets in the above equation defines the equation to determine the self-admittance which is the sum of all admittances connected in all the buses as well as to ground.

$$Y_{kk} = Y_{kG} + \sum_{m \neq k} \frac{1}{Z_{km}} \quad 3.26$$

Moreover, to find the negative inverse of the series impedance between the two connected buses, equation 3.27 is used.

$$Y_{km} = -\frac{1}{Z_{km}} \quad 3.27$$

In a large power system network, the formulation of the equation for each node might consume a lot of time and mistakes can be made due to the complexity of the network and also arrive at the solution a number of iteration will be needed due variability of the network. Hence the admittance matrix will not be ideal to solve such complex networks.

Power flow analysis can be performed through techniques such as Gauss-Seidel, and Newton-Raphson method which will be expressed below. These techniques both solve the equation as outline under the admittance matrix because of their simplicity in terms of data expression and interchange the admittance matrix.

In order to perform load flow through iteration algorithms, there are four parameters that need to specify. The parameter includes real and reactive power  $P$  and  $Q$  flowing into and out of the network, the specification of the bus voltage  $|V|$  and the reference bus voltage angle  $\theta$ .

### 3.3.1 Gauss-Seidel iterative technique

The gauss-seidel iterative method is developed to provide solutions to non-linear algebraic equations. In this method, the value of voltages is guessed in order to calculate the value of a particular variable such as current, real, or reactive power. The value of the voltage that has been guessed is set to the initial calculations. These calculations are recurring until the iteration convergence is achieved. In order to determine the new value of the voltage, equation 3.28 below is used.

$$V_i^{(k+1)} = \frac{\frac{P_i^{sch} - jQ_i^{sch}}{V_i^*} + \sum Y_{ij}V_i^k}{\sum Y_{ij}} \quad j \neq i \quad 3.28$$

In this process, Kirchoff's current law is applied, an assumption is made that the current flowing into the bus is positive, and the active  $P_i^{sch}$  and reactive power  $Q_i^{sch}$  also flowing into the buses (generator buses) will be positive. But the active and the reactive power flowing away from the load buses will have a negative polarity due to the flow direction. In order to calculate the values of the active and reactive power, equation 3.29 and 3.30 are used.

$$P_i^{(k+1)} = \text{Real} \left[ V_i^{*(k)} \left\{ \sum_{i=0}^n y_{ij} - \sum_{ji}^n V_i^{(k)} \right\} \right] \quad j \neq i \quad 3.29$$

$$Q_i^{(k+1)} = \text{Imaginary} \left[ V_i^{*(k)} \left\{ \sum_{j=1}^n y_{ij} - \sum_{ji}^n V_i^{(k)} \right\} \right] \quad j \neq i \quad 3.30$$

The power flow is often articulated in the form of a bus admittance matrix using both diagonal and non-diagonal elements of the matrix. Equation 3.31 below is the voltage equation using bus admittance matrix elements.

$$V_i^{(k+1)} = \frac{\frac{P_i^{sch} - jQ_i^{sch}}{V_i^*} - \sum Y_{ij} V_j^k}{Y_{ii}} \quad j \neq i \quad 3.31$$

The real and imaginary power through bus admittance matrix elements are determined as expressed in equation 3.32 and 3.33

$$P_i^{(k+1)} = \text{Real} \left[ V_i^{*(k)} \left\{ V_i^{*(k)} Y_{ii} + \sum_{i=1, j=1}^n y_{ij} V_j^{(k)} \right\} \right] \quad j \neq i \quad 3.32$$

$$Q_i^{(k+1)} = \text{Imaginary} \left[ V_i^{*(k)} \left\{ V_i^{*(k)} Y_{ii} + \sum_{i=1, j=1}^n y_{ij} V_j^{(k)} \right\} \right] \quad j \neq i \quad 3.33$$

### 3.3.2 Newton-Raphson iterative technique

This iterative power flow solution was developed in 1960 after Isaac Newton and Joseph Raphson. In this method, a nonlinear equation as being approximated with linear equations through Taylor series expansion. The advantage of this method over other iterative methods is its convergence characteristics which are more effective compared to other iterative methods. This method is also regarded as more reliable is it can solve events that result in divergence. This method can even be quick to obtain results if the assumed values are close to the solution. But if the assumed values are not as closer, then it can take some time for the completion of the computation. The non-linear equations are solved using this method through the application of the bus admittance matrix approach. The current injected at bus  $i$  the system can be expressed as in equation 3.34 below in the polar form.

$$I_i = \sum_{j=1}^n |Y_{ij}| |V_j| \angle \theta_{ij} + \delta_j \quad 3.34$$

The real and reactive power separated into real and imaginary parts with  $I_i$  substituted can be determined as expressed in equation 3.35 and 3.36 below

$$P_i = \sum_{j=1}^n |V_i| |V_j| |Y_{ij}| \cos(\theta_{ij} - \delta_i + \delta_j) \quad 3.35$$

And the reactive power is given as:

$$Q_i = \sum_{j=1}^n |V_i| |V_j| |Y_{ij}| \sin(\theta_{ij} - \delta_i + \delta_j) \quad 3.36$$

Equation 3.35 and 3.36 above are nonlinear and algebraic equations that are expressed in terms of voltage per unit and  $\delta$  expressed in radians. These two equations can be expanded further through the Taylor series in order to form linear equations as shown in equation 3.37 below.

### **3.4 Dynamic power system analysis and modeling approach.**

Traditional power system grid used to be dominated with a synchronous generation system. The power generation landscape has shifted from conventional to a modern type of generation system. The advantage of using a conventional generation system is its reliability and assured quality and continuity of supply for as long as there are resources such as fossil fuels. However, the conventional generation system mostly uses coal as the primary resource to energy, which has brought in some environmental impacts such as pollution, which also affected the ozone layer and introduces some global warming due to the greenhouse gases being produced in the process of power generation.

Due to the challenge the world is facing global warming, renewable energy systems were identified as the potential energy sources that guarantee security and mitigated pollutions to the atmosphere and the environment. The other advantage of renewable energy sources and other alternative energy resources is supplying electrical energy in both micro and large grids in an area where access is difficult such as rural area. The penetration rate of the energy resource is being observed to be as increasing. However, the impact or risk associated with their integration to the power system is still being investigated. This project's current focus is on the impact of distributed energy resources in power system frequency stability. The control measure to stabilize the power system grid are being explored as well. The theoretical aspects that need to be considered in frequency stability are being explored.

#### **3.4.1 Frequency stability**

Frequency stability refers to a power system's capability to regain steady frequency after the power system was subjected to severe disturbance resulting in the power imbalance between generation and load. When the power variation occurs, it results in continued frequency fluctuations, leading to cascaded tripping of generating units or loads. In the event of frequency variations, the protection

system relays such as under frequency load shedding relays, generator controls, and other protection equipment get triggered in a few seconds in responding to the frequency instability. The frequency instability can be short-term or long-term due to the response of control devices which some will respond quickly to the changes in power system whilst others such as prime mover energy supply systems and load voltage regulators respond after a few minutes.

The frequency variation can be classified into a number of stages based on the nature of dynamics associated with each of these stages to be defined independently. This is done to assist in demonstrating how the different power system changes develop. The power system dynamics stages can be understood requires and understanding the operation of the automatic generation control (AGC) as this is important in defining how the frequency will behave in response to a change in load.

#### **3.4.1.1 Automatic Generation Control**

A power system that consists of a number of generation units and loads with continuous variables throughout the day, its power demands are met in various ways. The large but slow power demand changes are met by deciding on which generating units need to be added or removed to the grid to cater to the change in power demand at daily interval considering the load profile. The medium load changes that are happening faster for about 30min, the economic despatch needs to take place to determine the amount of power required from each dedicated generation unit. In case of more minor load demand changes, happening at a faster rate requires to be regulated through an automatic generation controller. The purpose of automatic generation controller is to:

- maintain frequency within the predefined value (frequency control);
- maintain power exchanges with neighboring control areas at their scheduled values (tie-line control);
- The power is adequately allocated among the generation units based on area dispatching needs (energy market, security, or emergency).

The AGC is applied based on the configuration of the power system. Its three primary functions might not all be applicable in some systems. Hence the generation characteristics need to be considered.

#### **3.4.1.2 Generation characteristic**

In steady-state power system operation, the considerable equation representing the relationship between the generator's power and speed. Since the frequency

is directly proportional to generator rotational-speed. Equation 3.37 represents the relationship between the rotational speed of the generator and the frequency.

$$\frac{\Delta f}{f_n} = -\rho_i \frac{\Delta P_{mi}}{P_{ni}} \text{ and } \frac{\Delta P_{mi}}{P_{ni}} = -K_i \frac{\Delta f}{f_n} \quad 3.37$$

Under normal operation conditions, the system generation units are synchronized together meaning that they are operating at the same frequency. If there are any changes in the power system in regards to the power generated, its total deviation can be calculated according to equation 3.38.

$$\Delta P_T = \sum_{i=1}^{N_G} \Delta P_{mi} = -\frac{\Delta f}{f_n} \sum_{i=1}^{N_G} K_i P_{ni} = -\Delta f \sum_{i=1}^{N_G} \frac{K_i P_{ni}}{f_n} \quad 3.38$$

$N_G$  The above equation represents the number of generation units, the above equation is strictly for power generated through the turbine. The generation characteristic is demonstrated as the sum of speed droop characteristics of all generation units from Figure 3.20. It can be noted that the changes in frequency for generation unit one is the same as the change in frequency for generation unit two, the results into a change in total frequency of the system to remain the same while the changes in power for both units resulted into the double of each unit.

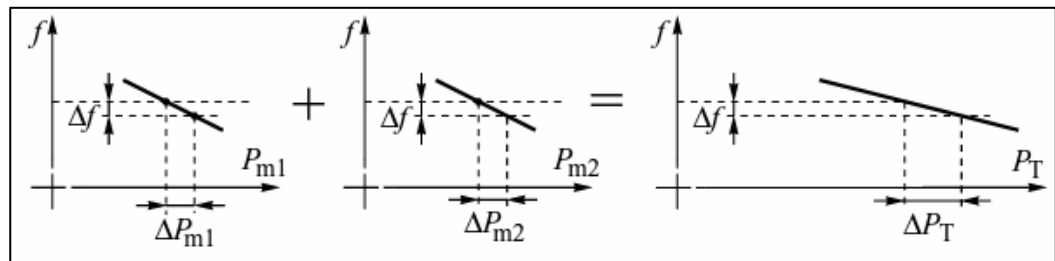


**Figure 3.20: The relationship between power and speed of the turbine generation units (Jan et al., 2005)**

This characteristic defines the capability of the system to compensate for any power deviations to regain the frequency stability. The benefit of the integration of more generation units in the power system results in small frequency differences. The turbine-generator characteristic has lower and upper limits. The lower limit is based on maintaining the basic operation of the system, for example, in coal-burn steam, its burners need to maintain stable operation, while upper limits are based on the thermal and mechanical operation.



An increase in power demand results in system frequency to drop. To compensate for the increase in power demand, the turbine generation needs to increase its power being generated and reduction in load can also assist in stabilizing the frequency. The change in power demand can be calculated using equation 3.39.

$$\Delta P_{demand} = \Delta P_T - \Delta P_L = -(K_T + K_L)P_L \frac{\Delta f}{f_n} = -K_f P_L \frac{\Delta f}{f_n} \quad 3.39$$

According to equation 3.39, it can be noted that the higher the change in load power, at the stable total change in power of the summed generation, the less the change in power demand resulting in more frequency deviations. Figure 3.21 is graphically representing equation 3.39. More frequency deviations could be experienced if the generation sensitivity coefficients are small.

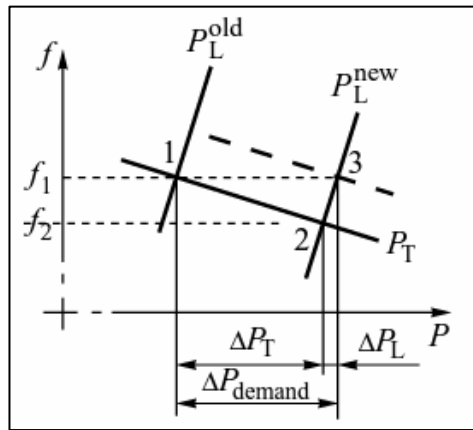


**Figure 3.21: The relationship between change in power demand and frequency (Jan et al., 2005)**

### 3.4.1.3 Frequency control

Power system frequency deviations occur when there is an imbalance between the power being produced at the generation against load demand. In the power system grid, the frequency needs to be maintained to be within the predefined limits of 0.1Hz at synchronous of 50Hz considering South African and some European grids. In the case where the frequency deviates exceeding the limits, control warning indications will be activated to action the change to bring the frequency to its nominal value. The power system can still operate and deliver the power to the load even though some parts of the network are experiencing not severe faults provided that the frequency of the grid is adequately controlled. Severe frequency deviations may lead to an inability to recover the frequency steady-state resulting in power system blackouts. The cause of blackout may be

due to an immense increase in load demand such that the generation capacity cannot supply the amount of demand.

A power system is designed to be able to maintain its stability in the event of contingencies (n-1). In the event whereby the frequency drops and the power system is expected to reach its steady-state shortly through activation reserved generation systems. If the steady-state is not met within the predefined time, the generation system is subjected to another state operation where it operates as the disturbed system. If there are no reserves available, to prevent the system from collapsing, implementation of load shedding would be ideal and it is encouraged. Another option is to split up the network to isolate the faulted part of the network that resulted in an emergency state.

The frequency control studies focus on assessing the contribution of distributed energy resources to power system stability while assessing over and under-frequency events, the events that lead to frequency rise, and drops. Furthermore, the contribution of frequency control stages such as primary, secondary and tertiary controls investigated.

The control stage of the system frequency is presented in Figure 3.22 below. The link between the stages is presented starting from the normal system before the disturbance to the last time control process for the long-term disturbance. The function of each control stage can be noted. The primary control is responsible to return the frequency to steady-state, the secondary control is set to activate the reserve capacity to cater to the deviation and also once that is done, it also needs to ensure that the frequency is restored to its normal value of 50Hz. The role of tertiary control is to supervise the actions of the secondary control if it fails to restore frequency to its normal value. The tertiary control can be performed manually or automatically. In the event of loss of load, the tertiary control needs to free some reserved and that enables the over frequency event to occur due to the loss of load to return to its steady state. In the event of an increase in load demand, the tertiary needs to bring online the reserved capacity to cater to the load demand increase.

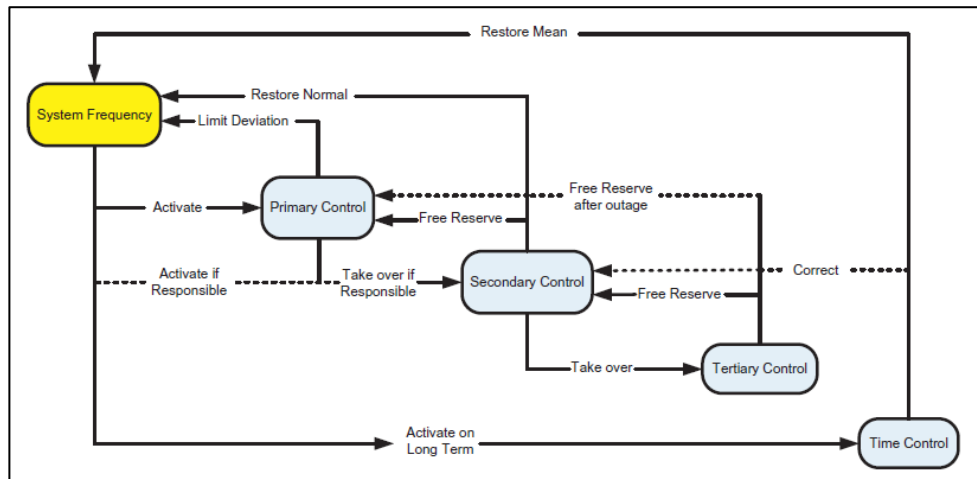


**Figure 3.22: Frequency control stages** (Laghari et al., 2013)

The role of the primary control function is to stabilize the frequency into the steady-state, while the role of secondary control is to ensure that the frequency is fully recovered to its nominal value of 50Hz considering the South African system. The tertiary frequency control system is always considered at a later stage when the primary and secondary control functions can no longer recover the frequency. The tertiary control system uses protection system equipment to perform disconnection of the generation system active on the grid in case of over frequency while performing load shedding in the event of under frequency.

Figure 3.23 below illustrates the modified frequency recovery process where primary, secondary, and tertiary control functions are activated following a disturbance. The time each control stage is expected to take in response to a disturbance can be noted.

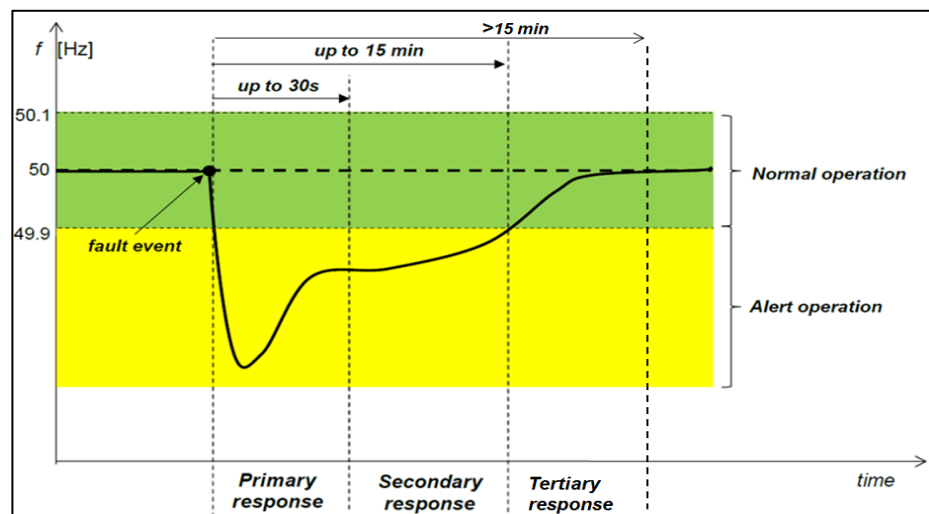


**Figure 3.23: Modified frequency recovery process** (Anca Daniela et al., 2016)

### 3.4.1.4 Primary control

Primary control is automatically activated to counteract the frequency deviation within 30 seconds of the system disturbance. This is done through frequency droop control at the by the generation which increases the speed of the generation units. When the frequency drops, these generating units immediately start producing more power to eliminate a further decrease of the frequency in the power system. Figure 3.23 above illustrates the function of primary control of bringing the frequency back to an acceptable steady-state level. The frequency of the system is brought to a stable level that is lower than the initial condition prior to the disturbance of the system. The frequency level is still on the alert level as per the color-coding. This diagram shows that it took less than 30 seconds to bring the frequency back to the stable level.

The power system is said to have met its state of equilibrium when the power generated is equated to the load demand, including power losses along the transmission line. The load and generation characteristics in response to frequency are expressed in the equations below. Equation 3.24 represents the load characteristics, while the equation represents generation characteristics in response to frequency. In both equations, any deviation, whether in load demand or in power generated (PT ), can influence the frequency also to change.

$$\frac{\Delta P_L}{P_L} = K_L \frac{\Delta f}{f_n} \quad 3.40$$

$K_L$  is the frequency sensitivity coefficient of the power demand

$f_n$  is the system nominal frequency

$\Delta f$  is the change in frequency

$P_L$  is the total system load power demand

$\Delta P_L$  is the change in power demand

$$\frac{\Delta P_T}{P_L} = -K_T \frac{\Delta f}{f_n} \quad 3.41$$

$K_T$  is the frequency sensitivity coefficient of the system generation power

$f_n$  is the system nominal frequency

$\Delta f$  is the change in frequency

$P_L$  is the total system load power demand

$\Delta P_T$  is the change in system generation power

The frequency sensitivity coefficient of the power demand ( $K_L$ ) ranges from 0.5 to the generation coefficient is approximated to 20 ( $K_T \approx 20$ ). In equations above the generation and load coefficients,  $K_T$  and  $K_L$  are opposite to one another to increase frequency to correspond to a drop in the generation and an increase in electrical load.

The relationship between the generation and load characteristic is demonstrated in Figure 3.24. The diagram below denotes the equilibrium point between generation and the load, which is expressed in the two equations above. Equation 3.42 below represents the link between the change in power demand, generation, and load demand.

$$\Delta P_{demand} = \Delta P_T - \Delta P_L = -(K_T + K_L)P_L \frac{\Delta f}{f_n} = -K_f P_L \frac{\Delta f}{f_n} \quad 3.42$$

A deviation in the total power required by the load  $\Delta P_L$  The load characteristic movement as indicated in Figure 3.24 below shifts the equilibrium point from 1 to 2. An increase in system load demand can be suppressed by increasing the change in generation power  $\Delta P_T$ , and by reducing the system change in power demand at the load side.

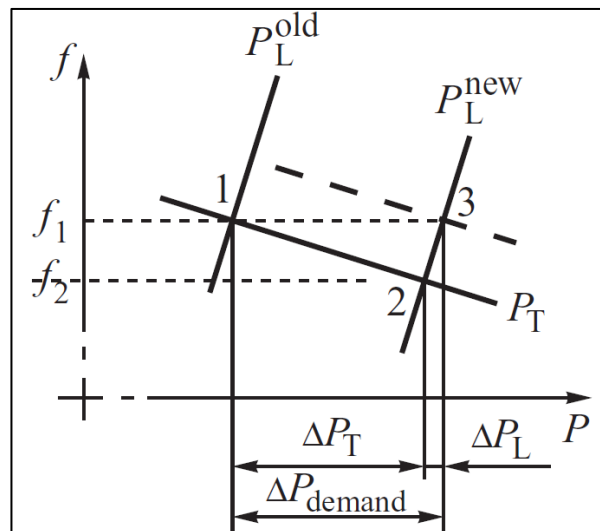


**Figure 3.24: Load and generation power characteristics** (Jan et al., 2005)

Due to the shift of the equilibrium point from 1 to 2, the new operating point, load demand, and frequency are reached. The new system frequency value is denoted as  $f_2$  at point 2, which is lower than the old frequency value  $f_1$  at point 1. The

above equation 3.7 represents the entire frequency response of the power system while the summation of the two coefficients  $K_T$  and  $K_L$  within the equation is the stiffness which is difficult to determine. The action of the turbine governor is configured such that  $\Delta P_T \gg \Delta P_L$  and this action is called primary frequency control. It is achieved by ensuring that the change in generation power is greater than the load demand through maintained reduced demand in the support of frequency sensitivity on the demand side. The action of primary control is done with respect to the regulator reference values which are kept constant.

In the event, the load demand increases resulting in frequency reduction, primary control is activated when there are generic units that are operating at an average level and are not fully loaded. Considering Figure 3.25 (b) below, it indicates that if the generation unit is already operating at its maximum, a reduction in frequency cannot influence the output of the generator to produce more power. However, the only those generation units that are moderately loaded which are carrying a spinning reserve be further loaded. In order to activate the primary control system, the system operator needs to ensure that there are enough spinning reserves and the generators are not being operated at the maximum power capacity. When the primary control is activated, uniformly distribute the spinning reserved power throughout the system in order to meet the required power demand. Since all the generation units will be in synchronism with one another, the spinning reserves will be released by all the generation units integrated to the system, this will also help to ensure that the power is evenly distributed to the system does not contribute to some other power system equipment being overload. If the spinning reserves are released from one region of the system, there are high chances of overload some apparatus.

An interconnected power system grid, the coordination of the generation units is very in regards to the actions of the primary control system and to effectively coordinate the interconnected power system grid, the power system grid code which underlines all the requirement needs to be considered as the reference.

In collaboration with other independent power producers, power system grid operators set out the limits of when should the spinning reserves be released to cater to the frequency deviations. It is their responsibility to set out the frequency limits as well as the activation time of the primary control when the system is subjected to some frequency deviations. Considering Figure 3.25 below, the frequency deviation is set to  $\pm 200\text{mHz}$  reliability primary frequency control. Time primary frequency control is expected to be activated within 15-30s of the

deviation. The governor will influence turbine speed to release the spinning reserves. The speed–droop characteristics are found in turbine governors of the synchronous generation units

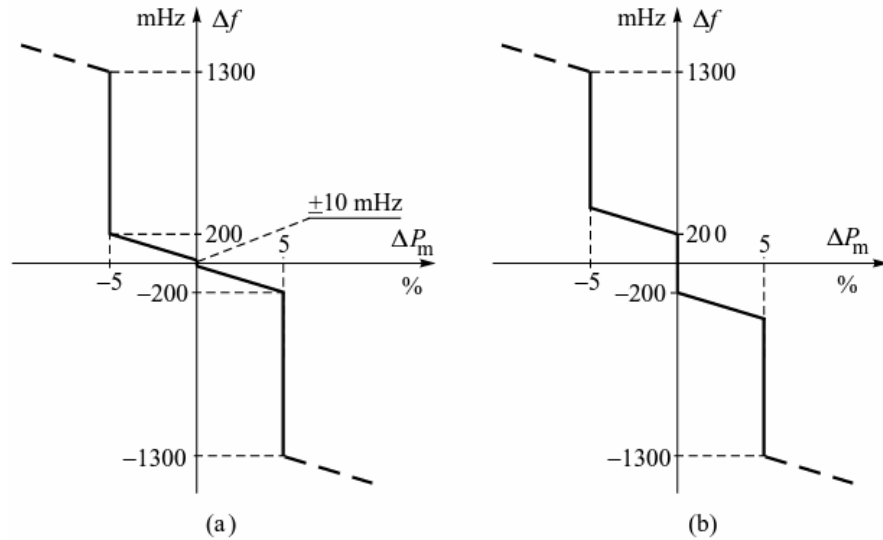


**Figure 3.25: Speed - Droop characteristic** (Jan et al., 2005)

### 3.4.1.5 Secondary control

The secondary control, also called Load Frequency Control (LFC) or Automatic Generation Control (AGC), is an additional control loop that slower than the primary control but faster than tertiary control, which redeploys load among the various generating units in order to bring back the frequency to its nominal value. The secondary control is activated after the primary control, where the power setpoints of the generators are adjusted to allow the power compensation to take while restoring the frequency error. The secondary control response time must be delivered within 15 minutes. Secondary control can be performed through an application of automatic generation control systems or through manual operation. This intervention can only be done by the system operators.

The turbine–generators that are equipped with governing systems can only bring the power system frequency to a steady-state after the system was subjected to some disturbances, they cannot restore it to its nominal value, hence a second intervention is required to restore the frequency to its initial nominal value.

Considering Figure 3.25, for the frequency to return to its initial nominal value, the generation characteristic needs to shift up to the dotted line for frequency restoration. Such a shift can be enforced by changing the  $P_{ref}$  setting in the turbine governing system at the load side. Figure 3.26 below demonstrates the

turbine speed-droop characteristic for different reference power. These changes also influence the characteristics of the corresponding generation power, such as  $P_{m(1)}$ ,  $P_{m(2)}$  and  $P_{m(3)}$ . A turbine cannot exceed its maximum power by only changing the governor settings, provided that it was already running on its limits or full capacity. In addition to this, the changing settings of the governor cannot override the turbine of the generator to produce power exceeding its maximum power rating. Changing the reference power settings  $P_{ref(1)}$  of each generator, governors will result in an upward shifting of the overall generation characteristic of the system provided that there are rotation reserves. Through that action, the power system frequency will be restored, reaching its initial condition. This condition will be met only when additional power is added to the grid, or the generators have released the rotating reserved power. The action of changing the reference power settings to shift the generation characteristic upwards, resulting in more power being produced is called secondary control. Figure 3.26 below demonstrates the process in which the initial frequency condition can be met by pref setting which directly influences the shifting of the generation characteristic upwards resulting in more power being produced. In this diagram  $P_{ref(1)}$  and  $P_{m(1)}$  are regarded as the initial conditions. When the load demand increases, the governor activates the primary control and after the action of primary control, the secondary control takes place to bring back the frequency to its initial condition. Through this action,  $P_{ref(2)}$  and  $P_{m(2)}$  is reached and the frequency is still at its initial condition.

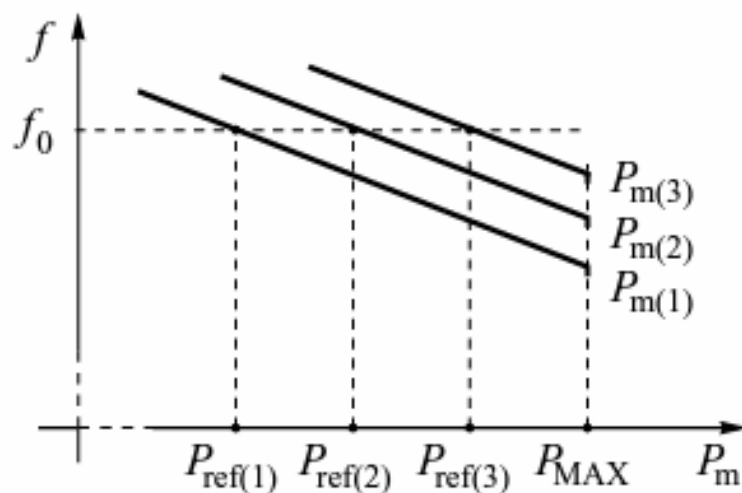


**Figure 3.26:** Turbine speed–droop characteristics for various settings of  $P_{ref}$  (Jan et al., 2005)



In a microgrid whereby a standalone generator feeds the system with decentralized control, the secondary control system can be achieved by integrating an additional control loop to the turbine-governor which will automatically perform the secondary control function. In Figure 3.27 below represent the turbine-governor block diagram before and post-modification. Dashed lines present the supplementary control loop for the generator to participate in secondary control connection and it comprises integration elements that produce a control signal that is linked speed error of the generator to the load reference point. The additional signal results in the new value of  $P_{ref}$  setting. The new setting of  $P_{ref}$  results in a new of stability as show to Figure 3.26 above

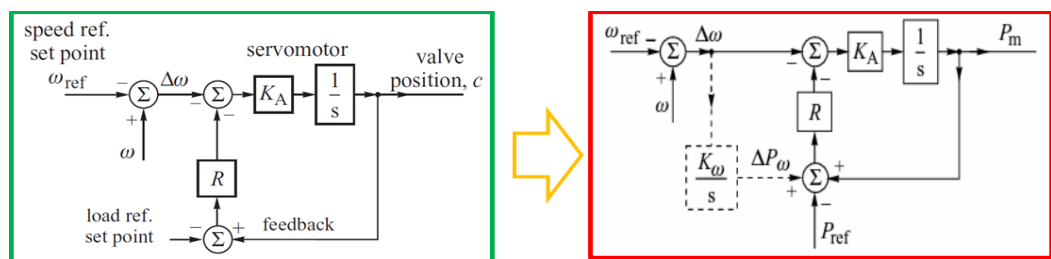


**Figure 3.27: Supplementary control added to the turbine governing system.**

(Jan et al., 2005)

In a decentralized control grid, the secondary control function can also be performed by integrating medium-sized generation units to regulate the system frequency by contributing power required by the load. These generation units are only tapped into the grid when the power demand increases. The availability of medium-sized generators in the system will supersede the implementation of the supplementary control loop for secondary control.

Considering an interconnected system, secondary control can only be utilized in a centralized control area to obtain information as to where the power imbalance occurs. This cannot be achieved in a decentralized control area because it would be impossible for the secondary control to obtain information as to where the power discrepancy is taking place. If the control system is not centralized, undesirable operation due to false information is received by the secondary control system, leading to the maloperation of the power system.

The implementation of centralized secondary control in an interconnected power system where an AGC is used in a manner that each subsystem has its dedicated central regulator can assist to deal with any power deviations between the generation of the load and to bring back the frequency to its nominal value.

The implementation of the centralized secondary will help to achieve the power system stability and equilibrium point whereby the power generated power will be equal to the summation of the power demand and net tie-line power (power losses) and the equation 3.9 and Figure 3.28 below illustrates the power system equilibrium. As presented in Figure 3.28 below, the control area where the secondary control takes place determines the additional power required to meet the power demand. It is the regulator within the control area that enforces the generator to produce more power.

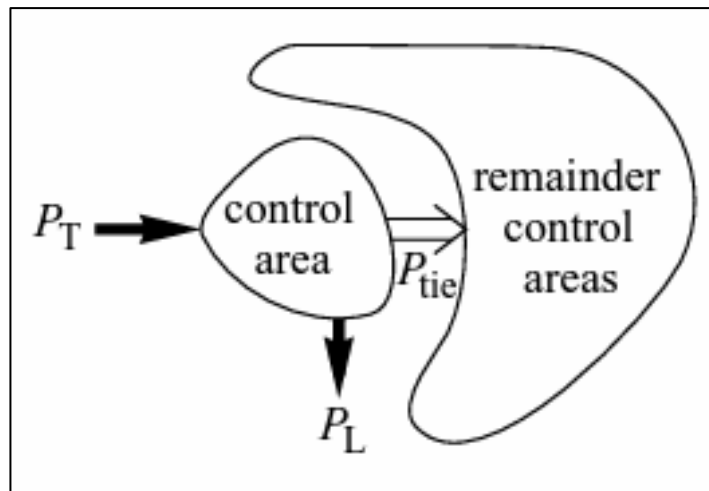


**Figure 3.28: Power balance of a control area** (Jan et al., 2005)

Equation 3.43 below illustrates the system equilibrium.

$$P_T = (P_L + P_{tie}) \quad 3.43$$

The aim of having a dedicated regulator is to keep the frequency at the predefined value/level and as well as to keep net tie-line power flow at a certain area to their predefined level. In the event whereby there is a huge power imbalance due to a generator that tripped, then a dedicated regulator within that subsystem should try to restore the frequency within that area without affecting other systems that are in normal operation. To regain the normal system operating condition, the regulator will enforce the generation to release the spinning reserves to reduce the power discrepancy, resulting in more power being produced by the generators within that specific area and maintaining the predefined net tie-line power exchange between generation and the load.

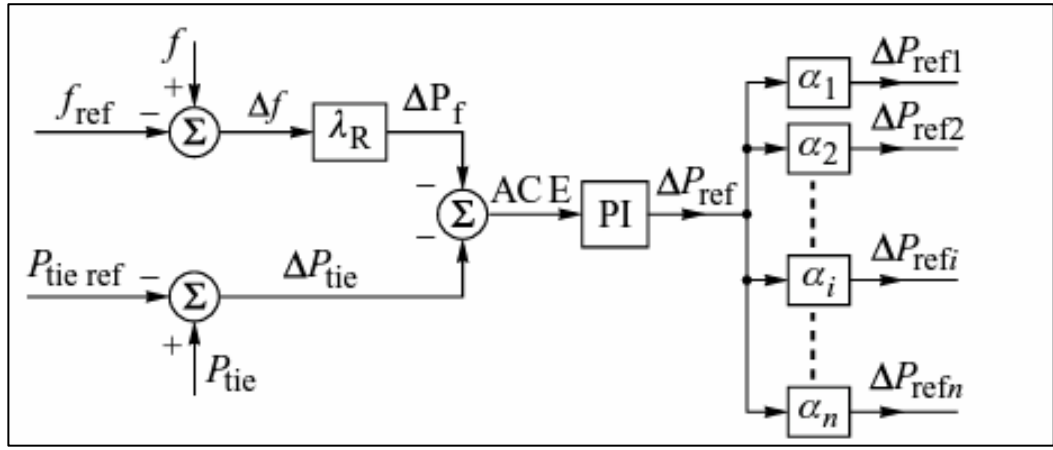


**Figure 3.29: Functional block diagram of a central regulator** (Jan et al., 2005)

The frequency regulation is made by varying  $p_{ref}$  of the specific area of concern, resulting in the change in power output of the turbine. The functional diagram of a central regulator has been demonstrated in Figure 3.29 above. The frequency is measured at the distribution level and gets compared with the generation frequency at the reference point when there is a deviation,  $\Delta f$  is produced. This also includes the power interchange between generation and the load which is also compared to one another and leads to the production of  $\Delta P_{tie}$ . This information is then delivered to the central regulator through a telecommunication system. The frequency bias factor is used to multiply the frequency deviation to obtain the change in generation power which is mathematically expressed in equation 3.44 below.

$$\Delta P_f = \lambda_R \Delta f \quad 3.44$$

The change in the generated power is forced through the controlled area to compensate for the frequency deviation, resulting in power discrepancy between generation and the load.

In the event of frequency drop due to shortage of generation capacity, considering equation 3.42 and 3.44

$$\Delta P_{demand} = -\left(\frac{K_f P_L}{f_n}\right) \Delta f \text{ and } \Delta P_f = \lambda_R \Delta f$$

The central regulator will enforce an increase in generation power to compensate for the shortfall resulting in a change in generation power equal to the change in power demand in opposite to the power flow

$$\Delta P_{demand} = -\Delta P_f \text{ and } \lambda_R \Delta f = -\left(\frac{K_f P_L}{f_n}\right) \Delta f$$

Therefore the frequency bias factor  $\lambda_R$  can be determined if the total power demand  $P_L$  and the stiffness constant  $K_f$  are known, resulting in the formulation of equation 3.45 below. The  $K_f$  MW/Hz represent the stiffness of the system. The value of the stiffness varies due to changes in power demand hence it is difficult to determine.

$$\lambda_R = -\left(\frac{K_f P_L}{f_n}\right) = K_f \text{ MW/Hz} \quad 3.45$$

The change in generation power is then summated with net tie-line power interchange error forming an area control error expressed in equation 3.46 below

$$ACE = -\Delta P_{tie} - \Delta P_f = -\Delta P_{tie} - \lambda_R \Delta f \quad 3.46$$

To remove an error like in a decentralized regulator, as shown in Figure 3.27 above, the integration element needs to be supplemented: a proportional integrator (PI) as indicated in Figure 3.29 above. The additional elements to be added like in the decentralized regulator, create the regulator output signal expressed in equation 3.47 below.

$$\Delta P_{ref} = \beta_R (ACE) + \frac{1}{T_R} \int_0^1 (ACE) dt \quad 3.47$$

In equation 3.47,  $\beta_R$  and  $T_R$  are the regulator parameters. An integral element is a regulator with small or zero proportional elements that participate in integration. The ACE is orientated such that the generated power is regulated to keep the frequency and tie-line power at a stable level as per the power being scheduled.

The output signal  $\Delta P_{ref}$  of the regulator produced through an integrating element is then multiplied by the participation factors of each dedicated generation unit  $\alpha_1, \alpha_2, \dots, \alpha_n$ . This determines the amount of power each generator needs to compensate to the grid to restore the grid's frequency while old maintaining the power demanded by the load. The produced control signals of each dedicated generation units  $\Delta P_{ref1}, \Delta P_{ref2}, \dots, \Delta P_{refn}$  are fed to the governing system of the turbine to influence to reference setpoint based on the change in power demand.

The frequency bias factors are programmed in the central generator based on the system stiffness which is estimated in the whole network on the annual energy production. The stiffness of the system is then divided between the subsystem control areas participating in generation regulation. The value estimated is set to

be the frequency bias factor for the whole year. To determine the magnitude of the frequency bias factor at a given control area, the participation factor will be given for that particular area and the system stiffness of the system for the whole, then equation 3.48 below can be used to determine the estimated frequency bias factor

$$\lambda_{Rn} = \alpha_n K_{fMW/Hz} \quad 3.48$$

The secondary frequency control has a time delay longer than the primary control. The system grid operators and the members of independent power producers need to agree on certain control measures and regulations.

- They need to agree on when and how the tie-line flow measurement should be sent to the central control and the allowable delay time.
- After how long should the central regulator issue instruction to the area control to change the reference set points
- At what time should the secondary control be activated following a change in frequency (15 min maximum)
- The participation factor per power station contributes to the secondary control based on the type of the plant and the range of operation of each power station. The primary control of thermal plant operates between 40% to 100% and the secondary control is within the range of  $\pm 5\%$
- Emphasis on how long the regulation should take place. This is, however dependent on the type of the generation unit, and it is expected that the speed of the regulation should not exceed the following limits: For petroleum units, it should not  $< 8\%$  of the rated power/minute, coal between 2-4% of the rated power/minutes, nuclear 1-5% rated power/minute, and for hydro  $< 30\%$  rated power per minute.

The operation regulation ranges of all the generating units participating in secondary are called the bandwidth. The positive value of the bandwidth is called the reserve of secondary control which is the value from the maximum to the actual point of operation. In the power system, the reserve value is normally set at 1% of the power generated at a specific control area. For contingency measures, the secondary reserves are set to be the size of the largest generation unit operation in the specific controlled area. This will assist in activating the control system in the event whereby the largest generation unit operating in that area is lost. The secondary control is expected to activate and release the reserves within 15 min quickly, the system needs to be at its stability point. In the event of these changes in the power system, power swings between the control

areas can occur if the changes are happening quickly. To avoid this, the values of the schedule power interchange are transmitted to the central regulator and the ramping occurs 5 min before and after the set time. Figure 3.34 illustrates the process of the power interchange schedule. The 10 min is the sum of the start and finishing time in the scheduling process

The proportional, integral, and derivative (PID) controller is the main component in the development of automatic generation control (AGC) or load frequency control or the so-called secondary controller. It is the one that damps those oscillations or error signals following a disturbance in the power system.

#### 3.4.1.6 PID controller background theory

The PID controller is widely applied in power systems controls. There are four different types of controllers that can be modeled from the PID control algorithm. These controllers include (Annam et al., 2017) and (Grobler, 2011):

- Proportional controller
- Integral controller
- Derivative control and
- Complete PID controller

The PID controller regulates and controls the input signal towards the setpoint. The iterative process is performed until the controlled signal difference with the setpoint value is equal to zero. To achieve this, the control process needs to take place in a closed-loop so that the output can be compared with the setpoint value. The operation of the PID controller can be understood when considering each part of the controller. PID controllers are developed to oppose two functions that can occur in the system. These functions include direct-acting and reverse-acting. When the increased input increases output, then this is known as direct action. When the increased input decreases output, then this is a reverse action (Grobler, 2011).

The four types of controllers are discussed below with their mathematical representation and block models. The controller model needs to eliminate the error from the output, which is then fed to the input. This error is the difference in setpoint and feedback signal from the output signal. In the direct-acting controller, the error signal is subtracted from the setpoint value.

$$\text{Error} = \text{Setpoint} - \text{measurement}$$

In the reverse-acting controller, the error is obtained by subtracting the setpoint value from the measurement value.

$$Error = \text{measuremet} - \text{sepoint}$$

### 3.4.1.6.1 P-the proportional term of PID

The proportional term of the which also now as the gain or tuning parameter influences. The proportional control is performed in a closed-loop. Consider Figure 3.30 below, in the input side of the controller, an error is obtained by subtracting the measured value from the setpoint. The error is feed to and multiplied by the proportional gain ( $K_p$ ). The output is obtained through the multiplication of the error by its constant ( $K_p$ ). The proportional controller is mathematically given in equation 3.49 below

$$P_{out} = K_p e(t) \quad 3.49$$

In equation 3.49:

$P_{out}$  is the proportion term output,

$K_p$  is the proportional gain and

$e(t)$  is the error at instantaneous  $t$ .

The proportional gain value should not be too high otherwise it can result in a high error value and consequently lead to an unstable system. Another aspect that needs to be considered is that, if the proportional gain is too small, then the controller will be less sensitive in a disturbance as there will be an uncontrolled large error magnitude (Grobler, 2011).

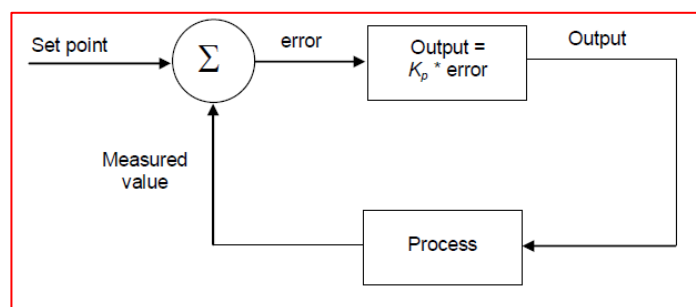


**Figure 3.30: Proportional controller block diagram** (Grobler, 2011)

The fine-tuning of the proportional gain of the controller needs to be as accurate as possible is required. An inaccurate controller due to large gain can lead to more oscillations and system instability.

The proportional band expression is used to achieve an adequate controller change in the controller output as indicated in equation 3.50 below (Grobler, 2011).

$$PB[\%] = \frac{100\%}{K_p} \quad 3.50$$

#### 3.4.1.6.2 I - the integral term of PID

The integral controller is the second term in the PID controller, also known as the resets proportional to the error magnitude and its duration. The integration of instantaneous error leads to accumulative error. The integrator is slow in reacting in its control mode. It is critical in applications of system stability as it restores the dynamic events such as frequency dips to the nominal state. It forces the error from the feedback signal loop to zero in the event of a disturbance. However, its disadvantages include its pole at the initial stage of operation as it can affect the system's stability because of the wind-ups it creates. The wind-ups are undesired signals generated when the integrator is in progress trying to integrate while the input is restrained. The high value of the integrator can result in the controller poorly respond to the transient disturbance. The integrator is mathematically expressed in equation 3.51 below (Grobler, 2011) and (Annam et al., 2017).

$$I_{out} = K_i \int_0^t e(t) \cdot dt \quad 3.51$$

Where:

$I_{out}$  is the integrator controller output value

$K_i$  is the integral adjustable gain parameter

$e(t)$  is the error difference between setpoint and measurement signal value. This error is obtained as the integral is direct-acting (error=setpoint value-measured value).

The integral control action is to adjust the process output value towards the setpoint value and eliminate the remaining steady-state error signal that normally occurs in the event when the proportional controller is in action. Since the integral controller responds to errors that accumulated, an overshoot can occur in the event of control action as the larger value of the gain the cause that but it also means that the steady-state can be accomplished at a shorter period. Any negative errors need to be eliminated before the stability is regained (Annam et al., 2017) and (Borase et al., 2020). The block diagram of an integral controller is shown in Figure 3.31 below.



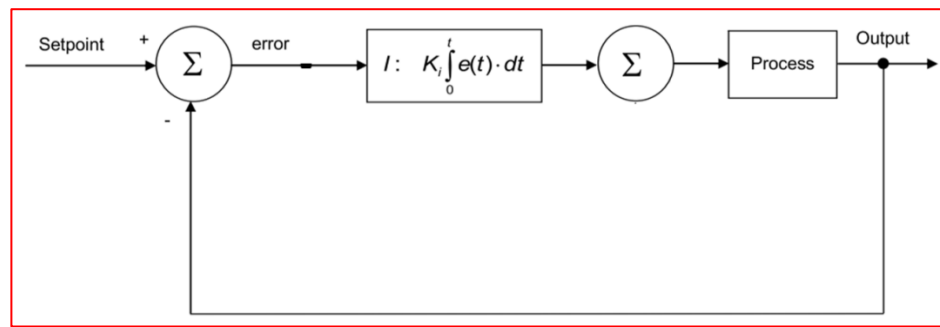


**Figure 3.31: Integral controller block diagram** (Grobler, 2011)

### 3.4.1.6.3 D- the derivative term of PID

The last part of the PID controller is the derivative controller. The derivative controller produces an output signal that is relative to the rate of change of the error. The derivative controller, also known as the predictive controller, is mainly dependent on nature. If the error is constant, then the derivative controller will not be active. It performs its function at a fast rate. One of its disadvantages is that it can produce large signals in response to large frequency deviations. The high-frequency error can be due to deviations at the setpoints and the noise-induced in the measurement process (Grobler, 2011). The expression represents derivative control is given in equation 3.52 below.

$$D_{out} = K_d \cdot \frac{de(t)}{dt} \quad 3.52$$

Where:

$D_{out}$  is the derivative control output value

$K_d$  is the derivative controller adjustable gain

$e(t)$  is the error signal (Error=setpoint-measured value)

The aim of implementing the derivative controller is to bring down the output rate concerning the input signal. When an overshoot occurs due to the integral controller, then the derivative controller will decrease the magnitude of the overshoot resulting in system stability. It is more critical to adequately set the value of the derivative gain of the controller. The high value of the derivative gain does reduce the overshoot; however, this might not adequately respond to transient response. This can result in the system's instability state due to the noise signal in error differentiation. The block model of the derivative controller is shown in Figure 3.32 below

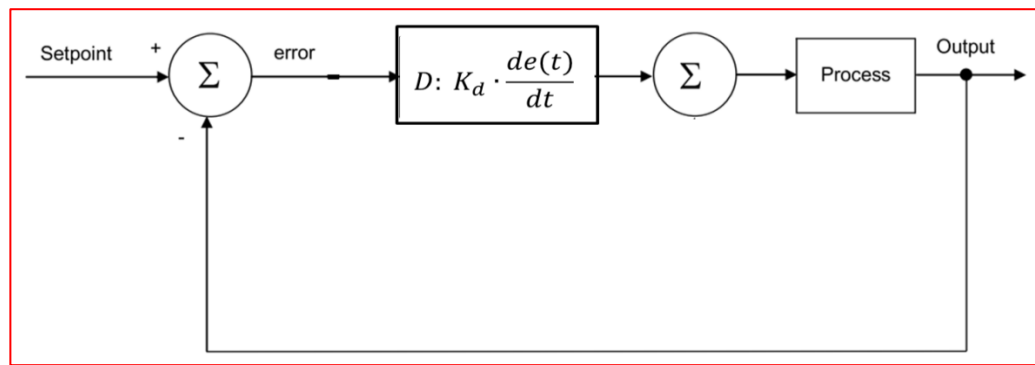


**Figure 3.32: Derivative controller block model** (Grobler, 2011)

To deal with the sensitivity of the derivative controller to noise, a low-pass filter at the measurement part of the controller to reduce the unwanted high-frequency signals. This implementation needs to be done through instrumentation to avoid the low-pass filter canceling out with the derivative control. Another option is to tune the derivative controller to have little loss in the control (Grobler, 2011).

#### 3.4.1.6.4 Full PID controller

PID controller is the combination of all the individual controllers such as proportional, integral, and derivative control. The PID controller can be mathematically expressed as in equation 3.53 below.

$$PID_{out} = P_{out} + I_{out} + D_{out} = K_p e(t) + K_i \int_0^t e(t) \cdot dt + K_d \cdot \frac{de(t)}{dt} \quad 3.53$$

In the PID controller, each part of the control has its own function which is separate from one another. The proportional controller regulates the active error signal it has received, the integral part is used to regulate all the error signals that have passed through the controller while the derivative part of the controller is sensing the rate of change of the error signal. The responsibility of the proportional controller in the event of an error signal received is to reduce the rise time of the signal, increase the signal overshoot, decrease the settling time while decreasing the steady-state error signal. The integral controller also responds similarly with the proportional controller for rising time, overshoot, and steady-state error, and the only difference is the integral controller increases the settling time of the signal. The derivative controller's responsibility is to lessen the error signal rise time, decrease an overshoot, also decrease the settling time while influencing the steady-state error signal. The other combination achieved through the PID controller is the Proportional Integral controller and Proportional Derivative controller. The application of these controllers is in load frequency

control to stabilize the power system frequency. Figure 3.33 below represents the PID controller block diagram (Satyanarayana et al., 2015) and (Grobler, 2011).

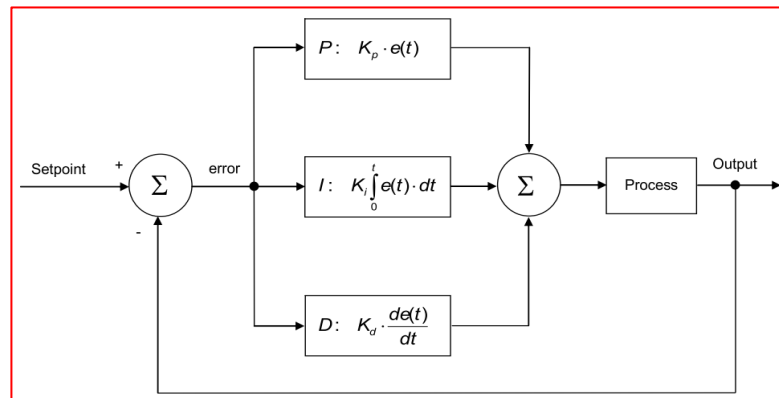


**Figure 3.33:** The full PID controller block diagram (Grobler, 2011)

### 3.4.1.7 Tertiary control

Tertiary control is an additional control system to primary and secondary frequency control which is slower than the other control systems in response to frequency deviations. The function of tertiary control is subjected to the power system and the power plant configuration structure. The operation setpoints of individual power plants can differ based on the economic or merit order power dispatching and generation capacity of each unit, optimizing the overall running cost of the power plants in the network. The tertiary control reference setpoints value are determined by optimal dispatching to meet overall demand, which will be satisfied with the schedule of power dispatching.

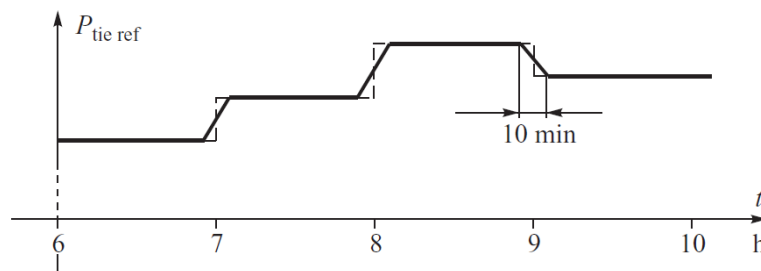


**Figure 3.34:** Changes in power interchange (Jan et al., 2005)

In some areas whereby the independent power producers dominate the power system grid, the system operator needs to determine the supply contracts to source the required primary and secondary reserves needed in the power system grid. This is done in an optimal power dispatching to meet the system constraints based on the power demand and generation capacity. In such a structure, the

tertiary control setpoint of each turbine governors can be manual or automatically adjusted to ensure the following:

- Adequate spinning reserve to contribute to primary control.
- Optimal dispatch of units to contribute secondary control.
- Restoration of the frequency bandwidth of secondary control at a given time.

Tertiary control looks after the actions of secondary control with the primary objective to correct the loading of each generation unit within the power system. The tertiary control is performed through:

- Automatic modification of the reference value of the power feed to the grid of individual units.
- Automatic or manual connection or disconnection of standby generation units of the tertiary control. The standby generation units can be integrated into the power system grid when a need arises through tertiary control manually or automatically within 15 min. In integrating these standby generation units, they need to ensure that the power system frequency is restored to its nominal value.

#### **3.4.2 Application of automatic generator control as a multi-stage control**

Figure 3.35 below illustrates a multi-level control scheme structure where an automatic generator controller is used as the key controller. Considering this Figure 3.35, the generator turbine governing system with an integrated system load is orientated at the lower level. The secondary and tertiary controls are position at a higher level. Since the governing system is installed on the power plant where the generator is located, it then receives all the commands from an external system such as secondary based on the system condition execution.

In the case of executing frequency control and tie-line control, the secondary control sends a signal to primary control to reduce the frequency and net tie-line variations

The role of tertiary control in the multi-level control system is to safeguard a suitable bandwidth of secondary control. Tertiary control is activated after the other two control system due to their configuration being delayed in response time more than the rest of the controllers. Must be slower than both primary and secondary control. The secondary and tertiary control can be used as a Load and Frequency Controller in control algorithms of SCADA–EMS (Energy Management System) to enhance the power's operation through adequate communication required in the energy management system by the system operator. SCADA–

EMS functions also enhances the control system due to its accessibility in a centralized control system.

Figure 3.35 below is equipped with a coordinated universal time (UTC) block UTC with the primary responsibility of measuring the time of the synchronous time based on the synchronous clocks corresponding to the system frequency. Due to power system frequency fluctuates, so synchronous clocks are subjected to an error concerning the integration of the system frequency, which is reduced by intermittently varying the reference value of the frequency.

The frequency regulation is done at the central control center by the system operator at the transmission level. This is done when the synchronous clocks are delayed or ahead, then the correction margin is set to 0.01Hz. The frequency correction will be in effect for a while and the regulation progress will be monitored.

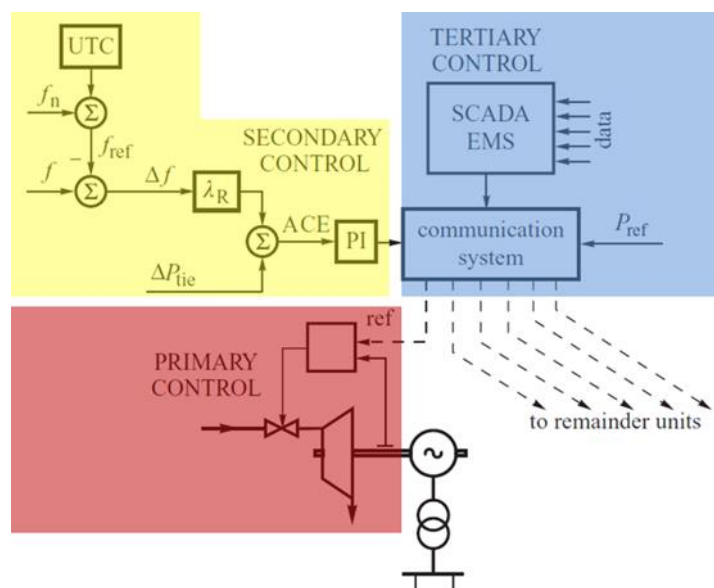


**Figure 3.35: The application of automatic generator controller in an integrated control system (Jan et al., 2005)**

### 3.4.3 Power system defense plan against frequency instability

Power system frequency defense is key to the system grid. The power system defense plan is mainly for unplanned disturbance in the system with real power imbalance or losing generation units producing real power of more 3000MW. The system operator uses this plan which the energy regulator supports. The defense is normally revised from time to time due to the energy production landscape leading towards renewable energy resources.

The defense plan stipulated on the distribution grid code is executed by the system operator who monitors the status of the network. The system operator can only action the defense plan when the system can no longer recover its stability followed by a severe disturbance. When the primary and secondary control can no longer recover the system stability, then the tertiary control takes place. In the event of an increase in load demand or generation unit tripped resulting in power more 3000MW required by the load, then the tertiary control needs to take place by the initiation of under load-shedding protection.

**Table 3.2: Power system frequency defense plan** (Jan et al., 2005)

$f(\text{Hz})$	$\Delta f(\text{Hz})$	Defense type
$f > 51.5\text{Hz}$	1.5 – 2Hz	Trip generation unit through protection
51.3Hz	1.3Hz	Mode of turbine governors (primary control discontinue) changes from power regulation to speed control based on droop characteristic
50.2Hz	200mHz	<ul style="list-style-type: none"> <li>Change the mode of hydro-pump storage system from generation to pump</li> <li>Stop fast start units such as open-cycle gas and diesel generators</li> <li>Activation of primary control set on the large dead zone of <math>\pm 200\text{mHz}</math></li> </ul>
50Hz	0Hz	<ul style="list-style-type: none"> <li>Normal operation</li> <li>Possible activation of primary control on generation units with a small dead zone of <math>\pm 10\text{mHz}</math></li> </ul>
49.8Hz	200mHz	<ul style="list-style-type: none"> <li>Change the mode of hydro-pump storage system from pump to generation</li> <li>Start of fast-start units such as open-cycle gas and diesel generators</li> <li>Activation of primary control set on the large dead zone of <math>\pm 200\text{mHz}</math></li> </ul>
49Hz 48.7Hz	1Hz 1.3Hz	<ul style="list-style-type: none"> <li>Implementation of stage two load-shedding</li> </ul>
48.7Hz	1.3	Mode of turbine governors (primary control discontinue) changes from power regulation to speed control based on droop characteristic
48.5Hz 48.3Hz 48.1Hz	1.5Hz 1.7Hz 1.9Hz	Implementation of stage three load-shedding
47.8	2.5Hz	Tripping of generation units, and system operator required to reconnect back to the grid islanded generation units. Activation of peak load generation units

In order to ensure that the power system does not reach complete collapse, load-shedding stages can be revised to accommodate severe disturbance that might lead to a large power imbalance between the generation and the load.

### **3.4.3.1 Emergency frequency control**

The implementation of emergency frequency control is regarded as the last resort in ensuring the stability of the power system. This type of control involves activation of under-frequency load shedding protection scheme, which is the load demand increase as the power system might not have enough reserved power to provide to the power being demanded by the load. In the event where a bulk load has been disconnected, over frequency protection gets activated to trip out one of the merited generators to restore the frequency to its nominal value. This can only happen when the primary and secondary are unable to recover the frequency, and in the event of low frequency is when the generation units are operating at their maximum as there would be no spinning reserves, the rotation of the turbines are also being slowed down due to the load demand being high.

### **3.4.4 Communication in the power system.**

In the power system monitoring and control, communication is very vital. The role of communication in the power system is for the transmission of information from the local power stations and substations to the SCADA system or control center. The communication system covers data signal transmission, tele-protection, tele-metering, and tele-control (Yousuf, 2018).

#### **3.4.4.1 Communication structure and medium in power system.**

Figure 3.36 below depicts the communication configuration between the local primary plant at the power station or substation and the master station, such as the SCADA system. Power plant status is obtained through the utilization of instrument transformers such as current and voltage transformers. These instrument transformers are used to convert the primary voltage and current to measurable values on the secondary side. The wiring from the instrument transformation is terminated at the junction box (JB), and it gets routed to the relay room to the designated relay panel of concern. The measured signal in the relay panel are converted to values suitable to be transmitted. The measured signal from the relay panel are routed to the Remote-Terminal-Unit via an intermediate distributed frame (IDF). All the signals from the relay panel are hardwired. In the IDF, each status or control signal has its dedicated pair of cable. The control signals from the relay panel are transmitted via the specific communication medium as per the compatibility with RTU (Van Der Walt et al., 2011).

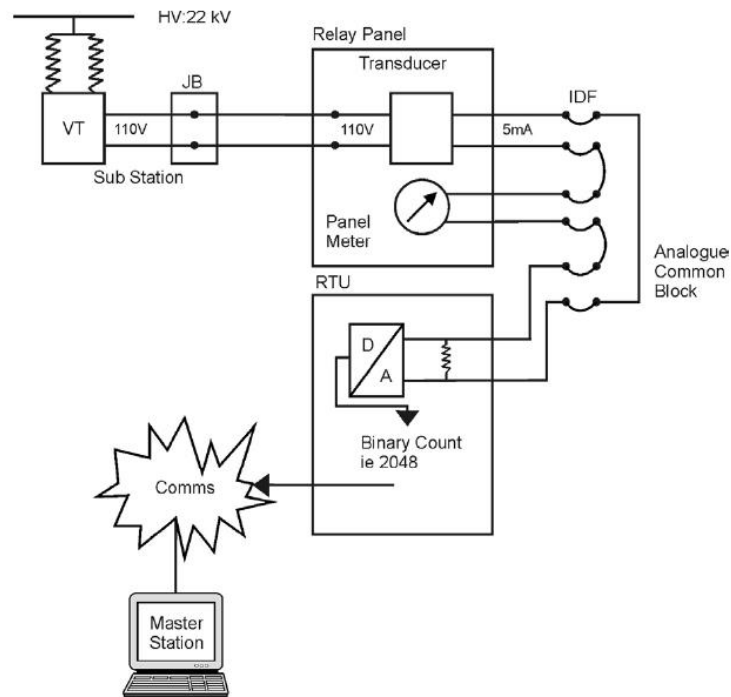


**Figure 3.36: A typical configuration between the primary plant and the control center (Van Der Walt et al., 2011).**

There are various communication mediums found in the power system, these communication mediums include: (Yousuf, 2018):

- Power line carrier
- Dedicated links
- Radio system
- Microwave, and
- Fiber optic cable.
- Packet-switched network
- Substation communication network architecture

#### 3.4.4.1.1 Power line carrier

The power line carrier (PLC) is used to transmit a radio band of frequency signals ranging from 10kHz to 490kHz. 150W of the PLC can be used to transmit signals up to 240Km of distance. The government restricts its frequency range, and it is vulnerable to lightning surges. Another disadvantage is that communication can no be maintained between the control center and the remote site during the disturbance. It is also distance restrictive (Yousuf, 2018).



#### 3.4.4.1.2 Dedicated links

The dedicated links can be pilot wires owned by the utility company or leased from the telephone companies. The advantage of using this type of communication medium is when the remote site is located in areas with a lack of connectivity. In this type of communication medium, the frequency bandwidth ranges between 0-4KHz (Yousuf, 2018).

#### 3.4.4.1.3 Radio system

It is a wireless communication medium where a satellite provides an option to transmit data covering an extensive range. The disadvantages of this method are the delay in signal transmission as well as the cost to install. The data transmission can be done by utilizing conventional radio, trunked radio, or the spread spectrum radio. The frequency can be very high frequency (VHF) or ultra-high frequency (UHF), depending on the country's orientation. Another method within the radio system is cellular radio communication. This method transmits the information via electromagnetic waves between the transmitter and the receiver. Figure 3.37 below illustrates the configuration of the cellular radio communication system. Cellular radio communication is categorized as the mobile communication system, therefore is network can be the mobile telephone switching office (MTSO), or the mobile switching center (MSC), or the public switched telephone network (PSTN) (Yousuf, 2018) and (Chauhan et al., 2017).

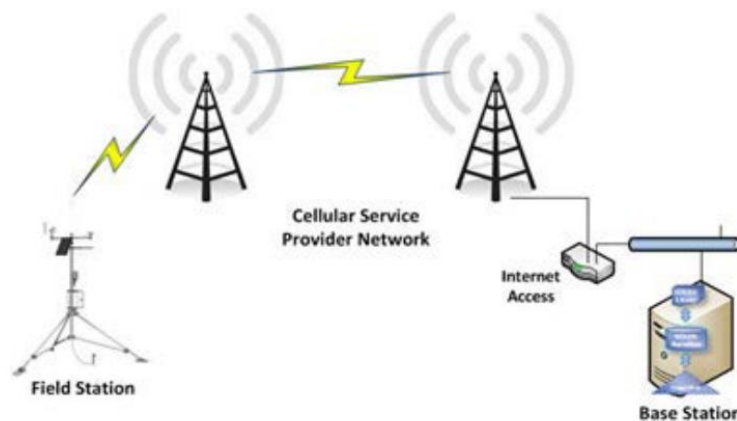


**Figure 3.37: Cellular radio communication configuration system (Yousuf, 2018).**

#### 3.4.4.1.4 Microwave system

A microwave system is also a radio signal transmission in the range of 150MHz to 20GHz. The disadvantage of this communication medium is that it is possible to a line of sight between the antennas, and it is subject to atmospheric

conditions. The delay time between the adjacent antennas can be up to 100 milliseconds before the signal can be transmitted where a modem is used. (Yousuf, 2018).

#### 3.4.4.1.5 Fiber optic cable

Fiber optic system is the latest promising technology in data transmission in the power system control and protection as it allows large data transportation frequently and the real-time communication is improved with its quick response. Its disadvantage is its installation cost, which is outweighed its benefits. Some of the fiber optic system properties include its high bandwidth, security is guaranteed, immune to electromagnetic interferences, and low attenuation (Yousuf, 2018) and (Chauhan et al., 2017).

#### 3.4.4.1.6 Packet-switched network (PSN)

This communication network organizes the data to be transmitted in small packets through a low-power ultrahigh-frequency (UHF) spread spectrum, and its typical frequency is about 935MHz. The organized data includes the IP address of the source, the IP address of the destination, and other unique data identifiers. This communication medium uses the computerized data transmission network to send digital information through low-power radios. It is used on local networks and the internet for real-time supervisory control and data acquisition (SCADA) and energy management systems (EMS). There is no physical link between the source and the destination in this configuration, as shown in Figure 3.38 below.



**Figure 3.38: Packet-switched network configuration (Yousuf, 2018).**

#### 3.4.4.1.7 Substation communication network architecture.

This is a modern power system communication method that can be divided into three levels, and the first level is the local station level where Intelligent Electronic Devices (IEDs) are used to performed power system either control or protection functions. Level 1 can also consist of Programmable Logic Controllers (PLCs), which also perform either control or protection functions. Level 2 is also local-based, and it consists of a substation server where power system monitoring and control occur. Level 3 is the control server, which oversees the entire system

operations and control. The communication between the control center server and the local station can be achieved by using a fiber distributed data interface or local area network (LAN) Ethernet to achieve substation automation. Figure 3.39 below shows the configuration of the substation communication network architecture (Yousuf, 2018).

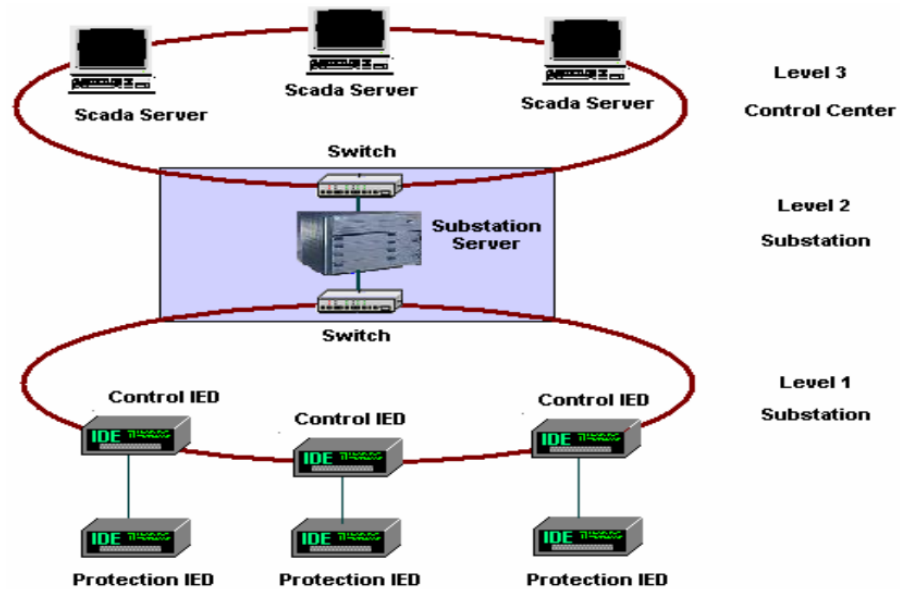


**Figure 3.39: Substation communication network configuration (Yousuf, 2018).**

The power system controllers or operators need to oversee the overall system and see the statuses of the apparatus. The automation communication protocol between the power plant and the master station has been standard to IEC 61850. The latest control and protection IED of intelligent electronic devices used in substations are capable of communication using IEC 61850, and in most parts of the world, this communication protocol is being implemented.

#### 3.4.4.2 Power system communication protocols.

In the power system communication hierarchy, various communication protocols are used. The protocol enables the ability for the master station to communicate and automatically retrieve data from the remote station. Communication protocols also enable the control local or remote and manually or automatically (Das & Kanabar, 2015). These protocols were developed to achieve multivendor interoperability and to simplify data communication commissioning. The commonly used communication protocols in the power system include the Modbus and the DNP3 protocol (Mohagheghi et al., 2009). The emerging communication protocol with advanced technology and communication is IEC

61850. The interoperability and interchangeability is guaranteed from different vendor complying to the standard. The communication has been standardized irrespective of the device manufacture (Mohagheghi et al., 2009).

#### 3.4.4.2.1 Modbus communication protocol

Modbus communication is the messaging protocol used for client/server between the connected devices on the same network. The messaging can be a query or a response type or broadcast/no response type. This type of communication can be used for remote operation initiation. Modbus protocol can be configured in three different ways in transmission protocol (Mohagheghi et al., 2009):

- Asynchronous Serial Transmission: this is for serial connection where RS-232,422 or 485 connection wire is used. Fiber and radio connection also forms part of the Asynchronous Serial Transmission. This configuration has two modes of transmission, the Modbus RTU and the Modbus ASCII. Modbus RTU is regarded as the binary representation of data, which is faster processing and is used under normal operation. While the Modbus ASCII is used for test purposes and is human-readable.
- TCP/IP over Ethernet
- Modbus Plus:

The Modbus protocol configuration is shown in Figure 3.40 below. The diagram below in Figure 3.40 shows that the different transmission configuration protocols can be used as gateways in a single communication network.

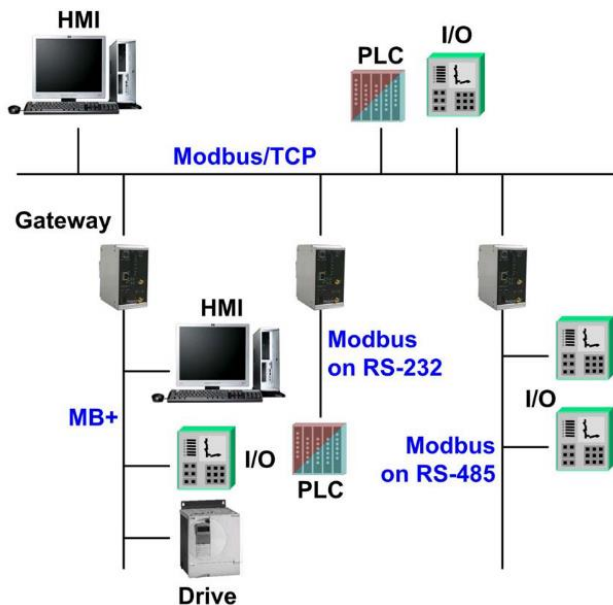


**Figure 3.40: Modbus implementation configuration (Mohagheghi et al., 2009).**

#### **3.4.4.2.2 DNP3 communication protocol**

The DNP3 protocol is used between the client station, RTUs, and other IEDs. This protocol was initially developed for the SCADA system to acquire information and issue commands between the separate physical computing devices. However, it is now widely used in power systems, water infrastructure, oil, gas industries etc.

The DNP3 is used to transmit small packets of data sequentially and reliably. Long messages are broken into multiple small packets for reliable data transmission. This helps to minimize the control errors.

#### **3.4.4.2.3 IEC 61850 communication protocol**

The IEC 61850 is an advanced communication standard used in power systems for substation automation systems. The communication within the substation environment is divided into three levels, as illustrated in Figure 3.41 below:

- Process level: this is where intelligent sensors and actuators are located, including the recording of sampled value exchange.
- Bay/Unit level: this is the control or protection device orientation.
- Substation level: The control desk, system operators, and interfaces with nearby substations are performed.

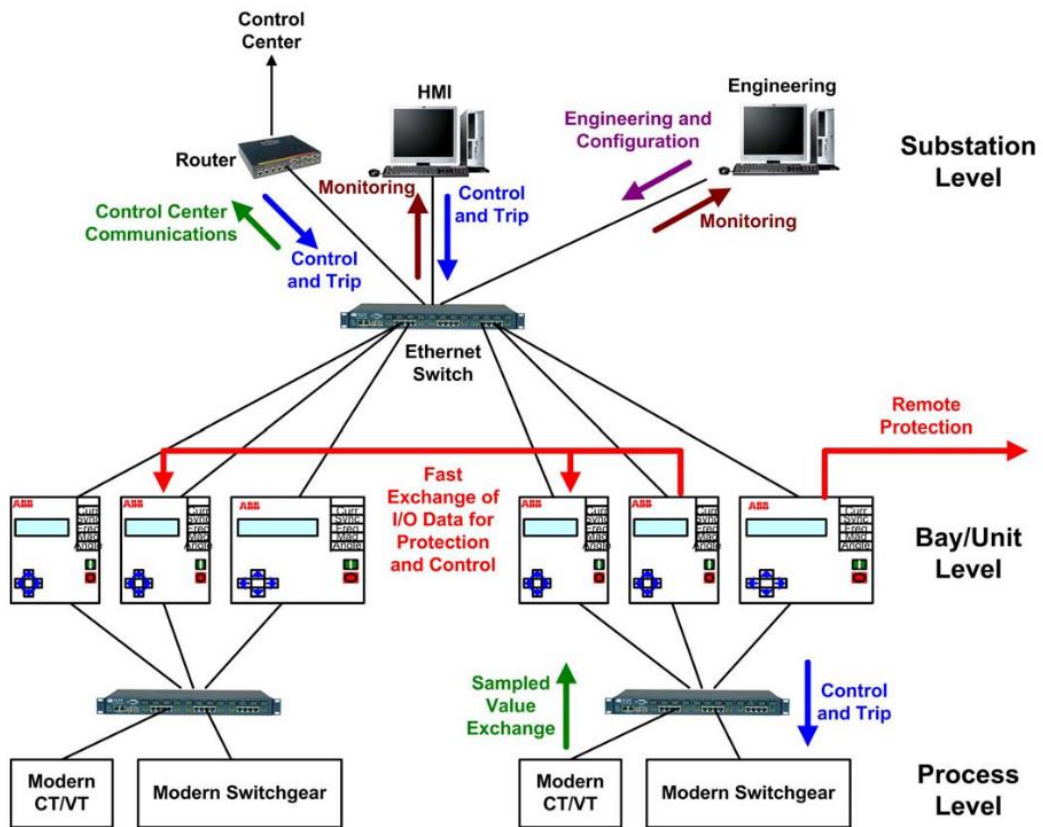


**Figure 3.41: IEC 61850 standard communication architecture (Mohagheghi et al., 2009).**

In the IEC 61850 standard, the operation of the control or protection devices is broken into smaller units called Logical Lodes. These units are objects that are defined in the object-oriented context of the IEC 61850 standard. The unique identification of the logical nodes in the IEC 61850 standard is the advantage over the legacy protocols. In the IEC 61850 standard, there are 92 logical nodes defined to correspond to protection, control, metering, and monitoring functions, including the power system physical devices such as circuit breaker and transformers. Figure 3.42 below shows the logical node representation following the basic IEC 61850 architecture (Mohagheghi et al., 2009) and (Das & Kanabar, 2015).

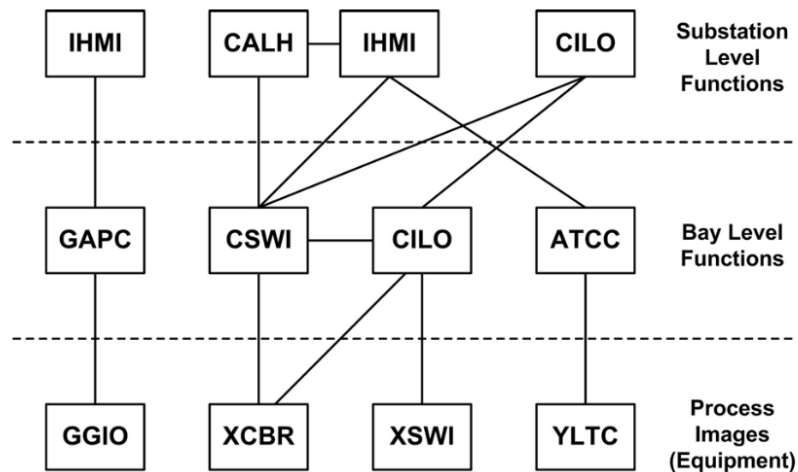


**Figure 3.42: IEC 61850 standard logical node representation (Mohagheghi et al., 2009).**

In Figure 3.42 above, examples of logical nodes are shown. At the substation level: IHMI is human-machine interface, CALH is alarm handler, CILO is interlocking. At the bay/unit level: GAPC is generic automatic process control, CSWI is circuit breaker control, ATCC is automatic tap changer controller. At process level: GGIO is generic input-output, XCBR is circuit breaker, XSWI is isolator, and YLTC is tap changer.

Each logical node has data objects which belong to the Common Data Class. An IED (logical device) can have several logical nodes, and the logical nodes can be either be for measurement, status, or control.

In practice, the Sampled Values information gathered from the primary power plant such as voltages and currents, is transmitted to the protection and control IEDs through client/server or GOOSE peer-to-peer communication. The communication medium used is the local area network (LAN) ethernet link. The practical IEC 61850 standard configuration structure is shown in Figure 3.43 below (Mohagheghi et al., 2009) and (Das & Kanabar, 2015).

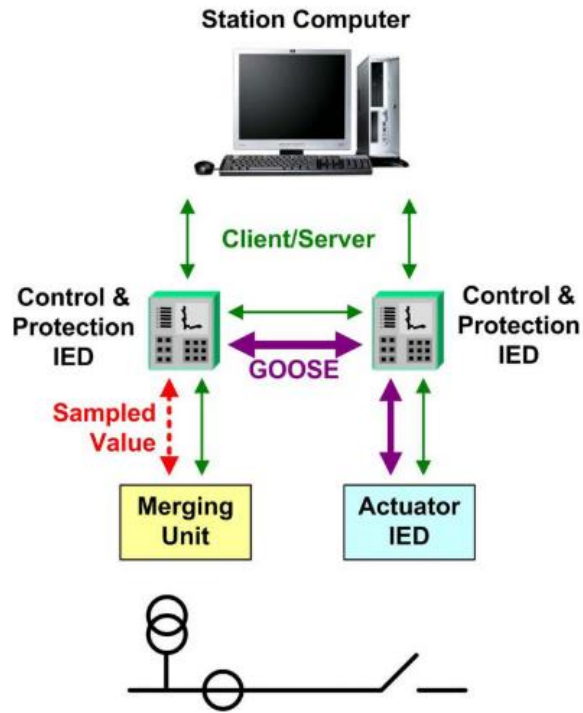


**Figure 3.43:** The practical IEC 61850 standard communication structure (Mohagheghi et al., 2009).

### 3.5 Conclusion

This chapter covered the theoretical overview of the power system frequency control strategies ranging from primary control, secondary control, tertiary control to emergency control. The conventional frequency control schemes utilized in the power system grid and their supporting theories are discussed. The configuration of the frequency control scheme in the power system is also described. The communication medium and protocols used between the primary power plant and the control center have been discussed in this chapter.

The next chapter described the modeling and simulation analysis of the selected network under the steady-state and dynamic-state conditions.



## CHAPTER FOUR

### MODIFIED IEEE 14 BUS NETWORK MODELLING AND ANALYSIS

#### 4.1 Introduction

Frequency stability is crucial in the power system network, and it needs to be maintained within the operating range. This is done to ensure that the quality and security of supply to the end-users are maintained. In the conventional power system, synchronous generators are utilized for based load supply. These generators are equipped with various control systems such as speed governors (GOV), automatic voltage controllers (AVR), and power system stabilizers (PSS). The automatic voltage controller is responsible for controlling the generator's excitation, and the power system stabilizers are an additional control loop to the AVR for the stability of both the rotor angle and the voltage at the stator terminals of the generator. The speed governor regulates the active power. Its responsibility is to balance the active power between the load of the generations, resulting in the frequency of the power system grid maintained at its nominal value of 50Hz. Frequency stability is one of the critical variables to be controlled in the power system. The consequences of not being controlled are dire as the load equipment would be operating out of their frequency range. This could lead to damage as well as system collapse. During steady-state, the acceptable operating frequency range is between 49.5Hz to 50.5Hz, and this is expected to be carried out through a speed governing system (NERSA, 2019a).

This chapter aims to demonstrate that the conventional speed governors are not good enough to maintain frequency stability when various disturbances than can occur in the power system network. To supplement the active power, wind turbine generation system are utilized as the power reserves. The integration of aggregated wind turbine generators is considered in the modeling. These wind turbines are not primarily supplying any active and reactive power in the grid. Their role is to compensate for active power during load change conditions to maintain the power grid frequency. To perform the event analysis and understand the power system operation for the case studies, a modified IEEE 14 bus network is modeled in DIgSILENT power factory software. The analysis is performed according to the flowchart shown in Figure 4.1 below.

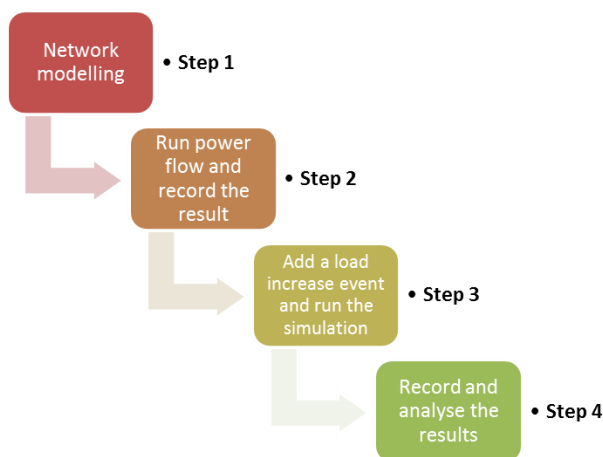


**Figure 4.1 Workflow stages**

The IEEE 14 bus system network consists of the following interconnected components as:

- 15 overhead lines
- 4 transformers
- 11 loads
- 14 buses / nodes
- 5 synchronous generators

The IEEE 14 bus system network consists of two synchronous generators and three synchronous reactive power compensators (connected on buses 3, 6, and 8). The three synchronous generators that were previously generating reactive power are now modified to produce both active and reactive power (G3, G6, and G8). The modifications are done to increase the total generation capacity to accommodate the load growth and have adequate spinning generation reserves.

The modified IEEE 14 bus network is a multi-level voltage grid system that consists of 132kV, 33kV, and 11kV. 132kV level denotes the sub-transmission portion; both 33kV and 11kV are regarded as part of the distribution grid. Grid code compliance is essential when developing the power system Grid. The modifications made to the IEEE 14 bus system are in line with South Africa Transmission and Distribution grid code / IEEE and IEC standards. (NERSA, 2019b) is the South African Network Grid Code standards, which outlines both frequency and voltage tolerances during normal operation. The frequency is set to be between 49.5Hz to 50.5Hz and the voltage is set to be 0.95pu to 1.05pu. Figure 4.2 below shows the modified IEEE 14 bus network with all the associated elements.

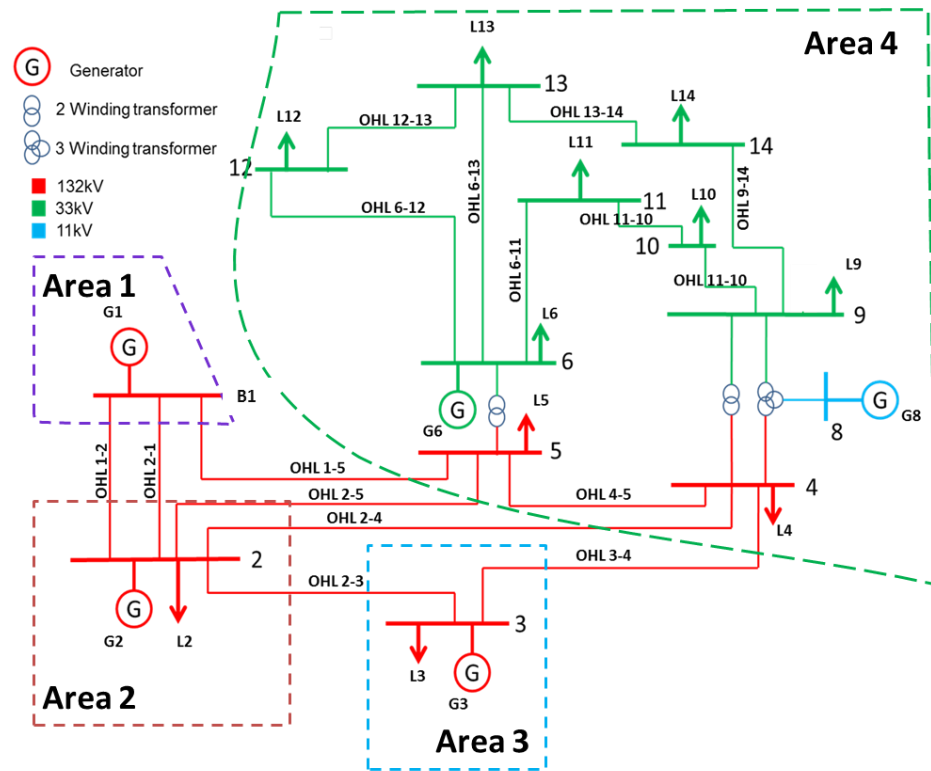


**Figure 4.2: Modified IEEE 14 bus power system network**

The IEEE 14 bus system network data of the above-illustrated network is presented in Tables 4.1, 4.2, and 4.3 below. Table 4.1 below represents the bus data with entail the bus types, the active and reactive power of the load, and the generator as well as the voltage rating in real-time and in per-unit form.

**Table 4.1: Bus, generator, and load data**

Bus Data								
Bus no	Type	$V_{pu}$	V (kV)	Generator			Load demand	
				(MW)	(MVA <sub>r</sub> )	MVA	P(MW)	Q(MVA <sub>r</sub> )
1	Slack	1.03	132	163	-6	200	-	-
2	P-V	1.01	132	42	42.4	60	21.7	12.7
3	P-V	1.01	132	31	20	60	94.2	19
4	P-Q	1.00	132	-	-	-	47.8	-3.9
5	P-Q	0.99	33	-	-	-	7.6	1.6
6	P-V	1.05	33	19	16.5	30	11.2	7.5
7	P-Q	1.03	1	-	-	-	-	-
8	P-V	1.04	11	19	16.5	30	-	-
9	P-Q	1.02	33	-	-	-	29.5	15.9
10	P-Q	1.02	33	-	-	-	9.0	5.8
11	P-Q	1.02	33	-	-	-	3.5	1.8

12	P-Q	1.02	33	-	-		6.1	1.6
13	P-Q	1.01	33	-	-		13.5	5.8
14	P-Q	1.00	33	0	0	120	14.9	5.0
<b>Total</b>				<b>274</b>	<b>89.4</b>	<b>380</b>	<b>259</b>	<b>72.82</b>

The transmission line data is given in Table 4.2 below. These parameters are presented as actual impedance in rectangular and in polar form. The rated line voltage is also given as well as termination at the buses. The transformer data is given in Table 4.3 below, which comprises the transformer reactance and the tap ratio. The termination of the transformer as well as the voltage rating (LV and HV) are included.

**Table 4.2: Transmission and distribution lines data**

Transmission and distribution line Data						
Line	From Bus	To Bus	V (kV)	Line impedance		Susceptance
				R in $\Omega$	X in $\Omega$	B in S
OHL 1-2	1	2	132.0	6.754	20.620	151.5152
OHL1-5	1	5	132.0	9.414	38.862	282.3691
OHL2-3	2	3	132.0	8.188	34.494	251.3774
OHL 2-4	2	4	132.0	10.125	30.722	214.6465
OHL 2-5	2	5	132.0	9.923	30.297	195.1331
OHL 3-4	3	4	132.0	11.676	29.800	198.5767
OHL 4-5	4	5	132.0	2.326	7.337	73.4619
OHL 6-11	6	11	33.0	1.0343	2.166	0.0000
OHL 6-12	6	12	33.0	1.338	2.786	0.0000
OHL 6-13	6	13	33.0	0.720	1.417	0.0000
OHL 9-10	9	10	33.0	0.346	0.9207	0.0000
OHL 9-14	9	14	33.0	1.384	2.944	0.0000
OHL 10-11	10	11	33.0	0.894	2.092	0.0000
OHL 12-13	12	13	33.0	2.406	2.177	0.0000
OHL 13-14	13	14	33.0	1.861	3.790	0.0000

The transformer data is also essential when modeling the network. Transformer data such as impedances, transformer ratio helps to understand the power flow through the transformer as well as protection settings computation. The

transformer is shown in Table 4.3 below. The per-unit data is computed using 100MVA base power.

**Table 4.3: Transformer data**

Transformer	MVA	HV (kV)	LV (kV)	R (PU)	X (PU)	Turns ratio
TRFR 4-7	150	132	1	0.0	0.20912	0.978
TRFR 4-9	100	132	33	0.0	0.55618	0.969
TRFR 5-6	100	132	33	0.0	0.25202	0.932
TRFR 7-8	150	11	1	0.0	0.17615	0.000
TRFR 7-9	9	33	1	0.0	0.11001	0.000
TRF WT Type 3	100.5	33	0.69	0.001	0.059992	

## 4.2 Modeling of the modified IEEE14 bus system and its associated control systems.

The power system consists of components such as generators, transmission lines, composite load, and reactive power compensators. The configuration of these components may differ based on the application. The network is modeled on DIgSILENT simulation software with all the parameters presented in Table 4.2, 4.2, and 4.3. The current IEEE 14 bus network model is generic and suitable for voltage stability analysis, therefore to fulfill the study's objectives, the load modeling needed to be edited such that it is frequency-dependent. This is done to investigate the frequency stability in the power system under different contingencies. The power system components and associated control systems needed to be modeled to respond quickly to frequency disturbing events as opposed to voltage.

### 4.2.1 Synchronous generator model parameters

The input parameters configured on the synchronous generator 1 model in DIgSILENT are captured in Figure 4.3 below. The data is captured as per Table 4.1 above. The process of capturing the data is the same for all the other four generators. This type of generator is set as the “reference machine” since it is defined as a slack generator. To view the parameters of the generator, double click on it, and select load flow.

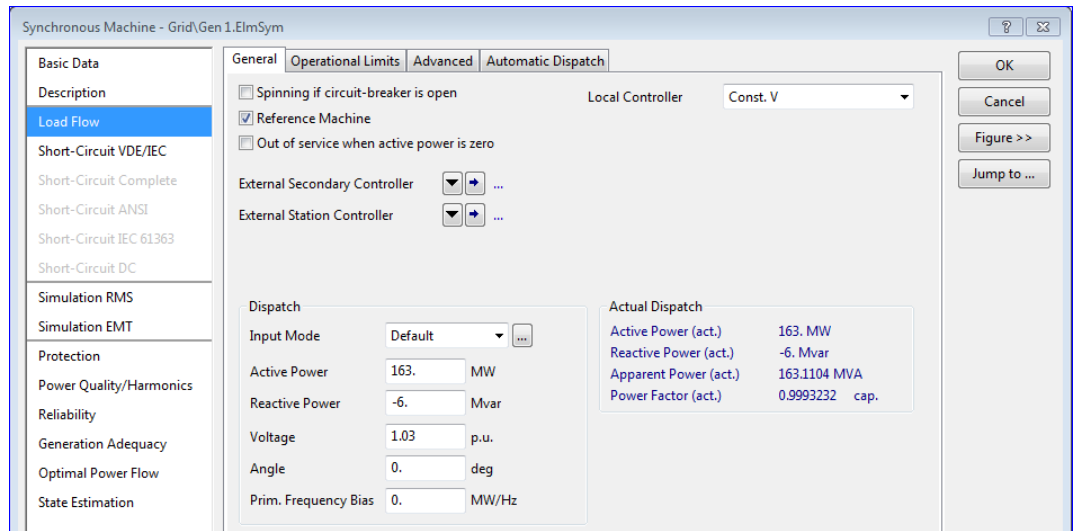


**Figure 4.3: Synchronous generator parameters**

The generation plant is equipped with a control system such as a speed governing system (GOV), automatic voltage regulator (AVR) as well as the power system stabilizer (PSS). The purpose of the governing system is to regulate the active power between the load and generation. Feedback is used to send the error signal to the turbine such that the valve positions can change accordingly based on the error signal sent by the governor. This operation is called a primary active power control. The reactive power is controlled through AVRs and power system stabilizers to maintain the power system voltage at the busbars. The conventional generation systems are equipped with the three control system as shown in Figure 4.4 below. The four-part system includes a generator (GEN), governor (GOV), power system stabilizer (PSS), and automatic voltage regulator or excitation system (AVR).

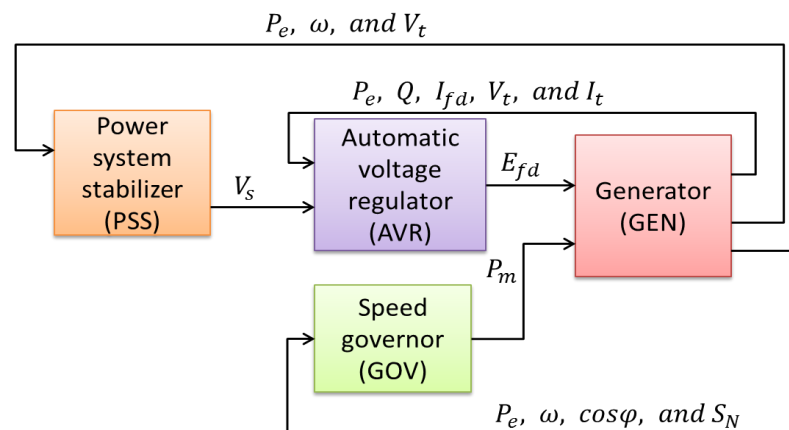


**Figure 4.4: Generation system model frame structure** (Zhao et al., 2013).

In the block diagram shown in Figure 4.4 above,  $V_s$  is an output voltage signal of the power system stabilizer,  $E_{fd}$  and  $I_{fd}$  are the excitation voltage and current,

$P_m$  is the mechanical power signal from the governor,  $P_e$  and  $Q$  is the active and reactive power,  $V_t$  and  $I_t$  is the voltage and current at bus terminals,  $\cos\varphi$  is the power factor and  $S_N$  is the nominal apparent power (Zhao et al., 2013).

The generation control system plays a huge role in ensuring that the power is operating within limits even when it is subjected to a disturbance. This can only be achieved through the proper integration of the generation control system. The absence or improper integration of the generation control system can cause the system to complete a power system instability. The control systems within the generation plant need to be modeled to fulfill the grid code requirement during dynamic analysis.

#### 4.2.2 Transmission line model parameters

For the transmission line equivalent circuit data as indicated in Table 4.2 above, the model of each line will be different as their parameters are not the same. The parameter capturing on DigSILENT for the other lines will be the same as the line 1-5 parameter capturing, hence other transmission and distribution lines data capturing process will not be shown. Figure 4.5 below illustrated the data for the transmission line below bus 1 and 5. To view the line data as shown in Table 4.2 above, double click on the line and select simulation RMS.

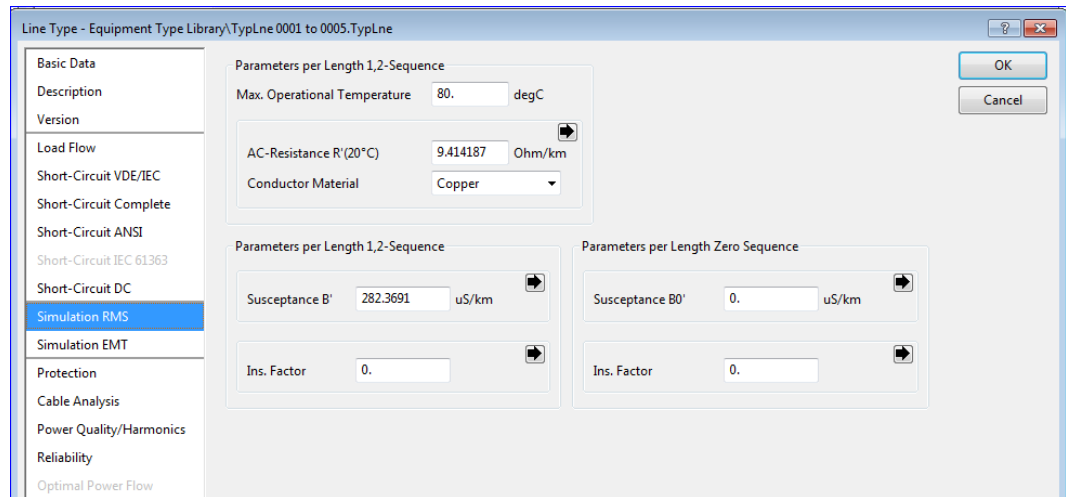


**Figure 4.5: Transmission line data (line 1-5)**

#### 4.2.3 Power transformer model parameter

The use of transformer 5-6 in the model is to step down the system voltage from 132kV to 33kV. The data of transformer 5-6 is shown in Figure 4.6 below. This transformer is connected between bus 5 and bus 6. To view the data of the transformer, double-click on the elements, and the element window will pop-up. Under basic data-general, under type, click the right-pointing direction, and the

transformer data will pop-up. This process is the same for the other two transformers.

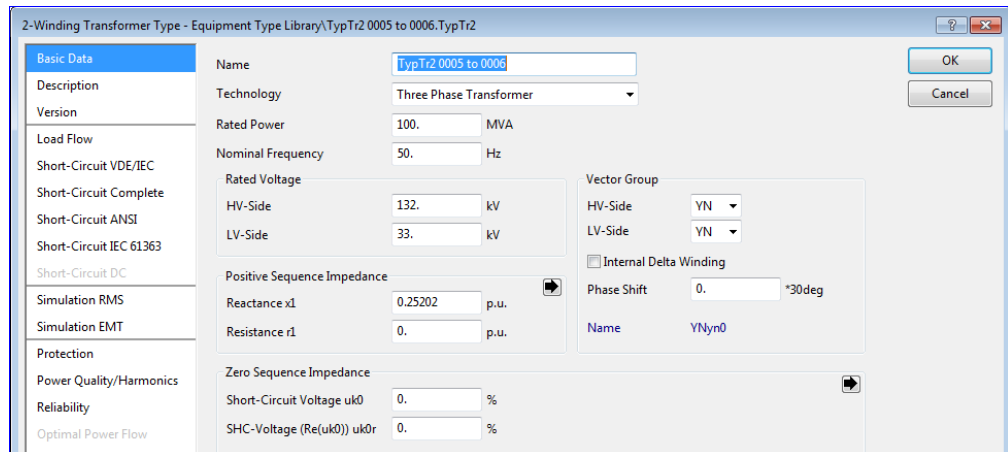


**Figure 4.6: Transformer parameters**

#### 4.2.4 Frequency-dependant load model

The load model computed on DigSILENT is voltage-dependent; therefore performing a frequency-based study can be erroneous as the impact of the load will mostly affect the system voltages rather than frequency. The selection of the type of load is critical, hence frequency dependant load needs to be model. The frequency dependant load is achieved through multiplying either the polynomial or exponential load model by the factor  $(1 + \alpha_f(f - f_0))$  and  $\Delta f = f - f_0$ . Equation 4.1 and 4.2 below are the exponential load model that has been multiplied by the factor indicated above to achieve a frequency-dependent load. Where  $\alpha$  is the frequency sensitivity parameter,  $f$  is the actual system frequency while  $f_0$  is the rated frequency (Jan et al., 2005) and (Hachmann et al., 2020).

$$P = P_0 \left( \frac{V}{V_0} \right)^\alpha \left( 1 + \Delta k_{Pf} \left( \frac{\Delta f}{f_0} \right) \right) \quad 4.1$$

$$Q = Q_0 \left( \frac{V}{V_0} \right)^\beta \left( 1 + \Delta k_{Qf} \left( \frac{\Delta f}{f_0} \right) \right) \quad 4.2$$

The coefficient factors are presented in Table 4.5 below. The approximated coefficient was Tabled by (Jan et al., 2005) according to different types of load, this includes the residential, commercial, and industrial load.

**Table 4.4: Load model sensitivity coefficients(Jan et al., 2005)**

Type of load	$\Delta k_{Pf}$	$\Delta k_{Qf}$
--------------	-----------------	-----------------



Residential	0.7 to 1	-1.3 to -2.6
Commercial	1.2 to 1.7	-0.9 to -1.6
Industrial	-0.3 to 2.9	0.6 to 1.8

The frequency-based load model has to reflect the realistic application approach where all load types are considered. To do this, the average sensitivity coefficients for active and reactive power are chosen as shown in Figure 4.7 below where the  $\Delta k_{Pf} = 0.5$  and  $\Delta k_{Qf} = 0.5$ . In the load modeling settings shown in Figure 4.7 below  $\beta = 0.96$  and  $\alpha = 0.62$ . were chose. The aim of choosing these parameters is to set to load to be very sensity to load event that influences the frequency of the power system grid.

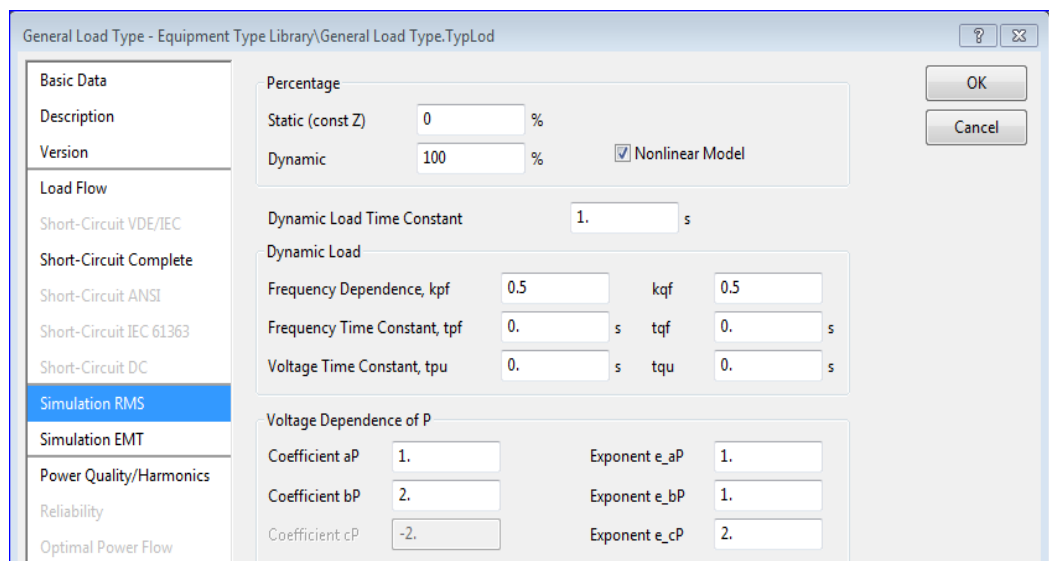


**Figure 4.7: Frequency-dependent load model parameters**

Figure 4.8 below represents the modified IEEE 14 bus network configured on DIgSILENT simulation software. Area 1, Area 2, and Area 3 represent the sub-transmission part of the network with a voltage level of 132kV. Area 4 represents the distribution section of the network, and this is categorized based on the bulk load connected to this area and the voltage level. The color coding is shown based on the voltage levels. 132kV level is represented by red color, 33kV is green, 11kV is illustrated in blue, 1kV is present by orange color, and 690V is presented by army color.

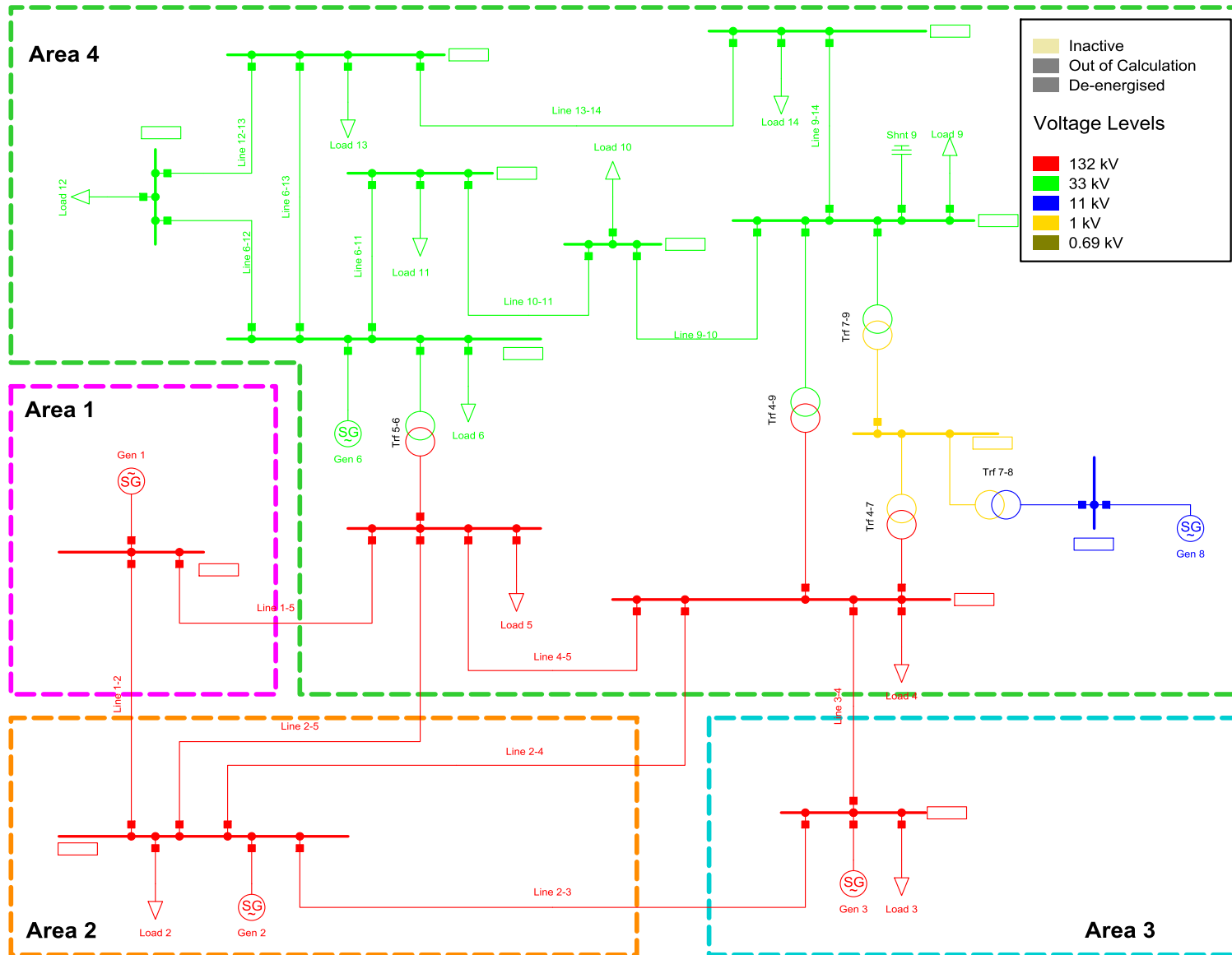


Figure 4.8: Modified IEEE 14 bus network in a de-energized state

The power system analysis is a broad study that focuses on the impact of various parameters on network stability. Two states of analysis need to be assessed, which include the steady-state and dynamic state. The steady-state analysis is when the power system is operating with no disturbances. At steady-state, the generated active power is equal to the sum of active load power demand and system power losses; hence, the system's frequency is at its nominal value of 50Hz. The method used to perform this state of analysis is the power flow analysis (Venkatasubramanian & Tomsovic, 2005). However, the dynamic state is when the system is subjected to a disturbance due to load changes, planned and unplanned power outages due to faults, and equipment maintenance. When the power system is subjected to a disturbance, the voltage and frequency will change. The magnitude of the frequency and voltage deviation also depends on the type and severity of the disturbance. These types of contingencies are performed during dynamic-state analysis. However, before the dynamic analysis is performed, steady-state analysis is initiated to analyze the system before any disturbances.

### 4.3 Steady-state analysis and results analysis

During steady-state analysis, power flow equations are used to determine the magnitudes of bus voltages as well as their angles, including the transmission line currents. The bus voltages need to be maintained within the strict grid code tolerances. There is an allowable normal operational voltage in the power system which ranges from 0.95 to 1.05pu. The allowable continuous operating frequency is between 49.5Hz and 50.5Hz (NERSA, 2019b).

Various methods can be used to perform load flow/ power flow, to analyze the modified IEEE 14 bus network illustrated in Figure 4.8 above, the Newton-Raphson algorithm is used on DlgSILENT power system simulation software. The iterative load flow method is highlighted with a red box in Figure 4.9 below.

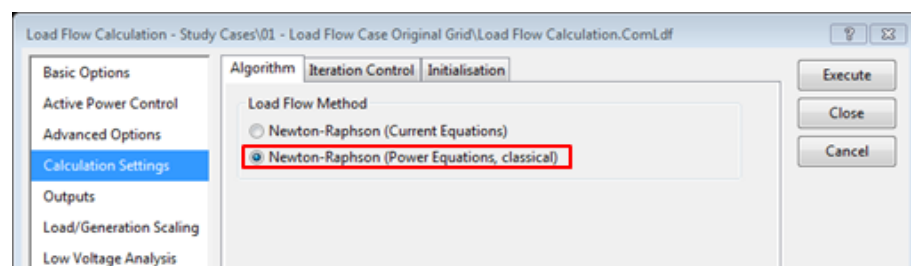






**Figure 4.9: Selected load flow method**

During the execution of load flow, the network parameters were monitored. Table 4.5 below shows the voltage profile during steady-state analysis. From the Table

4.5 below, the bus bar voltages are indicated. It can be noted that bus 4 have a less voltage while bus 1 is shown with the highest voltage. All these bus voltages are within the acceptable normal operating range of +/-5%, as illustrated in (NERSA, 2019b) which is the South Africa Network Grid Code. In the Table below, the voltage tolerance is set to monitor the voltage to its acceptance tolerance. The maroon color legend within the Table indicates the voltage deviation of all busbars compared from the rated bus voltage.

**Table 4.5: Network bus voltage profile in steady-state**

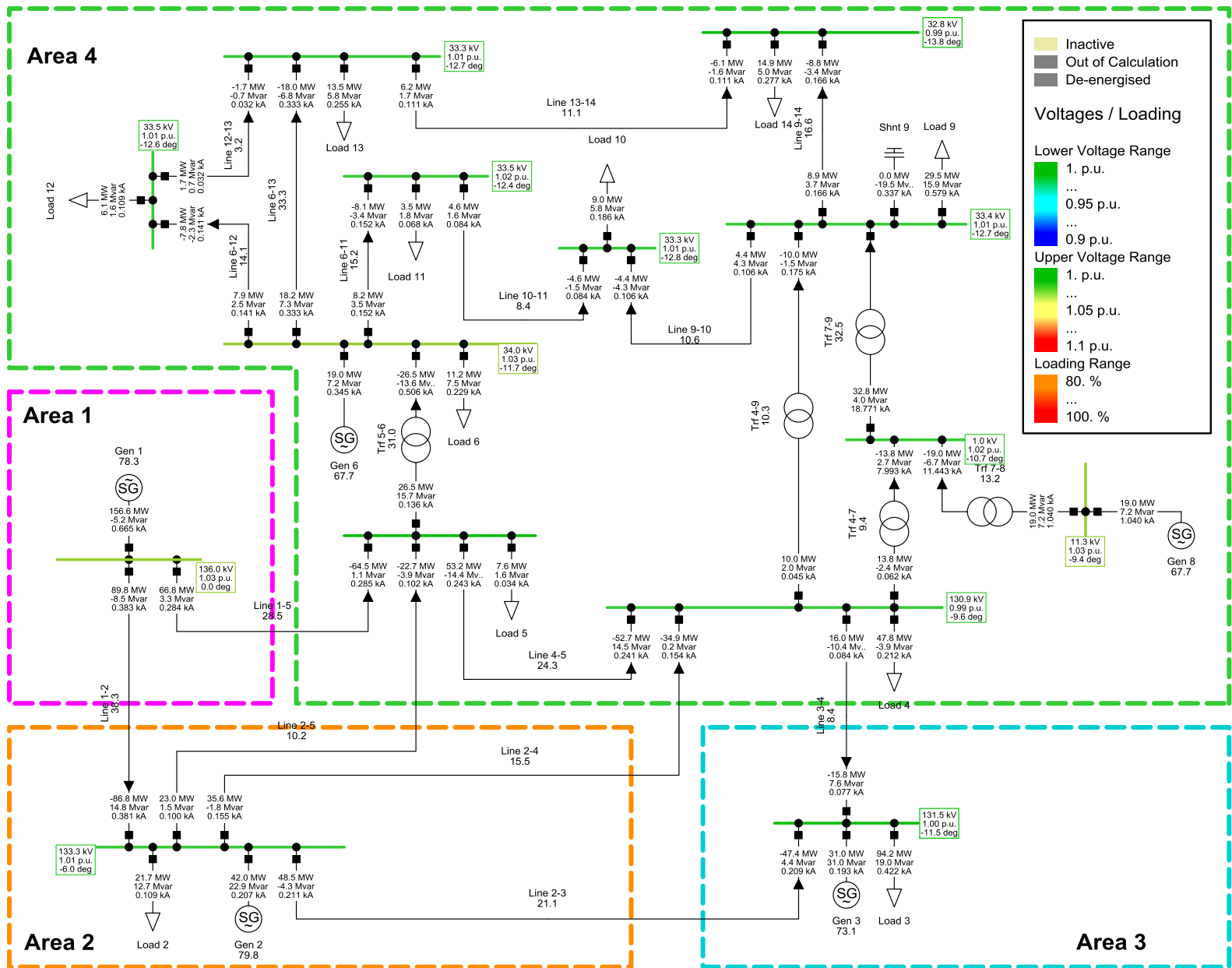
					DIGSILENT		Project:			
					PowerFactory		Date: 2021/04/22			
					2020 SP3					
Load Flow Calculation					Complete System Report: Voltage Profiles					
AC Load Flow, balanced, positive sequence			Automatic Model Adaptation for Convergence			No				
Automatic tap adjustment of transformers			Max. Acceptable Load Flow Error							
Consider reactive power limits			Bus Equations (HV)			1.00 kVA				
			Model Equations			0.10 %				
Grid: Grid		System Stage: Grid			Study Case: 01 - Load Flow Case Origin			Annex: / 1		
rtd.V		Bus - voltage			Voltage - Deviation [%]					
[kV]		[p.u.] [kV] [deg]			-10		-5		0 +5 +10	
Bus 1	132.00	1.030	135.96	0.00						
Bus 10	33.00	1.008	33.28	-12.82						
Bus 11	33.00	1.015	33.50	-12.39						
Bus 12	33.00	1.014	33.46	-12.63						
Bus 13	33.00	1.009	33.29	-12.73						
Bus 14	33.00	0.993	32.75	-13.79						
Bus 2	132.00	1.010	133.32	-6.01						
Bus 3	132.00	0.996	131.48	-11.53						
Bus 4	132.00	0.991	130.85	-9.60						
Bus 5	132.00	0.992	130.98	-8.19						
Bus 6	132.00	0.992	130.98	-8.19						

Grid: Grid		System Stage: Grid			Study Case: 01 - Load Flow Case Origin   Annex:					/ 2
	rtd.V [kV]	Bus - voltage [p.u.]	voltage [kV]	[deg]	-10	-5	Voltage - Deviation [%]			
							0	+5	+10	
Bus 7	33.00	1.029	33.97	-11.68						
Bus 8	1.00	1.017	1.02	-10.68						
Bus 9	11.00	1.025	11.28	-9.45						
	33.00	1.013	33.44	-12.68						

The color coding in DigSILENT helps to easily identify a part of the network that requires attention. Figure 4.10 below shows is the network diagram during load flow. The power flow direction is depicted on the network diagram below. The color legend are used to indicate the state of healthiness of the network. Tolerances are set to monitor the operation of the network.

In Figure 4.10 below, it can be noted that the normal operating voltage range must be between 0.95pu to 1.05pu. The extreme voltage tolerance is set to be between 0.9pu to 1.1pu. At 0.95pu, an alert color legend that is light blue indicates the low voltage state's potential at the particular busbar. The yellow colour in the legend is used as an alert indication of approaching an overvoltage state with an approximate voltage of 1.05pu. Another essential feature that is presented in the color legend is the system loading. Orange color is an alert when the loaded equipment is at approximately 80% of its maximum rating. The red color indicates that the equipment is in danger and it needs immediate attention and the loading percentage is 100%.

When the load flow simulation was executed, the network was found to be stable. The busbars' voltages were measured and found to be within the acceptable normal operating range (0.95pu-1.05pu). The loading of the lines, transformers, and generators is under 80%. The power flow direction is also indicated in the network to realize the amount of power exported from one area to another. The power system has been divided into four areas. Dividing the network into these areas has been done to monitor the power system dynamics per area adequately.





The modified IEEE 14 bus network grid summary results during steady-state load flow operation are shown in Table 4.6 below. The total number of power system components used in the network are also indicated. The Installed generation active power capacity is shown as 323MW, the total load demand is indicated as 259MW, the grid power losses are indicated as 8.60MW, and the generation active power is shown as 267.60MW. The generation spinning reserves are also shown as 42.65MW, this is power that is being utilized when load demand changes.

**Table 4.6: Network grid summary**

					DigSILENT	Project:	
					PowerFactory		
					2020 SP3	Date: 2021/04/22	
Load Flow Calculation				Total System Summary			
AC Load Flow, balanced, positive sequence				Automatic Model Adaptation for Convergence		No	
Automatic tap adjustment of transformers	No			Max. Acceptable Load Flow Error			
Consider reactive power limits	Yes			Bus Equations (HV)		1.00 kVA	
				Model Equations		0.10 %	
Total System Summary				Study Case: 01 - Load Flow Case Origin   Annex: / 1			
No. of Substations	0	No. of Busbars	14	No. of Terminals	0	No. of Lines	15
No. of 2-w Trfs.	5	No. of 3-w Trfs.	0	No. of syn. Machines	5	No. of asyn. Machines	0
No. of Loads	11	No. of Shunts/Filters	1	No. of SVS	0		
Generation	=	267.60 MW	63.13 Mvar	274.95 MVA			
External Infeed	=	0.00 MW	0.00 Mvar	0.00 MVA			
Load P(U)	=	259.00 MW	72.82 Mvar	269.04 MVA			
Load P(Un)	=	259.00 MW	72.82 Mvar	269.04 MVA			
Load P(Un-U)	=	-0.00 MW	-0.00 Mvar				
Motor Load	=	0.00 MW	0.00 Mvar	0.00 MVA			
Grid Losses	=	8.60 MW	9.82 Mvar				
Line Charging	=		-24.01 Mvar				
Compensation ind.	=		0.00 Mvar				
Compensation cap.	=		-19.51 Mvar				
Installed Capacity	=	323.00 MW					
Spinning Reserve	=	42.65 MW					
Total Power Factor:							
Generation	=	0.97	[-]				
Load/Motor	=	0.96 / 0.00	[-]				

Considering Table 4.6 above showing the grid summary results during steady-state, the sum of grid power losses and the load power should be equated to total power generation power. Therefore, equation 4.3 below can calculate either the total generation supply, total load demand, or total grid losses depending on the given variables.

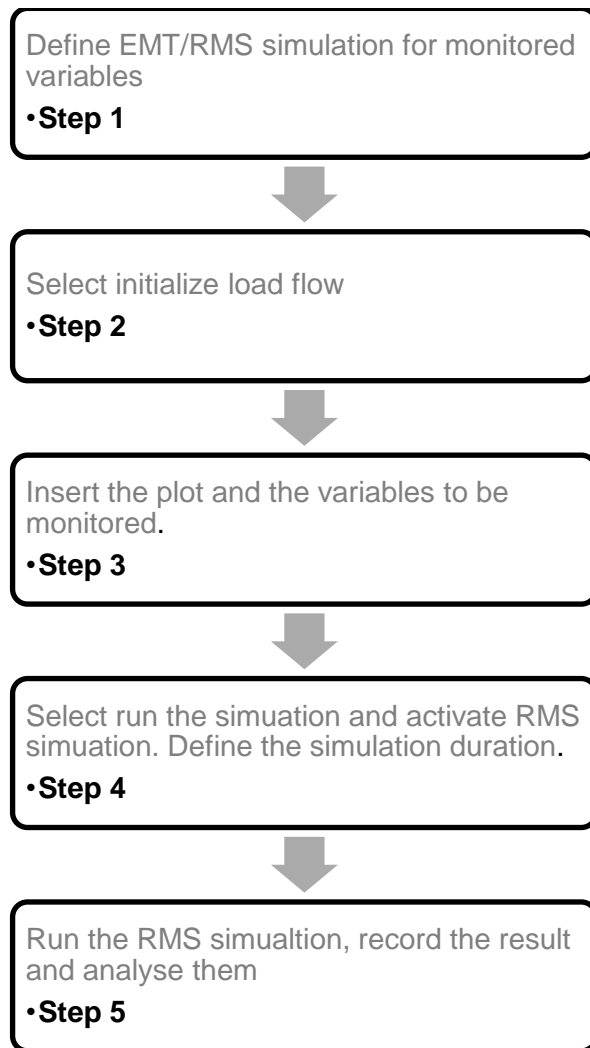
$$P_{gen} = P_{loss} + P_{load} \quad 4.3$$

In Table 4.6 above,  $P_{gen} = 267.60MW$ ,  $P_{loss} = 8.60MW$ , and  $P_{load} = 259MW$

$$\sum (P_{loss} \text{ and } P_{load}) = 8.60MW + 259MW = 267.60MW$$

When the active power generated is equal to the active load power and power losses along the transmission lines, the system frequency is stable at a nominal value of 50Hz. The available spinning reserves are shown as 42.65MW, and this is the active power that the governor will utilize to maintain the frequency within its standard operating range (49.5Hz to 50.5Hz).

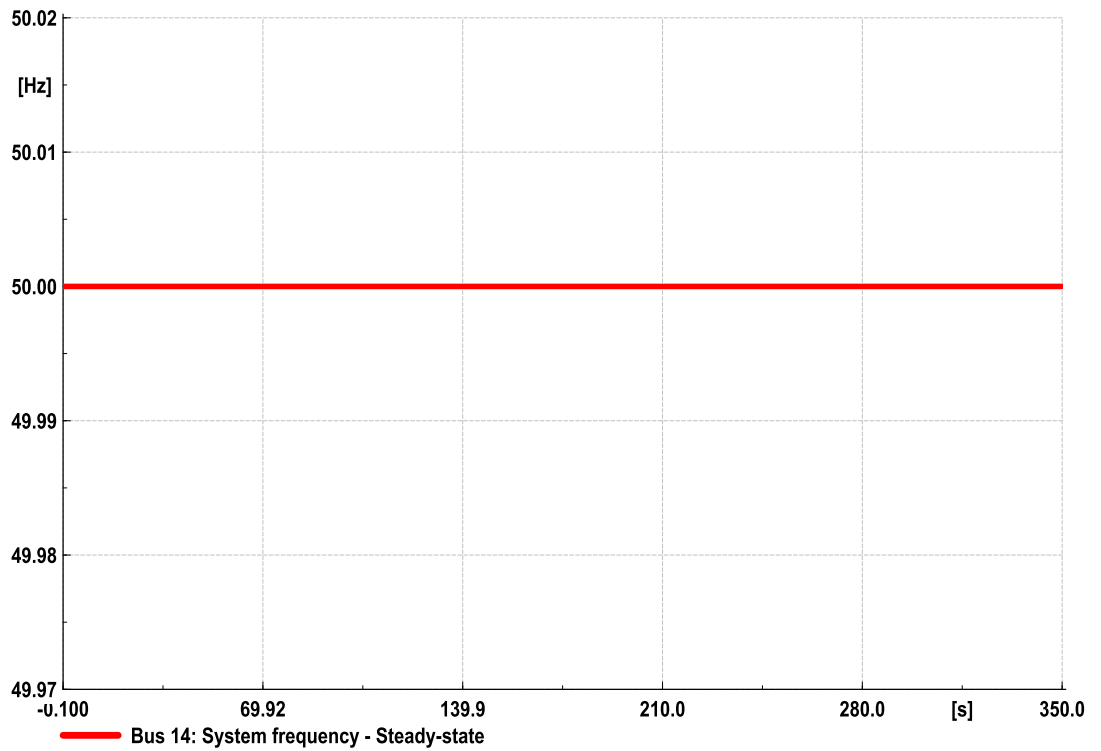
The monitored variables such as frequency, voltage, and active power are simulated in DIgSILENT by implementing the flow chart in Figure 4.11 below. EMT is the electromagnetic transient analysis tool for short-term dynamic analysis, while the RMS is the electromechanical transient analysis for mid to long-term dynamic analysis (DIgSILENT, 2020).



**Figure 4.11: Steady-state simulation flowchart**

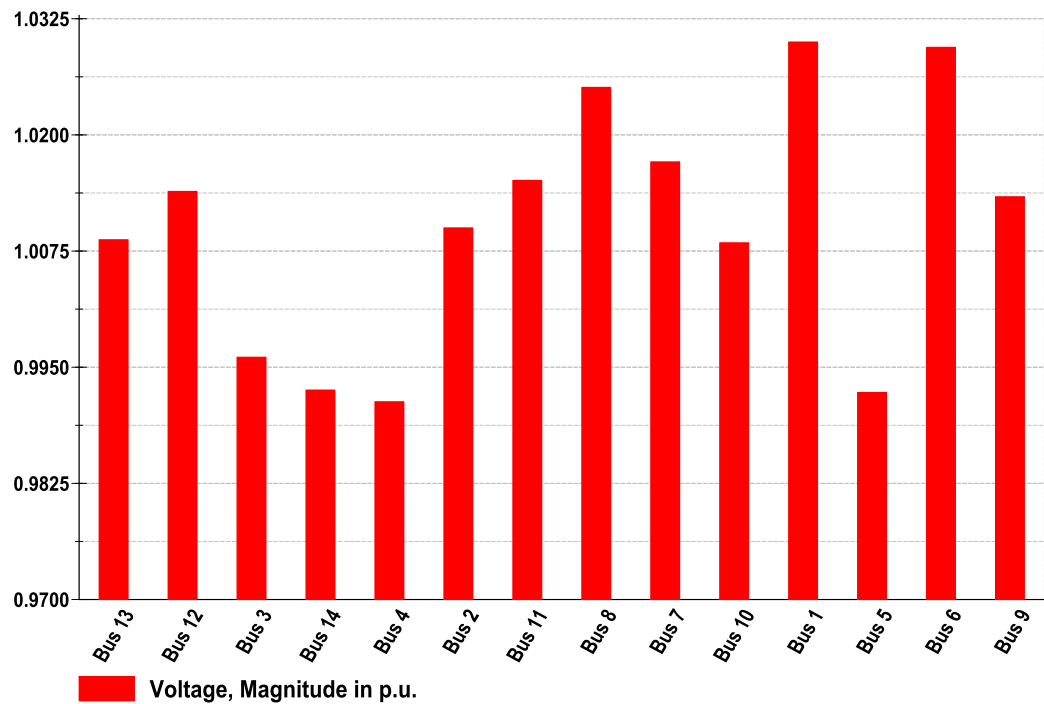
This simulation is performed when there is no active event contingency selected or defined. The simulation period on the x-axis of the plot was set to 350sec.

Figure 4.12 below shows the frequency measured at bus 14 during steady-state simulation. The system frequency is the same throughout the network. This is achieved by ensuring that all the generators are appropriately integrated into the power system grid and synchronized. The frequency is constant throughout the system at 50Hz. In Figure 4.12 below, the y-axis represents the frequency in hertz, while the x-axis is the simulation duration period; in this case, it is set at 350sec. When the frequency in the power system grid is at its nominal value, this means that the total power generation, which is equal to the total system load summated with total power losses along the transmission and distribution lines as indicated in equation 4.3 above. The power grid is regarded as being stable when all the system variables such as frequency and voltages are at the nominal state.



**Figure 4.12: Power system grid frequency during steady-state.**

Another fundamental consideration during the steady-state analysis is the system voltages. The system voltages are expected to be within the tolerances of +/- 5% of its nominal value. In per-unit terms, the system voltages should be within 0.95pu and 1.05pu. In Figure 4.13 below, the minimum measured bus voltage is 0.99pu (bus 4 and 5), and the maximum voltage measured 1.03pu (bus 1). In this figure, the y-axis represents the per-unit voltage measured at the bus terminals while the x-axis bus bar in the network.



**Figure 4.13: Network bus bar voltages**

The modified IEEE 14 bus network model is a true reflection of an interconnected power system grid, where there are areas involved which share the active power according to the load demand. The system is divided into four areas, area 1, area 2, area 3, and area 4 as shown in Figure 4.10 above. In area 1 there is no power active imported from other areas, and hence area 1 plot is not reflected in Figure 4.14 below. In area 2, an additional amount of active power is imported from area 1, and the area also exports active power to area 3 and area 4. Area 3 imports active power from area 2 and area 4. Area 4 also receives the active power from both areas 1 and 2.

Figure 4.14 below illustrate the net tie-line power interchange between the areas. Figure 4.14 (a) is the total power interchange imported to area 2, and based on the power flow performed, area 2 is receiving an additional active power of 86.81MW from area 1 as shown in Figure 4.10 above. In area 3 shown in Figure 4.14 (b), the additional active power of 63.20MW is imported from area 2 and area 4. Area 3 is the only area in the network with a single bulk load, and hence there is additional active power is required to meet the load demand. Area 4 is the distribution center of the grid, therefore a lot of customers are served in this area. An additional active power of 122.16MW is imported from area 1 and area 2

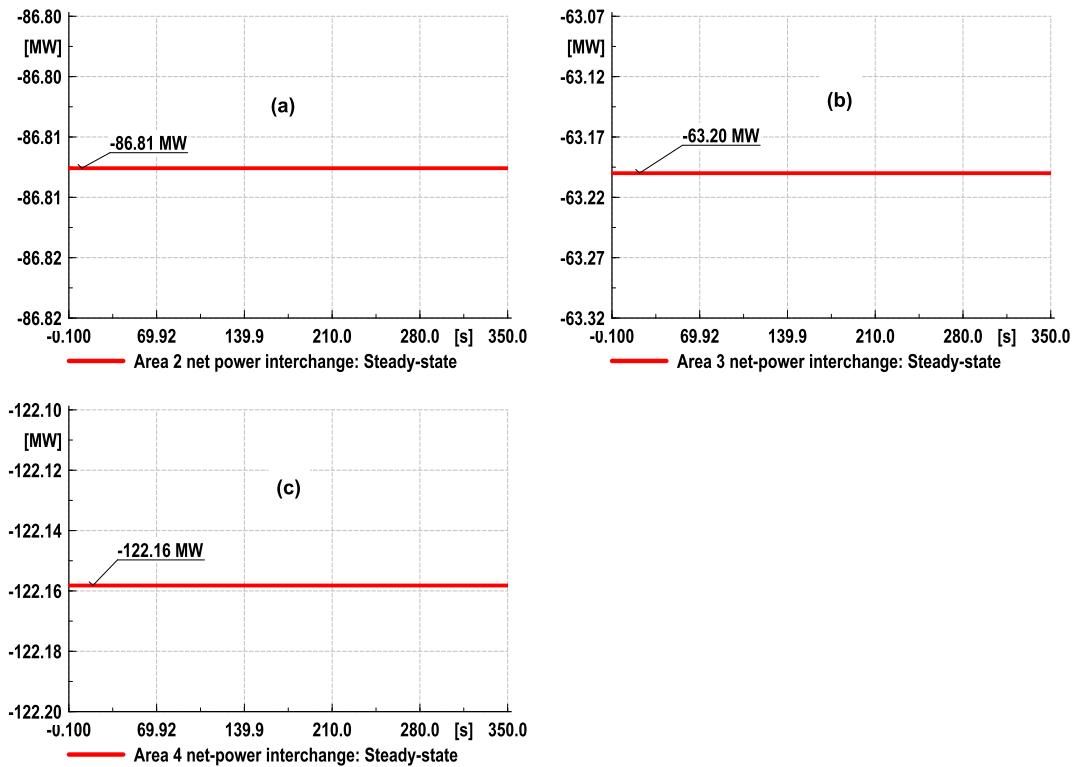


**Figure 4.14: (a) Scheduled tie-line active power interchange in area 2, (b) Scheduled tie-line active power interchange in area 3, and (c) Scheduled tie-line active power interchange in area 4**

The tie-line power interchange needs to be maintained as close as possible to the scheduled amount. This will ensure that there is adequate supply to the neighboring areas to meet the load demand.

When the network is subjected to a disturbance, be it a transient disturbance or significant system disturbance, then the state of operation changes from a steady state to a dynamic state.

#### 4.4 Dynamic state analysis

This analysis aims to analyze the behavior of the system frequency when the load suddenly increased. Also, to prove that the governing system is not good enough to regulate the frequency to the normal operating range. Load demand increases electrical torque, which leads to the electrical and mechanical torques becoming unequal, resulting in the speed of the turbine being slow down. Since the speed of the turbine is directly proportional to the angular speed of the turbine, the frequency will start to drop as the load demand increases. However, due to the inertia of the machine, the frequency is not immediately dropped. The acceleration time constant of the generator delays the decreased in the speed of

the governor. The moment of inertia can be calculated using the equation 4.4 below.

$$J = S_n \frac{T}{\omega_n^2} \quad 4.5$$

Where:

$J$  is the moment of inertia,

$\omega_n$  is the rated angular speed of the generator.

$T$  is the acceleration time constant at rated MVA of the generator ( $S_n$ )

$S_n$  is the rated MVA of the generator

#### 4.5.1 Dynamic state analysis - case study

The case study aims to analyze the contribution of the governing system to frequency regulation and stability. In the case study, a disturbance will be introduced by increasing the load demand, and the governor is expected to regulate the frequency through active power compensation by releasing the spinning reserves. The system frequency normal operating range is between 49.5Hz to 50.5Hz, and the governor is expected to ensure that the standard operating frequency is maintained by adjusting the turbine valve setpoints.

Since the frequency is the same throughout the system, its measurement will be done on bus 14. The event duration is set to 350sec, which is adequate when assessing the governing system contribution as its regulating process is within 15sec to 30sec after the event.

Table 4.7 below indicates the case study to be performed to assess the behavior of the power system during the dynamics state. The load demand increase disturbance is applied, and the response of the control system will be analyzed. The case study is performed on DlgSILENT simulation software.



**Table 4.7: Case study 1**

Case study name		Aim				Type of disturbance				Control method			
<b>Case study 1</b>		The case study proves that the governing system cannot maintain power system frequency to its nominal state following a load demand increase disturbance.				Load demand increase by 15% in steps of 1%				Generator governing system			
Monitored variables													
Lowest Bus Voltage (PU)		Frequency (Hz)		Area 2 net-power interchange (MW)		Area 3 net-power interchange (MW)		Area 4 net-power interchange (MW)		Total Load demand (MW)		Total Generation Supply (MW)	
before	after	after	before	after	before	before	after	before	after	before	after	before	after

#### 4.5.1.1 Case study 1 – load demand increase by 15%

After a 15% load demand increase, the system frequency dropped from 50Hz to 49.32Hz. The governor stabilized the system frequency below its operating range to 49.32Hz. The time the governor took to stabilize the frequency was recorded as less than 20sec. These results are shown in Figure 4.15 below, where the y-axis of the plot represents the frequency measured at bus 14, and the x-axis represents the event duration time. The load increment event is applied every 20 seconds, and a 1% load demand increase for 15 steps equivalent to 15%.

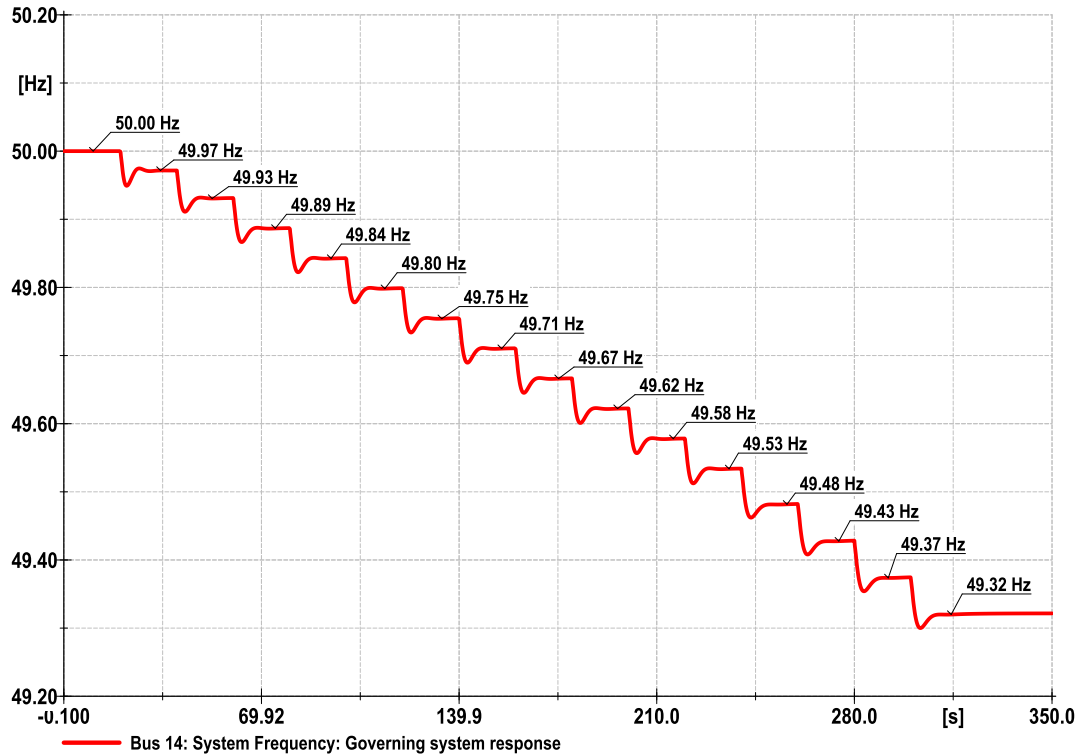


**Figure 4.15: Power system grid frequency on GOV response**

The load demand increase event resulted in a total load demand increase from 259MW to 297.02MW, as shown in Figure 4.16 below. The load event applied is a step increase; therefore, the increase occurs immediately.

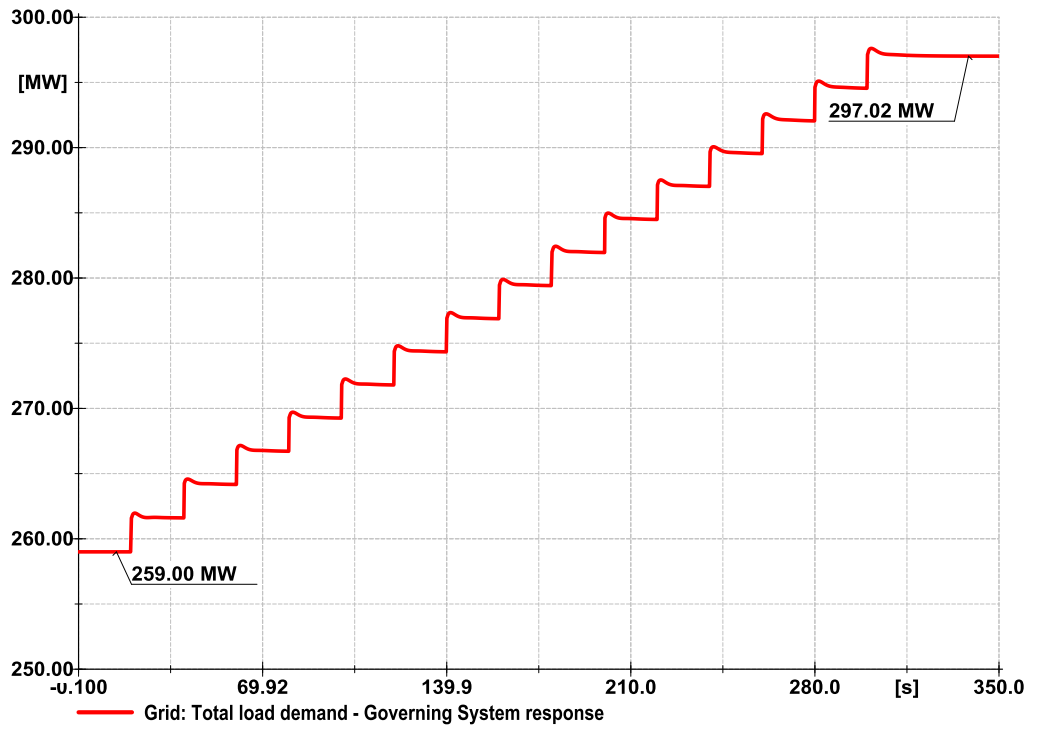


**Figure 4.16: Power system load demand on GOV response.**

As a result of the load demand increase, the generation system responded by delivering an additional active power of 307.14MW from 267.60MW of initial generation active power. Figure 4.17 below represents the total generation supply of the grid following the load demand increase event.

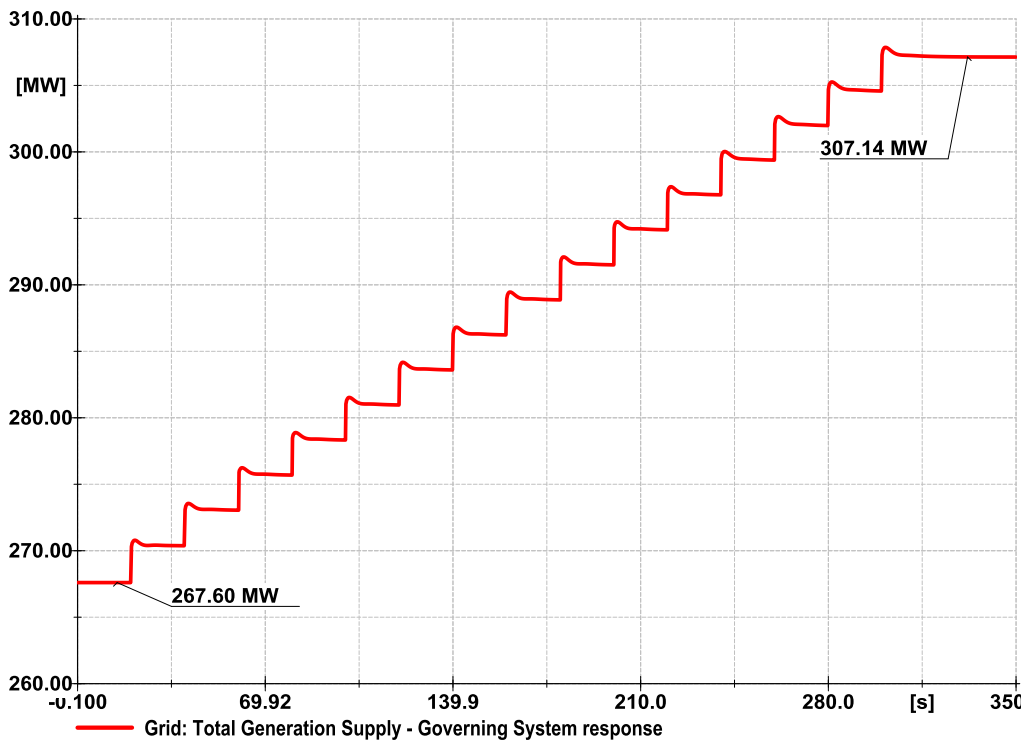


**Figure 4.17: Total Generation supply on GOV response.**

The scheduled tie-line active power flow between the areas has also deviated from their initial values. Deviation has occurred due to the load demand increase. Figure 4.18 to 4.20 below shows the net tie-line scheduled power interchange between areas. In Figure 4.18 below is the net tie-line power interchange in area 2. It can be noted that the schedule power interchange deviated from 86.81MW to 92.96MW following the load demand increase by 15%. The governing system response is observed failing to return the scheduled power interchange to its initial value. The increase in load demand increased net tie-line power interchange by 6.15MW in area 2.

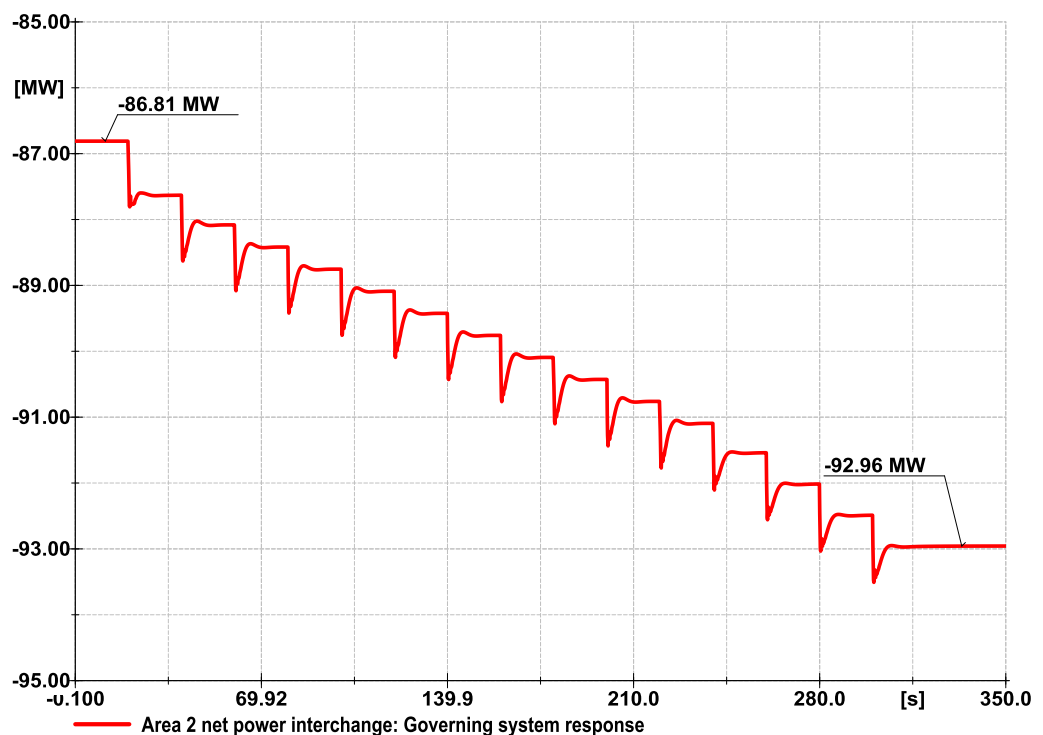


**Figure 4.18: Net Power Interchange in Area 2 on GOV response.**

In Figure 4.19 below, the net tie-line power interchange for area 3 is represented. The scheduled power interchange measured in area 3 has increased from 63.20MW to 65.91MW following the load demand increase. The load demand increase resulted in a 2.71MW increase in net tie-line power interchange in area 3.

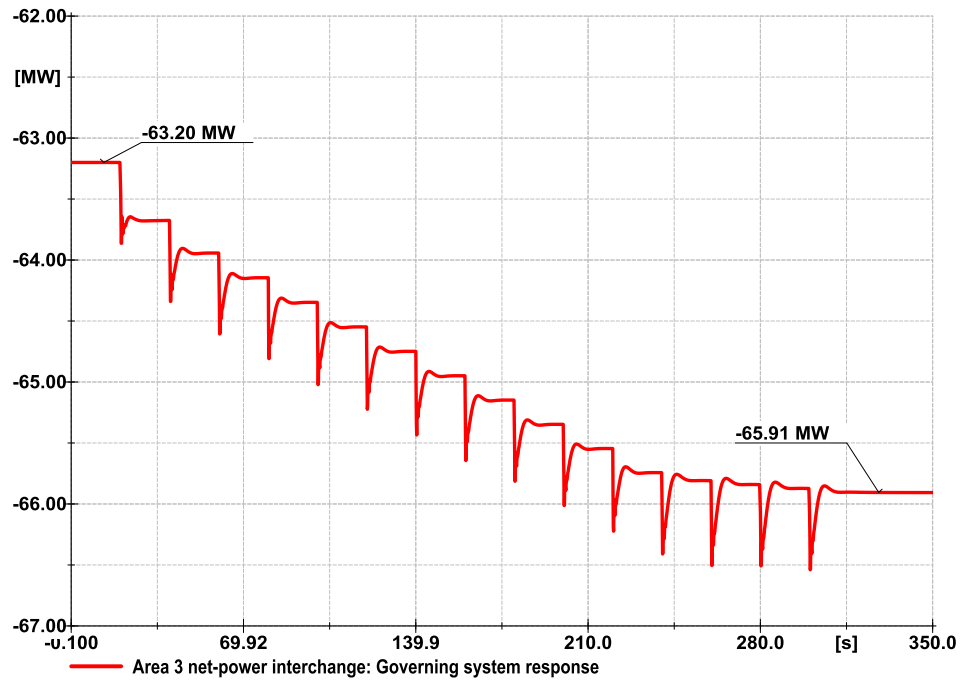


**Figure 4.19: Net Power Interchange in Area 3 on GOV response.**

Area 4 is the most is the part of the network with more load; therefore, an increase in load demand resulted in a net tie-line interchange to increase by 10.5MW. It is noted in Figure 4.20 below that the initial schedule power interchange was 122.16MW and changed to 132.66MW as a result of the load demand increase.

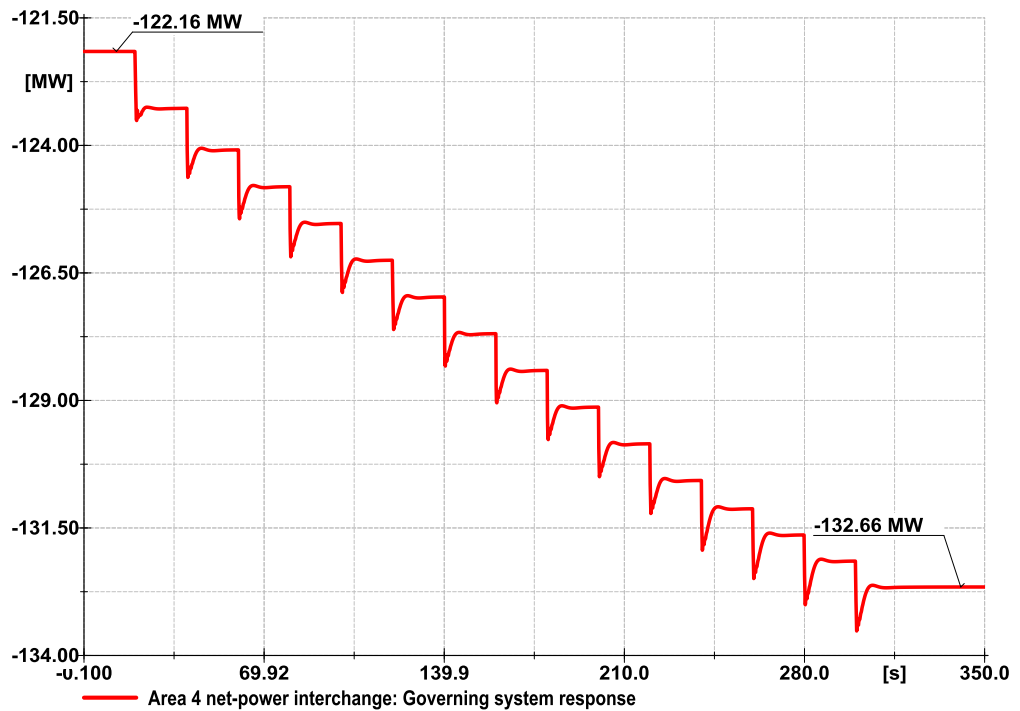


**Figure 4.20: Net Power Interchange in Area 4 on GOV response.**

The tie-line active power interchange is measured at the receiving end of each area fed; hence the sign is negative. The negative sign indicates the power flow direction towards the measurement point. The governing system controls the active power production, but it cannot maintain the scheduled tie-line power interchange.

The scheduled power interchange between the area must be adequately monitored. If the power interchange is not controlled, the transmission lines can experience stress, and the line protection scheme can be activated under overload conditions. The current carrying capacity of the line threshold needs to be maintained.

During a 15% load demand increase, bus 14 dropped from 0.99pu to 0.98pu, and if there is no control action activated, this busbar could be the weakest in the system as the load demand keeps on increasing. Busbar 14 voltage is still within the acceptable operating range. Although the focus of the study is on frequency stability, it is also crucial that the voltage stability is also maintained during the event simulations.

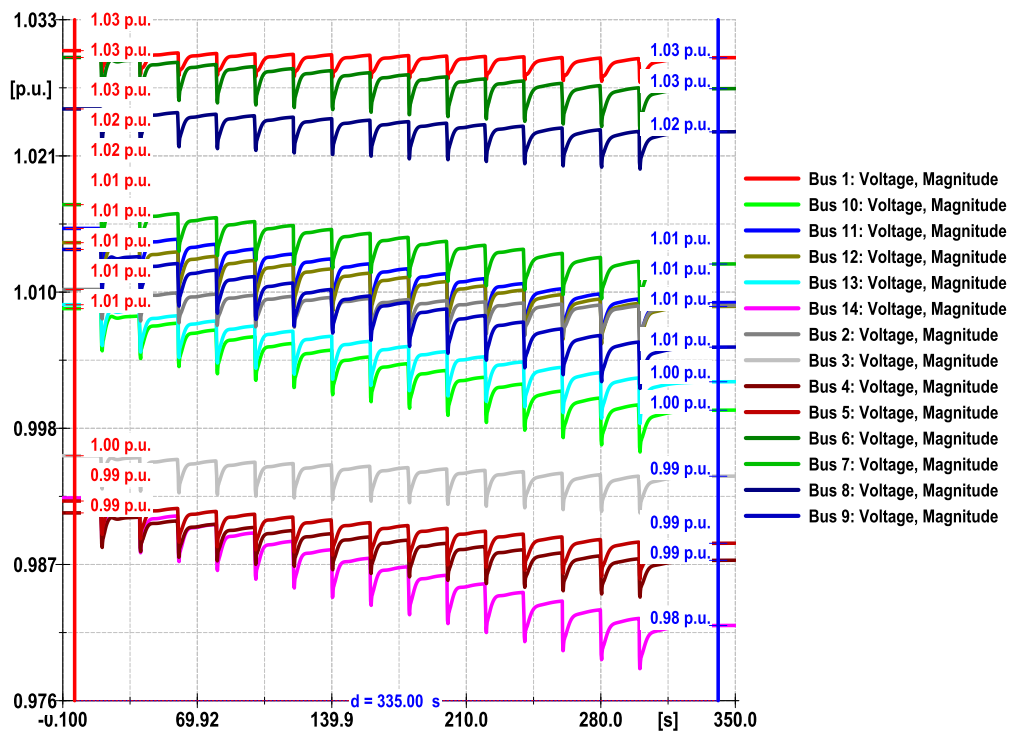


**Figure 4.21: Voltage response to 15% load demand increase.**

Table 4.8 below demonstrates the simulation results recorded before and after the load event was initiated.

**Table 4.8: Case study 1 results**

Case study name		Aim				Type of disturbance				Control method			
<b>Case study 1</b>		The case study proves that the governing system cannot maintain power system frequency to its nominal state following a load demand increase disturbance.				Load demand increase by 15% in steps of 1%				Generator governing system			
Monitored variables													
Lowest Bus Voltage (PU)		Frequency (Hz)		Area 2 net-power interchange (MW)		Area 3 net-power interchange (MW)		Area 4 net-power interchange (MW)		Total Load demand (MW)		Total Generation Supply (MW)	
before	after	after	before	after	before	before	after	before	after	before	after	before	after
0.99	0.98	50	49.32	-86.81	-92.96	-63.20	-65.91	-122.16	-132.66	259	297.02	267.60	307.14

#### **4.6 Discussion of results**

The results shown in Table 4.8 above were recorded before a load demand increase and after the load demand increase was implemented. The weakest busbar in terms of voltage was discovered to be bus 14. Before the execution of the load event, the voltage at bus 14 was 0.99pu, and after the load demand increase, the voltage on bus 14 was 0.98pu. The power system grid frequency before the load demand increase executed was at its nominal value of 50Hz. After the load demand increase, the frequency dropped to 49.32Hz. According to the revised South African Grid Code, stage 1 load-shedding is expected to be initiated to system frequency below 49.2Hz (NERSA, 2019a).

The net tie-line power interchange for all the areas has also deviated from their scheduled amount due to the load demand increase. Therefore, the governing system is not compelling enough to stabilize and recover the power system variables such as frequency and the voltage to their initial value, including the scheduled power interchange.

#### **4.7 Conclusion**

Based on the droop characteristic of the governing system, the frequency cannot be returned to its nominal value of 50Hz when the system is subjected to a disturbance unless the disturbance event is cleared. The control signal to the governing system is not as accurate as possible for the mechanical torque to be equal to the electrical torque to ensure the frequency is recovered. The speed deviation measured by the governing system between the turbine and generator is not as accurate, and hence it is challenging to restore frequency to its nominal value after the load event.

A secondary controller is required to assist the governing system with accurate signal deviation for the mechanical torque that can be equated with the electrical torque for frequency restoration to its nominal value of 50Hz. The modeling and development of secondary frequency control are introduced in chapter 5 for frequency restoration to the nominal value of 50Hz. This development will ensure that the power system frequency can be maintained at its nominal state, provided enough generation reserves are available.



## CHAPTER FIVE

### MODELING OF AUTOMATIC GENERATION CONTROL AND PERFORMANCE ANALYSIS USING DigSILENT SIMULATION SOFTWARE.

#### 5.1 Introduction.

The speed governing system has a significant contribution to the primary control of the conventional generation system. Its function is to control the active power production based on its droop characteristic. When a disturbance occurs in the power system network, the governor will respond to such disturbance by regulating the speed of the turbine of the generator. However, its speed regulation is not as accurate, and hence the system frequency cannot be returned to its nominal value. According to (NERSA, 2019a), the frequency operating range is expected to be maintained within 49.5Hz to 50.5Hz, and beyond these limits, an emergency control is required. The emergency control can result in load shedding.

In chapter 4, the response of the governing system was noted for the load demand increase of 15%, which resulted in a frequency deviation from 50Hz to 49.32Hz. It has been proven that, the governing system cannot maintain the frequency to its nominal value following a load demand increase. Therefore chapter seeks to solve the frequency instability issues experienced in chapter 4 through implementing an Automatic Generation Control (AGC). The AGC is the secondary control loop which will assist the primary control (GOV response) to recover the system frequency to its nominal value

#### 5.2 The implementation of Automatic Generation Control (AGC).

Power system frequency is maintained by balancing the load demand and generated power. As soon as there is an imbalance between generation and the load, resulting in a change of the net power interchange, the system frequency will subsequently change. There are three frequency control stages in the power system: primary control, secondary control, and tertiary control. Their activations are based on time-stamp. When the disturbance is introduced, the activation of the primary control (governing system) is between 15sec to 30s. The next stage is the activation of secondary control (automatic generation control) between the times of 30s to 15min. The last control stage is the tertiary control which is anticipated to be activated from 15min to several hours.

The modeling of the frequency controllers are based on the modified IEEE 14 bus network, which is modeled as the four area power system network as

demonstrated in chapter 4, Figure 4.2 above. All the generation units represented in Figure 4.2 are considered in the development of the frequency controllers and the power interchange between the areas. Each area has a dedicated controller to ensure both the frequency and tie-line power interchange are adequately maintained.

Figure 5.1 below illustrates a further demonstration of the four-area system. The purpose of illustrating these four areas is to indicate the interconnection between the areas and show the power flow direction between the areas. The power distribution or transfer amongst the areas needs to be controlled to ensure that the areas are not under-supplied or over-supplied. If they are under-supplied, there is a possibility of not meeting the load demand within the area, and when they are over-supplied, the power lines can be strained, the loading percentage will increase, and the possibilities of overload and activation of feeder protection under overcurrent conditions are likely.

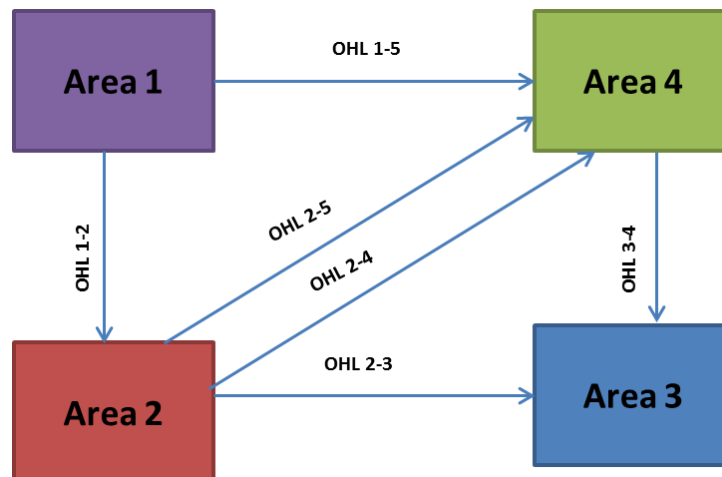


**Figure 5.1: A simplified diagram of a four area interconnected power system**

An automatic generation or load frequency control can be modeled in two ways, firstly as a decentralized controller, and the other configuration is a centralized controller. The difference between the two controllers is that the decentralized controller is a locally based control, while the centralized controller is remotely based. The input signal to the centralized controller is conventionally acquired through a telecommunication system, while in decentralized control, the input signals are locally acquired through a metering system and other measuring intelligent devices. In Table 5.1 below, the comparison between two types of controllers is made:

**Table 5.1: Comparison between the centralized and decentralized controller**

<b>Controller</b>	<b>Orientation</b>	<b>Application</b>	<b>Advantages</b>	<b>disadvantages</b>
Centralized	Remotely based in the central area	Secondary controller – balanced, active power between generation and load	Fewer components are required. Cheaper to install. It can accommodate more inputs	Too sensitive. If one input is lost, then the controller can no longer be used. It challenging to maintain scheduled power interchange
Decentralized	Local-based in each area	Secondary controller – balanced, active power between generation and load	Robust, reliable. If one controller is lost, the other controllers can still maintain the frequency stability control. Easy to maintain the schedule power interchange as well as the frequency.	Expensive. More components are required to install. Each area requires its controller

Though decentralized is expensive in its implementation, it has more advantages than the centralized controller. It very crucial in practice that the inter-areal power interchange and frequency are maintained. The advantages of a decentralized automatic generation control system considering schedule power interchange are the motivation of its implementation.

### **5.2.1 The modeling of decentralized automatic generation control approach**

In the decentralized frequency control model, each area has its designated control operating in isolation of other areal controllers. In most systems, the power interchange between the area is not considered in decentralized control (Tan et al., 2012). When the load changes in a particular area, all the controllers react to the load event, and however, this can put more strain is the transmission system when the power interchange is not being considered.

The modeling of the decentralized controller can be divided into two parts, one without considering the inter-areal power interchange, and the second is when the scheduled power interchange between the areas is considered.

The decentralized control model to be performed is when the power interchange between the areas is being considered. This model does ensure not only the maintenance of the frequency but also the inter-ariel scheduled power interchange.

In decentralized control, the change in system frequency and change in schedule power interchange are the input to the controller. In this case, the Proportional Integral (PI) controller is used to process the input signal to restore the system frequency. The block diagram of the decentralized control loop is shown in Figure 5.2 below. The highlighted part in a dashed red box is the decentralized frequency controller.

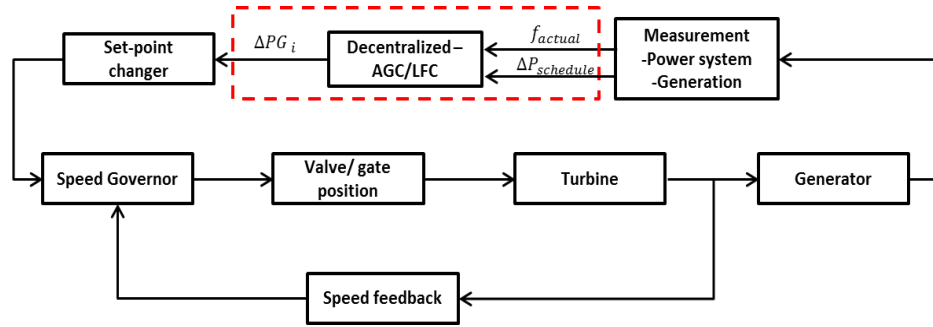


**Figure 5.2: Coordination of a decentralized frequency controller in the power system block diagram (Gjengedal, 2002)**

The mathematical modeling of the above block diagram is indicated below. The input signal to the controller, which is the frequency, is measured at the local busbar. In steady-state, the frequency measured will be 50Hz, and the reference setpoint frequency is also 50Hz; there will be no control signal sent to the controller. The change in tie-line schedule power between the areas and the change in frequency can be determined using equations 5.1 and 5.2 below. In equation 5.1,  $f_{ref}$  are the nominal frequency setpoint (50Hz), and  $f$  is the measured frequency at the bus terminals.

$$\Delta f = f_{ref} - f \quad 5.1$$

$$\Delta P_{net} = \frac{P_{net} - P_{net.ref}}{P_{base}} \quad 5.2$$

In equation 5.2,  $P_{net}$  is the measured total scheduled power flow at the receiving of each area,  $P_{net.ref}$  is the schedule power interchange setpoint between the areas,  $P_{base}$  is the base power to convert the change in tie-line power interchange to per unit value.

The area-control error is determined by multiplying the change in frequency with the frequency bias factor and subtracting the change in tie-line power interchange.  $\beta_i$  is the bias factor.

$$ACE = \beta_i * \Delta f - \Delta P_{net} \quad 5.3$$

The area control error is fed to the Proportional Integral Derivative (PID) controller, the control output from the PID-controller is then multiplied by the control participation factor, and the signal is sent to the governing system.

$$\Delta P_{set} = K_p(ACE) + \int_0^t ACE dt + K_d \cdot \frac{d(ACE)}{dt} \quad 5.4$$

$$\Delta PG_i = \Delta P_{set} * pf_i \quad 5.5$$

The mathematical modeling of the decentralized automatic generation control is presented through block diagrams, as demonstrated in Figures 5.3 and 5.4. The difference between the two diagrams is that Figure 5.3 is not considering the tie-line power interchange while Figure 5.4 considers the tie-line power interchange. The block diagram in Figure 5.4 is suitable to be applied in area 1 as there is no scheduled power being received in that area.

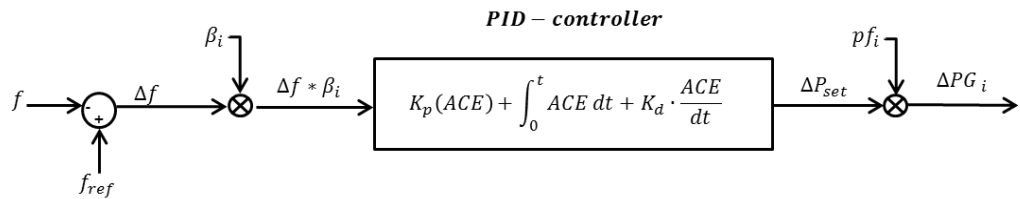


**Figure 5.3: Decentralised AGC block diagram without considering tie-line power interchange** (Pavlovsky & Steliuk, 2014)

The block diagram illustrated in Figure 5.4 is suitable for application in areas 2, 3, and 4. In this area, there is a scheduled power interchange that needs to be maintained.

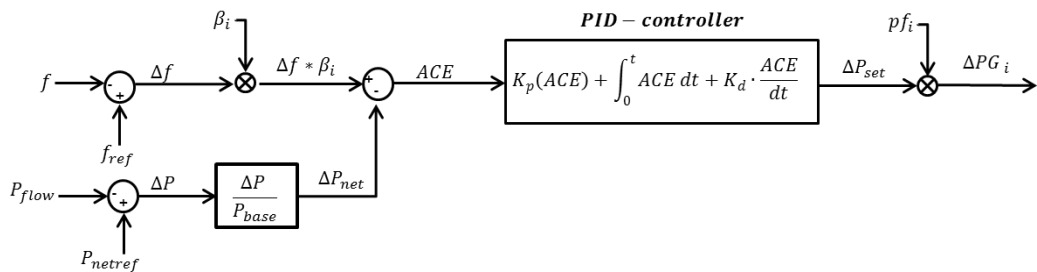


**Figure 5.4: Decentralised AGC block diagram considering tie-line power interchange** (Pavlovsky & Steliuk, 2014)

### 5.3 Modeling of a decentralized AGC in DigSILENT power factory software

The modeling of the AGC on DigSILENT is achieved by first creating the frame-block. The purpose of the frame-block is to define inputs and output assignments. The inputs to the controller to be defined include frequency measurements and the active power flow at the receiving end of the area. These analog signals are sent to the controller and processed for obtaining a desired control output signal.

The block diagrams for each area are shown from Figure 5.5 up to 5.8 below. In these block diagrams, the time delay has been included to delay the action of the secondary controller so that the primary control can have enough time to adjust and regulate the frequency until it reaches its steady state. The secondary control action only takes place once the primary control reaches its new steady-state.

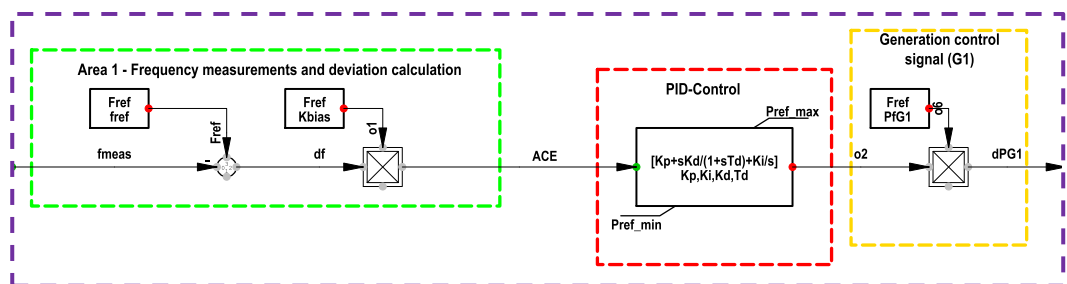


Figure 5.5: Area 1 decentralized AGC block diagram

Area 1 controller, shown in Figure 5.5 above, is used as an additional control loop to the governing system of generator 1, which supplies both areas 2 and 4; hence there is no power interchange control loop included on the controller. The input signal to the controller is the system frequency. The output control signal is sent to the generator 1 governing system.

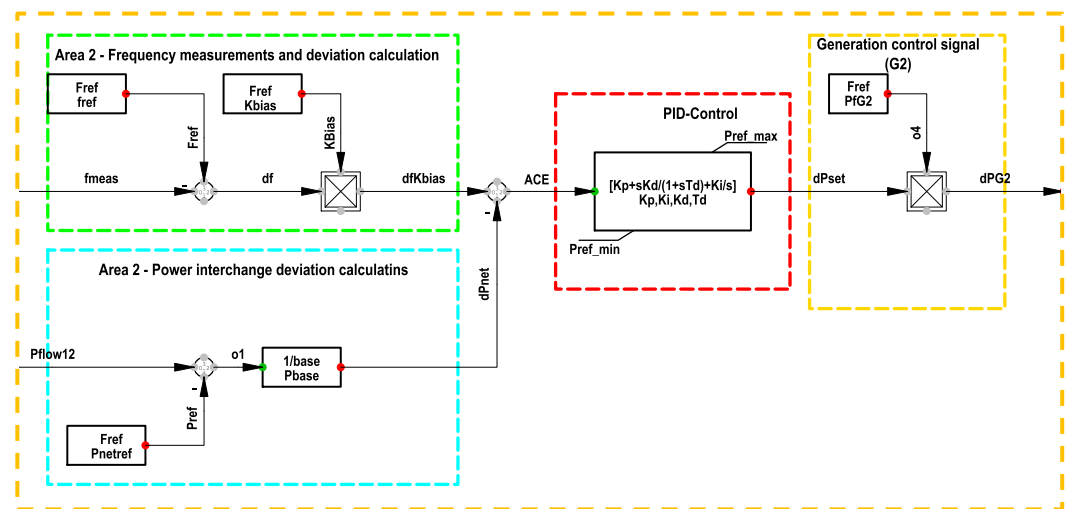
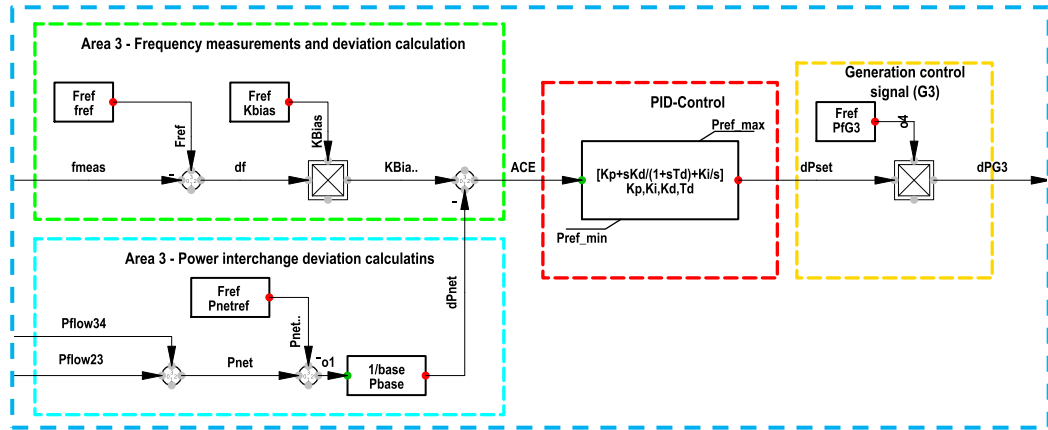


Figure 5.6: Area 2 decentralized AGC block diagram

Area 2 decentralized controller consists of two different input signals. The first signal is the system frequency, and the second signal is the tie-line flow from area 1 to area 2. The area control error is processed through the PID controller, and the output is multiplied by the generation participation factor. The output signal of the controller is sent to generator 2, as shown in Figure 5.6 above.



**Figure 5.7: Area 3 decentralized AGC block diagram**

The operation of areas 2, 3, and 4 controllers are the same. Their control loops facilitate two functions: ensuring the frequency stability while maintaining the scheduled tie-line power interchange. The output signal for the control loop in area 3 is sent to generator 3, as shown in Figure 5.7 above. For area 4 control loop, the output signal is sent to generators 6 and 8 governing systems as indicated in Figure 5.8 below.

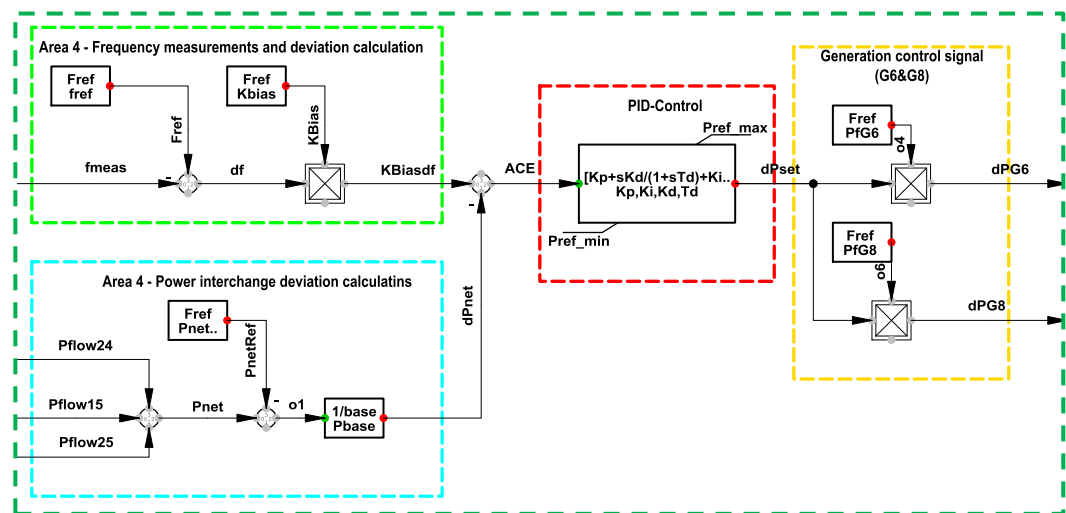


**Figure 5.8: Area 4 decentralized frequency controller**

To assess the effectiveness of the modeled decentralised automatic generation control loop for area 1 to area 4, Table 5.2 below is used. In Table 5.2 below, the case studies to be performed are described, the aim of conducting the case

studies is also outlined. The power system variables such as busbar voltages, frequency, and the net tie-line power interchange between the areas will be monitored before and after the disturbance. The total generation supply and the amount at which the load demand has increased will also be monitored.



**Table 5.2: Case study 2**

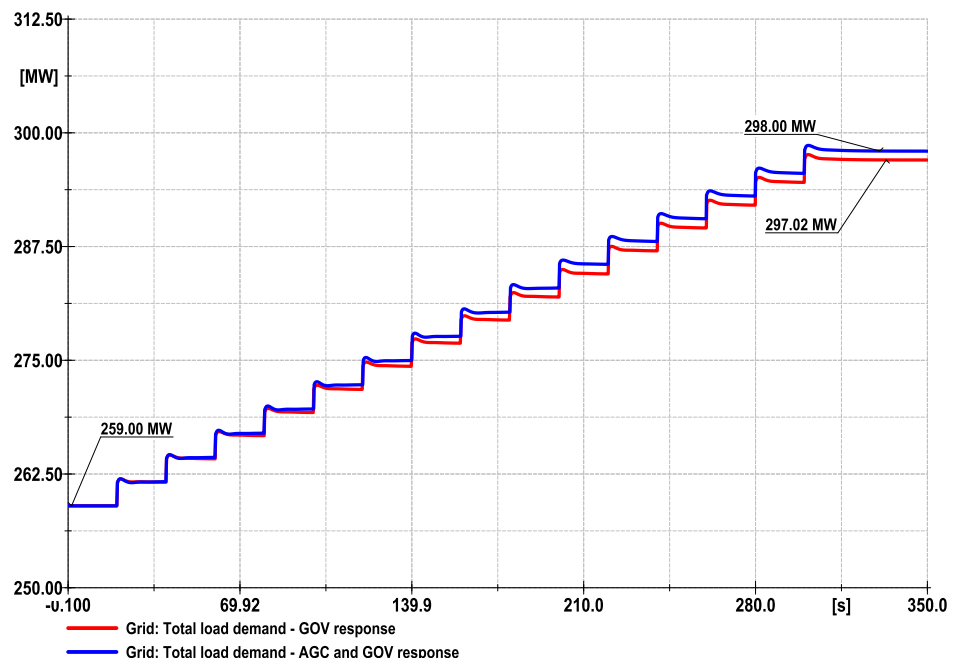
Case study name		Aim				Type of disturbance				Control method			
<b>Case study 2</b>		AGC was developed to assist the governing system in recovering the system frequency. Therefore the effectiveness of the modeled decentralized AGC control loop is assessed. The effectiveness of the AGC control and its response is compared to the GOV response.				Load demand increase by 15% in steps of 1%				Generator governing system and AGC			
Monitored variables													
Lowest Bus Voltage (PU)		Frequency (Hz)		Area 2 net-power interchange (MW)		Area 3 net-power interchange (MW)		Area 4 net-power interchange (MW)		Total Load demand (MW)		Total Generation Supply (MW)	
before	after	after	before	after	before	before	after	before	after	before	after	before	after

## 5.4 Decentralized AGC performance assessment and results

In chapter 4, a load demand increase event was implemented, resulting in a frequency dropping to 49.32Hz after the event. It was concluded that the governing system of the generator could not maintain the system frequency following a load demand increase. A secondary controller development was proposed to assist the governor in regulating the frequency of the grid. The automatic generation control has been modeled to assist the governing system in controlling the system frequency.

The simulations presented in Figure 5.9 to 5.14 indicate the results captured before and after implementing the automatic generation control. The presence of the AGC in the frequency control loop is compared to when there was only a governing system control. The governing system response alone is represented by the red graph, while the blue graph demonstrates the implementation of the AGC.

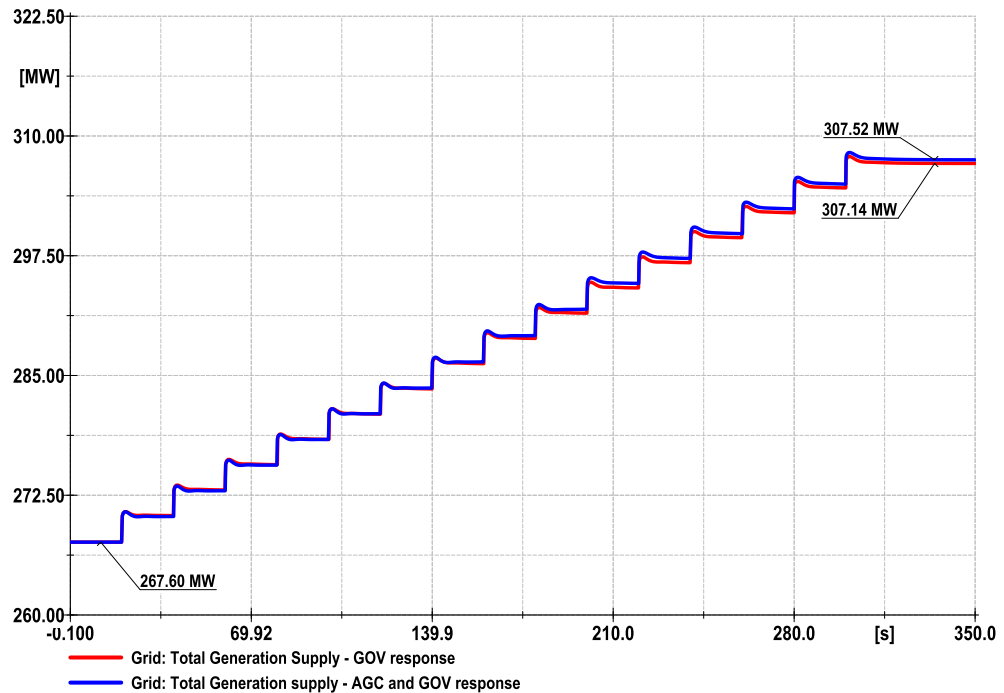
Figure 5.9 below illustrates the load demand increase from 259MW to 297.02MW before the AGC implementation and 298MW after the Implementation of AGC. Ideally, the 15% load increase of 259MW results in 297.85MW. It can be observed that during GOV response, there more power losses compared to when AGC is implemented; hence the load increase result in 298MW.



**Figure 5.9: Total Load Demand before and after AGC implementation.**

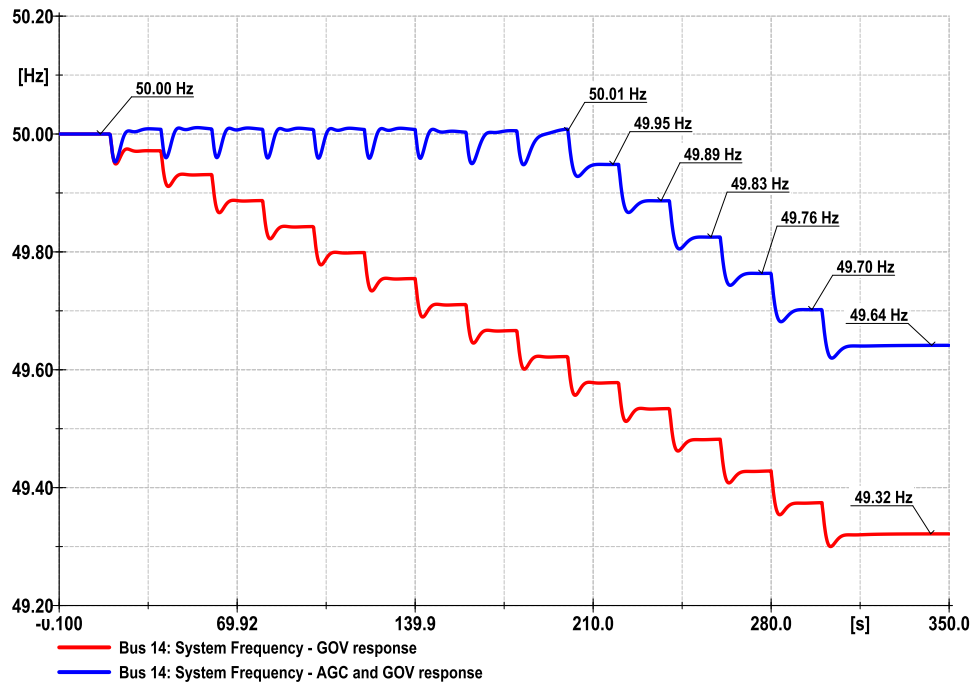
Due to the load demand increase, the generation supply has been adjusted to cater for the load increase from 307.14MW before the AGC implementation.

When the AGC was implemented, the generation supply increase to 307.52MW. Figure 5.10 below illustrate the generation response following a load demand increase before and after the implementation of the AGC.



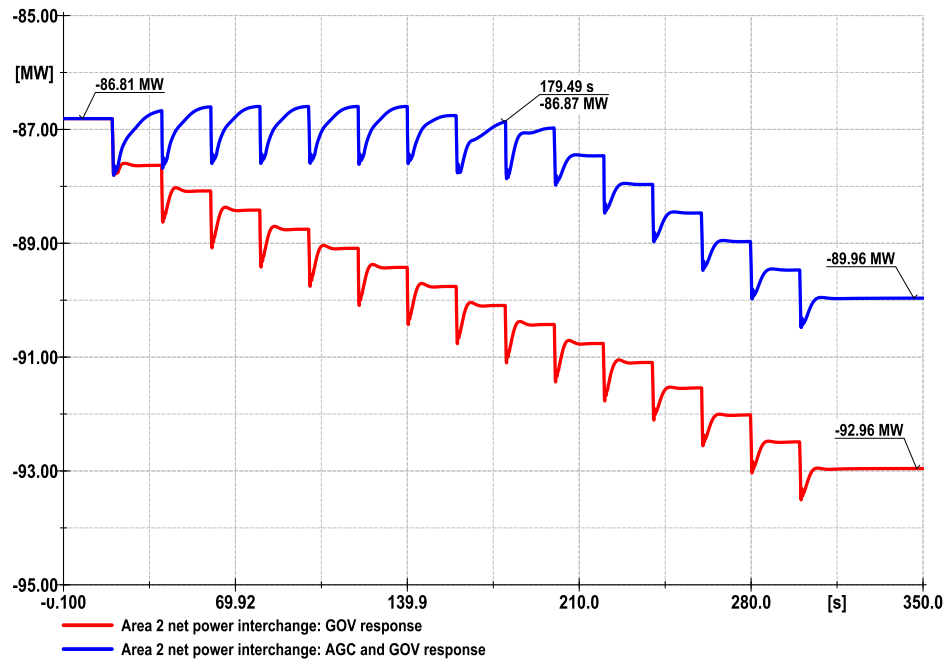
**Figure 5.10: Total Generation Supply before and after AGC implementation following load demand increase.**

Figure 5.11 represents the system frequency before and after the implementation of the AGC. Before the AGC was implemented, it can be seen that the governing system could not maintain the system frequency to its nominal state from the inception of the load demand increase. The system frequency fell to 49.32Hz, as shown by the red graph. The AGC was introduced as an additional control loop to the governing system of the generators. The frequency was recovered following a load demand increase to the 9<sup>th</sup> step (equal to a 9% load demand increase); however, at T=200sec, the AGC started to fail to maintain the system frequency. A new steady-state following a 15% load demand increase was reached at 49.64Hz, as indicated by the blue graph within Figure 5.11. The AGC utilizes the generation spinning reserves, and when those reserves are depleted and there is no additional supply to cater for the load growth, the power system will be subjected to instability.



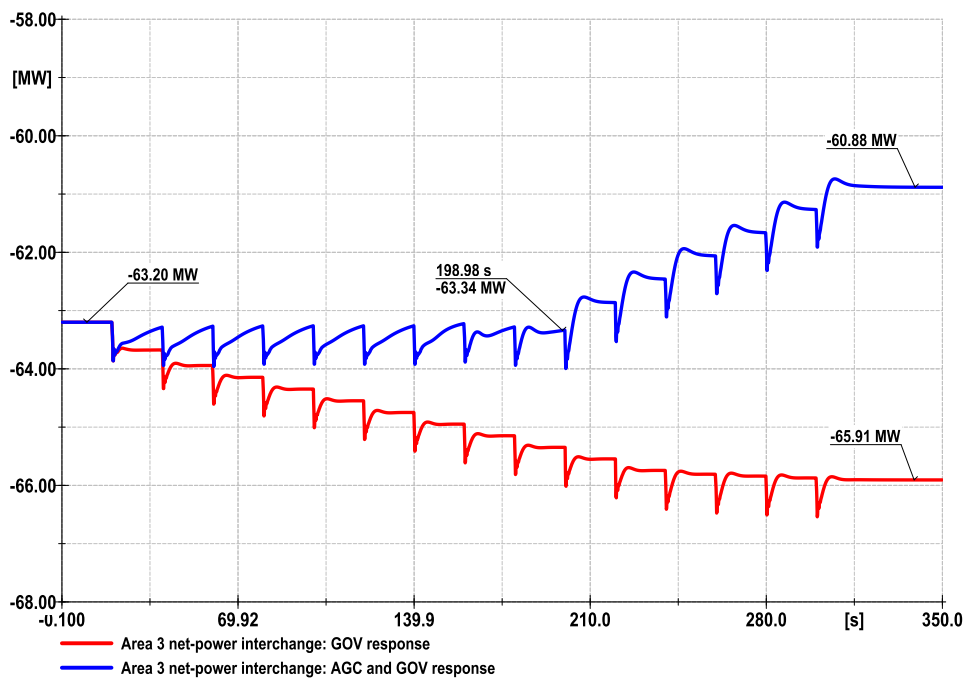
**Figure 5.11: System frequency before and after AGC implementation following load demand increase.**

Figure 5.12 below represents the net tie-line power interchange for area 2. Before implementing the AGC, the load demand increase resulted in a deviation of the scheduled power interchange of area 2 from -86.81MW to -92.96MW. When the AGC was implemented, the scheduled power interchange was recovered to the 8<sup>th</sup> step following a load demand increase. However, after the 8<sup>th</sup> step, where T=180sec, the AGC is failing to maintain the power interchange in area 2. A new state was reached where the power interchange was recorded as -89.96MW after the 15% load demand increase.



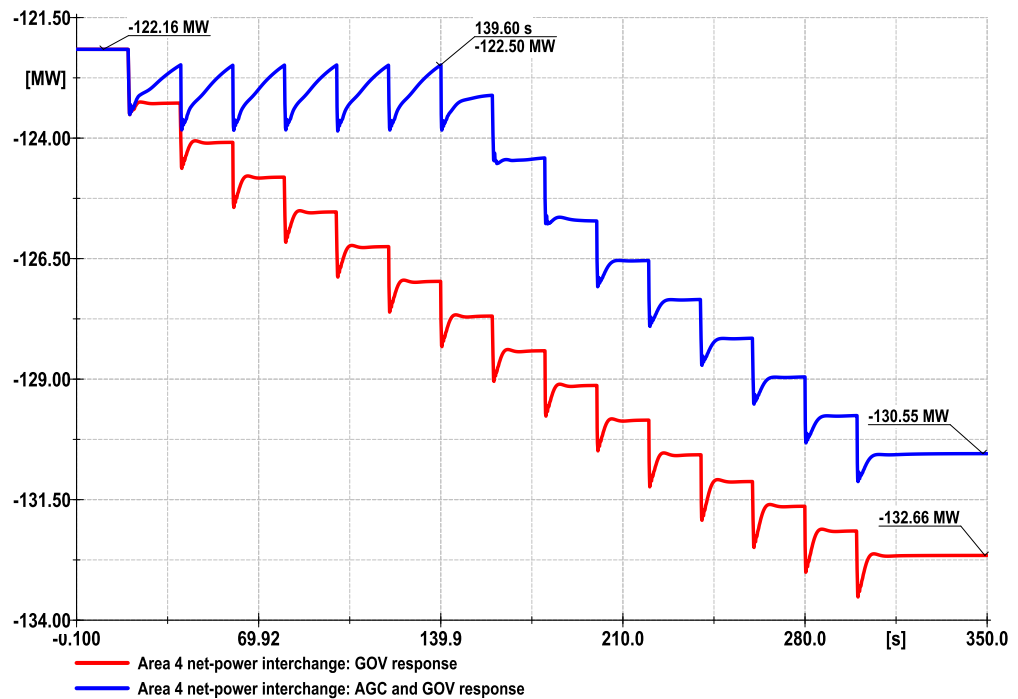
**Figure 5.12: Area 2 Net Tie-line Power Interchange before and after the implementation of AGC.**

In area 3, shown in Figure 5.13 below, the contribution AGC maintained the power interchange as close as possible to the scheduled amount until the 9<sup>th</sup> step at T=200sec following a load demand increase. As the load demand increased, the power interchange in area 3 dropped to -60.88MW after the 15% load demand increased.



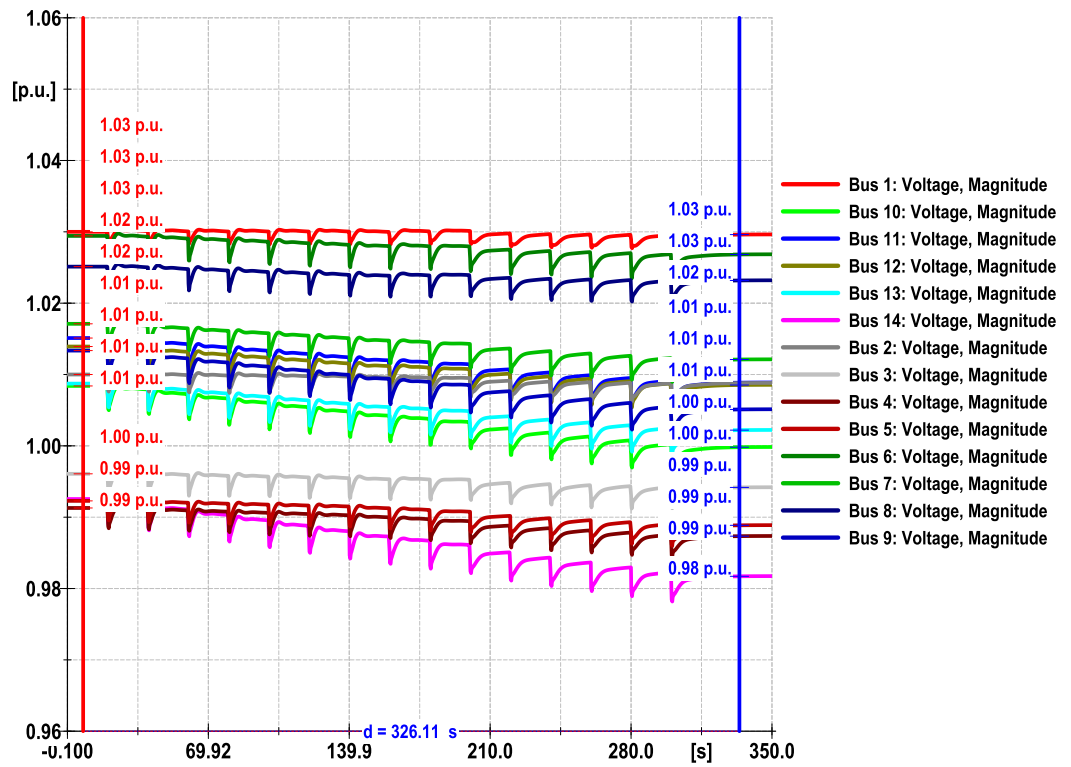
**Figure 5.13: Area 3 Net Tie-line Power Interchange before and after the implementation of AGC.**

Figure 5.14 below is the net tie-line power interchange for area 4. The AGC implementation has supported the power interchange to be maintained as close as possible to its scheduled value of 122.16MW. However, T=140s (7% load demand increase), the AGC started to fail to maintain the power interchange. As the results of a continued load demand increase, a new state of the power interchange, being -130.55 at area 4, was reached. Area 4 is the most vulnerable compared to other areas; therefore, a security supply to the load is critical. Area 4 losses its stability and healthiness quicker compared to other areas. At the 7th step of the load demand increase, area 4 is already becoming unstable while areas are still stable at this power demand level.



**Figure 5.14: Area 4 Net Tie-line Power Interchange before and after the implementation of AGC.**

Load demand increase affects the bus bar voltages because of its inverse proportionality according to Ohms law. Hence when the load demand increases, the bus bar voltages where the system loads are connected to are decreasing. It can be seen that bus 14 is the one that is experiencing more strain. After the load demand increase, bus 14 voltages have dropped from 0.99 to 0.98pu. This voltage is still within the acceptable tolerance. However, if the load demand keeps on increasing, voltage instabilities could be experienced. Figure 5.15 below demonstrates the bus bar voltage in the network grid.



**Figure 5.15: Bus voltages when AGC is activated during 15% load demand increase**

The case study results recorded from the simulation are documented in Table 5.3 below. The results before and after the implementation of automatic generation control are outlined.

**Table 5.3: Case study 2 results**

Case study name		Aim				Type of disturbance				Control method			
<b>Case study 2</b>		AGC was developed to assist the governing system in recovering the system frequency. Therefore the effectiveness of the modeled decentralized AGC control loop is assessed. The effectiveness of the AGC control and its response is compared to the GOV response.				Load demand increase by 15% in steps of 1%				Generator governing system and AGC			
Monitored variables													
Lowest Bus Voltage (PU)		Frequency (Hz)		Area 2 net-power interchange (MW)		Area 3 net-power interchange (MW)		Area 4 net-power interchange (MW)		Total Load demand (MW)		Total Generation Supply (MW)	
before	after	after	before	after	before	before	after	before	after	before	after	before	after
0.99	0.98	50	49.64	-86.81	-89.96	-63.20	-60.88	-122.16	130.55	259	298	267.60	307.52



## **5.5 Discussion of results**

Table 5.3 above represents the result for case study 2 performed to analyze the contribution of automatic generation control in power system stability. The results show that the AGC could not support voltage drop experience by bus 14 due to load demand increase. The voltage measure at bus 14 during the GOV response is the same as when the AGC was implemented.

The AGC has improved the system frequency from 49.32Hz during the GOV response to 49.64Hz. However, this is not good enough to declare the power system as being stable. If the load demand increase continues, the frequency will drop and result in an unstable system condition.

The AGC had also improved the tie-line power interchange between the areas compared to when the GOV was used alone. However, the most vulnerable area within the power system grid was discovered to be area 4. Therefore area 4 requires attention to ensure that the power supply to the end-users is secured.

## **5.6 Conclusion**

Power system stability is part of the day-to-day activity to all the utility custodians and those responsible for the smooth operation of the power system, such as system operators. Therefore, various control and monitoring strategies are explored every day. Therefore, it is essential to understand what each component within the sphere of control and operation can provide to enable and ensure the stability of the network grid.

Automatic generation control has been interrogated, its contribution to the power system is noticeable. However, a significant contribution of this control strategy could be realized more in a power system where there are enough generation reserves. Therefore, it has been realized that when there are not enough generation reserves in the power system, the contribution of the AGC to power system stability could be marginalized. It has been noticed that the AGC fails to maintain the power system frequency, the generation reserves are depleted.

Therefore a new control approach is required to deal with the drawback of the AGC. The AGC is mainly configured as an additional control loop to the governing system of the synchronous generator. Considering the restriction and prohibitory measures to mitigate the use of fossil fuel generators, which negatively impact the environment, has drawn more attention in an exploration of using distributed energy resources as an alternative supply. Therefore utilization of wind turbine generators as an alternative source of supply to stabilize the

power system grid is considered. The wind power plants need to be adequately integrated into the power system grid to avoid any impact that could lead to power system instability. Therefore a control system that will allow its smooth integration to the grid is proposed in chapter 5. The wind power plant is proposed as an active power compensator to control the power system frequency following a load increase disturbance.

# CHAPTER SIX

## MODELING OF AN AGGREGATED WIND FARM AND THE DEVELOPMENT OF WIND ACTIVE POWER COMPENSATOR ON DigSILENT

### 6.1 Introduction

The wind power plant has a significant contribution to the power system stability. Wind power plants are used in a weak power system grid to support both frequency and voltage stability. Several wind turbine producers are improving the output power that a single wind turbine generator can produce. GE, Vestas, Mitsubishi, and Siemens are the primary wind turbine producers. GE has already produced its first Haliade-X 12MW offshore wind turbine generator, which is the biggest in the world (Muyeen & Blaabjerg, 2019). The wind turbine generator can be onshore or offshore sited. Figure 6.1 below is the modified IEEE 14 bus network with the wind power plant integrated.

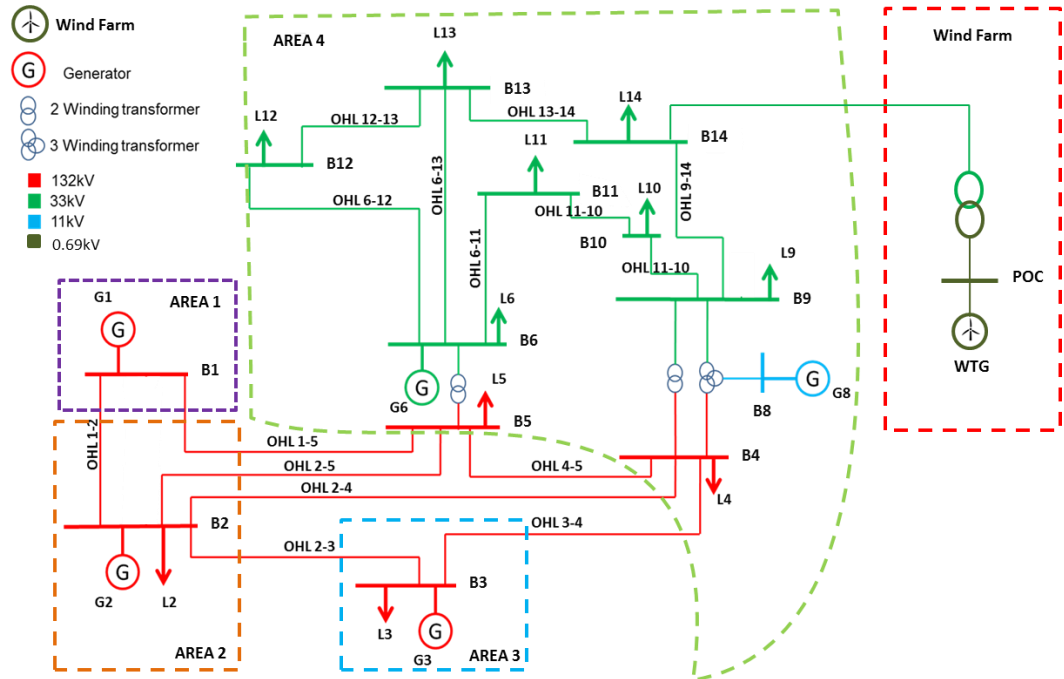


**Figure 6.1: Modified IEEE 14 bus network illustrated in four controlled areas with wind farm integrated**

The model used in this study is a type 3 wind turbine double-fed induction. The double-fed induction generator is widely used in power systems for its flexibility and efficiency in power generation. The wind turbine generators were aggregated to produce an output power of 40MW. In this model, each wind turbine generator produces 2MW. The total number of wind turbine generators is 20, hence the projected output power is 40MW. The measurement of the total output power was

done at the point of connection where all wind turbine generators are connected. Figure 6.2 below is the frame structure of the type 3 wind turbine generator, modeled with its associated control systems. In the frame structure shown in Figure 6.2 below, several control models are configured to enable the wind turbine generator to operate as per its design. These control models include pitch control, aerodynamics, torque control, plant control, electric control, drive-train, etc. The function of these control models differs from one another. The objective of these integrated controls, such as torque, drive-train, aerodynamics, and pitch control, ensures that the generator maintains its rated power output.

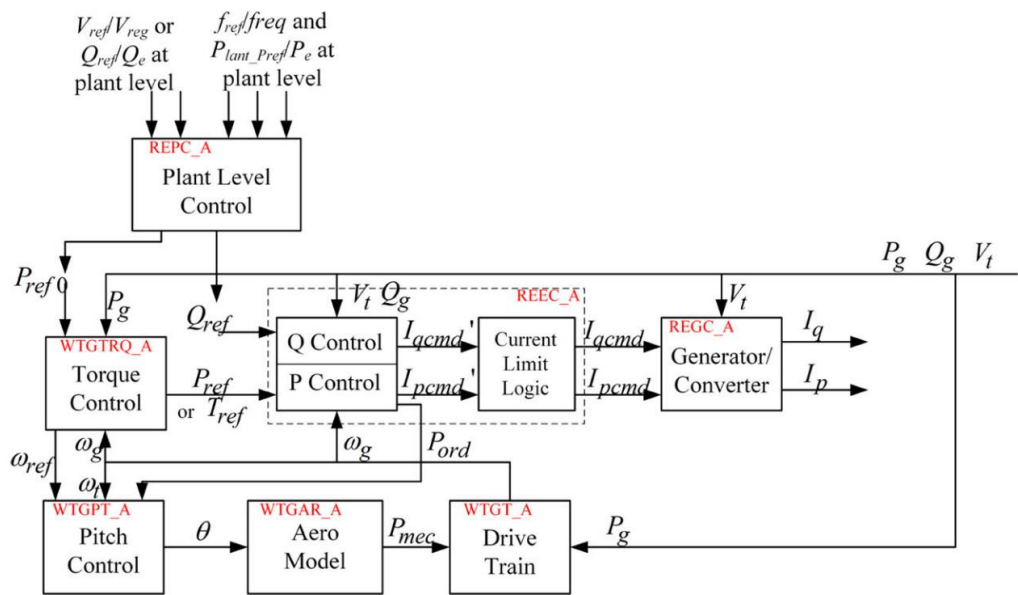


**Figure 6.2: Type 3 wind turbine generator frame structure diagram** (Motta et al., 2019)

A brief operation on each control is covered below to understand better each control model integrated into the wind turbine controls system.

### 6.1.1 Aerodynamic model (WTGAR\_A).

Aerodynamic model – the aero model only focuses on the pitch angle as its input. Ideally, the role of the aerodynamic model is to set the mechanical output power based on the rotor speed and the pitch angle. The model for the area-dynamic is shown in Figure 6.3 below. The mechanical output power that the wind turbine generators can produce is calculated using equation 6.1 below (Boyle et al., 2018), (Rueda et al., 2014), and (Motta et al., 2019).

$$P_m = \frac{1}{2} C_p(\lambda, \beta) \rho A v^3 \quad 6.1$$

Where (Boyle et al., 2018):

$P_m$  – is the mechanical output power

$C_p$  – is the power coefficient

$\lambda$  – is the tip speed ratio also known as lambda

$\beta$  – is the blade pitch angle

$\rho$  – is the air density

$A$  – is the blade swept area

$v$  – is the wind speed.

The swept area can be calculated using equation 6.2 below. In equation 6.2,  $R$  is the rotor radius

$$A = \pi \times R^2 \quad 6.2$$

The tip speed is calculated using equation 6.3 below

$$\lambda = \frac{\omega_T R}{v} \quad 6.3$$

From equation 6.3,  $\omega_T$  is the rotational speed of the hub or turbine, and  $R$  is the rotor radius (Rueda et al., 2014). In this simulation, the wind speed is regarded as constant. Therefore, the relationship between the mechanical and blade pitch angles can be a mathematical model as per equation 6.4 below (Motta et al., 2019).

$$P_{mech} = P_{mech0} - K_{areo} \beta(\beta - \beta_0) \quad 6.4$$

Where:

$P_{mech0}$  – is the initial mechanical power

$\beta_0$  – is the initial hub or blade pitch angle

The aerodynamic model is shown in Figure 6.3 below. The model below is the true reflection of equation 6.4 above.

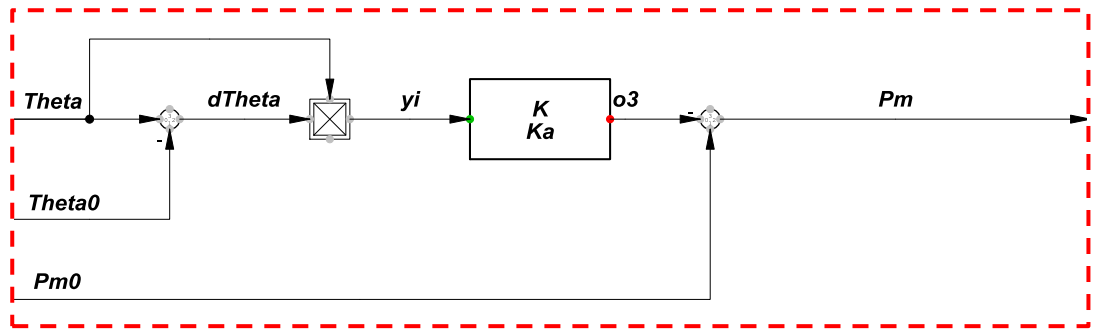


**Figure 6.3: Aerodynamic model for Type 3 wind turbine generator**

### 6.1.2 Wind turbine drive-train model

The output signal of the aero-dynamic model is fed to the drive-train, which couples the turbine and the generator to one rotating mass. Its mathematical model is present in equation 6.5 below. Where  $H$  is the total of generator and turbine inertial constants,  $D$  is the damping factor of the shaft,  $\omega_0$  is the turbine's initial speed.  $\Delta\omega_t$  represent the speed deviation of the turbine (Motta et al., 2019).

$$\omega_t = \frac{1}{2H(\omega_0 + \Delta\omega_t)} (P_{mech} - P_e - D\Delta\omega_t) \quad 6.5$$

The model of the above equation through DlgSILENT is shown in Figure 6.4 below.

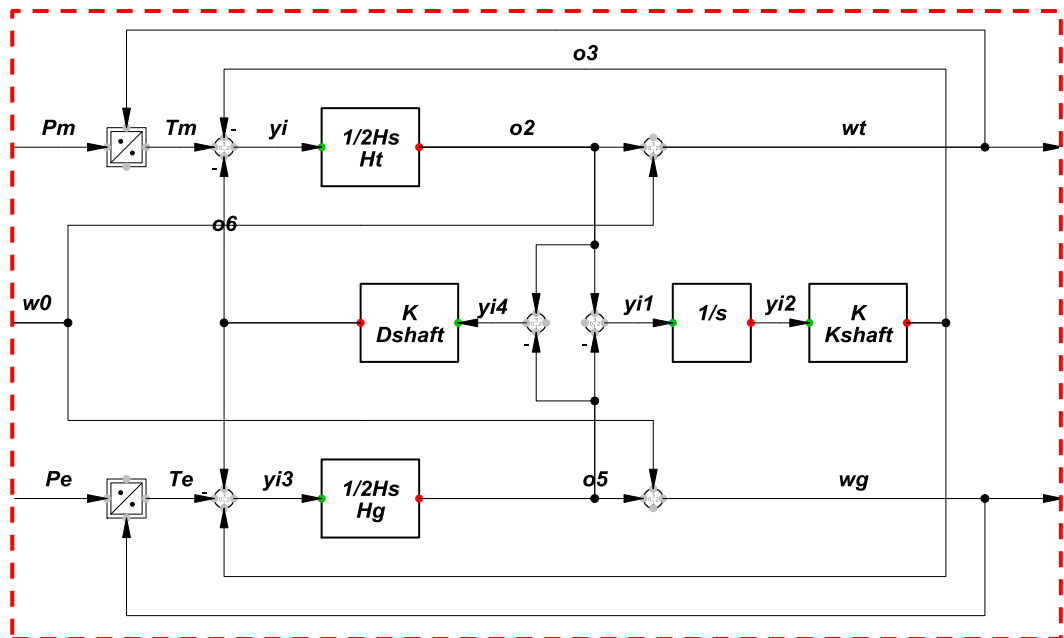


**Figure 6.4: Drive-train model for type 3 wind turbine generator**

The change in rotor speed from its reference point is used as an input to both pitch and torque control.

### 6.1.3 Pitch control model

The amount of mechanical power produced by the wind turbine generator depends on the pitch angle control. Pitch angle controller is activated when the power generated through wind kinetic energy is different from the power grid demand. The pitch controller ensures that the power available from the wind turbine generated is extracted as efficiently as possible through repositioning the blade pitching. The dynamic response of the blade pitching is control by two PI controllers by processing the speed and the power errors. Figure 6.5 below illustrates the pitch control model for a type 3 wind power plant.

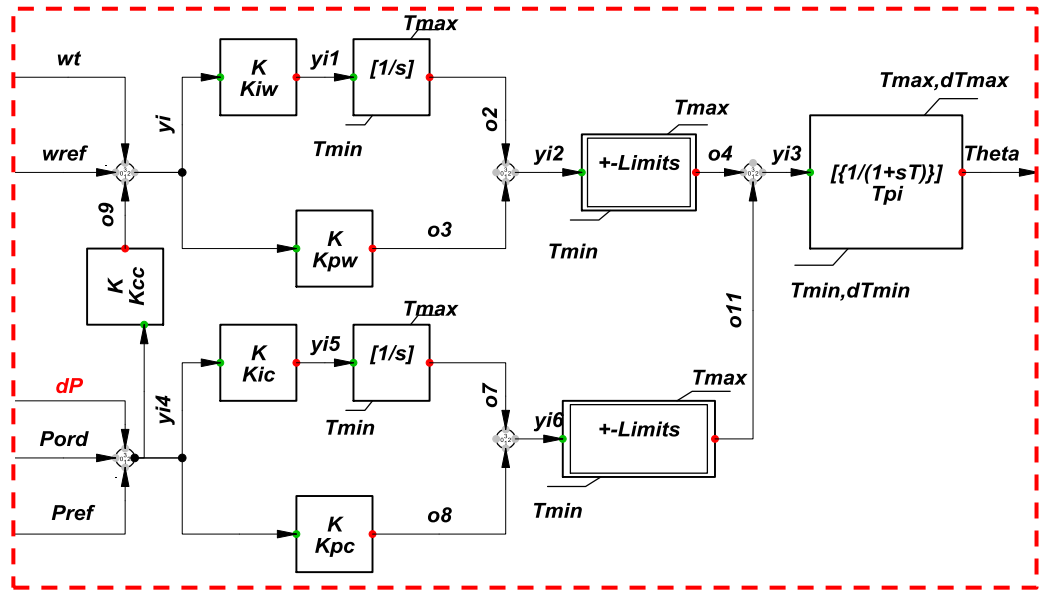


**Figure 6.5: Pitch control model for type 3 wind turbine generator model**

The mathematical model of the pitch compensation is shown in equation 4.9 below.

$$\dot{\theta} = \frac{1}{T_{pi}} (\theta_{pc} + \theta_{pco} - \theta) \quad 4.3$$

where

$$\theta_{pc} = K_{pw} [\omega_t - \omega_{ref} + K_{cc} (P_{ord} - P_{ref})] + s_0 \quad 4.4$$

And

$$s_0 = \int_{T_{min}}^{T_{max}} [\omega_t - \omega_{ref} + K_{cc} (P_{ord} - P_{ref})] dx \quad 4.5$$

The output signal  $\theta_{pc}$  is measured at point o4 on the diagram above and  $s_0$  refers to the speed PI control.

While

$$\theta_{pco} = K_{pc}(P_{ord} - P_{ref}) + S_1 \quad 4.6$$

Where

$$S_1 = \int_{T_{min}}^{T_{max}} (P_{ord} - P_{ref}) dx \quad 4.7$$

$\theta_{pco}$  is measured at point o11 in the diagram above, and  $S_1$  refers to PI control of the active power positioned at the bottom of the diagram.

### 6.1.4 Torque control model

The purpose of the torque control is to match the initial electrical torque. The torque reference can be determined in two techniques. The first technique is through maximum power tracking. In this technique, the turbine will try to meet them closer to the rotor speed to achieve maximum torque. Alternatively, a plant controller is used, which sets the active power reference to create the electrical torque. The plant controller is external. Tflag determines the active technique in the diagram, which sets the digital output when either control technique is activated. Tflag can be 1 or 0. The torque control model is represented in Figure 6.6 below.

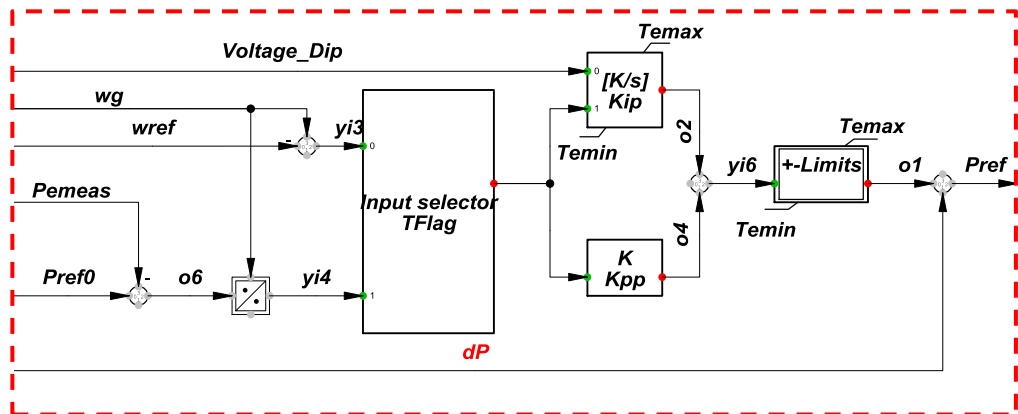


**Figure 6.6: Torque control model for type 3 wind turbine generator**

Torque and pitch control are the primary controllers that the wind turbine generator depends on to produce adequate electrical power provided wind is available.

The integration of the wind power plant to the modified IEEE 14 bus network is shown in Figure 6.7 below. The model below is demonstrated on a de-energized state on DigSILENT. The wind turbine generated is an aggregated model that



represents several parallel-connected wind turbine generators. The wind turbine generators are all connected to the Point Of Common Coupling (PCC). The voltage level at PCC is 690V phase-to-phase. Therefore, a power transformer is used to set up the voltage level of the wind turbine grid to 33kV for grid integration. The wind power plant is integrated at bus 14. The Point Of Connection (POC) is at bus 14. The wind power plant is integrated into this bus as seen as the weakest in the grid. Therefore this integration will also help to support the bus voltage at the point of connection.

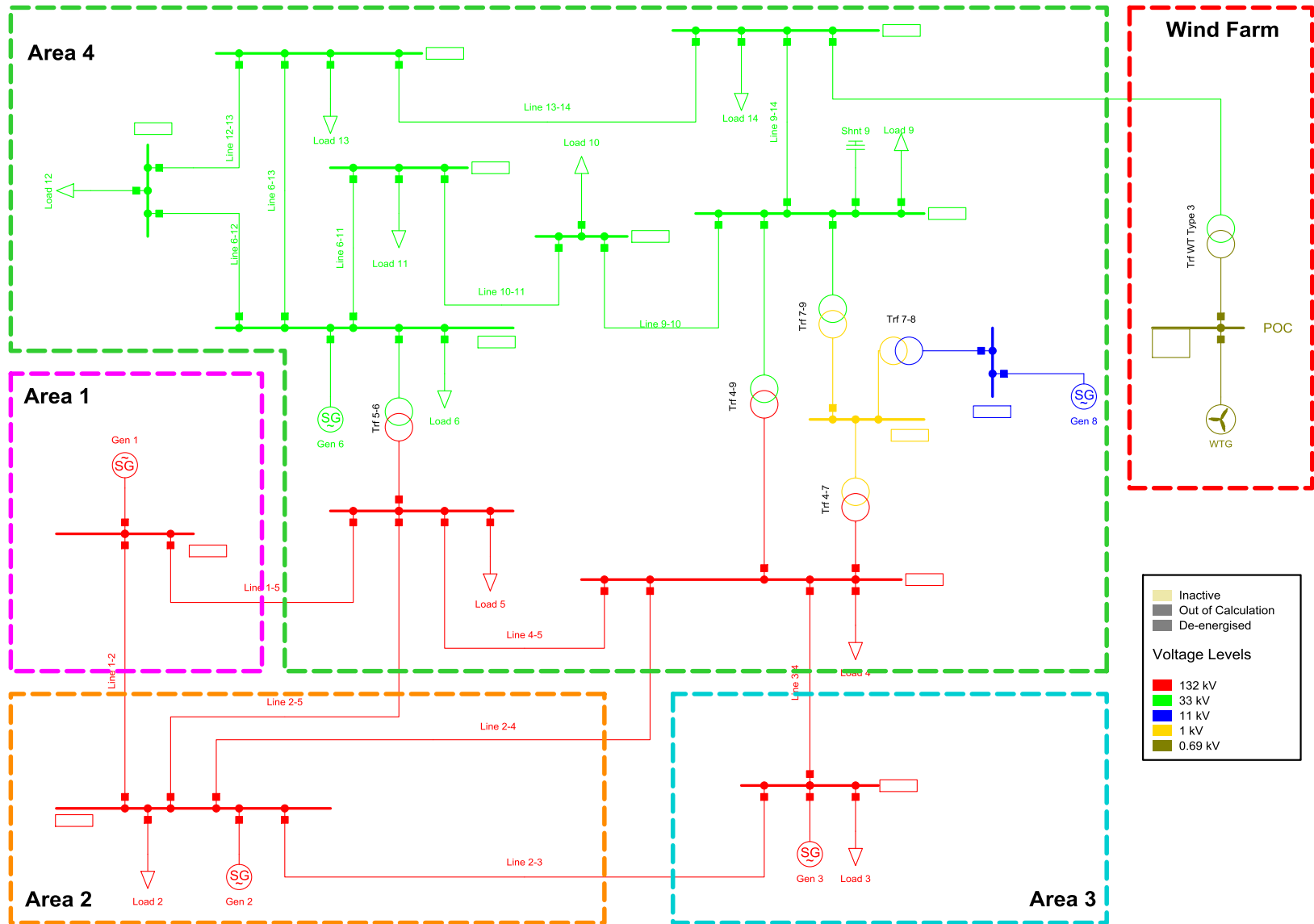


Figure 6.7: The modified IEEE 14 bus network with wind power plant integration

## **6.2 The role of the wind active power compensation in frequency control**

From chapter 5, the contribution of automatic generation control (AGC) system frequency control was assessed. It has been noted that when there are no spinning reserves available, the AGC cannot regulate the frequency. It has been observed in chapter 5 that when the load demand increase is at 9%, the AGC is starting to fail to maintain the frequency to its nominal value of 50Hz. When the load demand continued to increase and reached 15%, the governor maintains the frequency at 49.32Hz, while the AGC stabilizes the frequency to 49.64Hz.

The responsibility of the AGC is not only to support system frequency stability but also to assist in maintaining the power interchange between the areas to avoid transmission and distribution lines being overload. It was observed in chapter 5 that, when generation spinning reserves were depleted, the system frequency and power interchange between the areas could not be maintained at their initial schedules amount. In addition to this, the AGC and the governing system could not support the voltage drop experienced in bus bar 14.

Understanding the capability of the wind turbine generator and what it can offer in terms of maintaining power system stability, an aggregated model of 40MW is modeled using DIgSILENT power factory software. The wind farm model enables the compensation of the active power to the grid following frequency and tie-interchange power interchange deviations from their nominal and scheduled amount.

Wind power plant integration is proposed as an active power compensator to improve the system frequency without interrupting the supply to the consumers and avoiding under-frequency load-shedding scheme operation. For the wind turbine generator to release its active power based on system frequency deviation, an additional control loop needs to be integrated into its control systems. The wind turbine generator's supplementary frequency control loop is shown in Figure 6.8 below. In the control loop below, system frequency is measured, and a control signal sent to the PID control is subtracted from the reference frequency (50Hz). The signal processed through PID control is passed through a low pass filter. The output signal from the low pass filter is sent to the pitch control and the torque controller. This signal influences the pitch angle of the turbine and the torque control, a signal based on the aerodynamics of the wind turbine.

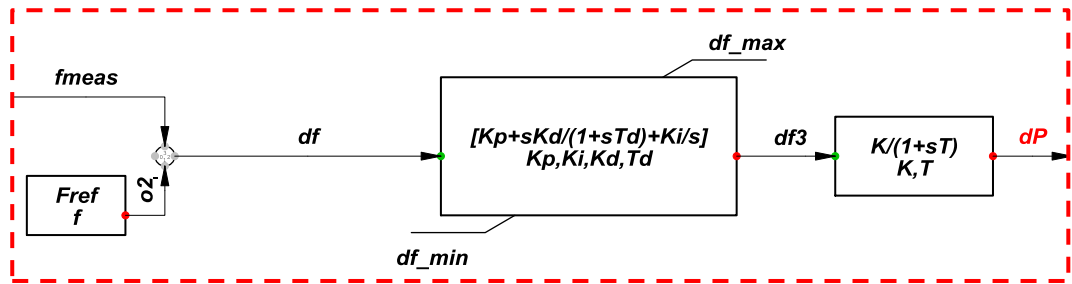


**Figure 6.8: Wind turbine generator primary frequency supplementary control loop**

When there is frequency deviation, the error signal ( $dP$ ) from the primary frequency control loop is subtracted from active power order ( $P_{ord}$ ) and reference active power ( $P_{ref}$ ) of the pitch controller. This will result in a new pitch angle position, as shown in Figure 6.5 above.

The wind turbine supplementary control loop ( $dP$ ) is also summated with the output signal of the torque control ( $P_{ref}$ ). When both pitch and torque control signals have deviated from their initial state, the active power of the wind turbine generator is released. In Figure 6.6 above, the wind turbine generator's supplementary control loop signal is summated with torque control output signal.

The integrated control scheme is proposed to perform its control actions as per the developed algorithm presented in a flow chart in Figure 6.9 below. When the load disturbance occurs, which will influence the stability point of frequency and shift the power interchange, the governing system will respond to the disturbance. If the frequency is not recovered through the governing system response, the AGC will be activated, and generation spinning reserves will be released until the frequency is recovered. If the load demand increases and the spinning reserves are depleted, the wind turbine generator will release active power based on the system frequency until the stability is regained and the scheduled power interchange is maintained.

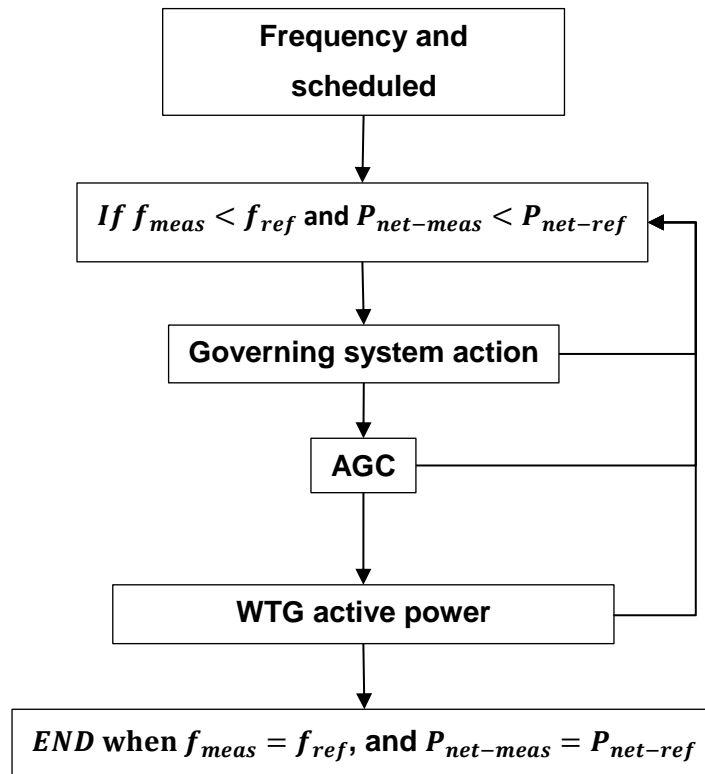


**Figure 6.9: Consolidated power system frequency and power interchange control scheme algorithm**

### 6.3 Simulations and results discussion

In order to assess the performance of the developed control loop supplementary to the control system of the wind turbine generator, the load demand increase will be applied as described in chapter 4. Table 6.1 below shows the case study to assess the developed wind turbine generator's active power compensation response effectiveness.

**Table 6.1: Case study 3 – Assessment of the effectiveness of wind turbine generator active power compensation control loop**

Case study name		Aim				Type of disturbance				Control method			
<b>Case study 3</b>		The developed wind turbine generator's active power compensation is assessed. Its response is analyzed, and it is compared to when the is a governing system only, or when the is a governing system and the automatic generation control, and when three control stages are active. Lastly, a consolidated controlled system includes AGC and wind turbine generation active power compensation is implemented and analyzed.				Load demand increase by 15% in steps of 1%				Generator governing system, Automatic Generation Control (AGC), and the wind turbine generator active power compensator.			
Monitored variables													
Lowest Bus Voltage (PU)		Frequency (Hz)		Area 2 net-power interchange (MW)		Area 3 net-power interchange (MW)		Area 4 net-power interchange (MW)		Total Load demand (MW)		Total Generation Supply (MW)	
before	after	after	before	after	before	before	after	before	after	before	after	before	after

Figure 6.10 below shows the simulation results for the system frequency following a load demand increase disturbance. In Figure 6.10, the red graph shows the system frequency during governing system response. The blue graphs represent the contribution of both the speed governing system and automatic generation control in frequency support. In comparison, the green graph shows the contribution of the wind turbine generator active power compensator with both governing system and automatic generation control activated to support system frequency following a load demand increase. On the top graph, the y-axis is the system frequency while the x-axis is the simulation duration. The improvement of the system frequency under the three different control conditions is remarkable. The AGC improved the frequency to 49.64Hz from 49.32Hz, and the active power from the wind turbine generation system resulted in a significant improvement of the frequency to 49.99Hz.

At  $T=160\text{sec}$ , the AGC is seen to be failing to maintain the power system frequency to its nominal value following a continued load demand increase. The benefits of the integrated wind power plants are noticeable at this stage, as they maintained the system frequency to as close as possible to the nominal value, and the recorded frequency is 49.99Hz.

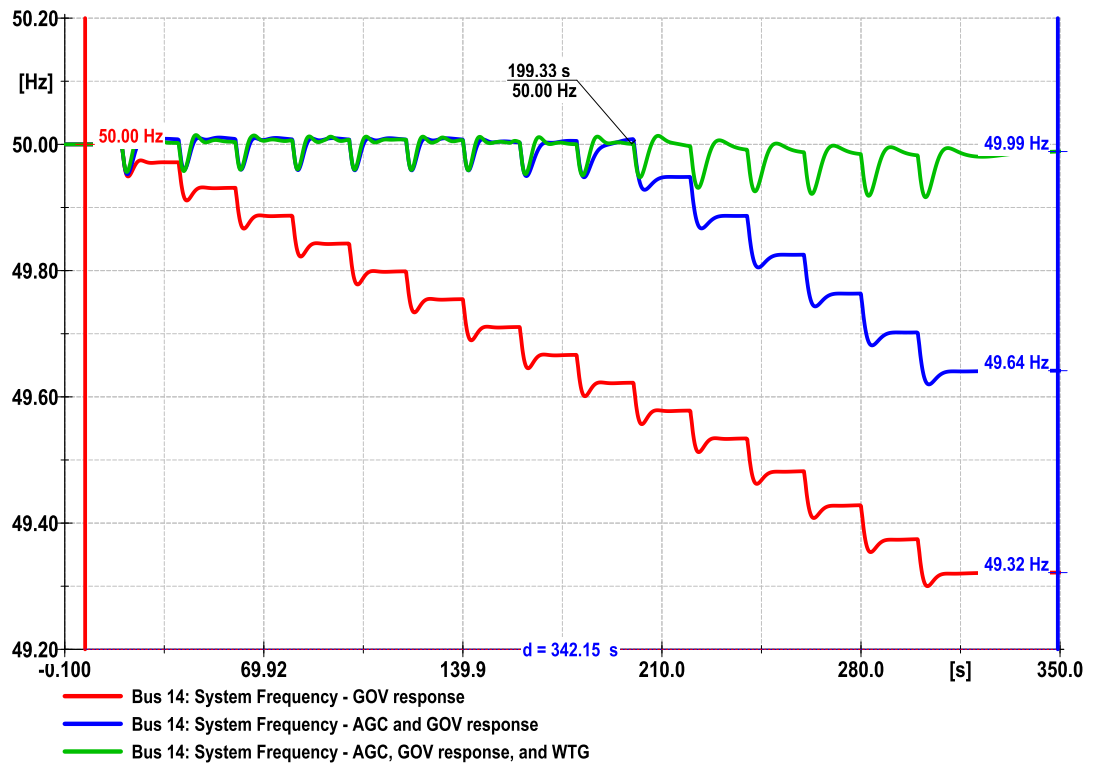


**Figure 6.10: System frequency before and after the AGC and WTG implementation following a 15% load demand increase.**

When the AGC with the governing system could not maintain the system frequency at its nominal value, the wind turbine generator active power compensator released an additional power to support the power system frequency. Since the AGC uses spinning reserves to assist the governing system to provide frequency support to the grid, at  $T=160$ sec is when the spinning reserves were starting to be depleted. At this time,  $T=160$ sec, the wind turbine generator started to release more active power to the grid, as indicated in Figure 6.11 below. The total active power contribution of the wind turbine generator to the grid is 9.09MW after a 15% load demand increase.



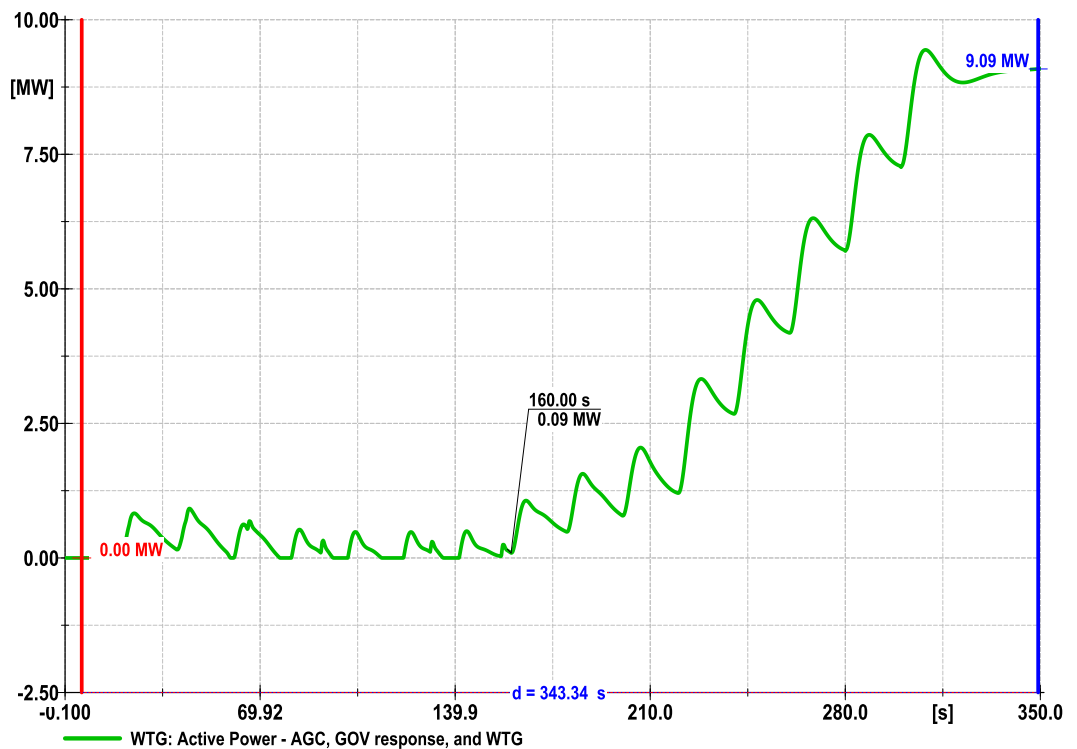


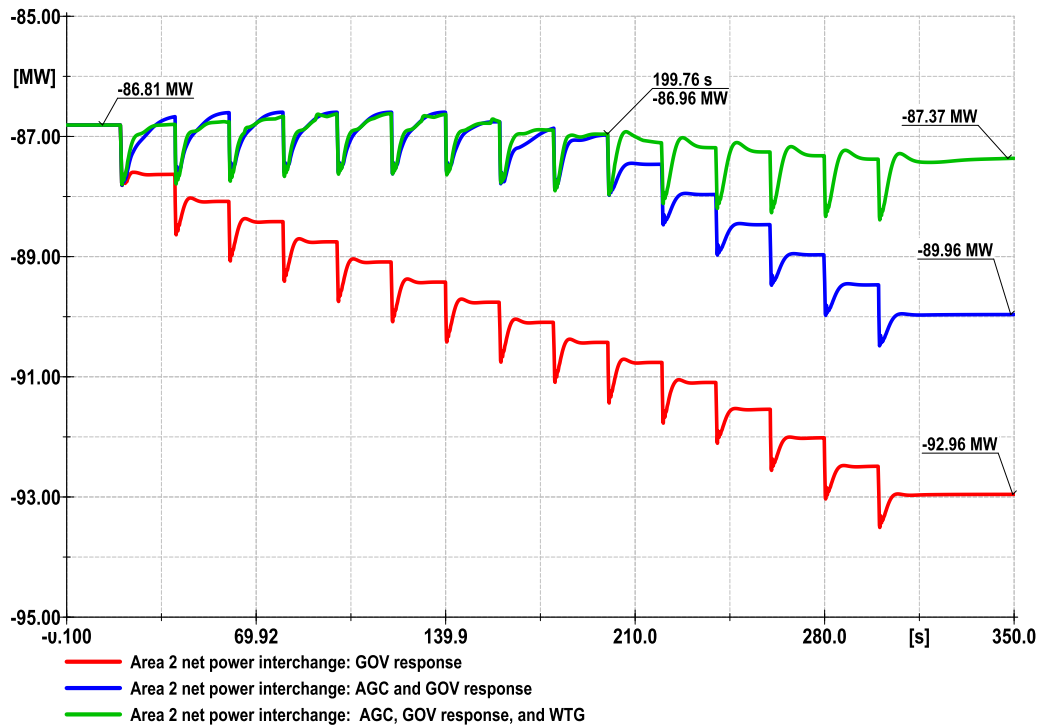
**Figure 6.11: Active power contribution of the wind turbine generator following load demand increase.**

Another essential function of the controllers in the power system is to ensure that the tie-line power interchange is maintained within the scheduled amount. When there were no controllers, the power interchange between the areas started to deviate following a load demand increase. When the AGC was introduced, the scheduled active power interchange was maintained up to 9% of the load demand increase. The power interchange deviated from the scheduled amount when the load was increased by more than 10%. The AGC could not maintain the power interchange amount.

The introduction of wind turbine active power compensation and AGC, including governing system, improved the maintenance of the scheduled active tie-line power interchange. After a 10% load demand increase, the scheduled tie-line power interchange was maintained as close as possible to their scheduled amount in each area.

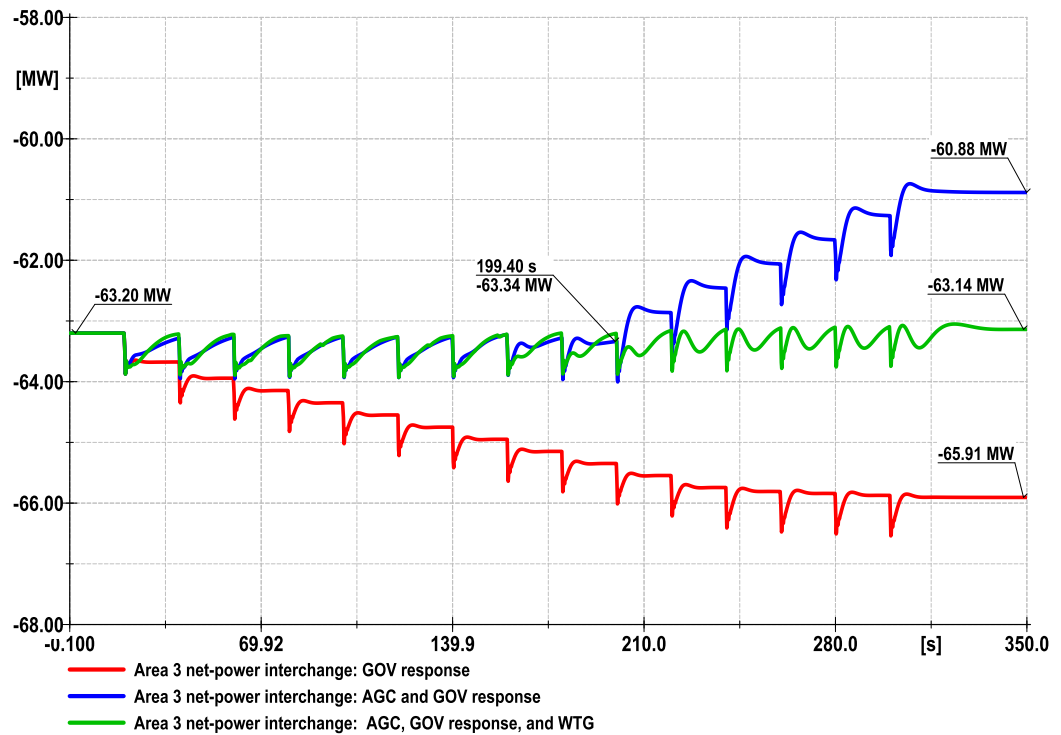
The tie-line power interchange is recorded as negative at the received end of the line. The negative sign indicates the power flow direction, which is toward the area of concern. Figure 6.12 below is the net tie-line power interchange at area 2. Before any disturbance, the scheduled power interchange was -86.61MW. When the load increase occurred, the AGC and the governing system maintained the

power interchange as close as possible to the scheduled amount up to the 9<sup>th</sup> step. At 200sec, the AGC was no longer able to maintain the power interchange, and the wind turbine generator started increasing its power output. At the 15<sup>th</sup> step of the load demand increase, the power interchange was maintained at -87.37MW.



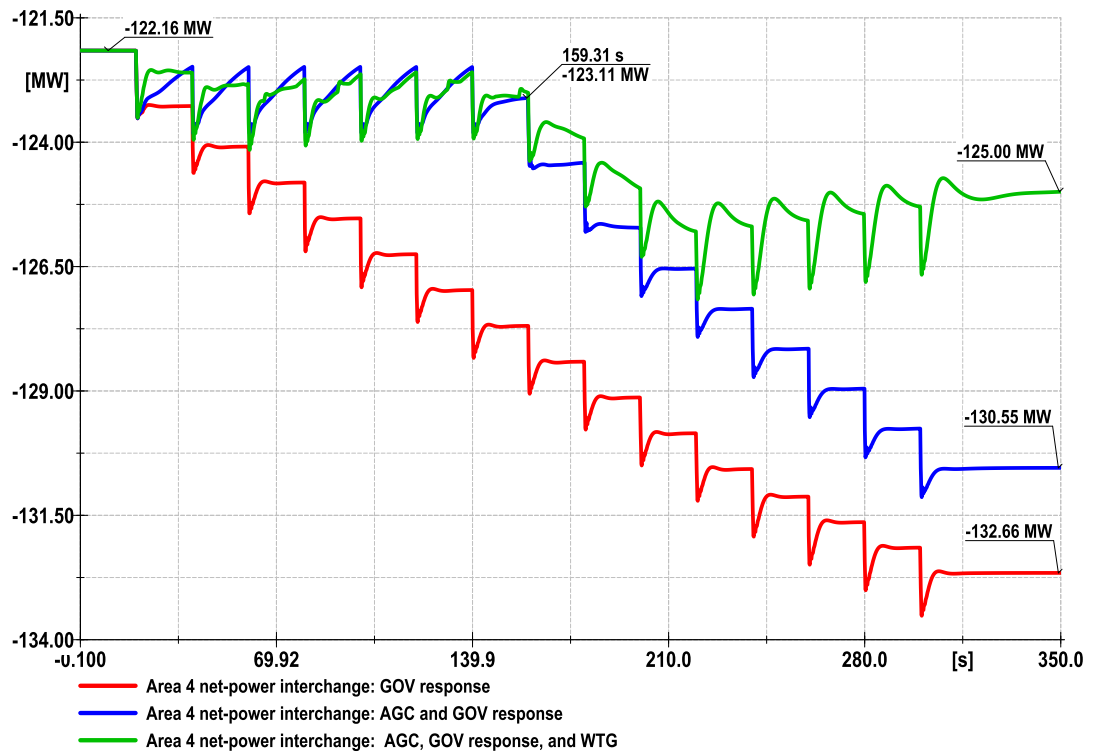
**Figure 6.12: Area 2 Net Tie-line Power Interchange before and after the implementation of AGC and the WTG active power compensator.**

In area 3, the wind turbine generator's active power compensator significantly contributed to maintaining the power interchange. At 200sec, when the AGC was starting to fail, the wind turbine generator contribution maintained the power interchange as close as possible to the scheduled value. At the 15<sup>th</sup> step load increase, the net tie-line power interchange in area 3 was recorded as -63.14MW. Figure 6.13 below represents the result of area 3 net-tie line power interchange under difference control system attempts.



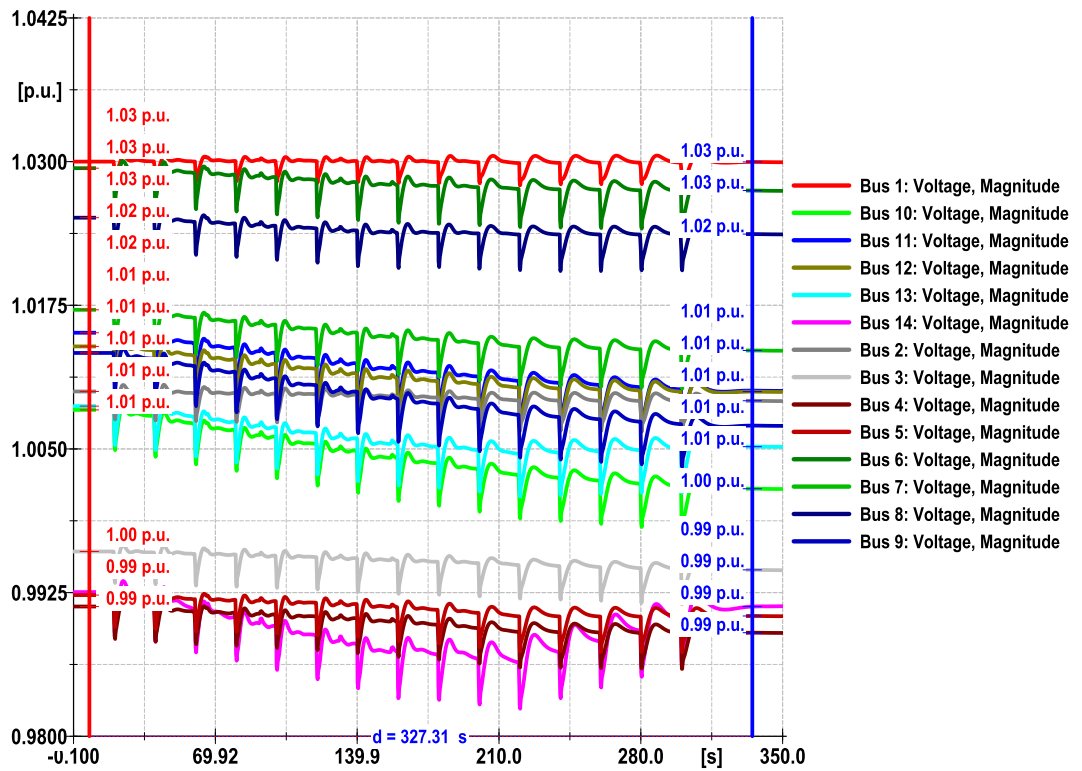
**Figure 6.13: Area 3 Net Tie-line Power Interchange before and after the implementation of AGC and the WTG active power compensator.**

Figure 6.14 below is the net tie-line power interchange for area 4. Before the initiation of the load demand increase, the scheduled power interchange was recorded as -122.16MW. When the load demand increase occurred, the AGC maintains the power interchange for 6% of the load demand increase. As the load demand continued to grow, the AGC started failing, as indicated in Figure 6.14 at T=160sec. The wind turbine generator provided additional support to the control system by keeping power interchange. This is a significant improvement compared to the response of the governing system and the AGC.



**Figure 6.14: Area 4 Net Tie-line Power Interchange before and after the implementation of AGC and the WTG active power compensator.**

Before activating the wind turbine generator control system, bus bar 14 voltage was 0.98pu, the contribution of wind turbine active power has improved bus 14 voltage back to its initial value of 0.99pu after a 15% load demand increase. Figure 6.15 below shows the system bus voltages after a 15% load demand increase. All the bus voltages are stable and maintained within the operating range. Before the load demand increase event, bus 14 voltage was above bus 4. After the load event, bus 14 is still more significant than bus 4 voltage when the wind turbine generator's active power is initiated.



**Figure 6.15: System bus voltage after 15% load demand increase when all control functions are activated**

The results representation for the simulations performed is indicated in Table 6.2 below. The Table covers the results before and after the load event is initiated. The aim is to analyze the response of the developed control system in grid stability with more emphasis on frequency.

Bus 14 results indicated in Table 6.2 below show a significant improvement during wind turbine generator active power compensation compared to only the governing and AGC active. The voltage of the system is maintained to its initial values as before the load demand increase.

The system frequency is also improved to as close as possible to a new value of 49.99Hz due to integrating the wind power plant and its developed control scheme. During the implementation of AGC and the governing system, the system frequency reached a steady state of 49.64Hz following load demand increase. Therefore the effectiveness of wind turbine generators with their control scheme is remarkable to the maintenance of the power system stability.

**Table 6.2: Case study 3 results– Assessment of the effectiveness of wind turbine generator active power compensation control loop**

Case study name		Aim				Type of disturbance				Control method			
<b>Case study 3</b>		The developed wind turbine generator's active power compensation is assessed. Its response is analyzed, and it is compared to when the is a governing system only, or when the is a governing system and the automatic generation control, and when three control stages are active. Lastly, a consolidated controlled system includes AGC and wind turbine generation active power compensation is implemented and analyzed.				Load demand increase by 15% in steps of 1%				Generator governing system, Automatic Generation Control (AGC), and the wind turbine generator active power compensator.			
Monitored variables													
Lowest Bus Voltage (PU)		Frequency (Hz)		Area 2 net-power interchange (MW)		Area 3 net-power interchange (MW)		Area 4 net-power interchange (MW)		Total Load demand (MW)		Total Generation Supply (MW)	
before	after	after	before	after	before	before	after	before	after	before	after	before	after
0.99	0.99	50	49.99	-86.16	-87.37	-63.20	-63.14	-122.16	-125.0	259	297.85	267.67	307.74

The net tie-line power interchange has been improved as well. In area 2, the initial power interchange was -86.16MW; when the load demand increase of 15% occurred, the power interchange was -92.96MW during the governing system response. The AGC improved it to -89.96MW. With the consolidated control scheme (governing system response, AGC, and wind turbine generator active power compensator), the power interchange improved to -87.37MW.

In area 3 the consolidated control scheme improved the power interchange from an initial amount of -63.20MW; after the load demand increase, the power interchange was recorded as -63.14MW.

The power interchange in area4 was improved from -122.16MW to -125MW when the consolidated control scheme was applied. The GOV response result to -132.66MW. When AGC was applied, the power interchange was improved to -130.55MW.

#### **6.4 Conclusion**

The integration of wind power plants in the power system significantly contributes to the power system's stability. The integration of these resources is made closer to the load. It also minimizes the transmission and cost and network losses transmission. Proper implementation of the control scheme enables the utilization of the DERs in various configurations. The developed control scheme proves that the DERs such as wind power plants can be utilized in the power system for stability purposes, mainly considering frequency instability. Its contribution does not only cover the frequency stability but also voltage stability is improved.

The verification of the developed control scheme in real-time is essential to assess the response of the control scheme in real-time implementation. In chapter 7, the modified IEEE 14 bus network is model and simulated using RSCAD Real-Time Digital Simulator. Software-based AGC and Wind turbine generator active power compensator are developed and analyzed under various case studies.

## CHAPTER SEVEN

### MODIFIED IEEE 14 BUS NETWORK AND IMPLEMENTATION OF THE DEVELOPED CONTROL SCHEME IN REAL-TIME DIGITAL SIMULATOR (RTDS)

#### 7.1 Introduction

In this chapter, the control schemes developed in chapter 5 and 6 using the DIgSILENT simulation platform are further implemented on the real-time digital simulation (RTDS) platform. The effectiveness of the developed control scheme is assessed based on the load demand increase contingency applied. Therefore the controller is anticipated to realize the frequency deviation and trigger the integrated wind turbine generator to release the active power to restore the frequency to the acceptable operating range of between 49.5Hz and 50.5Hz. The first control strategy used is the governing system response, followed by automatic generation control, and the last stage is the wind turbine generator active power compensator.

RTDS is an industrial real-time power system and controls simulation platform that integrates external hardware objects. This helps to analyze its behavior on a real-time operation basis. In this chapter, the control scheme is developed using RSCAD software and is implemented to the network under study. The primary function of the developed control scheme is to ensure that the power system frequency is maintained within its operating range and to ensure that the active power interchange between the areas is also maintained. The decentralized automatic generation control scheme was implemented. The decentralized automatic generation control scheme is categorized into two options, and the first option is when the only frequency is controlled. The second option is when both frequency and the tie-line power interchange between the areas are considered.

Implementing the control scheme on RTDS makes it easier to assess its behavior when fully implemented into the real-time power system. Various contingencies are applied to verify the effectiveness and appropriateness of the control scheme for an actual power system grid implementation. This control scheme is assessed on the IEEE 14 bus power system network modified to suit the application.

#### 7.2 Modeling of modified IEEE 14 bus power system network in RSCAD

The network diagram shown in Figure 7.1 was developed using the RSCAD draft of RTDS. The network diagrams were developed to evaluate the effectiveness of



the automatic generation control by applying the same load incremental contingency used in chapters four and five.

Figure 7.1 shows four subsystem names as area 1, area 2, area 3, and area 4. Area 1 is exporting power to both area 2 and area 4. T1 is the tie-line from area 1 to area 2 while T2, from area 1 to area 4. Generator 1 is also positioned in area 1.

Area 2 subsystem is receiving power from area 1 via T1 tie-line. Area 2 is also exporting power to areas 3 and 4. The tie-lines used for exporting power from area 2 to area 4 are T4 and T5. T3 is used to export power from area 2 to area 3. The rated apparent power of Generator two is 60MVA. This generator has enough power to cater to the load, and the excess electrical energy is exported to the neighbouring areas such as area 3 and area 4. The load demand in area 2 is 21.7MW

Area 3 is receiving additional power from area 2 and area 4 through tie-line T3 and T6 respectively. The area has a single bulk load of 94.2MW, which is the biggest single load in the network. Generator 3 has a rated apparent power of 60MVA, hence this area required an additional supply from neighboring areas.

Area 4 is the biggest area with the most loads. This area is regarded as the distribution area. Area 4 consists of two generators (generator 6 and 8) with a total rated apparent power of 60MVA. This total generation capacity available for this area is not enough to support the total load demand within the area. Hence areas one and two are supplementing this area for the deficit power. The total load demand in this area is 143.1MW.

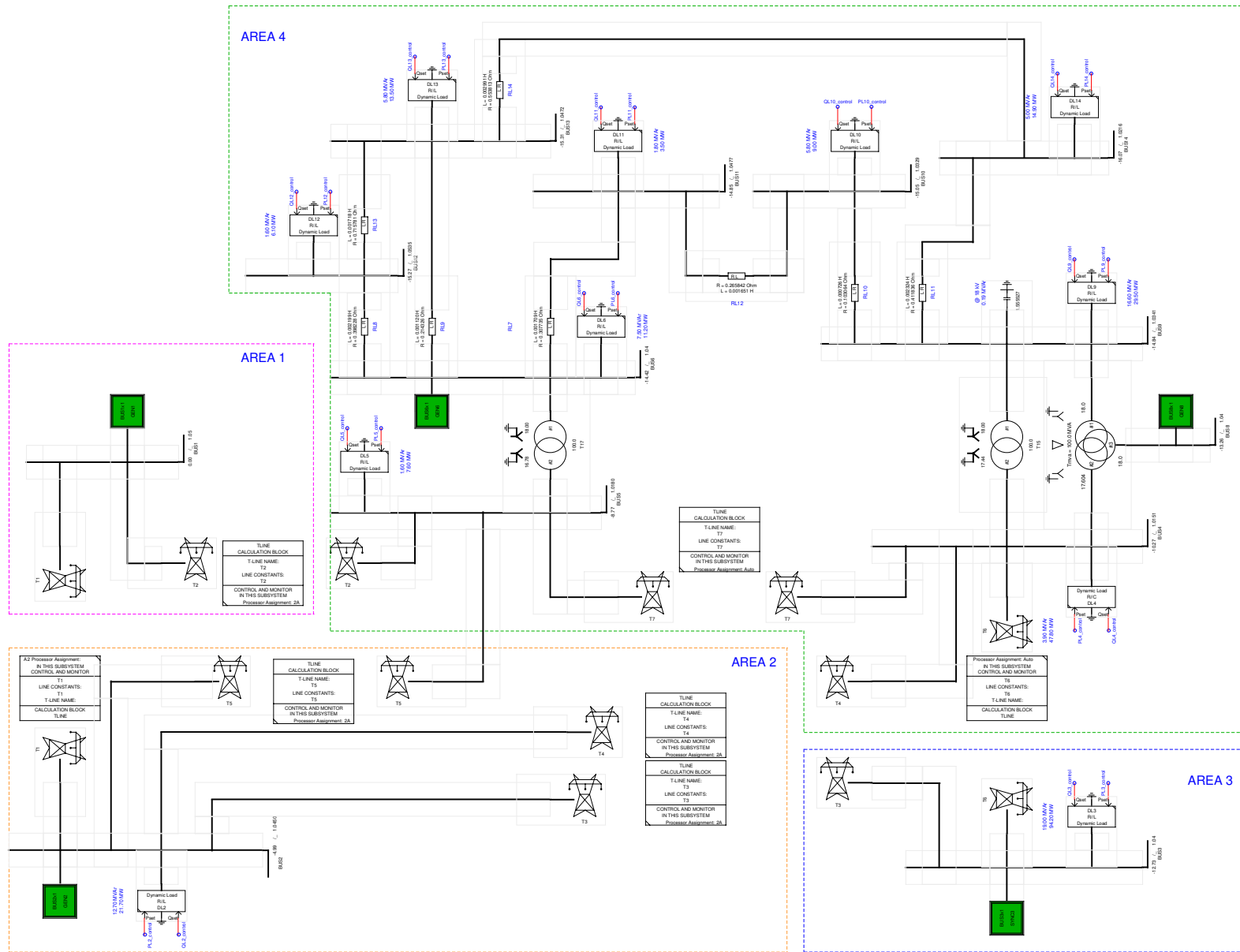
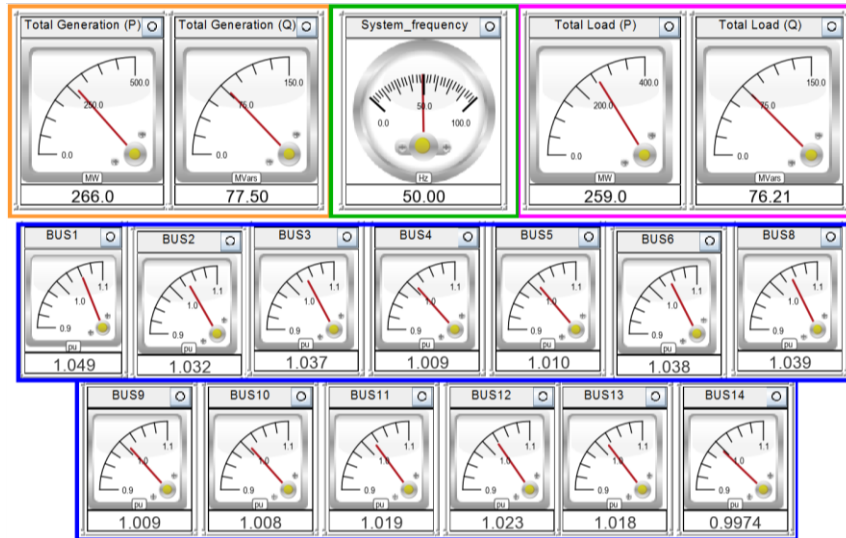


Figure 7.1: Modified IEEE 14 bus power system network model in RSCAD

### 7.2.1 Steady-state simulation and results analysis

This analysis is made to prove that the network is stable before the implementation of the contingencies. Bus voltages, generation supply, load demand, and system frequency are monitored. Figure 7.2 below shows the results for the total generation supply, total system load demand, bus voltages, and network frequency during steady-state analysis. According to the results recorded, the power system voltage is stable between 0.9947pu and 1.049pu. The system frequency was measured at bus 14, and it is also stable at 50Hz.

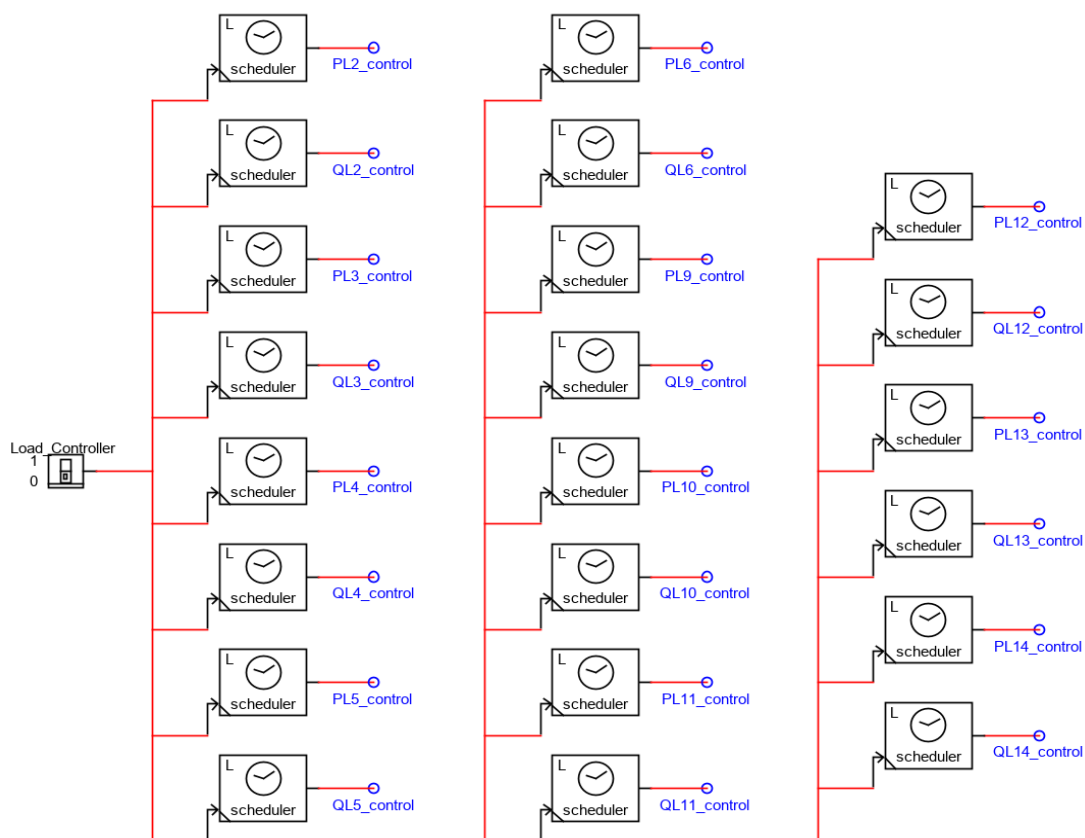


**Figure 7.2: Steady-state generation supply, bus voltages, load demand, and system frequency**

The power loss can be determined by subtracting the load demand power from the total generation supply. The results for the power losses are 7.2MW.

### 7.2.2 Dynamic state simulation and results analysis

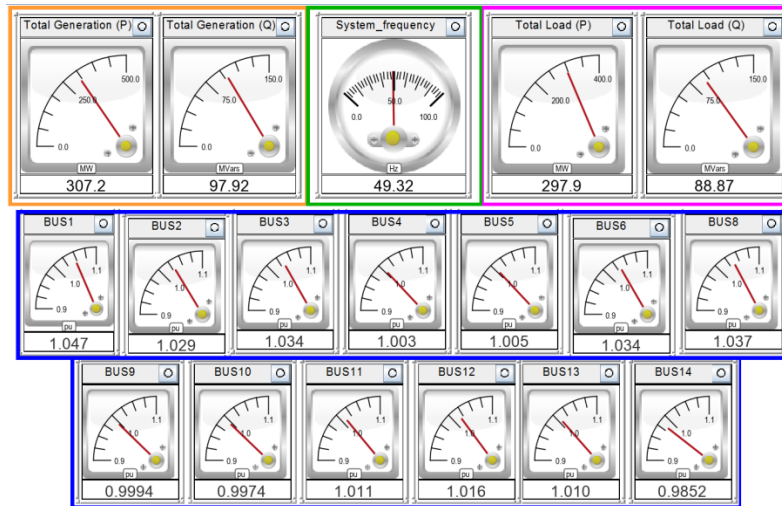
Unlike DIGSILENT power factory, the implementation of the load contingency on RSCAD is done by using load schedulers. In the load scheduler component, the load multiplier and the time at which the load demand increase should occur can be defined. The type of load demand component (active and reactive components) increase has its scheduler. Figure 7.3 below illustrated the load scheduler.



**Figure 7.3: Load scheduler**

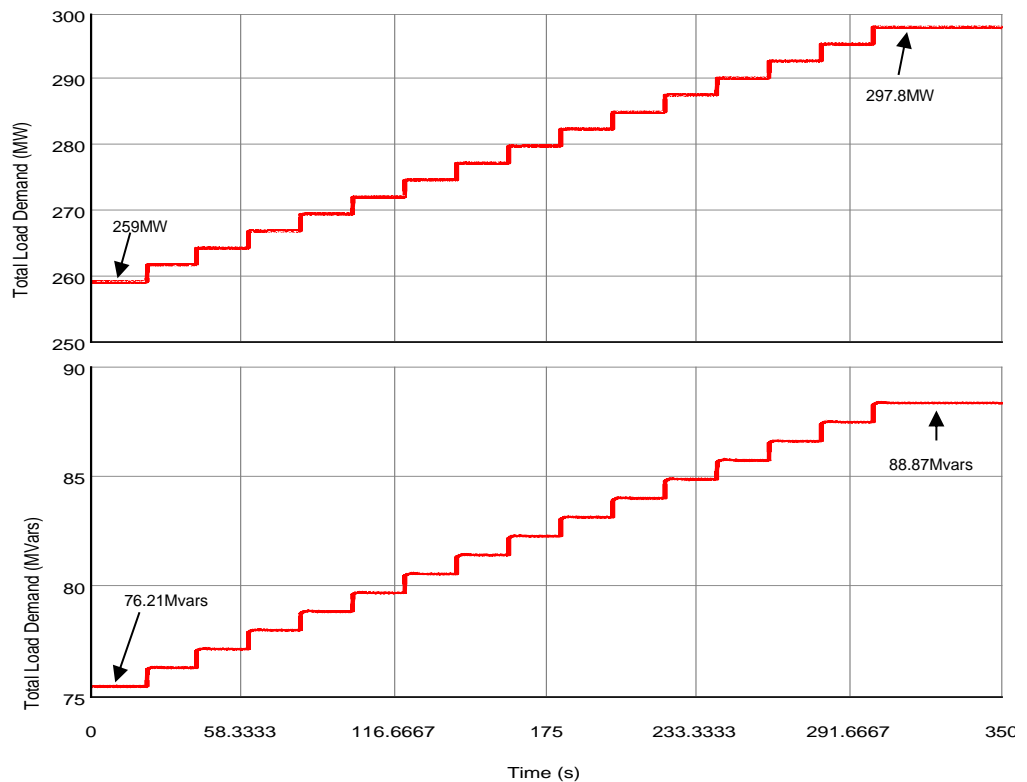
During dynamic state analysis, the load scheduler shown in Figure 7.3 above is utilized to increase the system load demand by 15% in steps of 1%. The load demand increase is done on both the active and the reactive components of the load. The aim of applying this contingency is to assess the response of the governing system during dynamic state condition. Case study 1 in chapter 4 is repeated in this analysis. Case study 1 described in chapter 4 investigates the response of the governing system to check its effectiveness and contribution in power system frequency stability.

Figure 7.4 below shows the results of the monitored signals of the power system after the load demand increase contingency. With the load demand increase contingency, the system frequency dropped from 50Hz to 49.32Hz. The total generation supply increase from 266MW to 307.3MW due to the load demand increase from 259.5MW to 297.9MW. Bus 14 voltage is seen as the lowest voltage bus in the system with a measured value of 0.9826pu.



**Figure 7.4: System monitored variables after a 15% load demand increase contingency**

The load demand increase is graphically represented in Figure 7.5 below. The load ramping starts at initial system loading of 259.8MW and increases by 1% steps to 15%, which is equated to 297.9MW as indicated in the wattage measurement meter shown in Figure 7.4 above. Within Figure 7.5 below, the reactive power before the application of load demand increase contingency was 76.21MVars, and after the load demand increase, it was recorded as 88.87MVars



**Figure 7.5: Total load demand after 15% load demand increase (1% incremental steps)**

The total generation supply active power increased from 266MW to 307.2MW and reactive power from 77.5MVars to 97.92MVars, respectively, following the applied load increment contingency. Figure 7.6 diagram shows the plot of the generation supply before, during, and after the load demand increase for both active and reactive generation power.

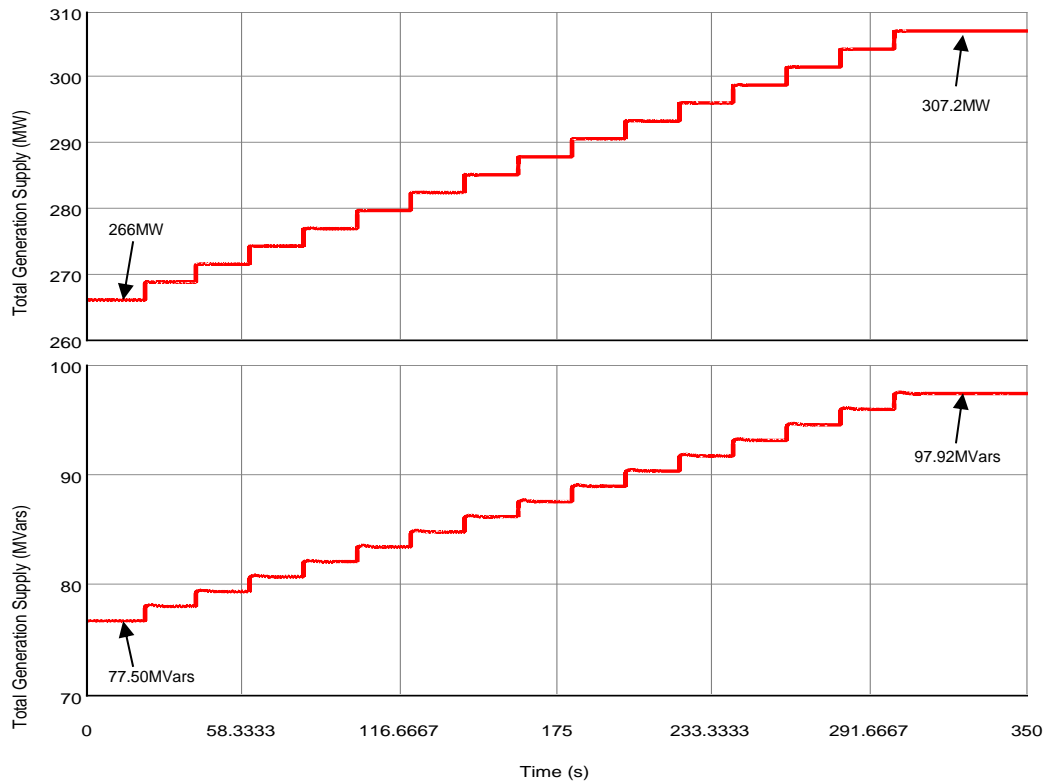


**Figure 7.6: Total generation supply after 15% load demand increase contingency (1% incremental steps)**

The load demand increase contributed to the decline in system frequency, which was initially recorded as 50Hz before the load demand increased contingency. After the load demand increase contingency, the system frequency was recorded as 49.32Hz. This level of system frequency is outside of the acceptable operating frequency (49.5Hz and 50.5Hz) as per the power system grid code standard in South Africa. The system frequency results are shown in Figure 7.7 below. It can be seen that the introduction of a 1% step load demand increase results in an approximately 46mHz deviation from the nominal value.



**Figure 7.7: System frequency during speed governing system response**

Due to the load demand increase, the active power transfer from one area to another is also affected. Figure 7.8 below shows the initial power transfer to area 2, measured at the receiving end of area 2. The measured value before the disturbance was 97.3MW, and post-disturbance was 111.14MW. In Figure 7.8 the results indicate a negative sign, which denotes the power flow direction as they are recorded at the receiving end.

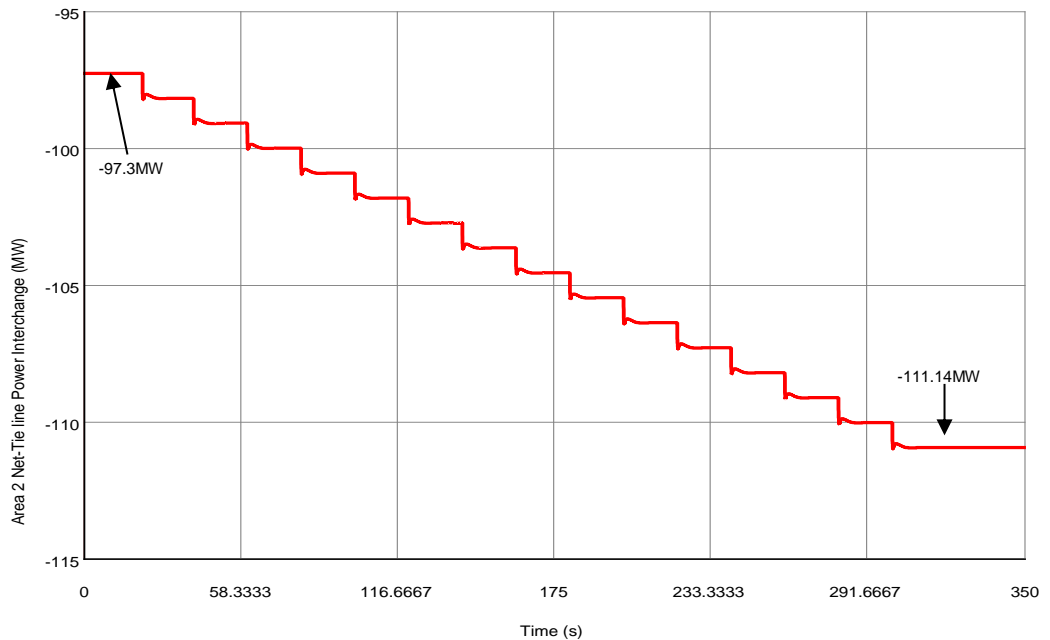


**Figure 7.8: Area 2 Net tie-line power interchange during the speed governing system response**

Area 3 and Area 4 were also affected. The active power for area 3 was recorded as 48.61MW and area 4 was 125.11MW, respectively, before the load demand increase. After the load demand increased contingency, the power transfer recorded in area 3 and area 4 was 56.22MW and 141.44MW. Area 4 is the most heavily loaded area with a total load demand of 143.1MW and followed by area 3, with total load demand of 94.2MW, while area 2 has a total load demand of 21.7MW. This results in more active power required to meet the load demand in these heavily loaded areas. Figure 7.9 and 7.10 shows the results of active power transfer to and area 3 and area 4, respectively

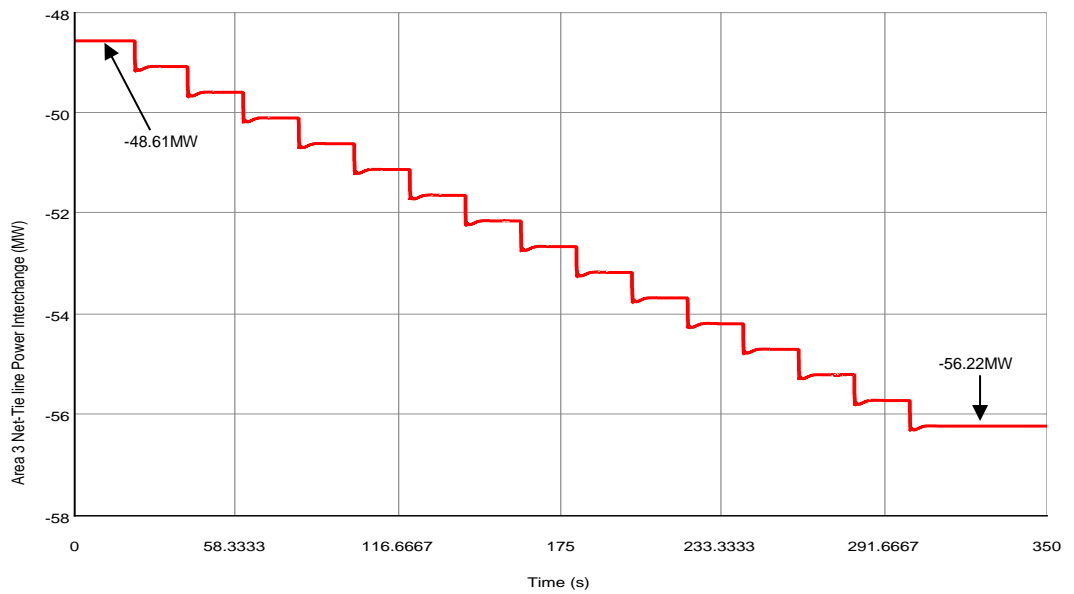


**Figure 7.9: Area 3 Net tie-line power interchange during the speed governing system response**



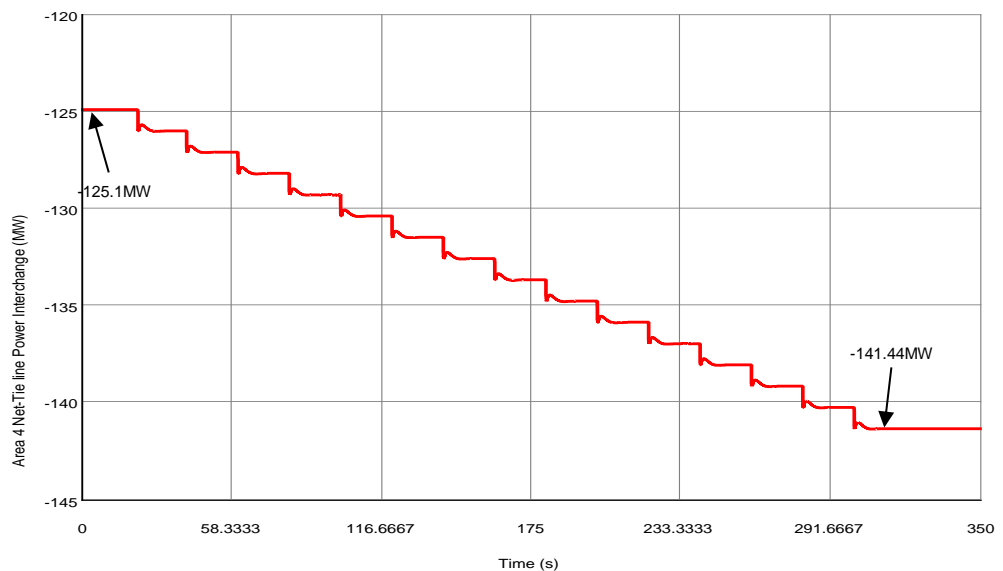
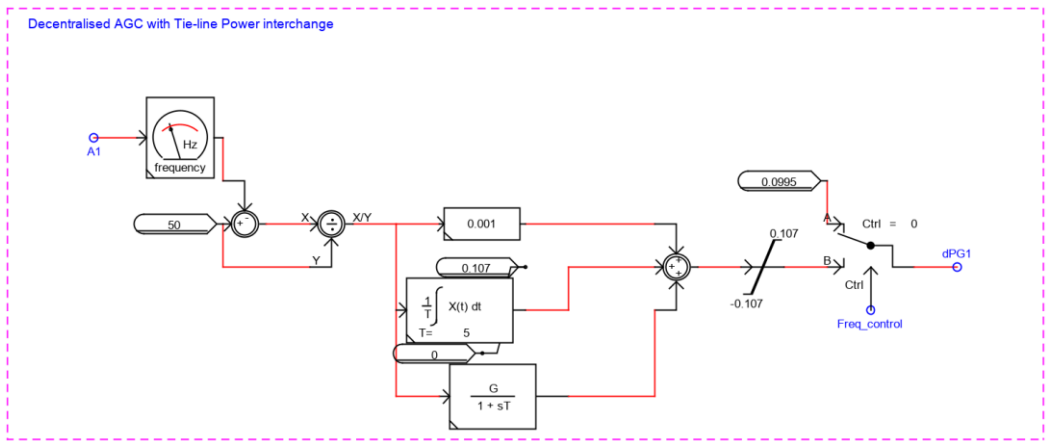


**Figure 7.10: Area 3 Net tie-line power interchange during the speed governing system response**

The speed governing system has brought the system frequency to a new steady-state 49.32Hz following a load demand increase event. The speed governing system is noticeable to be unable to fully recover the system frequency, hence an additional control system is required to restore the system frequency to its nominal state. An automatic generation controller (AGC) modeling is proposed to recover the system frequency to its nominal value of 50Hz. The decentralized AGC is considered for the application. Each area (from area 1 to area 4) will have its dedicated AGC to control both frequency and net-areal tie-line power interchange.

### 7.3 Modeling of decentralized automatic generation control (AGC)

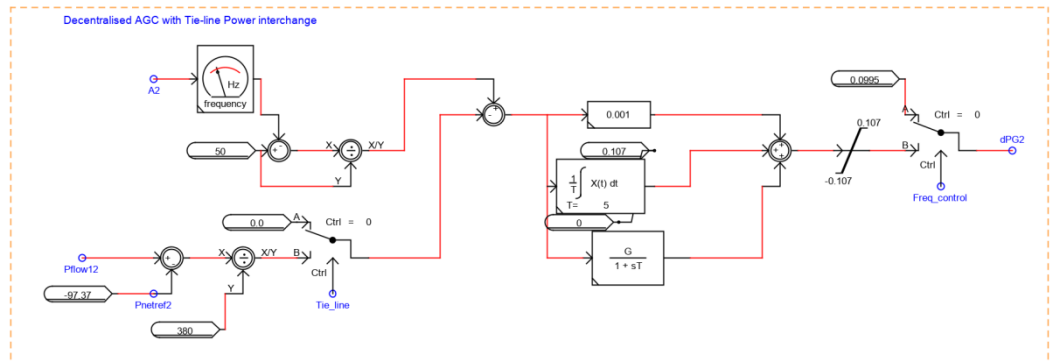
Area 1 AGC input is the system frequency measured in bus 1 (A1), and output  $df$  is the difference of reference angular frequency and the input angular frequency.  $df$  is divided with the reference angular frequency and converted to a per-unit signal  $df(\text{pu})$  fed to the PID controller. The output signal from an integral part and the proportional gain are summated together and fed to a signal limiter. The output signal of the limiter is sent to the signal selector. The signal selector is used for initializing the simulation so that the control logic is not immediately integrated. The power system needs to be first initialized, and once it is stable, the AGC control signal can be fed to the governor by operating the `freq_control` switch. The output signal of the signal selector is sent as an input to generator 1 governing system. Figure 7.11 below illustrates the AGC to be implemented in area 1.



**Figure 7.11: Area 1 Automatic Generation Control (AGC)**

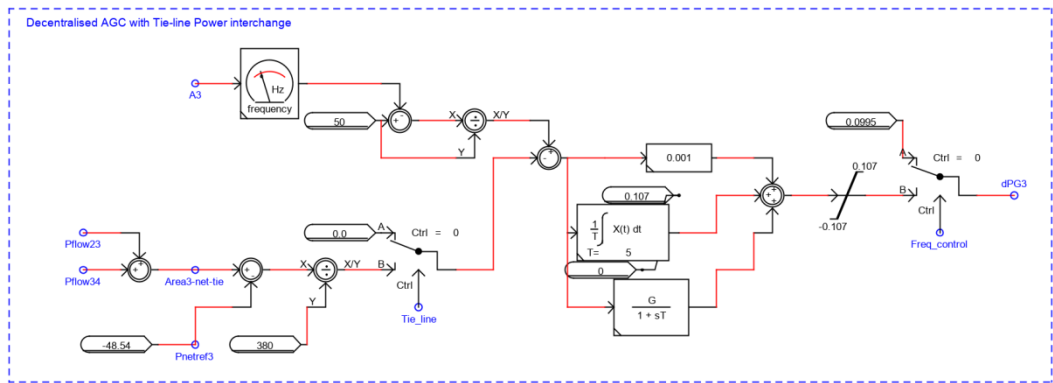
The approach in the development of the areal generation controller is identically for area 2 to area 4. The only difference in area is that there is no tie-line power interchange being considered in area 1. Area 1 is supplying both area 2 and area 4.

In area 2, the net tie-line power interchange is considered. The system frequency which is the input to the control is measured at bus 2 of the network. Area 2 is receiving and additional active power from area 1 through the transmission line 1-2. The power transfer input to area 2 is measured as pflow12 as an additional input to the AGC. Figure 7.12 below illustrate the automatic generation controller for area 2. The output dPG2 is fed to generator 2 governing system



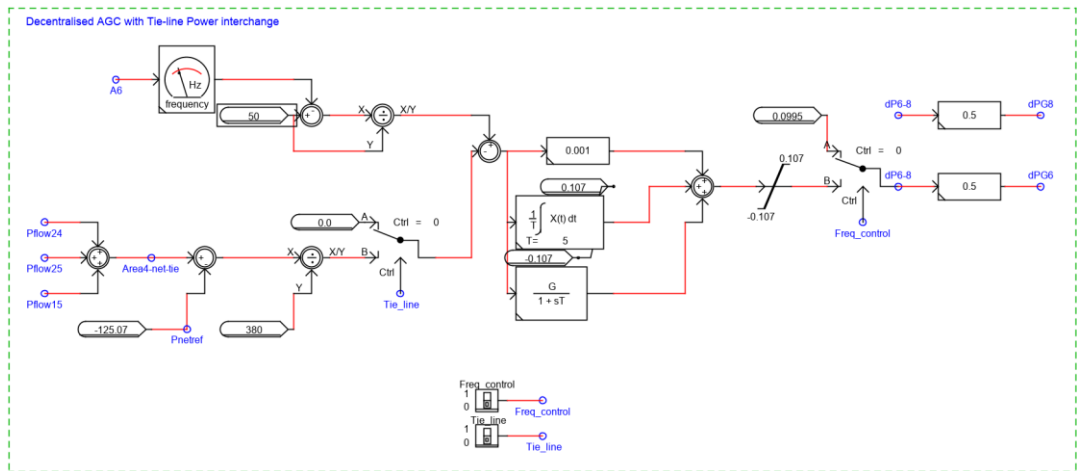
**Figure 7.12: Area 2 Automatic Generation Control (AGC)**

The automatic generation controller for area 3 is shown in Figure 7.13 below. The inputs to the controller are A3 (measured in bus 3) and the net tie-line power interchange (Area3-net-tie) which is the result of summing power measured on line T3 (pflow23) and T6 (pflow34). The output signal of area 3 is sent to dPG3 governing system.



**Figure 7.13: Area 3 Automatic Generation Control (AGC)**

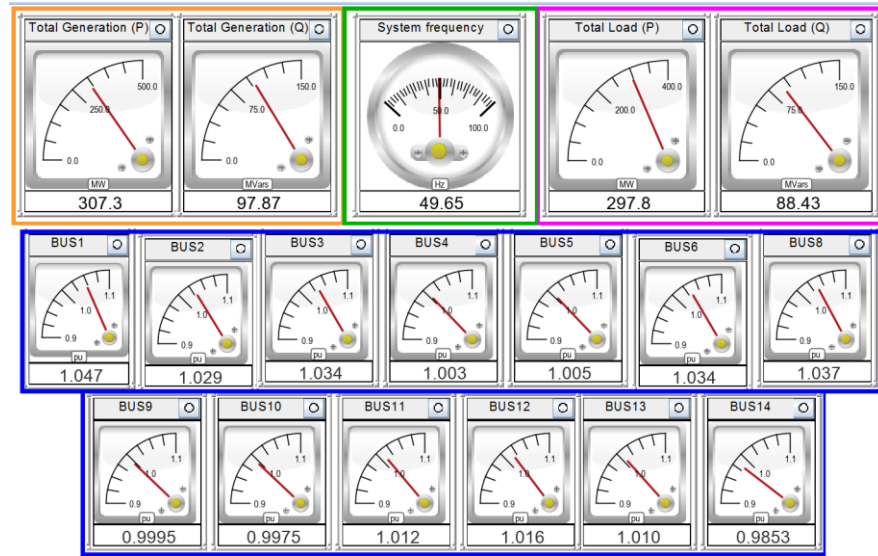
The automatic generation control logic presented in Figure 7.14 is modelled for area 4. The input signals to the controller includes frequency measured at A6 (bus 6), and the Area4-net-tie which is the total power interchange interchange measured at T2 (plow15), T4 (plow24), and T5 (plow25). There are tow output signals from this controller (dPG6 and dPG8). The output dPG6 is sent to generator 6 governing system while dPG8 is fed to generator 8 governing system. Two switches are shown in Figure 7.14 below. Freq\_control switch is used to control to initialized the frequency control of AGC to the governing system while Tie-line is used to initialize the the power interchange measurement to the controller.



**Figure 7.14: Area 4 Automatic Generation Control (AGC)**

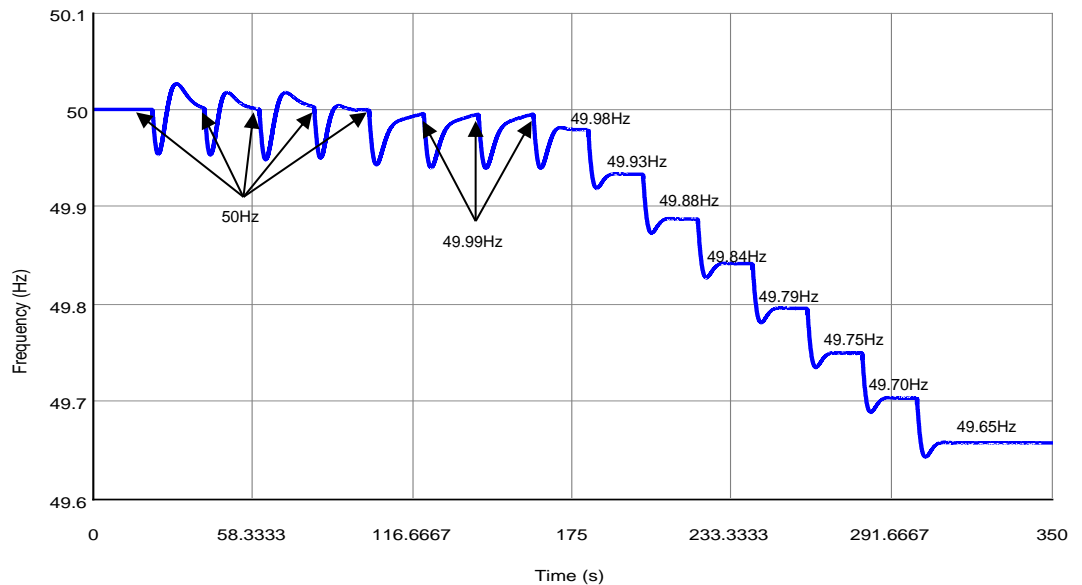
When the AGC was activated to improve the system frequency, initial power stability was performed to ensure that the power system is stabilize before applying any contingencies. When the system was stable, the incremental load contingency of 15% was applied. The results were obtained, and the system frequency was recorded as 49.65Hz using the measurement meters, as shown in

Figure 7.15 below. The AGC has improved the system frequency from 49.32Hz, as presented in Figure 7.4 above to 49.65Hz as shown in Figure 7.15 below.



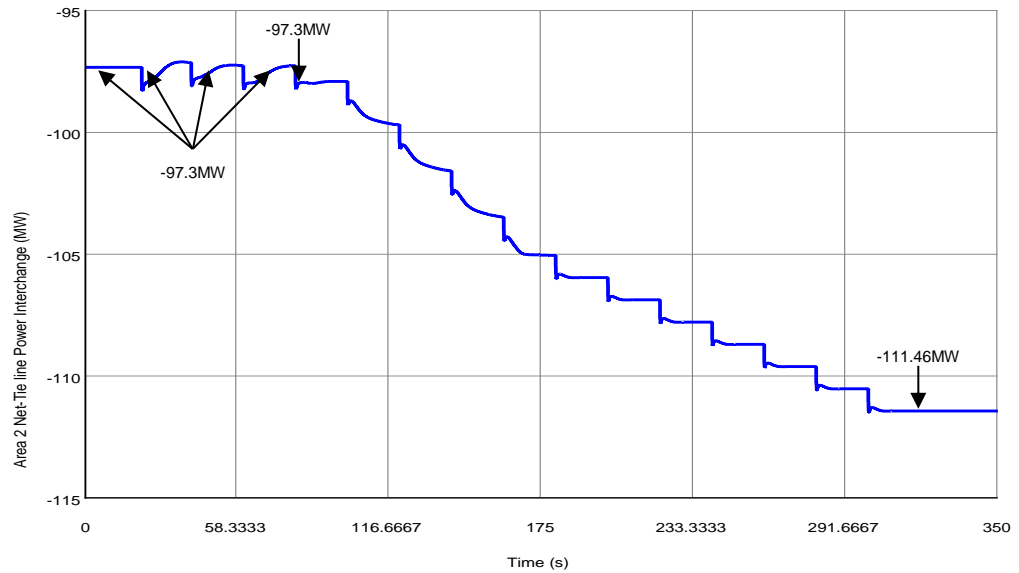
**Figure 7.15: System grid meters results after the implementation of AGC following a 15% load demand increase.**

Figure 7.16 below is the system frequency plot which shows the system frequency changes as the load demand increases. It can be seen that after the 4<sup>th</sup> incremental stage, the frequency started to drop to 49.99Hz. At the 8<sup>th</sup> stage, the system frequency started to decay and reached the last stage (15<sup>th</sup> stage), where the frequency stabilized at 49.65Hz.



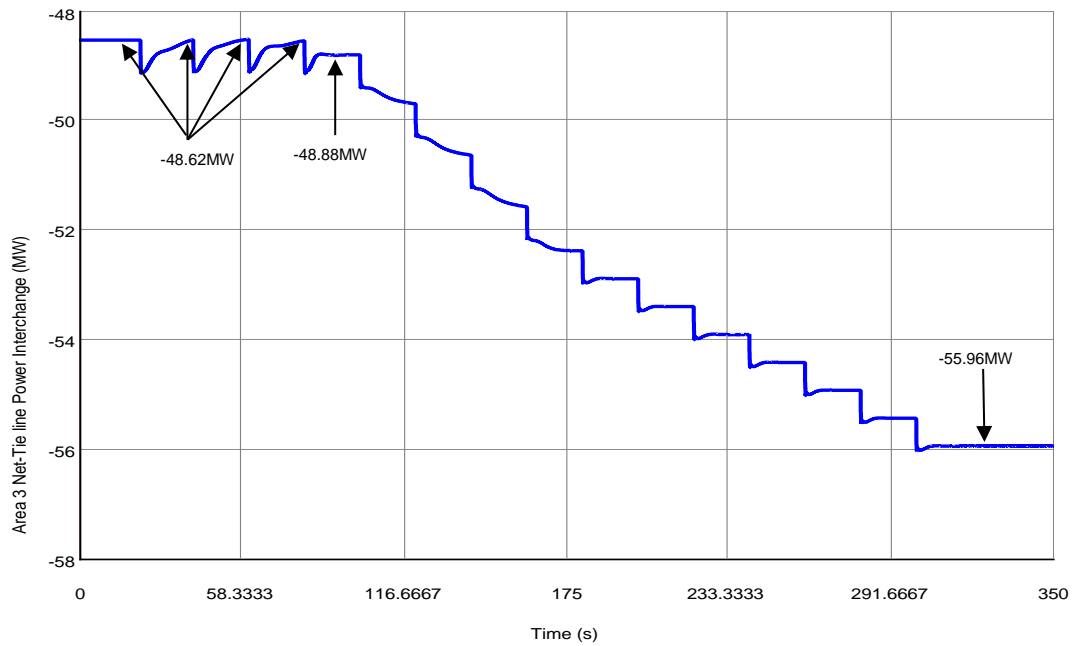
**Figure 7.16: System frequency response after the implementation of AGC following a 15% load demand increase.**

The AGC tried to maintain the net tie-line power interchange in area 2 for three stages. In the third stage, the active power interchange recorded in area 2 started to divert from its scheduled value of -97.53MW to a new value of -111.46MW. The net tie-line power interchange is measured at the receiving end of the area fed; hence the active power shared is seen as negative. Figure 7.17 below is shows the area 2 net tie-line power interchange when AGC is active.



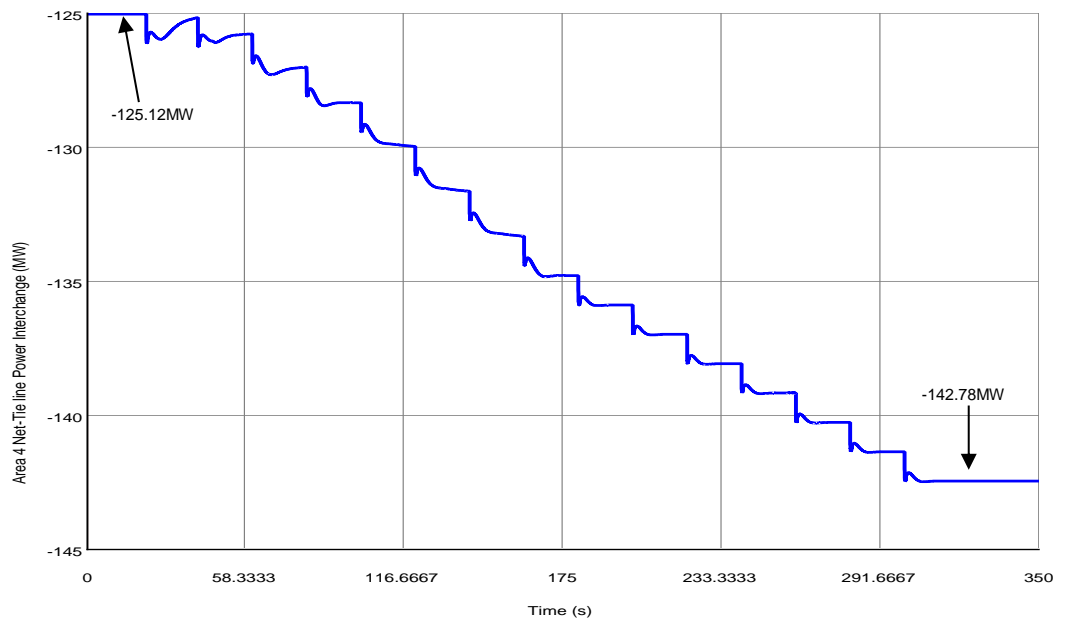
**Figure 7.17: Area 2 Net tie-line power interchange after the implementation of AGC following a 15% load demand increase.**

Figure 7.18 below is area 3 net tie-line power interchange when the AGC was implemented. The active power transferred to area 3 also diverted at the fourth stage of the load increment, from -48.80MW to -55.96MW. There is a slight improvement in these results as compared to when there was only a speed governing system controlling the active power supply of the grid.



**Figure 7.18: Area 3 Net tie-line power interchange after the implementation of AGC following a 15% load demand increase.**

Area 4 is the most critical portion of the system as several loads are supplied from this area. The AGC could not even sustain a single load demand increase in this area. The active power interchange immediately diverted from the scheduled amount of -125.11MW to -142.78MW. Figure 7.19 below is the plot for area 4 net tie-line power interchange when the AGC is implemented following a load demand increase.



**Figure 7.19: Area 4 Net tie-line power interchange after the implementation of AGC following a 15% load demand increase.**

The system frequency needs to be controlled towards the nominal value of 50Hz. The contribution of automatic generation control has brought the system frequency to a new steady-state value of 49.65Hz. This system frequency is acceptable in power system operation as it is within the acceptable frequency operating range between 49.5Hz and 50.5Hz. However, it would be risky to maintain the frequency at the lowest acceptable level; a further disturbance to the power system could lead to a catastrophic situation which could even result in a complete power system collapse. It is therefore recommended that the system in maintaining as close as possible to its steady-state condition. Further energy resource alternatives could be explored to ensure the power system stability is maintained at all times.

Wind power plants are not fully utilized to support frequency control by providing the required amount of active power based on the load demand, which results in frequency dropping. In the following section, a wind power plant control loop is modeled using RTDS in RSCAD software. The active power control loop is to activate the wind power plant to supply the required active power based on the system frequency.

#### **7.4 The modeling and integration of the wind turbine generator active power compensator**

The wind turbine generator system was integrated to supplement the active power deficit to improve the power system frequency, as outlined in section 6.3 above. The system frequency recorded in section 6.3 above was 49.64Hz. Integrating the wind energy system aims to improve the system frequency towards the nominal frequency of 50Hz.

To use the wind energy system as the active power compensator when the frequency is deteriorating, an additional control loop to release active power based on the system frequency deviation is required. The wind energy system will be integrated into the grid but not supply any power to the grid; therefore, its output power is set to minimum (approximately zero) at steady-state.

##### **7.4.1 Wind Turbine generator active power supplementary control loop**

System voltage measured point of connected node is converted to frequency. The system frequency deviation output is obtained by subtracting the system frequency from the reference frequency of 50Hz. The difference is converted to per unit signal, which is fed to the proportional gain, integrator and derivation. The output signals of the proportional gain, integral and derivative (PID) are

summated. The scale component further amplifies the signal. The output of the scale component is sent to the wind power plant. The scaling component sets the output of the wind power plant based on the frequency deviation.

The mathematical modeling of the wind turbine generator active power compensator scaling is given in equation 7.1 below. Equation 7.2 is used to calculate the frequency error signal to the controller.

$$Scale = (P_{out} + I_{out} + D_{out})G = \left( K_p e(t) + K_i \int_0^t e(t) \cdot dt + K_d \cdot \frac{de(t)}{dt} \right) G \quad 7.1$$

And

$$e(t) = \frac{f_{ref} - f_{meas}}{f_{ref}} \quad 7.2$$

The output power of the wind power plant is dependent on the system frequency. When the system frequency is at a nominal value of 50Hz, there is no signal sent to the scaling component of the wind power plant; hence the output power of the wind power plant is zero. When the load demand increases, the frequency will change depending on the amount of change in frequency; the wind power plant will only supply when the difference in system frequency is realized. Figure 7.20 below shows the wind power plant active power compensator logic developed on RSCAD. The frequency input signal to this control is measured at bus 14 and the output of the control is sent to the wind power plant control scheme for active power scaling based on system frequency deviations.

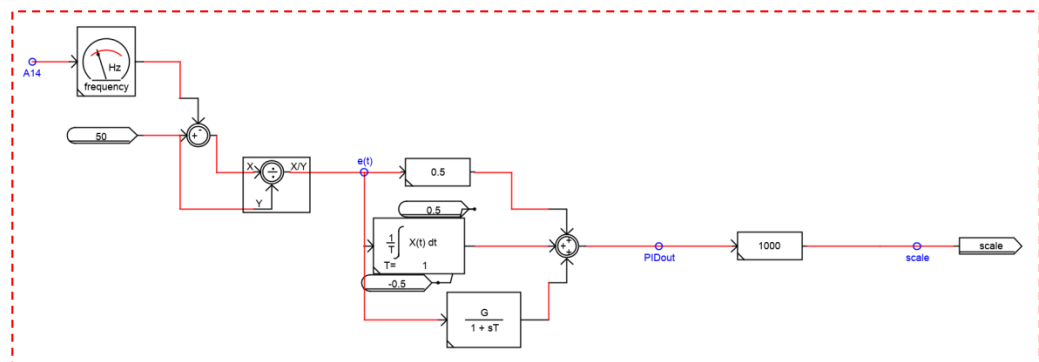


**Figure 7.20: Wind power plant active power scaling control**

## 7.5 Contingency application and results

Case study 3 performed in chapter 5 was repeated to assess the effectiveness of the AGC and the wind power plant active power compensator in real-time simulation. In Figure 7.21 below, it can be seen that the AGC maintained the system frequency for the first four stages of the load demand increase. In the fourth stage, the wind power plant was activated and started to supply the active



power to the grid. The supplied active power by the wind turbine generators stabilized the frequency at 50Hz. The impact on wind variation also contributed to system frequency fluctuation between 49.99Hz and 50.01Hz; this is due to the small-time constant of the wind power plants as well as the wind resource variation. Figure 7.21 below shows the system frequency results obtained from the RTDS runtime simulation platform.

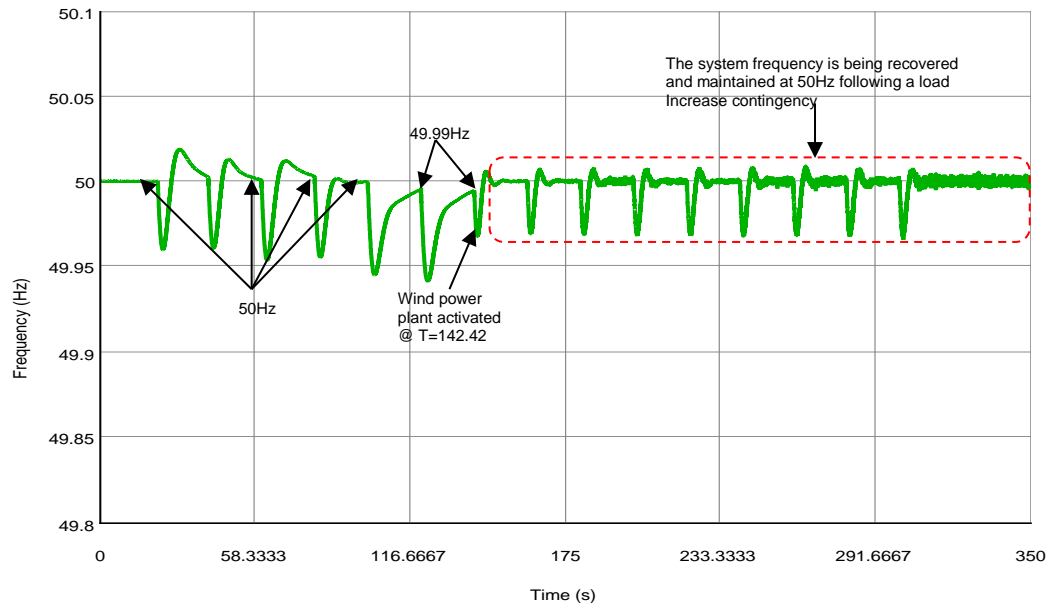


**Figure 7.21: System frequency when the governing system, AGC and WTG were active after the 15% load demand increase**

Figure 7.22 below shows the wind turbine generator active power measured at the sending-end. At the initial state, when the system frequency is stable at 50Hz, the wind power plant is not supplying power to the grid. When the load contingency was applied and the governing system and the AGC failed to maintain the system frequency, the wind power plant was activated. It can be seen in Figure 7.22 below that the wind power started supplying the active power plant at  $T=83.46s$ , and the wind supplied more power as the load demand increase to a value of 20.55MW. The wind power plant's activation contributed to the maintenance of the system frequency at its nominal value following load demand increase contingency.

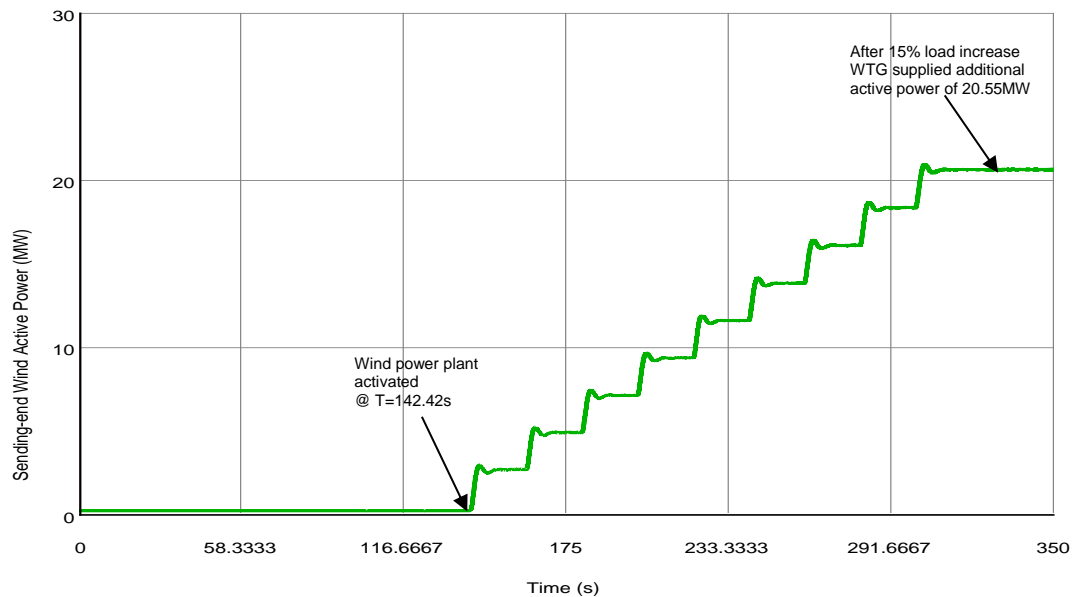


**Figure 7.22: Active power delivered by the wind power plant measured at the sending-end.**

The active power is transmitted to the distribution grid utilizing the transmission line. The integration of the wind power plant is done at bus 14.

The introduction of wind power plants as an active power compensator has improved the tie-line power interchange between the areas. Figure 7.23 shows the improved results of the net tie-line power interchange in area 2. For the first three stages of the load demand increase, the consolidated control system, which comprises the governing system, AGC, and wind power plant, succeeded in maintaining the power interchange at its scheduled amount. The integration of the wind power plant is located where there is more load compared to other areas considering the availability of the wind resource. Hence there is no power fed to other areas as more load is in area 4. However, there is a slight improvement compared to when there was no active power support from the wind power plant. This is seen when the wind power plant was activated at the 7<sup>th</sup> stage of the load demand increase. After the 15<sup>th</sup> stage of the load demand increase, the net tie-line power interchange recorded was -104.99MW, as shown in Figure 7.23 below.

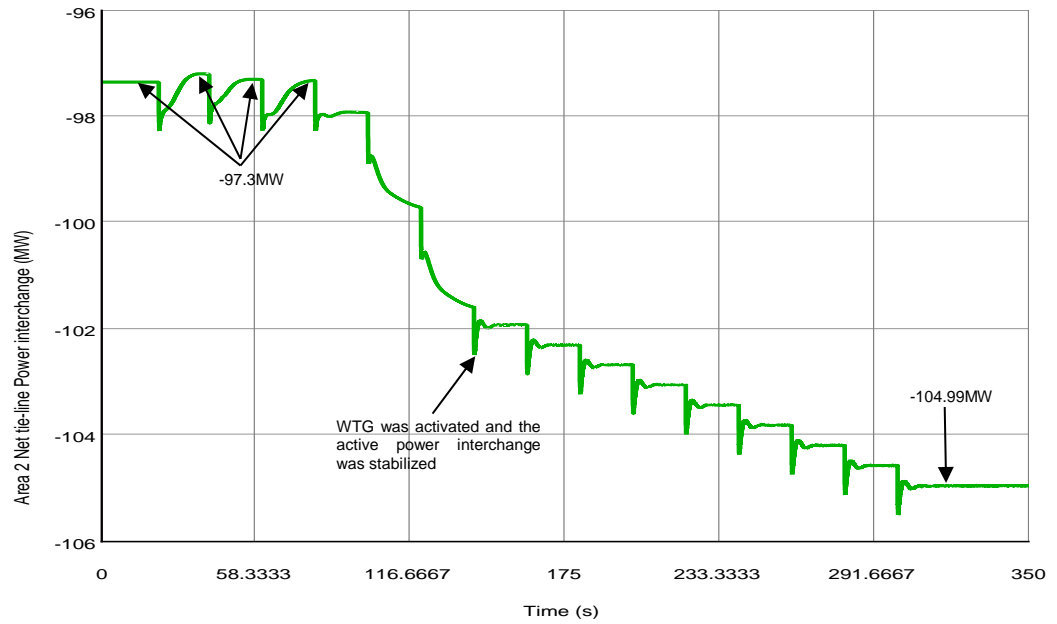


**Figure 7.23: Area 2 net tie-line power interchange when the wind power plant was activated.**

In area 3, the control system could only maintain the power interchange for the first four stages of load increment. As the load demand increases, the power interchange kept on deviating from the scheduled amount of -48.54MW to a new value of -59.28MW. Figure 7.24 below shows the net tie-line power interchange measured at area 3.

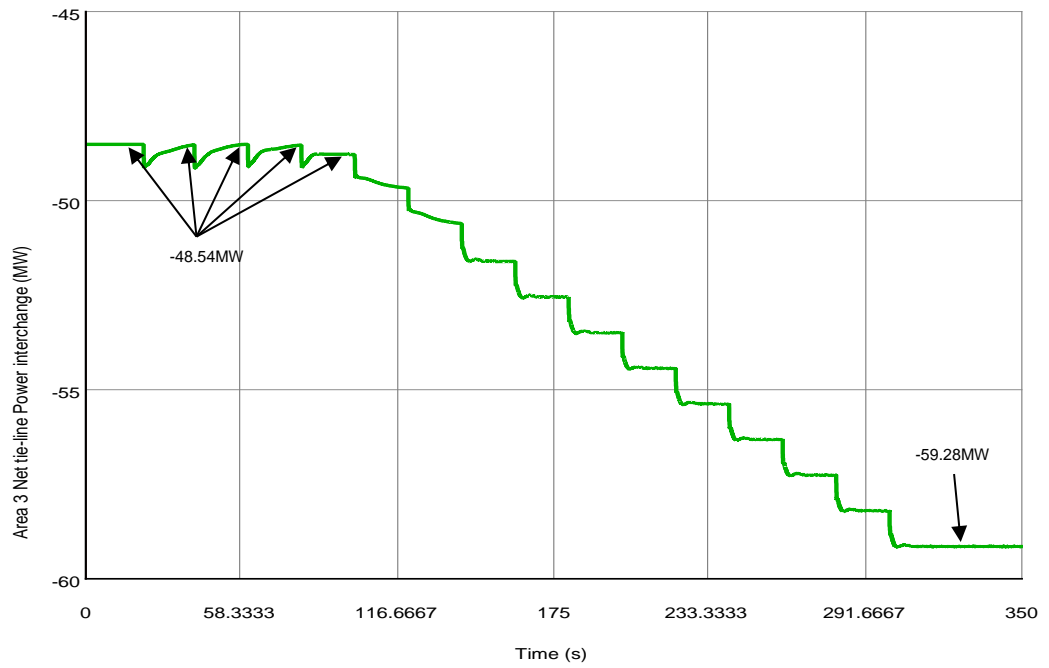


**Figure 7.24: Area 3 net tie-line power interchange when the wind power plant was activated.**

The wind power plant was integrated into area 4. When the load demand increase was initialized, the power interchange instantly changed from its scheduled amount of -125.1MW. On the 7<sup>th</sup> stage of the load demand increase, the wind power plant was activated, and the power interchange also started to improve. The net tie-line power interchange was recovered towards the scheduled amount. After the load demand increase contingency, the new level of the power interchange in area 4 was -129MW. Figure 7.25 below shows the net tie-line power interchange measured at area 4.

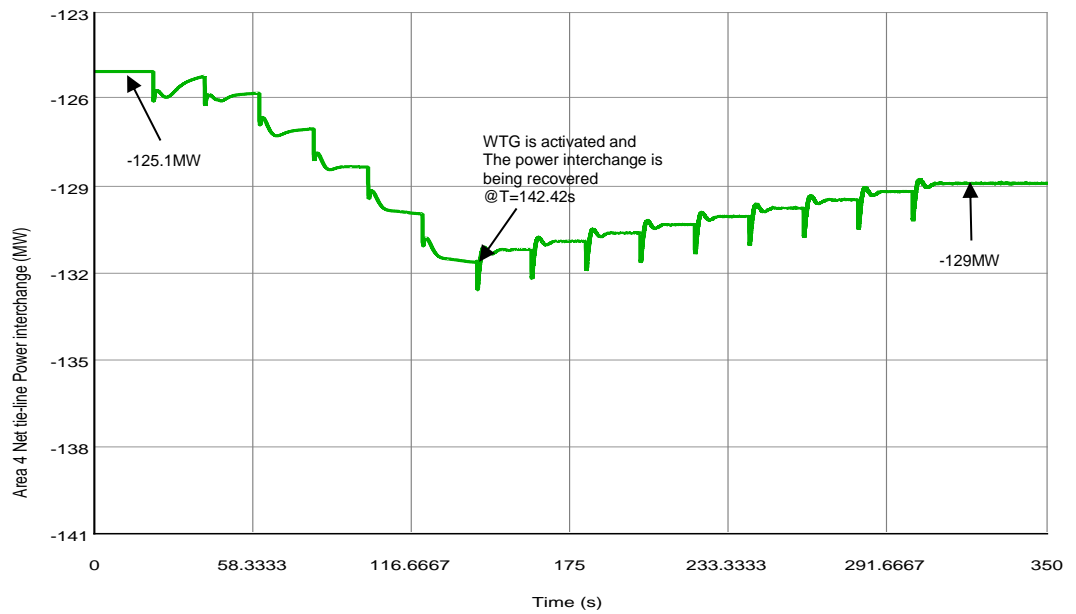


**Figure 7.25: Area 4 net tie-line power interchange when the wind power plant was activated.**

The consolidated control scheme, which comprises of the governing system, the automatic generation control and the wind active power compensator, has improved the power system stability following a load demand increase contingency. The system load was increased by 15% in steps of 1%. When the generation system started to experience a severe load and started to decay, the wind power plant was activated. The metering results shown in Figure 7.26 below were captured after the 15% load demand increase. It can be seen that the bus voltages are maintained within the nominal operating range. The power system was stabilized after the load demand increase.

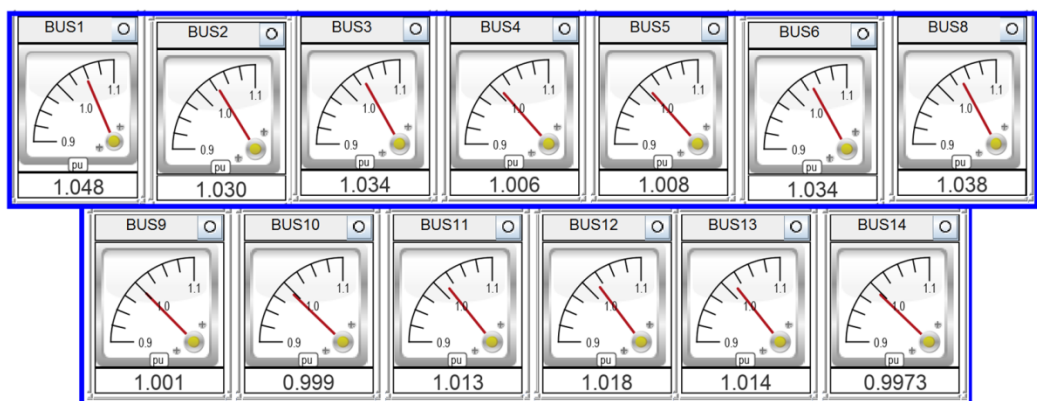


**Figure 7.26: Bus voltage results recorded after the load demand increase contingency.**

## **7.6 Conclusion.**

Wind power plants are widely used in the power system as means of providing additional power to the grid. The utilization is mainly on the baseload supply, though their intermittent energy is regarded as unreliable due to the wind variation. Their contribution to the power system stability is remarkable, although they are not widely used as active power compensators.

In this research, the utilization of a wind power plant as an active power compensator following a frequency deviation could result from a generator trip or increased load demand. The investigation of the utilization of wind power plants in this research was mainly focused on load demand increase contingency. The aim was to ensure that the system frequency is controlled towards the nominal level following a load increment contingency. The results obtained from DIgSILENT power system simulation software were verified using the RTDS simulation platform, which enables the hardware-in-the-loop implementation.

The control scheme that was developed and evaluated using the DIgSILENT simulation platform was further evaluated using the RTDS simulation platform. The results obtained in these simulation platforms show some resemblance. The system frequency was controlled and maintained at its nominal value following a load demand increase contingency.

The developed control scheme in the two simulation platforms (DIgSILENT and RTDS) needs to be implemented and its operation needs to be evaluated in real-time. The utilization of a hardware system integrated into the RTDS simulation platform will enable evaluation of the developed control and protection scheme to be through. Chapter 8 details the practical implementation of the control and protection scheme and the IEC 61850 communication standard implementation.

# CHAPTER EIGHT

## IEC 61850 STANDARD IMPLEMENTATION ON THE DEVELOPED FREQUENCY CONTROL AND PROTECTION SCHEME FOR SMART STABILITY

### 8.1 Introduction

The Automatic Generation Control (AGC) in the power system network is implemented using Programmable Logic Controllers (PLC). These PLCs require many signal processing cards. The configuration of the PLC requires more time, and troubleshooting is difficult as there is much wiring involved. The availability of the utilized technology is also a challenge.

The development of the IEC 61850 standard was to ensure the advancement of the energy management systems and improve the system reliability and communication. This advancement has improved the power system security. Multivendor has produced several Intelligent Electronic Devices (IEDs) to advance power system automation. The control system has been improved by applying intelligent electronic devices from various vendors guided by the IEC 61850 standard.

This chapter proposes the practical implementation of the system frequency control scheme using SEL-3555 Real-Time Automation Controller (RTAC). There are several functions that the SEL-3555 RTAC can perform. It has a wide range of application. It can be used as a gateway communication device between the power plant and the intelligent electronic devices or as an automation control using IEC61131 programming functions.

The SEL-3555 Real-Time Automation Controller (RTAC) is configured as a decentralized Automatic Generation Control (AGC) and wind active power compensation. The modified IEEE 14 bus network is divided into four areas, and each area has its controller. The wind power plant control is also decentralized; hence it is equipped with its controller. The orientation of the controllers, the configuration, and their performance is covered in the following sections of this chapter.

### 8.2 Development of a test bed for Hardware-In-The- Loop (HIL) implementation

The developed testbed is a configuration of the modified IEEE 14 bus power system network modeled on the RSCAD simulation platform and integrated with RTAC 3555 which is performing the frequency control and active power compensation. The inputs to the SEL-3555 RTAC device are both the frequency

and the power interchange. The system frequency and the power interchange are analog signals which are measured at the bus bars. These signals are published through IEC 61850 Generic Object Oriented Substation Event (GOOSE) messaging system and they are transmitted using Ethernet via the communication switch. RTDS is equipped with the Giga-Transceiver Network (GTNET) Communication Card, which enables the transmission and receiving of signals the physical device (RTAC 3555) configured in the testbed. The SEL-3555 RTAC subscribes to the analog signals published by GTNET card and performance its control actions through a PID controller. The output of the PID controller configured in RTAC 3555 is then published back to GTNET via the communication switch. The GNET is RSCAD subscribes the control signals from the SEL-3555 RTAC and these control signals a sent to their respective control devices. For the automatic generation control, the control signal from the SEL-3555 RTAC is directed to the governing system of the generator (Pset). The developed test-bed configuration is shown in Figure 8.1 below. The green arrows dotted lines indicates the communication link between the agents. The the red dotted arrow indicates the communication link between the masters station and the controller.

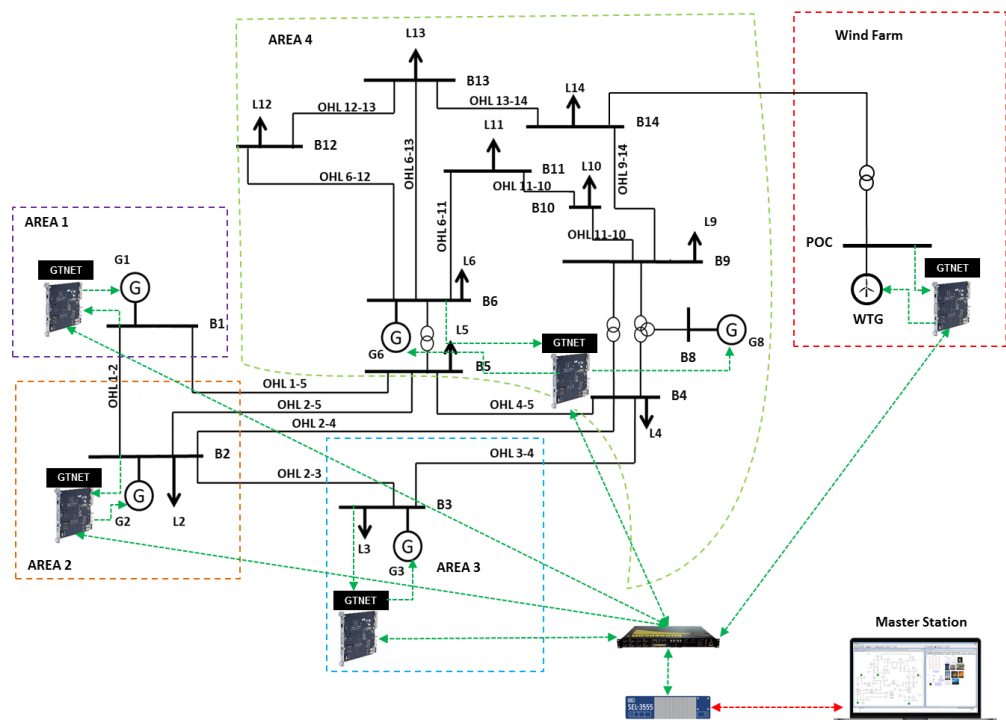


**Figure 8.1: Modified IEEE 14 fully integrated with SEL-3555 RTAC in hardware in the closed-loop configuration**

For the establishment of the communication between RTDS and the hardware device, a proper configuration is required. This is to ensure that the relevant



devices subscribe the signals that are being published. The communication configuration using IEC 61850 standard is introduced in the section below.

### 8.3 IEC 61850 standard communication configuration

The communication between the GTNET cards in RTDS/RSCAD and RTAC 3555 is established through the steps set out below. To configure the signals that need to be published, the GTNET-GSE component needs to be imported from the library. This component enables the IEC 61850 standard communication using the GTNET hardware. Right-click to edit and navigate to IEC 61850 Substation Configuration Language (SCD) template as shown in Figure 8.2 below

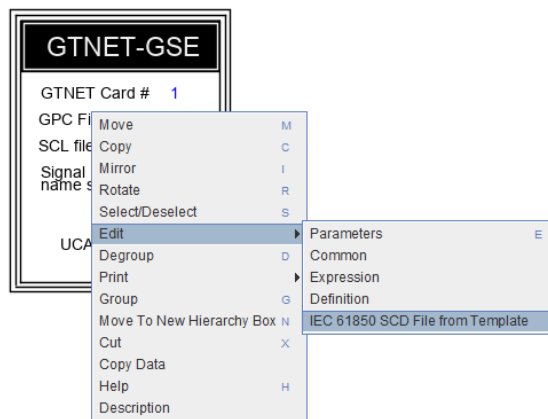


**Figure 8.2: GNET-GSE Communication configuration**

When the SCD template is open, the definition of the IED name will be required. The SCD configuration enables to development of a virtual RSCAD soft IED that will communicate with the external device (RTAC 3555). Program the IED name and press OK, then an SCD file editor will be open as shown in Figure 8.3 below.

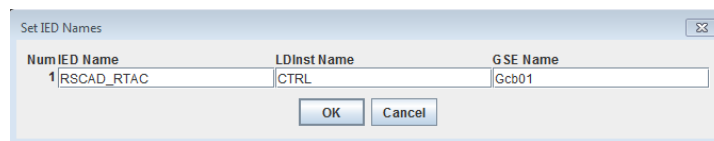


**Figure 8.3: IED name tab**

Once the SCD file editor is open, navigate to edit, select output/datasets, and click to configured IED name (RSCAD\_RTAC). Define the dataset and the signal type to be published and press OK. Click the save button and exit the SCD file editor as illustrated in Figure 8.4 below.

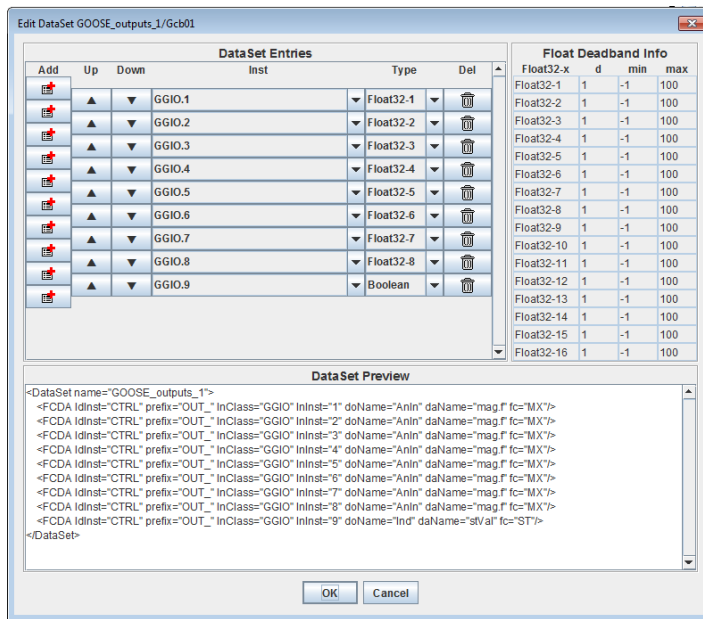


**Figure 8.4: Define datasets and signal type to be published**

The next step is to double-click on GTNET- GSE component to map all the outgoing analog signals, as shown in Figure 8.5 below.

Name	Description	Value	U...	M...
IED1...	Output 1 Type	FLO...	0	12
nIED...	Output 1 Signal Name	BUS1_F	0	0
IED1...	Output 1 Boolean bitmap bit num (32..1)	1	1	32
IED1...	Output 2 Type	FLO...	0	12
nIED...	Output 2 Signal Name	BUS2_F	0	0
IED1...	Output 2 Boolean bitmap bit num (32..1)	1	1	32
IED1...	Output 3 Type	FLO...	0	12
nIED...	Output 3 Signal Name	Pflow12	0	0
IED1...	Output 3 Boolean bitmap bit num (32..1)	1	1	32
IED1...	Output 4 Type	FLO...	0	12
nIED...	Output 4 Signal Name	BUS3_F	0	0
IED1...	Output 4 Boolean bitmap bit num (32..1)	1	1	32
IED1...	Output 5 Type	FLO...	0	12
nIED...	Output 5 Signal Name	AREA3_...	0	0
IED1...	Output 5 Boolean bitmap bit num (32..1)	1	1	32
IED1...	Output 6 Type	FLO...	0	12
nIED...	Output 6 Signal Name	BUS6_F	0	0
IED1...	Output 6 Boolean bitmap bit num (32..1)	1	1	32
IED1...	Output 7 Type	FLO...	0	12
nIED...	Output 7 Signal Name	AREA4_...	0	0
IED1...	Output 7 Boolean bitmap bit num (32..1)	1	1	32
IED1...	Output 8 Type	FLO...	0	12
nIED...	Output 8 Signal Name	BUS14_F	0	0
IED1...	Output 8 Boolean bitmap bit num (32..1)	1	1	32
IED1...	Output 9 Type	BOOL	0	12
nIED...	Output 9 Signal Name	Auto_Ma...	0	0
IED1...	Output 9 Boolean bitmap bit num (32..1)	1	1	32

**Figure 8.5: Output signals mapping published through GTNET-GSE**

Once the output signal from RSCAD has been mapped, the next step is to save the draft file and compile the project. Once the compilation is done, run the simulation and verify the output signals published by GTNET using GOOSE inspector. Figure 8.6 below shows the published data from GTNET using GOOSE inspector.

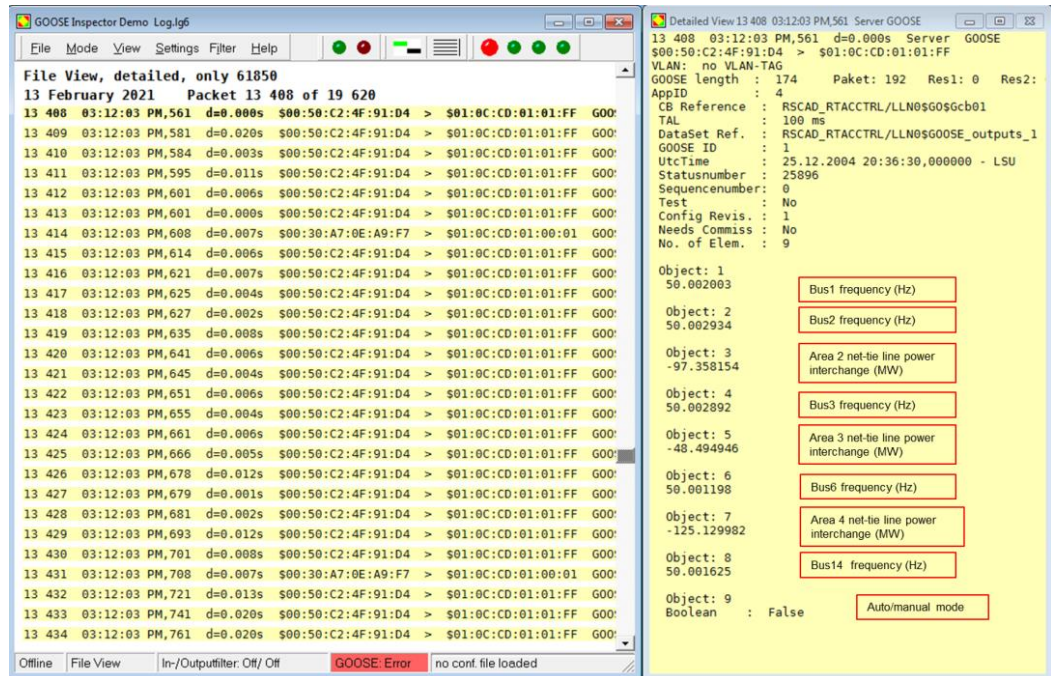


**Figure 8.6: Data published from RSCAD is displayed using GOOSE inspector**

The output data published by the GTNET correspond with the data measured on RSCAD runtime. The data being published is arranged in ascending order, as given in Figure 8.6 above.

The next step is to ensure that the output signals that are being published by the GTNET to be subscribed by the Real-Time Automatic Controller (RTAC). This is done by configuring the IEC 61850 SCD file using AcSelerator Architect, which is then uploaded to AcSelerator RTAC. Figure 8.7 below shows the mapping of the GNET output signal to RTAC 3555 as well as the configuration of the logical node for the signals to be published the SEL-3555 RTAC to GTNET card in RSCAD.

When AcSelerator Architecture is open, the next step is to import the configured IED Description (CID) file developed on RSCAD. This is done by right-clicking on the IED pallet and select import, and navigate where the IED was saved. Once imported, drag and drop the RSCAD cid file to the project editor. Also, drag and drop the SEL RTAC IED to project editor to prepare for the mapping of the input

as well as the output signal accordingly to be received and transmitted, respectively.

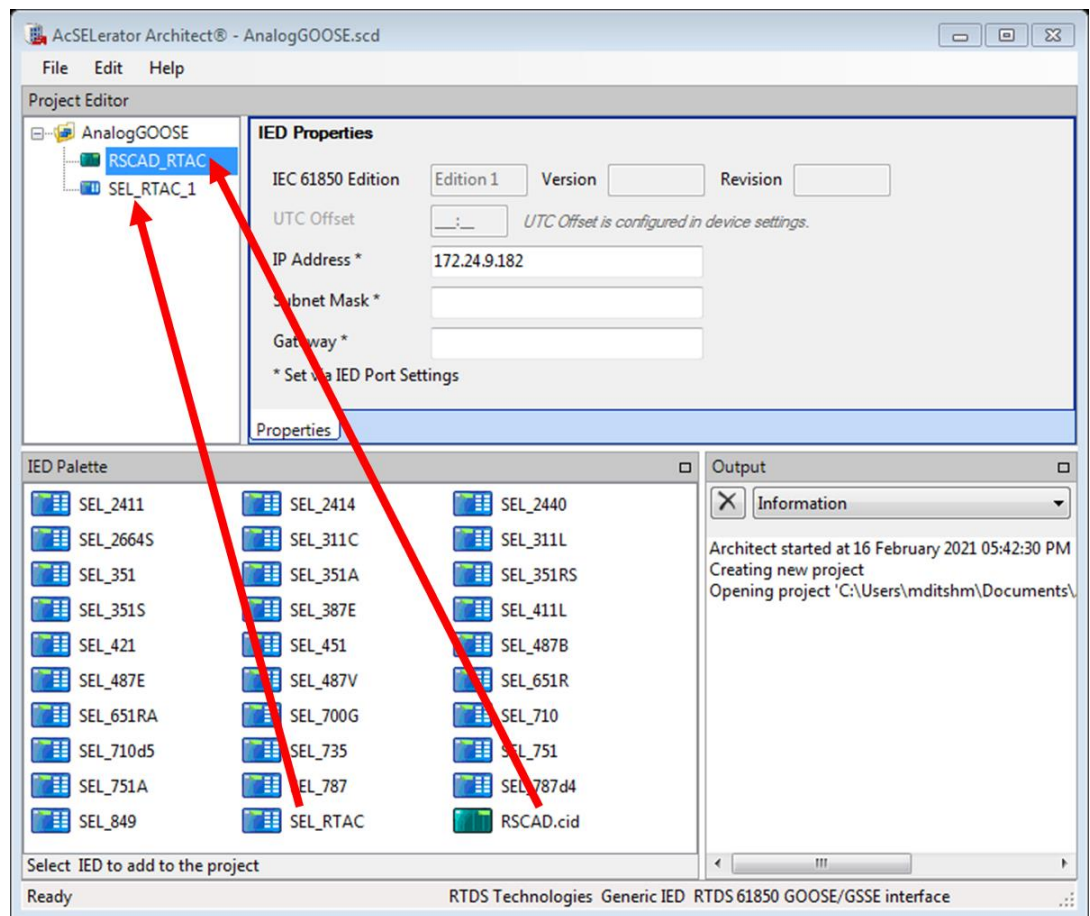


**Figure 8.7: IEC 61850 GOOSE messaging configuration on AcSelerator Architect**

By clicking on RSCAD\_RTAC IED, the properties of the IED, such as its IP address, IEC 61850 version support, are displayed. Selecting SEL RTAC, also its properties are shown, the IP address of the SEL-3555 RTAC in use is shown. The next tab is GOOSE receive which enables the mapping of the logical nodes, which will be subscribed by the SEL-3555 RTAC. The mapping is done by dragging the logical node signal to its appropriate type (analog to analog and digital to digital), as shown in Figure 8.8 below.

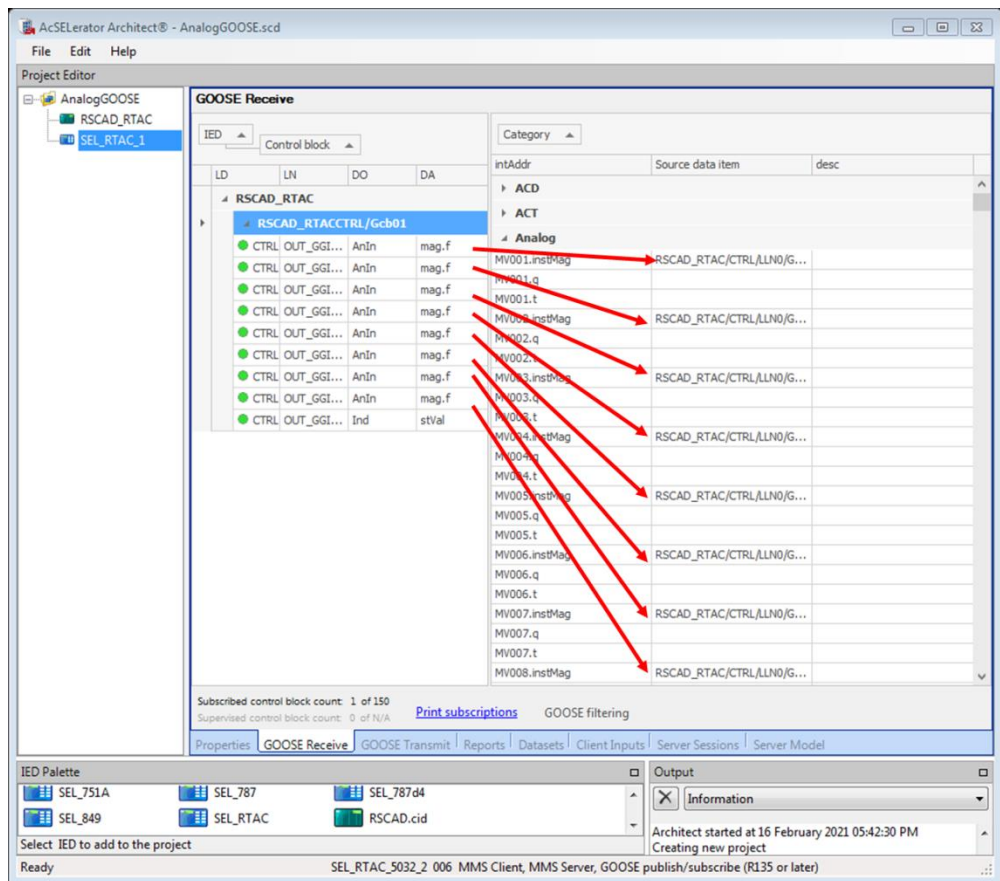


**Figure 8.8: IEC 61850 GOOSE Receive messaging subscription configuration on AcSelerator Architect**

The SEL-3555 RTAC does not have preconfigured analog datasets that can be used for GOOSE message transmission. Therefore these datasets need to be configured to map the output of the SEL-3555 RTAC to GTNET IED in RSCAD. This is done by selecting the server model and configure a logical device, then select the logical node. The logical node class Generic Process I/O (GGIO) is selected, which enables the configuration of the analog signal output from the SEL-3555 RTAC to GTNET, as shown in Figure 8.9 below. Six analog signals will be published, the SEL-3555 RTAC to GTNET. Five of these output signals are sent to the governing system of the generator that is contracted for automatic generation control. The other signal is sent to the wind power plant as contracted for active power compensation.

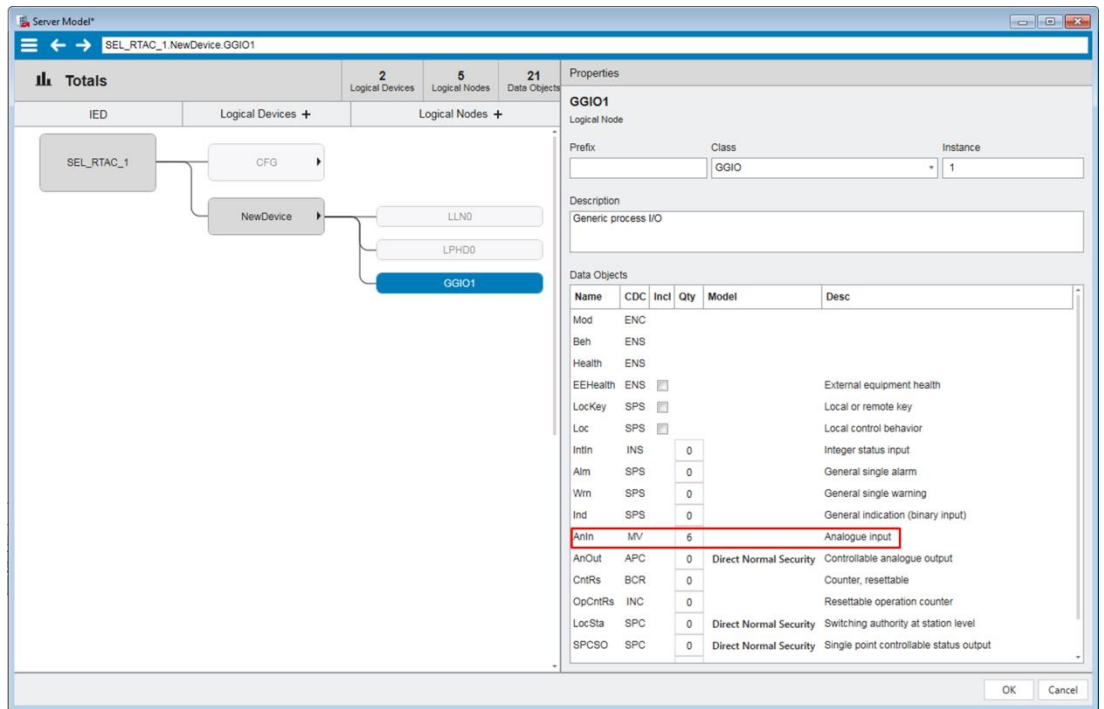


**Figure 8.9: Dataset configuration for analog signal transmission from the SEL-3555 RTAC to RSCAD**

Under the dataset tab, the GOOSE transmission type to be published needs to be adequately defined. Measurement functional constraint needs to be selected and open the type of analog signal to be published. Drag to the right under datasets, as shown in Figure 8.10 below.

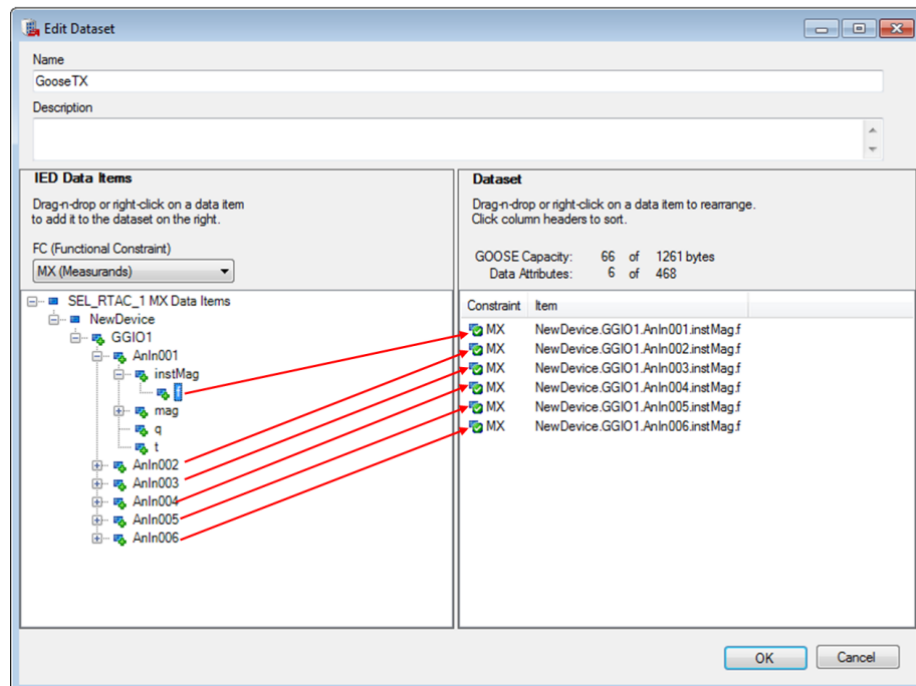


**Figure 8.10: Dataset type and arrangement configuration for analog signals transmission the SEL-3555 RTAC to RSCAD**

The datasets have been defined and arranged. The next step is to configure these datasets for IEC 61850 GOOSE transmission messages. This is achieved by opening the GOOSE transmission tab. Figure 8.11 below shows that the device that will be publishing the transmission GOOSE message is SEL\_RTAC\_1, as highlighted within the Figure. The dataset to be published is also highlighted.

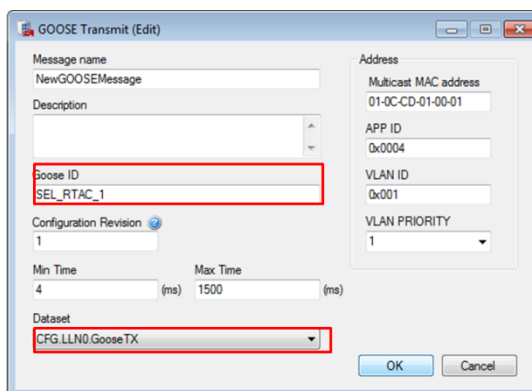


**Figure 8.11: IEC 61850 GOOSE transmission analog signals the SEL-3555 RTAC to RSCAD**

Once the communication configuration is done, the IEC 61850 SCD file is saved (AnalogGOOSE). The next step is to open AcSelerator RTAC, where the automatic generation controller and wind power active compensator are being modeled.

#### **8.4 Development of Automatic Generation Control (AGC) and wind active power compensator using SEL-3555 RTAC.**

RTAC 3555 can be used in various configurations. To achieve hardware configuration of an automatic generation control as well as the wind power plant active power compensator, the SEL-3555 RTAC was chosen. It is selected based on its features, modern technology, which can replace the utilization of PLC for control purposes as its IEC 61850 compliant; therefore, the communication establishment is more reliable as compared to the conventional methods such as the utilization of pilot cables and radio communication.

##### **8.4.1 IEC 61850 configuration on AcSelerator RTAC**

Once AcSelerator Software opens, the SCD file developed using AcSelerator Architect is imported by selecting IEC 61850 tab on the software's toolbar and select the configuration. The configuration is uploaded with both receive and

transmission datasets. The received dataset is from RSCAD\_RTAC, and the transmission is from SEL\_RTAC\_1. Figure 8.12 below shows the IEC 61850 configuration uploaded on AcSelerator RTAC software.

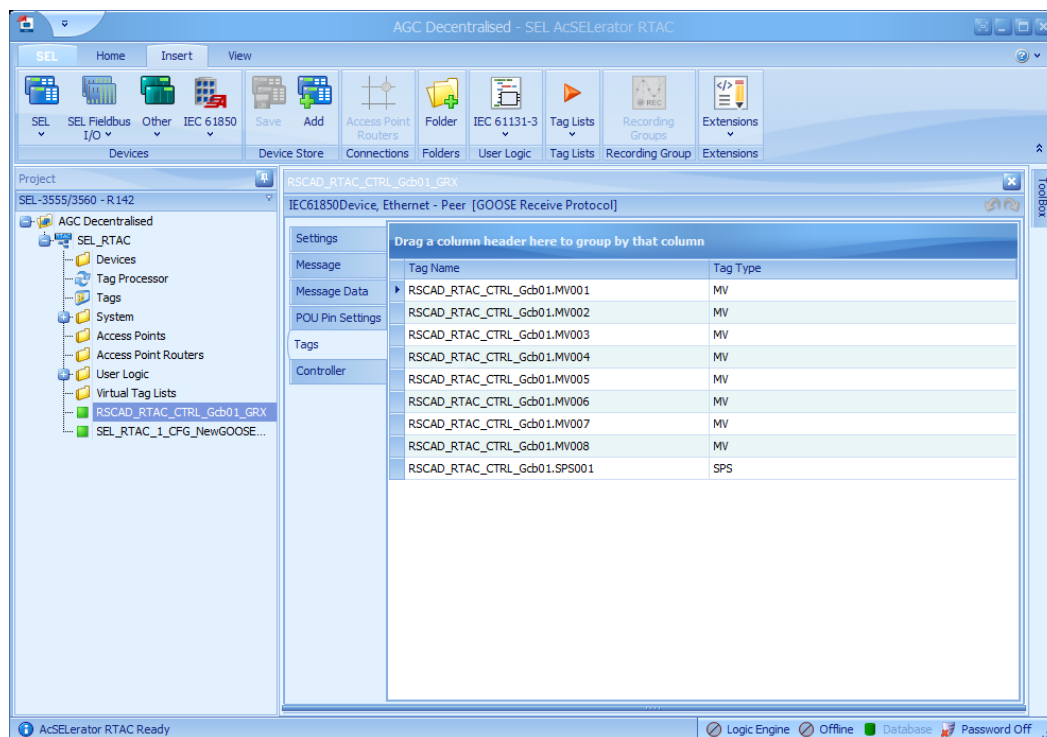


**Figure 8.12: IEC 61850 configuration file upload on AcSelerator RTAC platform**

The tags currently displayed in Figure 8.12 above are for receive GOOSE messages from GTNET. These are the tags that will be mapped to control logic for both receive and transmit GOOSE messaging.

#### 8.4.2 Development of customized programmable logics using IEC61131-3

Control logic within the RTAC 3555 environment can be developed using various options of IEC 61131-3 depending on the type of control logic to be customized. For this project, the option to program the block diagram logics for the automatic generation control as well as wind active power compensator was selected on the IEC 61131-3 drop down.

Once the software is opened, select IEC 61131-3 drop-down and select program. This will appear on the right-side tools under user logic. The toolbox will be shown on the left side of the page. This enables the drafting of the block diagram required. The control logic is being developed using Continuous Function Chart (CFC) language, which uses the toolboxes shown on the left side of accelerator RTAC software in Figure 8.13 below.



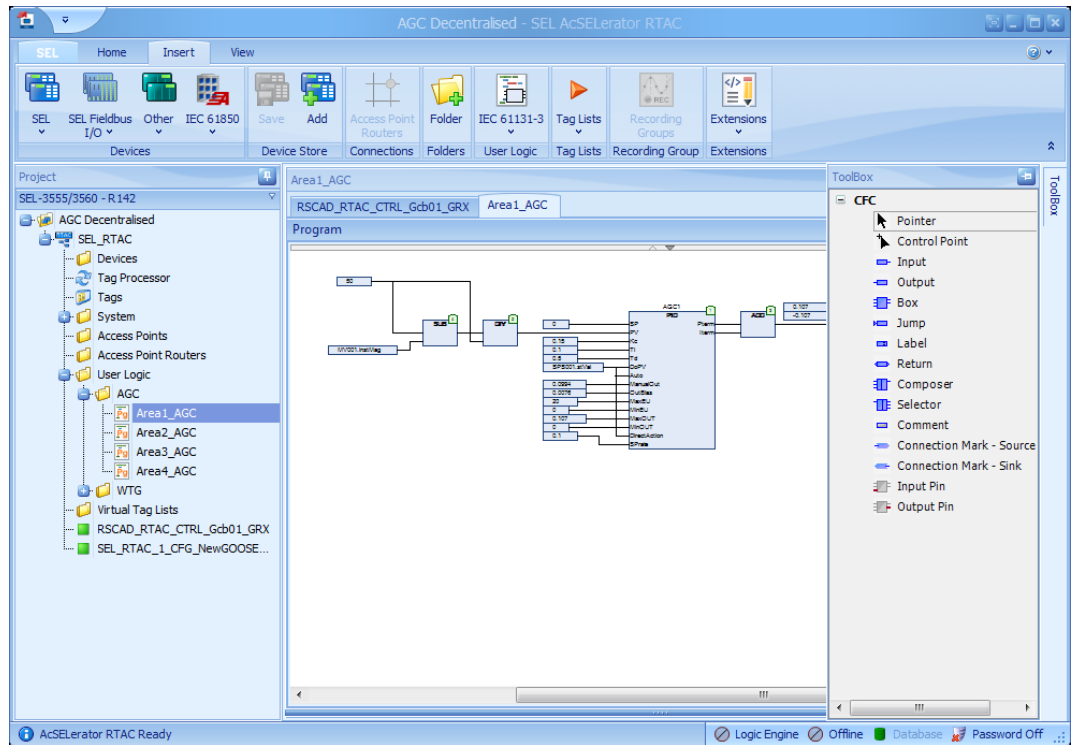


**Figure 8.13: Area 1 logic development using IEC 61131-3 language (CFC)**

Figure 8.14 to 8.17 below are the developed automatic generation control logics modeled using AcSelerator RTAC. The PID control has two operation modes, the first one is the manual mode and the second one is the automatic mode. When the PID is set to manual mode, the generator governing system performs the control function, the automatic generation control is inactive (no control function performed). When auto mode is select, then the automatic generation control PID will be active and perform its control function.

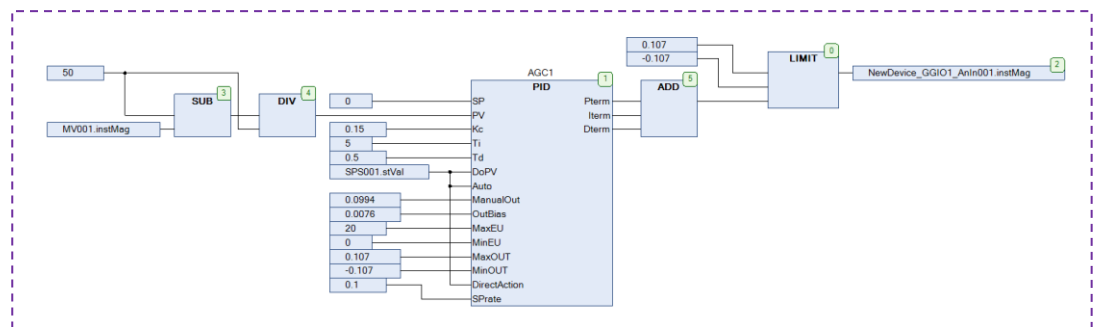


**Figure 8.14: Area 1 automatic generation control configuration**

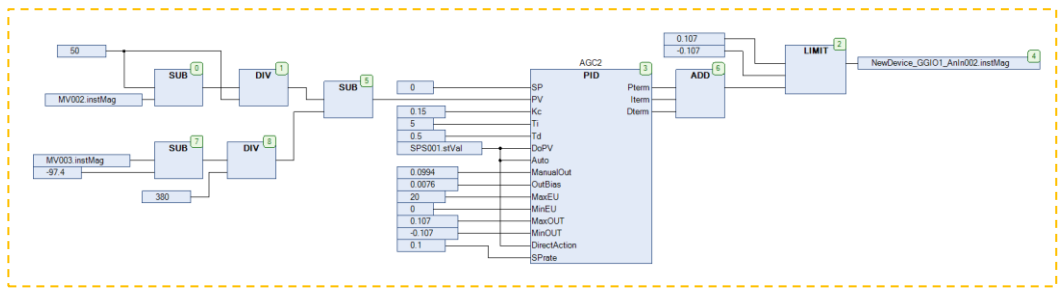


**Figure 8.15: Area 2 automatic generation control configuration**

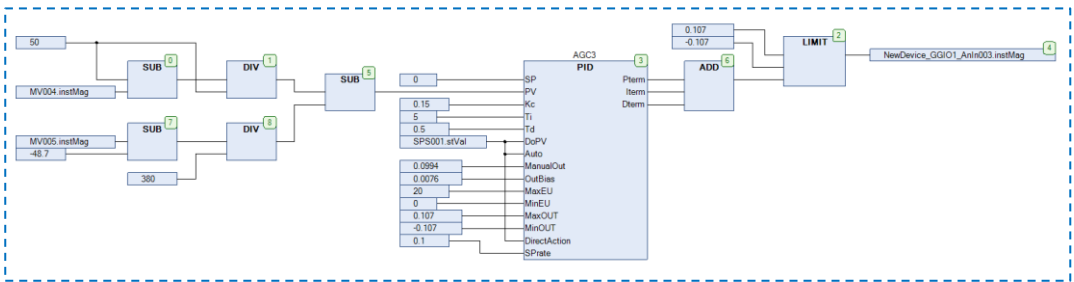


**Figure 8.16: Area 3 automatic generation control configuration**

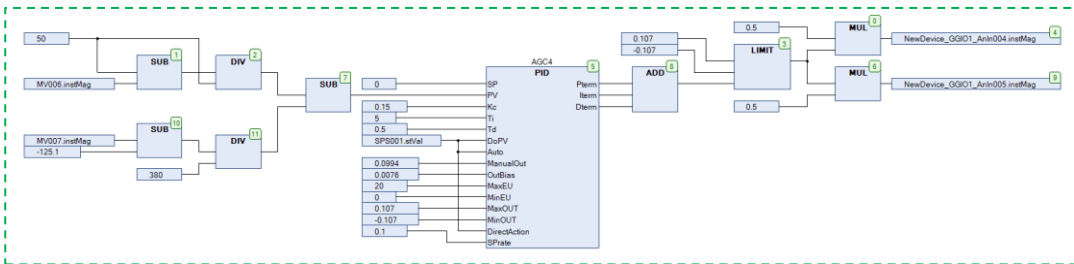


**Figure 8.17: Area 4 automatic generation control configuration**

Figure 8.18 below illustrates the control logic for the wind power plant active power compensation. This control logic is activated when there is a notifiable difference between the reference frequency setpoint and the system's measured frequency.

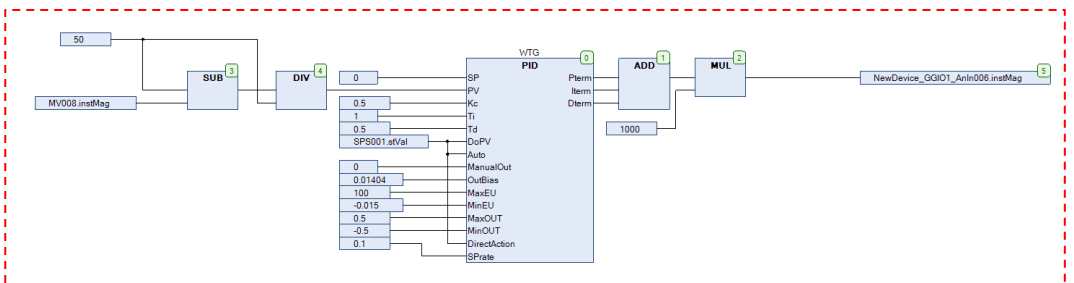


**Figure 8.18: Wind active power compensation scaling logic**

Once the control logic's development is complete, the project needs to be sent to the SEL-3555 RTAC IED. This is done by clicking “Go online,” then a password

to login will be required. This is for safety and security purposes so that an unauthorized applicator does not log in and interfere with the configure control program. The IP address of the SEL-3555 RTAC device needs to be programmed correctly. Figure 8.19 below indicates the software requirements to enable uploading a project to the SEL-3555 RTAC device.

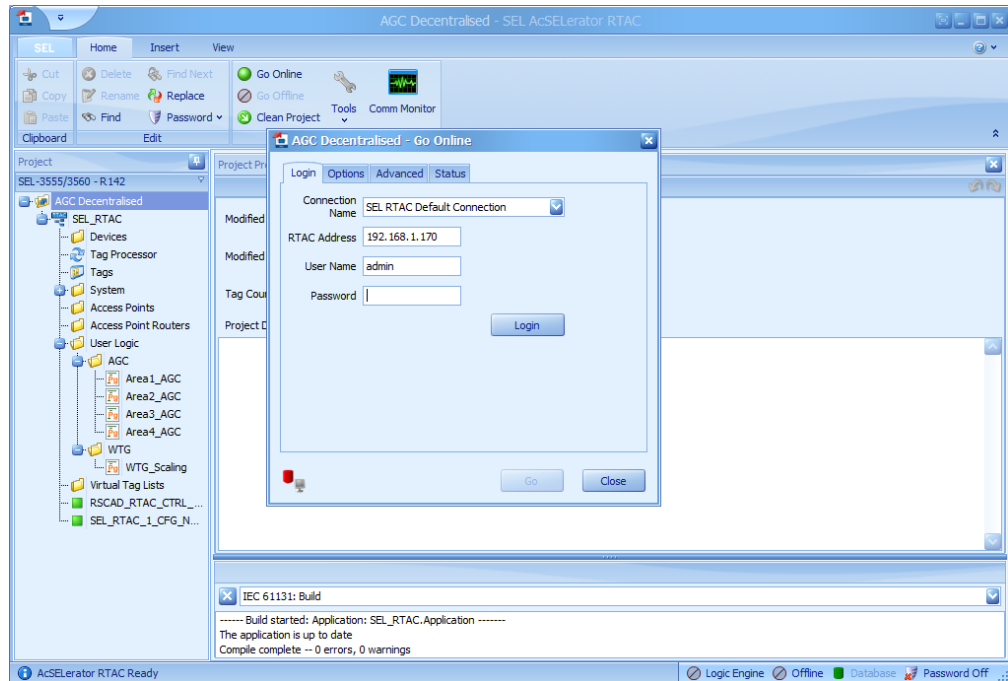


**Figure 8.19: Uploading the configured control logics and settings to the SEL-3555 RTAC device**

When there are errors in the logic developed, the SEL-3555 RTAC will not allow the settings and the logic to be uploaded to it. When there are no errors, the settings, and the logic will be uploaded to the device. Once the task is complete, the device will be online. Figure 8.20 below is the SEL-3555 RTAC configuration when it is online.

RSCAD-RTAC GOOSE received (GRX) is selected; these are the configured receive GOOSE message signal. The instantaneous message value of 50.06379Hz is the system frequency on RSCAD. This confirms that the IEC 61850 GOOSE SCD file is configured correctly, and RSCAD publishes the correct subscribed signal.

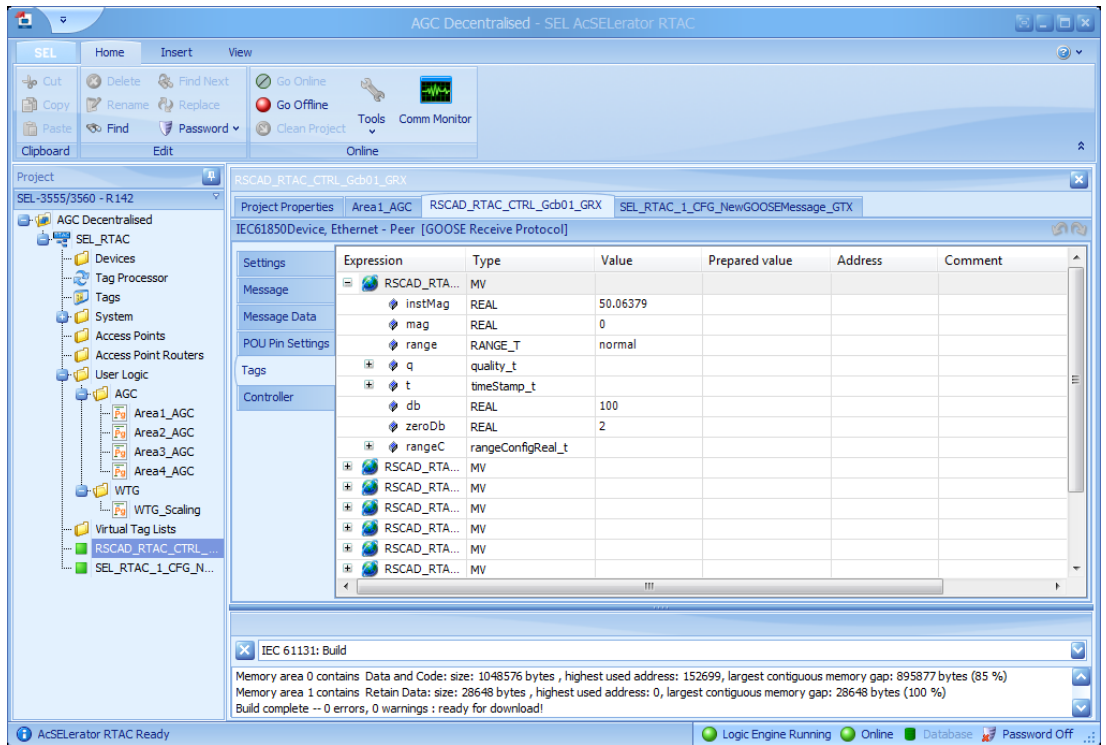


**Figure 8.20: Control signal data from GTNET received by SEL-3555 RTAC via GOOSE messaging**

In Figure 8.21 below, SEL\_RTAC GOOSE transmit (GTX) has been selected; the GOOSE transmission configuration and the output control signals are mapped. The instantaneous value displayed is the control signal to the generator governing system.

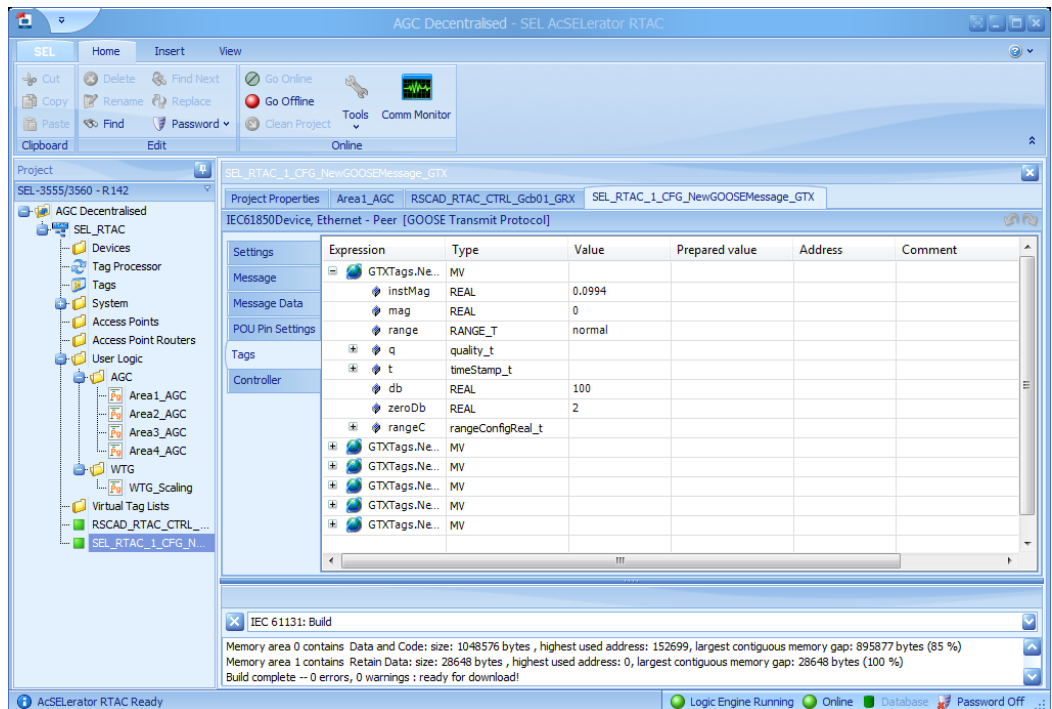


**Figure 8.21: Output control signal published by SEL-3555 RTAC to GTNET**

The output control signal from SEL RTAC becomes the input to the GTNET-GSE card on RSCAD. The control signals SEL RTAC are mapped onto the IEC 61850 SCD file of the GTNET card. This is done by opening the SCD file, then click Edit, and select import. This will enable navigation to where the SCD file configuration was saved using ArSelerator Architect. Once the SCD file is imported, the SEL RTAC IED will be placed under IEDs on the RSCAD SCD file, as shown in Figure 8.22 below. When the IED is open, the datasets will be shown. These datasets need to be dragged to the input module, as shown in Figure 8.22 below.

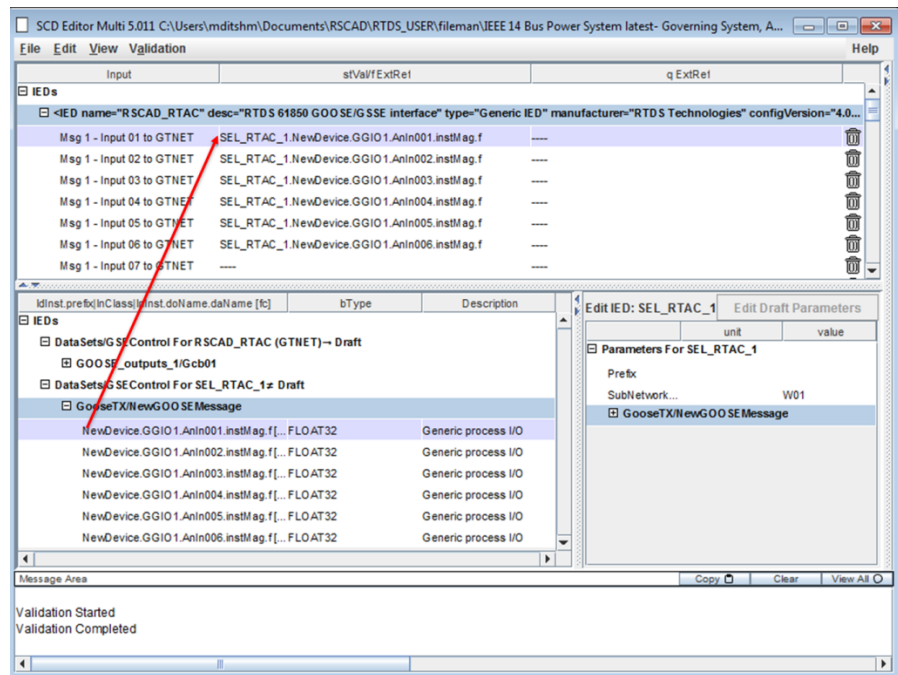


**Figure 8.22: Mapping the IEC 61850 GOOSE messaging signals transmitted by SEL-3555 RTAC to GTNET**

When configuring the GOOSE messaging, careful attention is required. This will enable an appropriate mapping of control signals so that those signals are not mismatched and are correctly mapped to their appropriate destination. Figure 8.23 shows the control signals from SEL RTAC 3555 via GOOSE messaging. These signals are mapped in ascending order, and this mapping corresponds to signals published from GTNET, as indicated in Figure 8.5 above. The floating signals shown on the left side of Figure 8.23 indicates the origination and destination of the control signals for adequate mapping to the GTNET communication card.

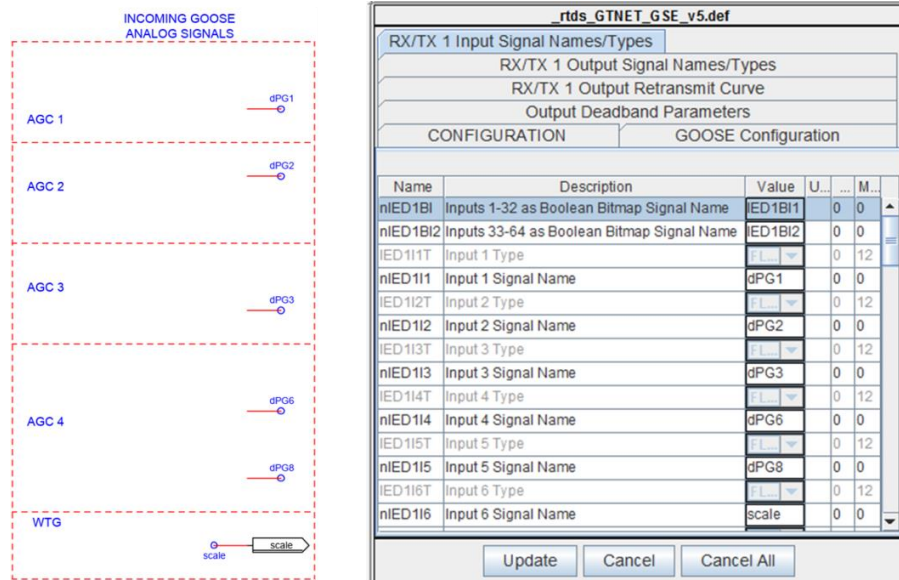


**Figure 8.23: Control signals signal from SEL-3555 RTAC to GNET arrangement on GNET-GSE communication module**

The SEL RTAC output control signal to RSCAD GTNET is transmitted through IEC 61850 GOOSE communication protocol. Figure 8.24 below shows the SEL-3555 RTAC control signal to RSCAD GTNET card captured using GOOSE Inspector. The arrangement is made in an ascending order starting from the generator 1 governor control signal to wind turbine generator active power compensator. In Figure 8.24 below, from dPG1 to dPG8, these are the supplementary control loops signal to the governing system of generator 1 to generator 8.

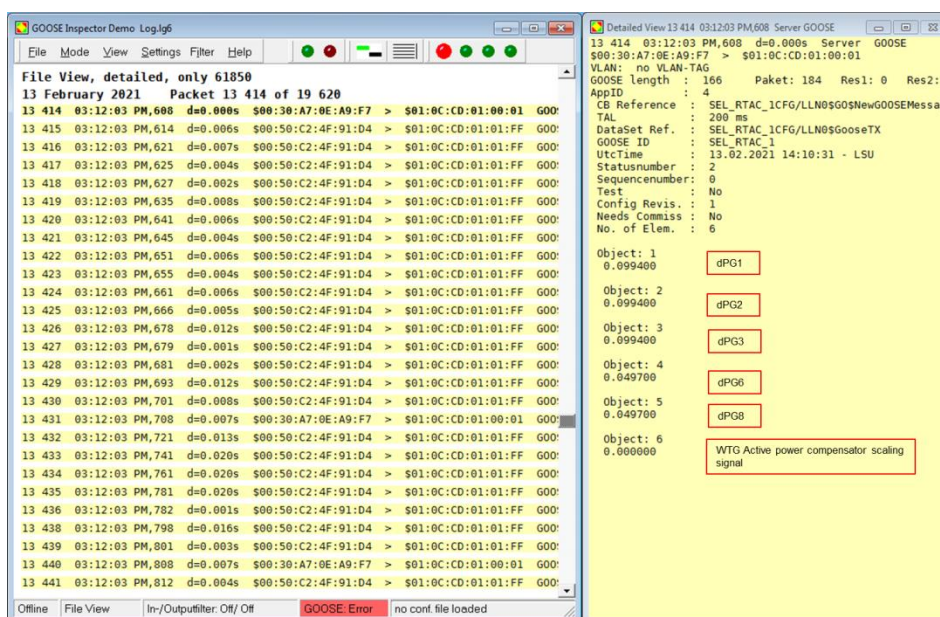


**Figure 8.24: Data published from SEL-3555 RTAC via GOOSE messaging to GTNET is viewed using GOOSE Inspector**

The output control signals from SEL-3555 RTAC were measured on RSCAD RUNTIME, as shown in Figure 8.25 below. These control signals were compared with the SEL-3555 RTAC device signal shown in Figure 8.21 above, also verified on the GOOSE message captured through GOOSE Inspector as shown in Figure 8.24 above.

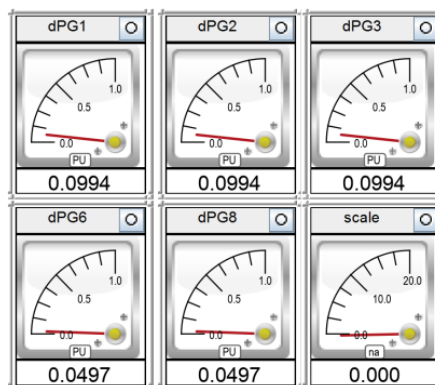


**Figure 8.25: Control signal from SEL-3555 RTAC to RSCAD generator governing system and WTG active power compensator scaling captured on RSCAD RUNTIME**

The developed control scheme's effectiveness on hardware needs to be tested and verified by applying system disturbance contingencies. The response of the developed control scheme will be monitored under the applied contingencies.

## **8.5 The application of contingencies to validate the effectiveness of the developed control scheme.**

Case studies introduced in chapter 4, 5, and 6 are repeated to validate the developed control scheme's effectiveness. Case study 1 is assessing the governing system's response when the AGC and wind power plant are inactive while they are integrated into the system. This can be the time where maintenance is taking place. Case study 2 assesses the effectiveness of the AGC to support the governing which performs the primary control. Case study 3 is the consolidated control scheme that includes both AGC and the wind turbine generator active power compensation control loop. This case study assesses the effectiveness of the whole scheme in frequency restoration.

### 8.5.1 Case study 1 – Response of the governing system.

During case study 1, the SEL-3555 RTAC is set to manual mode, and this control mode sets the controller's output to be a constant, which is defined as ManuaOut on the PID controller. For area 1 to area 4, the manual output is set to 0.0994pu. However, for area 4, since there are two synchronous generators active, the output control signal is divided in two for the control signal to generator 6 governing system as well as generator 8 governing system. Overall the constant control signal to generator 1 is 0.0994pu, generator 2 is 0.0994pu, for generator 3 is 0.0994pu, for generator 6 is 0.0497pu, and this is the same for generator 8 as well as shown in Figure 8.25 above.

Manual mode can be activated when maintenance needs to be done on the controller or settings to be updated on the SEL-3555 RTAC while still activated. The SEL-3555 RTAC enables the change of settings while the device is in service without creating any grid disturbances.

When case study 1 contingency (the load demand increase) was applied, the system frequency started dropping from 50Hz to 49.32Hz. This proves that the governing system alone cannot recover the system frequency back to its nominal value of 50Hz. Figure 8.26 below shows the response of the governing system when the RTAC 3555 is set to manual mode, and the disturbance occurs.

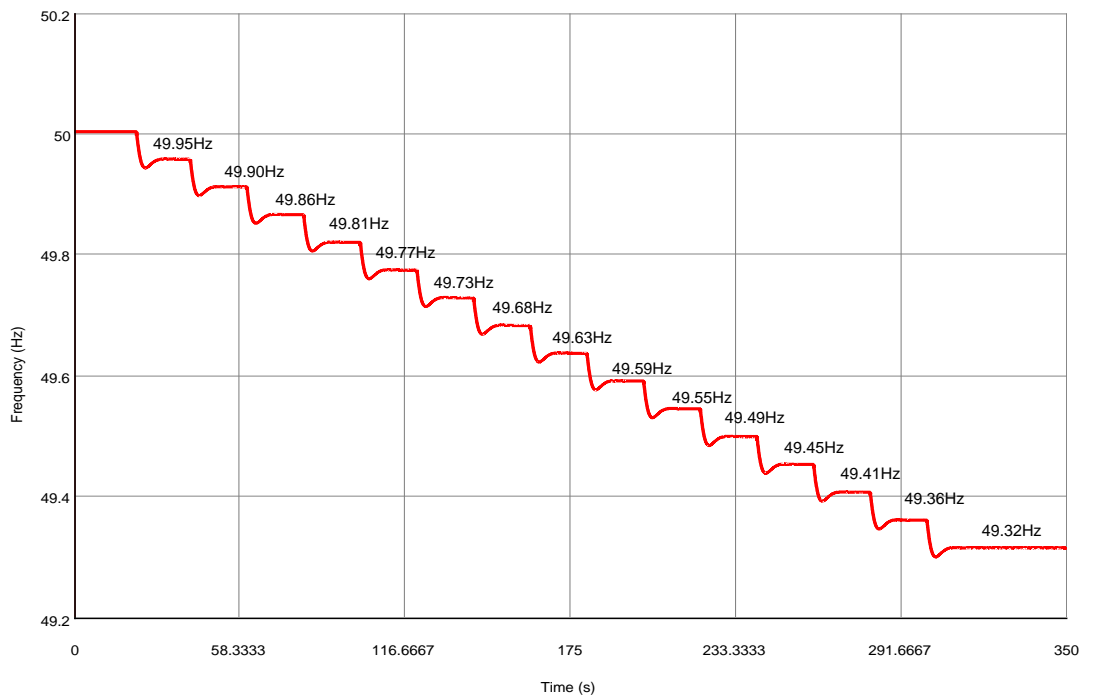


**Figure 8.26: System frequency during speed governing system response and SEL-3555 RTAC on manual mode**



The governing system regulates the active power of the system based on its droop characteristic. Figure 8.27 below shows the net-tie line power interchange in area 2. The governing system also failed to maintain the power interchange to their schedule amount. The droop characteristic is set such that the generator does not release all of its power capability. This is also done to protect the generator so that it does not operate its full scale. The scheduled power interchange pre-disturbance was 97.3MW, and post-disturbance was 111.1MW as shown in Figure 8.27 below

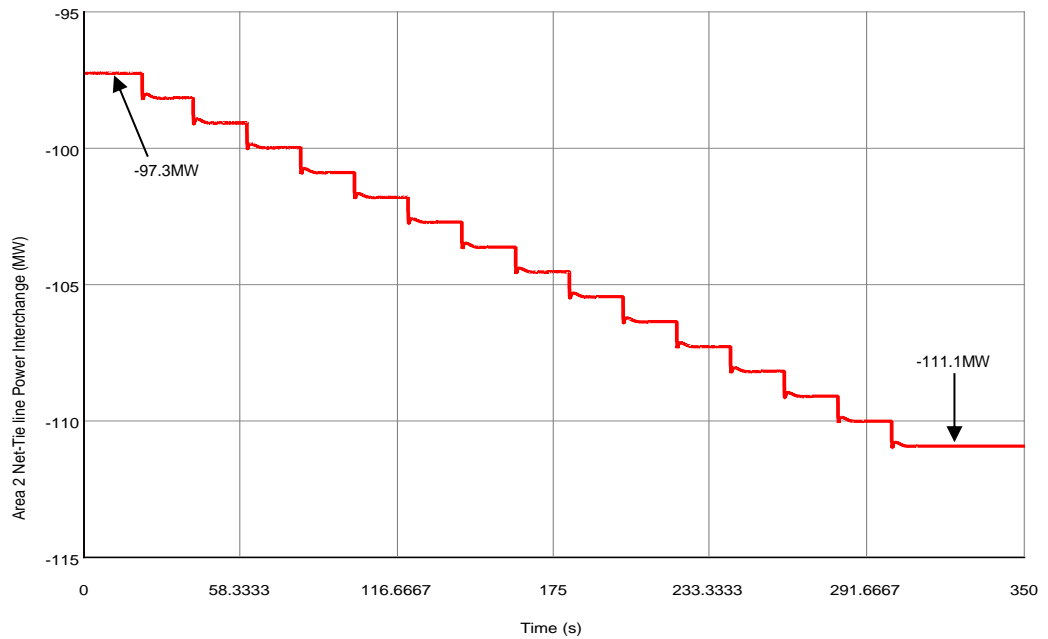


**Figure 8.27: Area 2 Net tie-line power interchange during the speed governing system response and SEL-3555 RTAC on manual mode**

In area 3, the power interchange was recorded as 48.61MW before the load demand increase contingency. After the 15% load demand increase, the power interchange increased to 56.22MW as shown in Figure 8.28 below

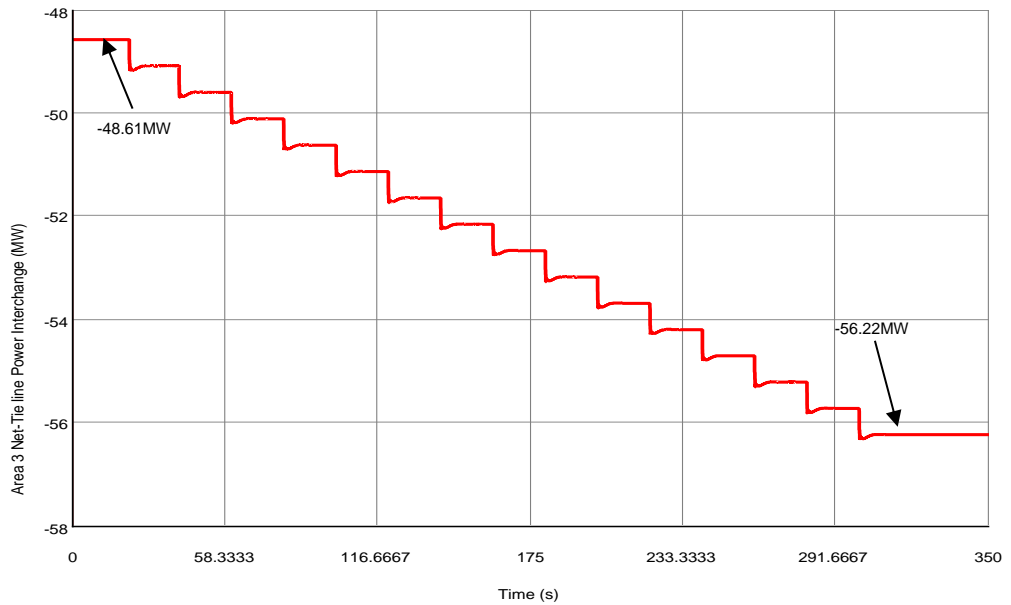


**Figure 8.28: Area 3 Net tie-line power interchange during the speed governing system response and SEL-3555 RTAC on manual mode**

In area 4, shown in Figure 8.29 below, the power interchange shifted from 125.11MW to a new value of 141.44MW. An uncontrolled power interchange could result in overloaded transmission lines and possibly triggering the feeder protection scheme in an overcurrent condition.

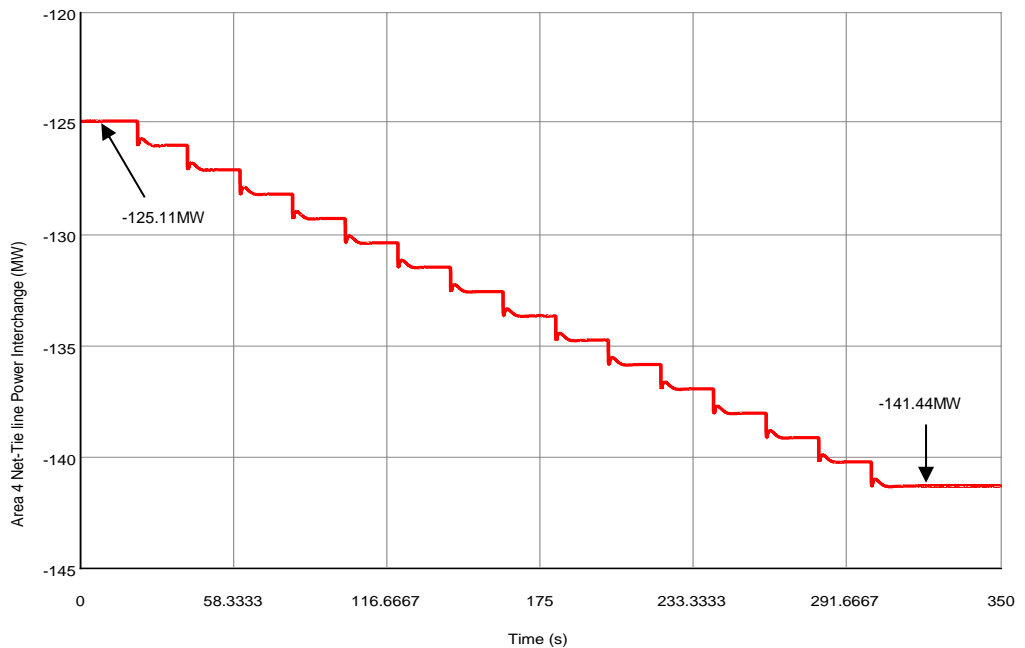


**Figure 8.29: Area 4 Net tie-line power interchange during the speed governing system response and SEL-3555 RTAC on manual mode**

From the measured bus voltages, it can be seen that bus 14 is the weakest bus of the network based on its voltage drop. There is a high probability that if the

load keeps increasing, the voltage at bus 14 will severely decrease. Therefore an additional control system needs to address the state of this busbar. Figure 8.30 below illustrates the bus voltages of the system following a load demand increase.

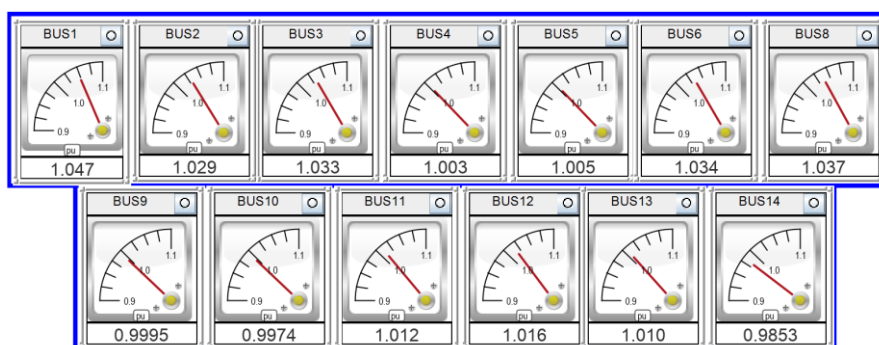


**Figure 8.30: Bus voltages during speed governing system response and SEL-3555 RTAC on manual mode**

To assist the governing system in providing an accurate control signal to enable the gate opening positions for the pressure inlet to run the turbine as the power demand changes, an additional control loop is required. An automatic generation control loop was developed using SEL-3555 RTAC. The control logic developed earlier as indicated from Figure 8.14 to Figure 8.17 above. The automatic generation control provides an accurate control signal to the governing system to control the active power based on the load demand changes. This is an additional control signal to the droop characteristic of the governing system. The response of the governing system with the automatic generation control is assessed through case study 2 below.

### 8.5.2 Case study 2 – Response of the governing system and automatic generation control.

Case study 2 described in chapter 5 is repeated. In this case study, the response of the governing system with support from the automatic generation control, which was developed on the SEL-3555 RTAC, is analyzed. From the previous subsection, the response of the governing system was assessed, and it was found that the governing system cannot restore the system frequency when the load has increased even if there are enough spinning reserves. Its droop characteristic allows it to set the mechanical power according to its setpoint. However, to return the system frequency to its nominal value, an additional control loop was required; hence, the automatic generation control development was made possible.

To activate the automatic generation control function, the PID mode of the control needs to change from manual to automatic mode. When a load demand increase contingency was applied, the governing system and the automatic generation control maintained the system frequency for a 4% load demand increase. From 5% to 8%, the load system frequency dropped to 49.99Hz. From 9% to 15% of the load demand increase, the system frequency kept on decreasing to a steady-state value of 49.66Hz, as shown in Figure 8.31 below.

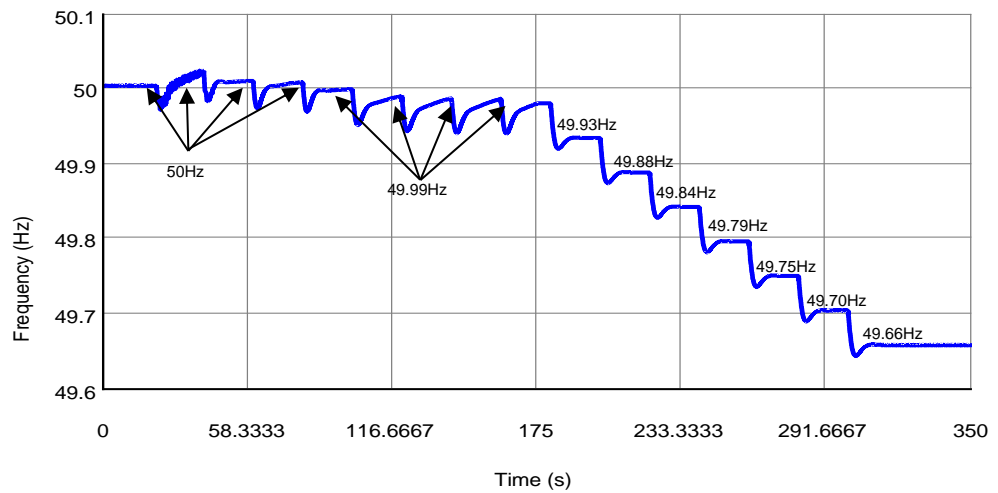


**Figure 8.31: System frequency response after the implementation of AGC on SEL-3555 RTAC**

The automatic generation control sends an accurate control signal to the governing system based on the frequency change. The governing system then sends an accurate control signal to the turbine gate or valve position. This detects how wide the pressure opening is to rotate the turbine and produce the required amount of active power to compensate for the load demand. When the spinning reserves are depleted, the automatic generation control and the governing cannot regulate the system frequency; hence the frequency has dropped to 49.66Hz, as shown in Figure 8.31 above.

The AGC's contribution is noticeable as the net power interchange in area 2 was improved compared to when only the governing system was activated to control the active power. For the first 3% load demand increase, the net power interchange was maintained around its scheduled value of 97.3MW, as shown in Figure 8.32 below. As the load demand increase, the net power interchange also increased and transgressed to a new value of 111.58MW after the load demand increase.

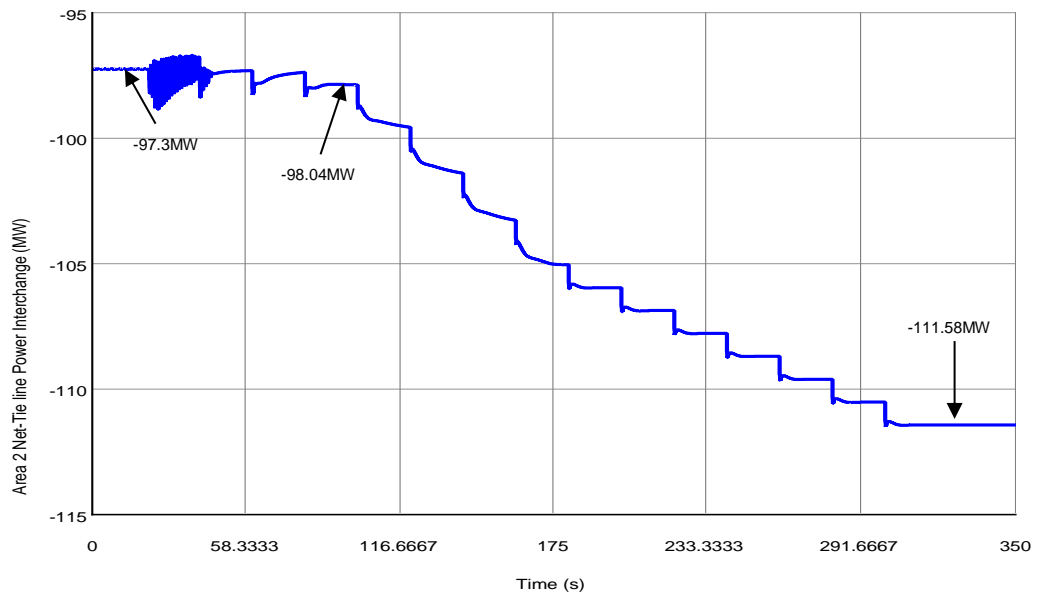


**Figure 8.32: Area 2 Net tie-line power interchange after the implementation of AGC on SEL-3555 RTAC**

The AGC and the governing system maintained the net power interchange for area 3 between 48.61MW and 48.88MW for the first four steps of the load demand increase, as shown in Figure 8.33 below. After the load demand increase, the net power interchange was improved from 56.22MW as indicated in Figure 8.28 to 55.97MW, as shown in Figure 8.33 below after the load demand increase event.

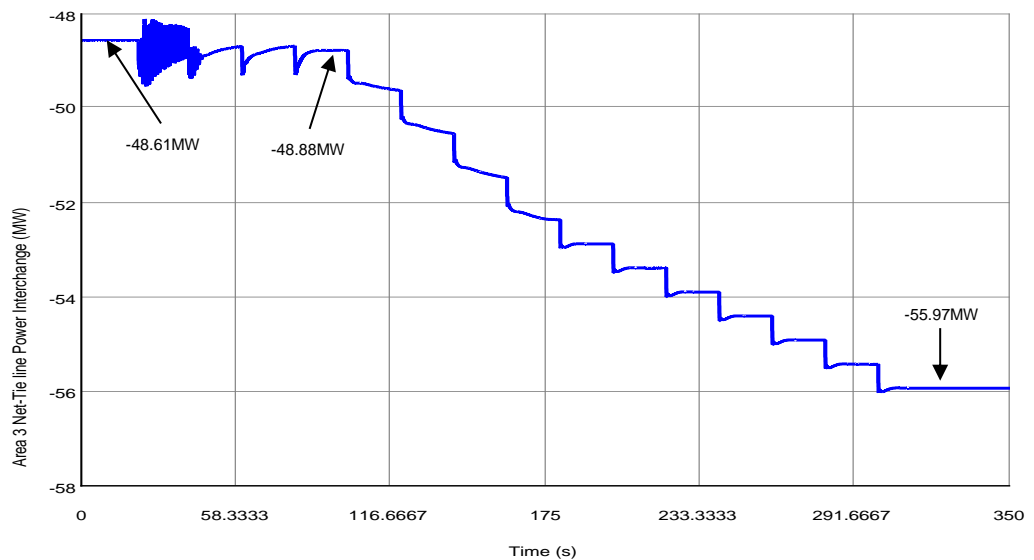


**Figure 8.33: Area 3 Net tie-line power interchange after the implementation of AGC on SEL-3555 RTAC**

The activation of AGC and the governing system did not make any significant improvement to the power interchange at area 4; instead, the power interchange

has risen from 141.42MW in the presence of governing system alone, as shown in Figure 8.29 above to 142.47MW in the presence of the AGC as shown in Figure 8.34 below. This is a critical area within the network as there is a bulk load fed from this area.

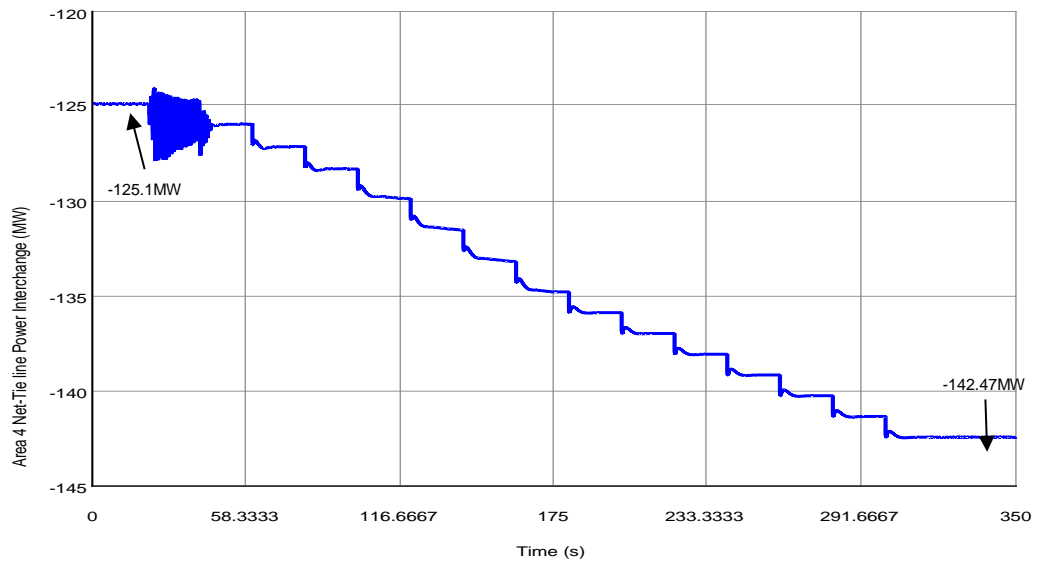


**Figure 8.34: Area 4 Net tie-line power interchange after the implementation of AGC on SEL-3555 RTAC**

The bus voltages were recorded after the load demand increase contingency, as indicated in Figure 8.35 below. Bus 14 has a lower voltage measurement than other buses; bus 14 voltage measurement was 0.9855pu. This is an indication that this is the weak bus of the network. This needs to be addressed, otherwise, if the load increases, the system can become unstable, and the load connected to this busbar will be severely affected by low voltage.

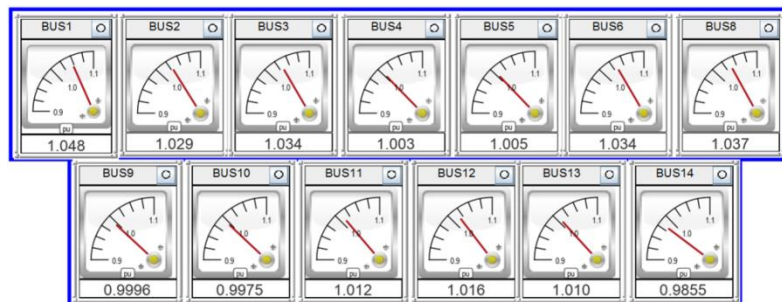


**Figure 8.35: Bus voltages after the implementation of AGC on SEL-3555 RTAC**

The AGC utilized in case study 2 is seen to provide some improvement to the system frequency and the power interchange between the areas. In addition, there is an improvement in the bus voltages. However, the AGC can only help ensure the balance between the power being generated and the load demand,

provided that there are enough spinning reserves. When the spinning reserves are depleted, the power system can shift from its stability point in the event of incremental load contingency.

An additional supply and control loop is required to address the declining power system frequency and voltages. The integration of wind power plants has a significant impact on improving the power system stability. Section 8.5.3 below focuses on assessing the contribution of wind active power compensation to the declining system frequency while maintaining both the system voltages and the power interchange between the areas.

### **8.5.3 Case study 3 – Response of the governing system, automatic generation control, and wind active power compensator.**

Case study 3 performed in chapter 6 is repeated. This case study seeks to validate the consolidated control scheme comprised of governing system, automatic generation control, and wind active power compensation. This is performed to validate the effectiveness of the control scheme developed.

The wind turbine generator active power compensator scaling logic described in Figure 8.18 above was developed to activate the wind turbine generator to supply the active power required to the system based on the frequency deviation.

The load demand increase contingency was applied to assess the effectiveness of the control logic developed to allow active power compensation to the grid.

The governing system and the automatic generation control were able to keep the frequency as close as possible to its initial value following a load demand increase for the first four steps. At the fifth step, load demand increase, the AGC and the governing system were struggling to keep the frequency at 50Hz, the wind power plant was activated to support the grid with the required active power based on the frequency deviation load kept on increasing. Figure 8.36 below shows the response and the contribution of the wind power plant to power system frequency control. The Wind power plant is noted that it started to activate its control when the frequency became less than 50Hz at T=112.67s. The stability was maintained throughout until the 15 step load demand increase was complete at the rate of 1% of the load at each step. Therefore the maximum load demand increase was 15% which equates to 38.85MW

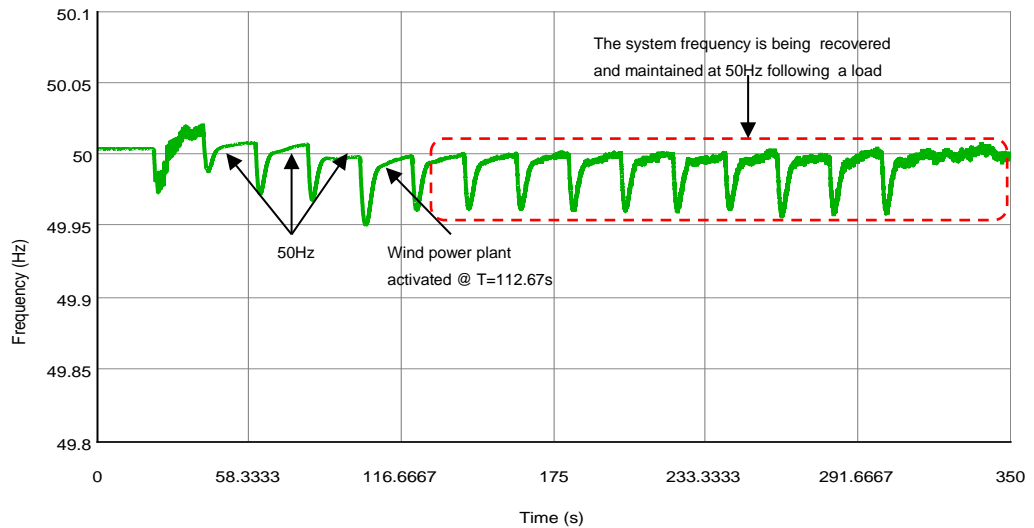


**Figure 8.36: System frequency when the governing system, AGC and WTG were active on SEL-3555 RTAC**

The wind power plant was activated when the AGC and the governing system could not contribute any additional active power to the grid. This was due to insufficient spinning reserves. In Figure 8.37 below, the activation time of the wind power plant is indicated as  $T=112.67\text{sec}$ . This is the response of the controller in real-time as this controller was developed using SEL-3555 RTAC. The response time of the wind power plant is faster by 29.67sec compared to the response of the control developed on RSCAD, which resulted in wind power being activated at  $T=142.42\text{sec}$  as shown in chapter 7, Figure 7.22 above. The total active power compensated by the wind power plant is 19.98MW, as shown in Figure 8.37 below

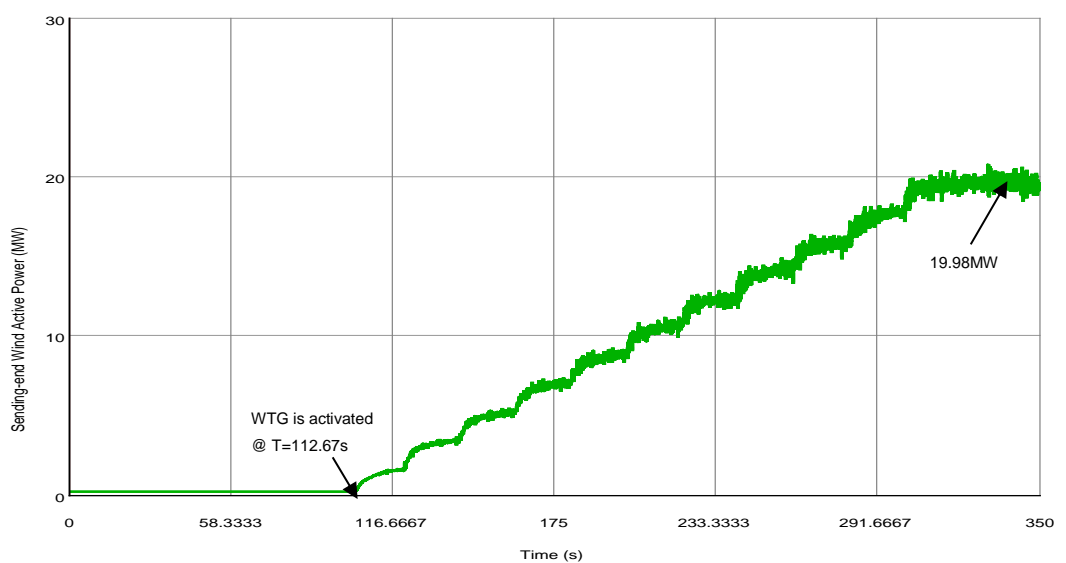


**Figure 8.37: Active power delivered by the wind power plant measured at the sending-end controlled through SEL-3555 RTAC**



The contribution of the wind active power compensation to the improvement of the net power interchange is noted. After the load demand increase contingency, the power interchange was recorded as 105.8MW at the receiving end of area 2. Figure 8.38 shows the contribution of the wind turbine generator's active power compensation to the power interchange at area 2. Before the wind power plant activation, area 2 net power interchange was recorded as -111.58MW as indicated in Figure 8.32.

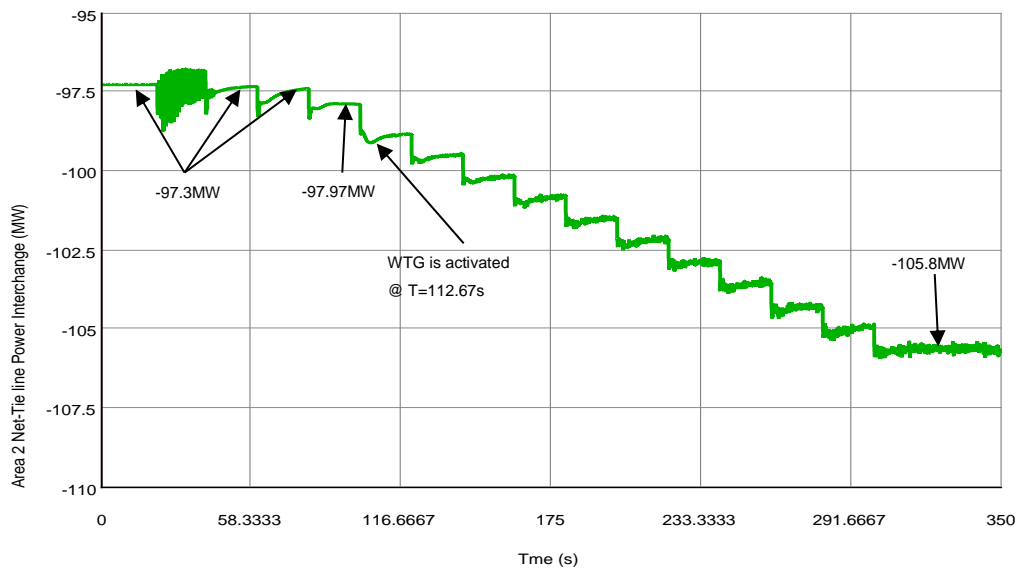


**Figure 8.38: Area 2 net tie-line power interchange when the wind power plant was activated through SEL-3555 RTAC**

For area 3, there was not a significant contribution of the wind power plant to the net tie-line power interchange. Instead, the power interchange increased from 55.97MW in Figure 8.33 during the response of the governing system and the AGC to 59.27 during the response of the governing system, AGC, and the wind power plant in Figure 8.39 below. This is due to the bulk load connected in area 3, which requires active power support as the demand increases. Therefore, for area 3 to maintain its power interchange as scheduled, an additional supply is recommended.

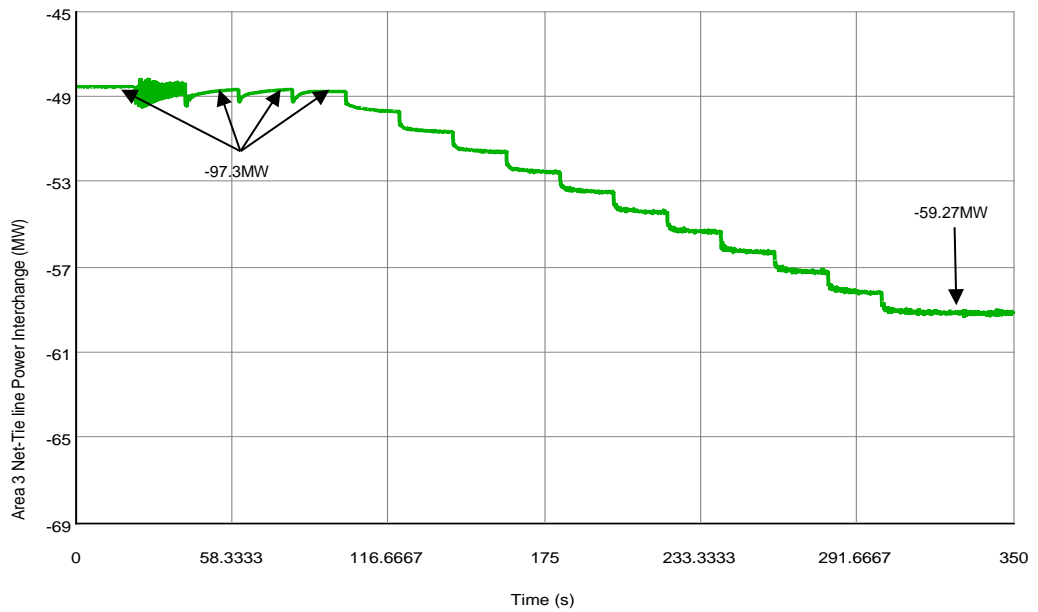


**Figure 8.39: Area 3 net tie-line power interchange when the wind power plant was activated through SEL-3555 RTAC**

Considering Figure 8.34, during the response of the governing system and the AGC, area 4 power interchange was -142.47MW after the load demand increase contingency applied. When the wind power plant was activated, the power interchange was improved to -130MW, as shown in Figure 8.40 below.

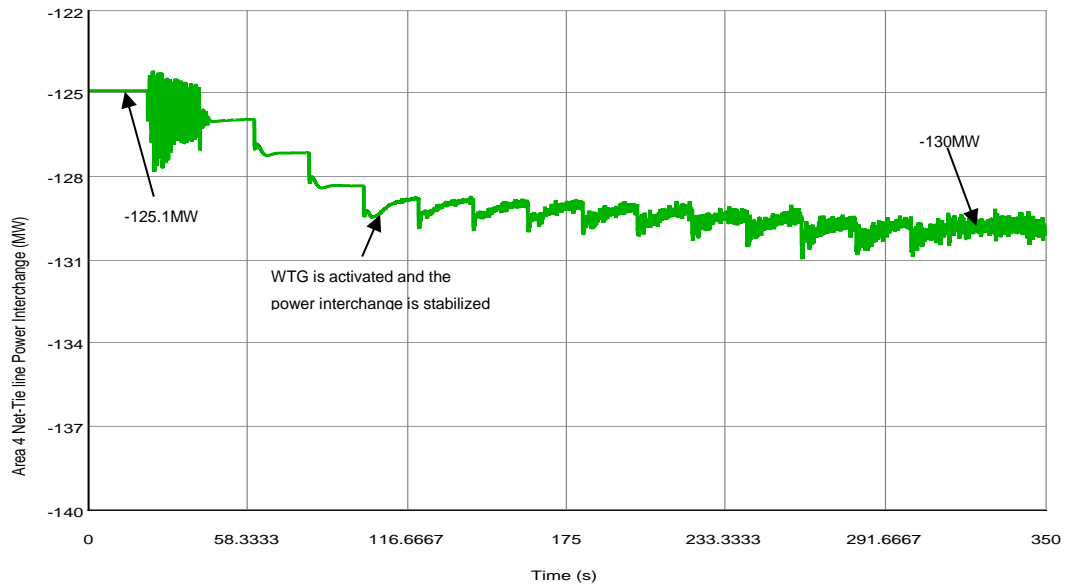


**Figure 8.40: Area 4 net tie-line power interchange when the wind power plant was activated through SEL-3555 RTAC**

The power system network can be declared as stable when both the system's frequency and power interchange are within the acceptable operating range. Both the system frequency and the system bus voltages are equally important

when considering power system stability. Therefore a focus on power system stability cannot be on one variable such as frequency. The voltage needed to be considered as well. Hence Figure 8.41 is also critical to assess the bus voltage status after the load demand contingency.

It can be noted that the wind power plant has also improved the system bus voltages. Bus14 has been improved from 0.9855pu as indicated in Figure 8.35 to 0.9965pu, as shown in Figure 8.41 below.

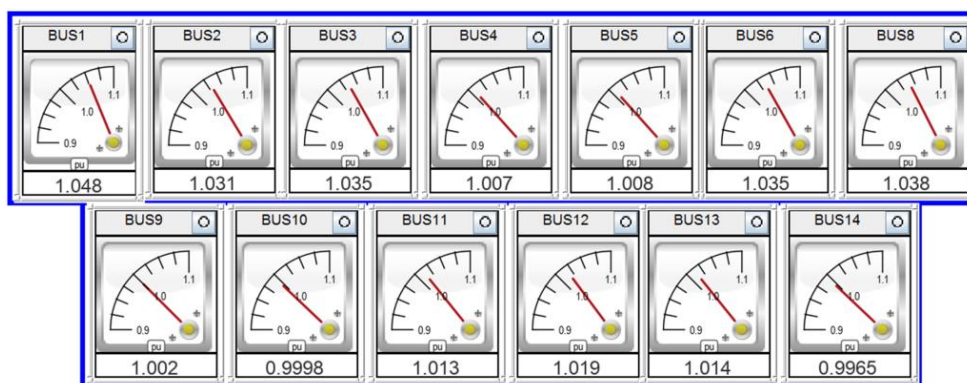


**Figure 8.41: Bus voltage results recorded when the wind power plant was activated through SEL-3555 RTAC**

## 8.6 Conclusion

Maintaining the stability of the power system is crucial. The developed frequency control scheme has proven that renewable energy resources can contribute to the power system frequency stability. Although these energy resources are well-known for their quick reaction to system disturbance, the developed control scheme has shown that they can remain stable when adequately configured using the latest technologies.

The decentralized automatic generation control (AGC) with wind active power compensator control loop has been proven effective in power system frequency regulation. The developed control scheme will benefit power utility companies when it comes to frequency stability. The developed control scheme can also help avoid load-shedding when supply cannot withstand the load demand.

This innovation will also enable the power utility companies to explore these control and protection schemes to maintain the power system frequency stability. The heavily dependent system on PLCs for control functions can now utilize the SEL-3555 RTAC controller as it offers a wide range of control options, and it has been proven to be effective when applied in frequency control of the power system network. This controller is using the latest communication IEC 61850

standard protocol. This standard allows data retrieval in remote areas through Ethernet connectivity. The data can be retrieved even if the controller is locally based.

# CHAPTER NINE

## CONCLUSION AND RECOMMENDATIONS

### 9.1 Introduction

The quality of supply is essential to end-users. Power system variables such as voltage and frequency change under different conditions, but the power system grid's stability must be maintained following any system disturbances. Compromising the power's stability would result in low supply quality to the customers, which can consequently cause more equipment damages and maloperation.

This thesis focuses on developing the control scheme to integrate renewable energy resources in the event power system frequency instability using IEC 61850 standard. A control algorithm determines the operation of the control scheme in light of the frequency stability.

The IEEE 14 bus network was modified and used as the network under study to achieve the objectives of the thesis. Load flow analysis in steady-state conditions was performed. Under dynamic-state, load demand increase contingencies were applied. The aim was to prove that the governing system cannot recover the system frequency following the load demand increase contingency. The impact of the load demand increase resulted in a drop in power system frequency.

The automatic generation control was developed as the secondary controller to assist the governing system in frequency regulation. When the load kept on increasing, an additional control loop was recommended, which will activate the active wind power following frequency deviation from its nominal value of 50Hz

The control scheme development was initiated through DIgSILENT simulation software, verified on RSCAD, and practically implemented on the hardware in the loop using SEL-3555 RTAC and tested on RSCAD.

Therefore, this chapter summarizes the work performed to achieve the aim and objective of the thesis. Section 9.1 is the introduction of this chapter, and section 9.2 outlines the deliverables of this study. Section 9.3 outlines the applicability of the study performed in academics as well as in industrial environments. Section 9.4 highlights the future work that is recommended and propose within the power system stability environment. Section 9.5 indicates the progress made in publications.

## **9.2 Thesis deliverables**

This section outlines the summary of the work performed in achieving the aim and objectives of the thesis.

### **9.1.1 Literature review**

A literature review was performed in this study to evaluate the progress made in frequency stability and control. The power system instability phenomena, as well as the mitigation factor, were explored. The integration of wind power plant in the distribution grid and the issue they pose to the grid were explored

Power system textbooks, ebooks, journals, and digital library platforms were used to construct the literature, which will guide the study's aim and objectives.

### **9.1.2 Theoretical outline.**

The utilization of digital libraries, ebooks, textbooks, and journals was used to develop the theory for power system frequency stability, power system model and analysis, and the concepts in developing control schemes.

### **9.1.3 Modeling and simulation of the modified IEEE 14 bus system DlgSILENT**

The IEEE 14 bus network was modified to be suitable for the study performed in chapter 4. Ideally, this network consists of 3 synchronous generators and two reactive power compensators later modified to become two additional generators. Load flow analysis was performed to ensure that the network is stable before introducing any disturbances.

When the load demand increase contingency was applied, it was proven that the governing system could not restore the system frequency following the load demand increase; instead, it can only stabilize it to a new steady-state. As the load kept increasing, a need arose to develop a controller, which will help the governing system recover the system frequency following a load demand increase contingency. The development of the controller is described in chapter 5. These simulations were conducted in this chapter using DlgSILENT power factory simulation software version 2020. After the 15% load demand increase contingency, the system frequency was stabilized at 49.32Hz.

### **9.1.4 Modeling of automatic generation control and performance analysis using digsilent simulation software**

In chapter 5, an automatic generation control scheme was developed to address the governing system's ineffectiveness to recover the system frequency following a load demand increase contingency. The control scheme logics were developed

using DlgSILENT simulation software. The control's effectiveness was evaluated using the same software, and repeating the same load demand increased contingency. The developed control scheme operating as a secondary control loop has improved the system frequency to a new steady-state of 49.64Hz. This was a significant improvement, although this control is supplementary to the governing system. Therefore, when the generator spinning reserves are depleted, the secondary control loop cannot help the system recover the system frequency. Hence the new steady-state value frequency was recorded as 49.64Hz.

#### **9.1.5 Modeling of an aggregated wind farm and the development of wind active power compensator**

The introduction of distributed energy resources to compensate for the required amount of power following a load demand increase contingency was explored. The wind power plant control loop was developed in chapter 6 to enable the active power compensation based on the system frequency deviation. The control loop was tested, and its effectiveness was proven to resolve the system frequency issue while also aiming to ensure that the power interchange between the areas is also maintained at their scheduled amount. After the load demand increase contingency, the consolidated control scheme, which consists of automatic generation control and wind active power compensator, was proven to have recovered the system frequency to 50Hz.

#### **9.1.6 Modeling and simulation of the modified IEEE 14 bus system on RSCAD**

The network modeling performed in the chapter using DlgSILENT was repeated on the RSCAD simulation platform. All the contingencies performed in chapter 4 were repeated in chapter 7. The aim of developing this network modeling was to verify the behavior of the developed control scheme effectively.

#### **9.1.7 Development of frequency control scheme logic and integration of wind power plant and simulations using RSCAD.**

The automatic generation control and wind active power compensation scheme were evaluated by implementing the same contingencies in chapters 5 and 6. The result showed that the developed control scheme with wind power integration could improve the system frequency.

### **9.1.8 Practically implementation of the developed control scheme using SEL-3555 RTAC and simulations**

A test bench was developed in chapter 8, where the developed control scheme using different simulation platforms such as DigSielnt and RSCAD was practically implemented on the SEL-3555 RTAC device. Load demand increase contingencies were applied, the effectiveness of integrating wind power plant as the active power compensator was assessed, and its effectiveness was proven based on the applied contingencies.

### **9.3 Academic and industrial application**

This research has developed a test bench where academics can utilize to expand knowledge in power system frequency control schemes in real-time. This will also help students understand the control system's behavior and its application in the power system environment.

The developed control scheme can replace automatic generation control, which uses Programmable Logic Controllers (PLC). Troubleshooting and fault-finding in a congested system with much wiring can be complex. The developed control scheme is IEC 61850 standard-based, with reliable communication and less wiring. The signal input is transmitted via Ethernet communication.

The utility companies will also benefit from utilizing this controller to assist them in ensuring that the system stability is maintained following load demand increase, provided there is enough active power reserve capacity. This will help to avoid the implementation of load-shedding.

### **9.4 Future work**

The modeled automatic generation control was developed as a decentralized controller. In a decentralized control loop, each control area has its controller. This can result in a high cost due to more resources required for the implementation, although its advantage of overlapping the control function is noted when one controller fails.

The future work will focus on developing a centralized controller controlled remotely at a centralized control center. Integrating the load-shedding scheme as a backup control when there is no active power capacity to automatically implement load-shedding to avoid the power system collapse can be considered.



Also, the wind power plant's utilization as the primary frequency control in a conventional power system grid supports the governing system in frequency regulation.

## **9.5 Publication**

M. Mditshwa, M.E.S. Mnguni, and M. Ratshitanga, 2021. Integration of Wind Power Plant ( WPP ) for primary frequency regulation, published on IEEE PowerAfrica Conference 2021.

M. Mditshwa, M.E.S. Mnguni, and M. Ratshitanga, 2021. The Benefits of an Automatic Generation Control in an Interconnected Power System Under Various System Conditions, accepted for publication on International Journal of Electrical Engineering and Applied Sciences

## BIBLIOGRAPHY/REFERENCES

- Ahmad, F., Rasool, A., Ozsoy, E., Sekar, R., Sabanovic, A. & Elitaş, M. 2018. Distribution system state estimation-A step towards smart grid. *Renewable and Sustainable Energy Reviews*, 81: 2659–2671. <https://www.sciencedirect.com/science/article/pii/S1364032117310134> 21 May 2018.
- Alan S, M. & Hall, M. 2019. The G20 Transition Towards a Net-zero Emissions Economy - South Africa. *Brown to Green*: 1–20. [www.britannica.com](http://www.britannica.com).
- Alhejji, A. 2017. L1 adaptive load frequency control of single-area electrical power system. *2017 4th International Conference on Control, Decision and Information Technologies, CoDIT 2017*, 2017-Janua: 595–598.
- Anca Daniela, H., Ejnar Poul, S., Zeni, L. & Altin, M. 2016. *Frequency control modelling - basics*.
- Annam, S., Rani, K.R. & Naick, J.S. 2017. Automatic Generation Control of Three Area Power System with Artificial Intelligent. : 6576–6591.
- Apostolov, A.P. 2009. Modeling systems with distributed generators in IEC 61850. *2009 Power Systems Conference: Advance Metering, Protection, Control, Communication, and Distributed Resources, PSC 2009*: 77–82.
- Basler, M.J., Schaefer, R.C. & Member, S. 2008. Understanding Power-System Stability. *Industry Applications, Transactions on*, 44(2): 463–474.
- Bergen, A.R. & Vittal, V. 2007. *Power Systems Analysis*. [http://www.ugr.es/~bioestad/\\_private/cpfund10.pdf](http://www.ugr.es/~bioestad/_private/cpfund10.pdf).
- Beukman, C., Claassens, F., Lawrence, B., Smit, N. & Tarrant, D. 2011. *GENERATION GROUP, POWER STATION ELECTRICAL PLANT, GENERATOR BASIC ENGINEERING MANUAL*.
- Bevrani, H. 2014. Power System Control : An Overview. In 1–17.
- Bevrani, Hassan. 2014. *Robust Power System Frequency Control (Power Electronics and Power Systems)*.

Borase, R.P., Maghade, D.K., Sondkar, S.Y. & Pawar, S.N. 2020. A review of PID control, tuning methods and applications. *International Journal of Dynamics and Control*, (July). <https://doi.org/10.1007/s40435-020-00665-4>.

Boyle, J., Littler, T. & Foley, A. 2018. Review of frequency stability services for grid balancing with wind generation. *The Journal of Engineering*, 2018(15): 1061–1065.

Bragantini, A. 2019. *Investment Planning for Distribution Networks in Multi Carrier Energy Systems*. Swiss Federal Institute of Technology (ETH).

De Carne, G., Buticchi, G., Liserre, M. & Vournas, C. 2018. Real-Time Primary Frequency Regulation using Load Power Control by Smart Transformers. *IEEE Transactions on Smart Grid*, 10(5): 5630–5639.

Chauhan, V.S., Sharma, R. & Shah, H. 2017. Modern Trends in Power System Communication: A Review. *International Journal of Advanced Research in Electrical, Electronics and Instrumentation Engineering*: 3285–3289.

Chris, Y. 2020. André de Ruyter reflects on restructuring needed to meet future vision. , (3).

Daniela, A., Ejnar, P., Basit, A., Hansen, A.D., Sørensen, P. & Gamst, M. 2014. large-scale wind power Wind power integration into the automatic generation control of power systems with large-scale wind power.

Darussalam, R. & Garniwa, I. 2019. The effect of photovoltaic penetration on frequency response of distribution system. *Proceedings - 6th International Conference on Sustainable Energy Engineering and Application, ICSEEA 2018*: 81–85.

Das, R. & Kanabar, M. 2015. Centralized Substation Protection and Control. *IEEE PES Report of Working Group K15 of the Substation Protection Subcommittee Members*.

DIGSILENT. 2020. PowerFactory 2020 User Manual. : 1–1253. <https://www.digsilent.de>.

Ding, X., Xu, J., Sun, Y., Liao, S., Chen, R., Lan, T., Li, P. & Yu, L. 2020. A Closed Loop Load Control Scheme for Stabilizing Frequency in Power System

with Block Events. *2020 IEEE/IAS Industrial and Commercial Power System Asia, I and CPS Asia 2020*: 391–396.

Duymaz, E., Pourkeivannour, S., Ceylan, D., Sahin, I. & Keysan, O. 2018. Design of a power plant emulator for the dynamic frequency stability studies. *Proceedings - 2018 23rd International Conference on Electrical Machines, ICEM 2018*: 152–157.

El-Hawary, M.E. & Ali, M.-S. 2020. Load Frequency Control in Variable Inertia Systems. *IEEE Transactions on Power Systems*, 22(10): 43.

Endegnanew, A.G. & Uhlen, K. 2016. Global analysis of frequency stability and inertia in AC systems interconnected through an HVDC. *2016 IEEE International Energy Conference, ENERGYCON 2016*.

Forsyth, P. & Kuffel, R. 2007. Utility applications of a RTDS x00AE; Simulator. *Power Engineering Conference, 2007. IPEC 2007. International*: 112–117.

Ghafouri, A., Milimonfared, J. & Gharehpetian, G.B. 2015. Coordinated control of distributed energy resources and conventional power plants for frequency control of power systems. *IEEE Transactions on Smart Grid*, 6(1): 104–113.

Gjengedal, T. 2002. System Control of Large Scale Wind Power by use of Automatic Generation Control ( AGC ). : 15–21.

Grobler, J. 2011. *Development and adaptation of dynamic models for new power generation sources JH Grobler Dissertation submitted in partial fulfilment of the requirements for the degree Magister in Engineering in Electrical Engineering at North-West University*.

Gu, J.C., Liu, C.H., Yang, M.T. & Tsai, D.L. 2019. Research on Integrating Wind Turbine into Intelligent IEC 61850 Substation Automation. *2019 2nd Asia Conference on Energy and Environment Engineering, ACEEE 2019*: 54–58.

Gu, M., Meegahapola, L. & Wong, K.L. 2018. Review of rotor angle stability in hybrid AC/DC power systems. *Asia-Pacific Power and Energy Engineering Conference, APPEEC, 2018-October*: 7–12.

Hachmann, C., Lammert, G., Lafferte, D. & Braun, M. 2020. Power system restoration and operation of island grids with frequency dependent active power

control of distributed generation. *NEIS 2017 - Conference on Sustainable Energy Supply and Energy Storage Systems*: 45–50.

Jan, M., Janusz, W., James, And, B. & R, B. 2005. *The Power System in the Steady State*.

Johnson, B., Denholm, P., Kroposki, B. & Hodge, B. 2017. Achieving a 100% Renewable Grid. *IEEE Power and Energy Magazine*, (april): 61–73.

Kuffel, R., Ouellette, D. & Forsyth, P. 2010. Real Time Simulation and Testing Using IEC 61850. *Proc. Modern Electric Power Systems conf.*: 1–8.

Kumar, S. & Anwar, M.N. 2019. Fractional order PID Controller design for Load Frequency Control in Parallel Control Structure. *2019 54th International Universities Power Engineering Conference, UPEC 2019 - Proceedings*.

Kundur, P. 2004. Definition and Classification of Power System Stability IEEE/CIGRE Joint Task Force on Stability Terms and Definitions. *IEEE Transactions on Power Systems*, 19(3): 1387–1401.

Kundur, P. 1994. *Power System Stability And Control*. N. B. J. & M. G. Lauby, eds. McGraw-Hill, Inc.

Kundur, P., John, P., Venkat, A., Göran, A., Anjan, B., Claudio, C., Nikos, H., Hill, D., Alex, S., Carson, T., Thierry, V.C. & Vittal, V. 2004. Definition and classification of power system stability IEEE/CIGRE joint task force on stability terms and definitions. *IEEE Transactions on Power Systems*, 19(3): 1387–1401.

Laghari, J.A., Mokhlis, H., Bakar, A.H.A. & Mohamad, H. 2013. Application of computational intelligence techniques for load shedding in power systems: A review. *Energy Conversion and Management*, 75(August 2003): 130–140. <http://dx.doi.org/10.1016/j.enconman.2013.06.010>.

Li, C., Wu, Y., Sun, Y., Zhang, H., Liu, Yutian, Liu, Yilu & Terzija, V. 2020. Continuous Under-Frequency Load Shedding Scheme for Power System Adaptive Frequency Control. *IEEE Transactions on Power Systems*, 35(2): 950–961.

Liu, Yong, You, S. & Liu, Yilu. 2017. Study of Wind and PV Frequency Control in U.S. Power Grids—EI and TI Case Studies. *IEEE Power and Energy Technology*

*Systems Journal*, 4(3): 65–73.

Luna, A.C., Rodriguez, E., Vasquez, J.C., Meng, L., Luna, A. & Dragicevic, T. 2016. Flexible System Integration and Advanced Hierarchical Control Architectures in the Microgrid Research Laboratory of Aalborg University Savaghebi, Juan Vasquez, Josep Guerrero Moisès Graells Fabio Andrade. , 52(2): 1736–1749.

Machowski, J., Bialek, J.W. & Bumby, J.R. 2008. Frequency Stability and Control.

Magdy, G., Shabib, G., Elbaset, A.A. & Mitani, Y. 2019. Renewable power systems dynamic security using a new coordination of frequency control strategy based on virtual synchronous generator and digital frequency protection. *International Journal of Electrical Power and Energy Systems*, 109(January): 351–368. <https://doi.org/10.1016/j.ijepes.2019.02.007>.

Marchesan, G., Muraro, M.R., Cardoso, G., Mariotto, L. & De Morais, A.P. 2016. Passive Method for Distributed-Generation Island Detection Based on Oscillation Frequency. *IEEE Transactions on Power Delivery*, 31(1): 138–146.

Mnguni, M.E.S. & Darcy, Y. 2020. An approach for a multi-stage under-frequency based load shedding scheme for a power system network. *International Journal of Electrical and Computer Engineering*, 10(6): 6071–6100.

Mohagheghi, S., Stoupis, J. & Wang, Z. 2009. Communication protocols and networks for power systems - Current status and future trends. *2009 IEEE/PES Power Systems Conference and Exposition, PSCE 2009*: 1–9.

Mohamed, A, E., Magdy, G. & Mitani, Y. 2018. Digital frequency protection for micro-grid coordinated with LFC considering high PV/wind penetration level. *Proceedings - 2018 6th International Istanbul Smart Grids and Cities Congress and Fair, ICSG 2018*: 62–66.

Mohamed, E.A., Magdy, G., Shabib, G., Elbaset, A.A. & Mitani, Y. 2018. Digital coordination strategy of protection and frequency stability for an islanded microgrid. : 3637–3646.

Motta, R.T., Dotta, D. & Wilches-Bernal, F. 2019. Development and assessment of second generation WTG models in an open source platform. *Energy Systems*. <https://doi.org/10.1007/s12667-019-00337-z>.

Munoz-Hernandez, G.A., Mansoor, S.P. & Jones, D.I. 2013. *Power system dynamics*.

Musau, M.P., Chepkania, T.L., Odero, A.N. & Wekesa, C.W. 2017. Effects of renewable energy on frequency stability: A proposed case study of the Kenyan grid. *Proceedings - 2017 IEEE PES-IAS PowerAfrica Conference: Harnessing Energy, Information and Communications Technology (ICT) for Affordable Electrification of Africa, PowerAfrica 2017*: 12–15.

Muyeen, S.M. & Blaabjerg, F. 2019. Special issue on 'large grid-connected wind turbines'. *Applied Sciences (Switzerland)*, 9(5): 10–12.

Nayak, P.C., Bisoi, S., Prusty, R.C. & Panda, S. 2019. Performance analysis of PDF+(1+PI) controller for load frequency control of the multi microgrid system using genetic algorithm. *Proceedings - 2019 International Conference on Information Technology, ICIT 2019*: 448–453.

NERSA. 2016. Grid Connection Code for Renewable Power. , 9(July): 122. <http://www.nersa.org.za/>.

NERSA. 2019a. The South African Grid Code - System Operation Code. , 10(August): 24. <http://www.nersa.org.za/>.

NERSA. 2010. The South African Grid Code – Network Code. , (July): 1–21.

NERSA. 2019b. The South African Grid Code The Transmission Tariff Code. , 10(August): 1–65.

Obaid, Z.A., Cipcigan, L.M., Abraham, L. & Muhssin, M.T. 2019. Frequency control of future power systems: reviewing and evaluating challenges and new control methods. *Journal of Modern Power Systems and Clean Energy*, 7(1): 9–25. <https://doi.org/10.1007/s40565-018-0441-1>.

Ortega, Á. & Milano, F. 2018. Frequency Control of Distributed Energy Resources in Distribution Networks. *IFAC-PapersOnLine*, 51(28): 37–42. <https://doi.org/10.1016/j.ifacol.2018.11.674>.

Ozansoy, C. 2016. Design of an adaptive protection system for microgrids with distributed energy resources in accordance with IEC 61850-7-420. *ELECO 2015 - 9th International Conference on Electrical and Electronics Engineering*: 474–

478.

Patel, N.C. 2017. Load Frequency Control of a Non-Linear Power System with Optimal PID Controller with Derivative Filter. *IEEE International Conference on Power, Control, Signals and Instrumentation Engineering (ICPCSI-2017)* Load: 1515–1520.

Pavlovsky, V. & Steliuk, A. 2014. Modeling of Automatic Generation Control in Power Systems. : 157–173.

Philip, K. 2004. *Electrical Equipment Handbook: Troubleshooting and Maintenance*. <https://eur-lex.europa.eu/legal-content/PT/TXT/PDF/?uri=CELEX:32016R0679&from=PT%0Ahttp://eur-lex.europa.eu/LexUriServ/LexUriServ.do?uri=CELEX:52012PC0011:pt:NOT>.

Rahmann, C., Ortiz-Villalba, D., Alvarez, R. & Salles, M. 2018. Methodology for selecting operating points and contingencies for frequency stability studies. *IEEE Power and Energy Society General Meeting*, 2018-Janua: 1–5.

Rueda, J.L., Korai, A.W., Cepeda, J.C., Erlich, I. & Gonzalez-Longatt, F.M. 2014. *Implementation of Simplified Models of DFIG-Based Wind Turbines for RMS-Type Simulation in DlgSILENT PowerFactory*.

Sallam, A.A. & Malik, O.P. 2015. Power system stability overview. *Power System Stability: Modelling, Analysis and Control*: 1–10.

Satyanarayana, S., Sharma, R.K., Mukta, A. & Sappa, A.K. 2015. Automatic generation control in power plant using PID, PSS and Fuzzy-PID controller. *2014 International Conference on Smart Electric Grid, ISEG 2014*.

Schneider, K.P., Radhakrishnan, N., Tang, Y., Tuffner, F.K., Liu, C.C., Xie, J. & Ton, D. 2019. Improving Primary Frequency Response to Support Networked Microgrid Operations. *IEEE Transactions on Power Systems*, 34(1): 659–667.

Tan, W., Zhang, H. & Yu, M. 2012. Decentralized load frequency control in deregulated environments. *International Journal of Electrical Power and Energy Systems*, 41(1): 16–26. <http://dx.doi.org/10.1016/j.ijepes.2012.02.013>.

Tomsovic, K., Bakken, D.E., Venkatasubramanian, V. & Bose, A. 2005. Designing the next generation of real-time control, communication, and



- computations for large power systems. *Proceedings of the IEEE*, 93(5): 965–979.
- Umrao, R., Kumar, S., Mohan, M. & Chaturvedi, D.K. 2012. Load Frequency Control methodologies for power system. *ICPCES 2012 - 2012 2nd International Conference on Power, Control and Embedded Systems*.
- Ustun, T., Ozansoy, C. & Zayegh, A. 2011. Distributed Energy Resources (DER) object modeling with IEC 61850–7–420. ... *Conference (AUPEC), 2011 ...*: 1–6. [http://ieeexplore.ieee.org/xpls/abs\\_all.jsp?arnumber=6102505](http://ieeexplore.ieee.org/xpls/abs_all.jsp?arnumber=6102505).
- Ustun, T.S., Ozansoy, C. & Zayegh, A. 2012. Modeling of a centralized microgrid protection system and distributed energy resources according to IEC 61850-7-420. *IEEE Transactions on Power Systems*, 27(3): 1560–1567.
- Venkatasubramanian, M. & Tomsovic, K. 2005. Power System Analysis. *The Electrical Engineering Handbook*: 761–778.
- Vieira, J.C.M., Freitas, W., Xu, W. & Morelato, A. 2006. Efficient coordination of ROCOF and frequency relays for distributed generation protection by using the application region. *IEEE Transactions on Power Delivery*, 21(4): 1878–1884.
- Vieira, J.C.M., Freitas, W., Xu, W. & Morelato, A. 2008. Evaluation of the distributed generators frequency protection due to changes in the anti-islanding requirements. : 6 pp.
- Van Der Walt, T., Brown, K. & Mabuza, P. 2011. *Telecommunications and control - The bare basics*. Second edi. Eskom Holdings Limited.
- Wazeer, E.M., El-Azab, R., Daowd, M. & Ghany, A.M.A. 2019. Short-Term Frequency Stability Regulation for Power System with Large-Scale Wind Energy Penetration Using PID Controller. *2018 20th International Middle East Power Systems Conference, MEPCON 2018 - Proceedings*: 1059–1063.
- Wu, Y.K., Chang, S.M. & Hu, Y.L. 2017. Literature Review of Power System Blackouts. *Energy Procedia*, 141: 428–431. <https://doi.org/10.1016/j.egypro.2017.11.055>.
- Yang-Wu, S., Xun, M., Ao, P., Yang-Guang, W., Ting, C., Ding, W. & Jian, Z. 2019. Load Frequency Control Strategy for Wind Power Grid-connected Power Systems Considering Wind Power Forecast. *2019 3rd IEEE Conference on*

*Energy Internet and Energy System Integration: Ubiquitous Energy Network Connecting Everything, EI2 2019*: 1124–1128.

Yousuf, M. 2018. Current Communication Media in Power System. *International Journal of Research in Electrical Engineering*, (February): 2–5.

Zhang, Y., Xu, D., Yang, W., Bi, K. & Yan, W. 2020. Fault-Tolerant Control for Load Frequency Control System via a Fault Observer. *Proceedings of 2020 IEEE 9th Data Driven Control and Learning Systems Conference, DDCLS 2020*, (3): 855–859.

Zhang, Y.Y., Zhang, K.S., Sun, W.L. & Zhang, F. 2011. Control strategy of distributed generators in microgrid. *Proceedings 2011 International Conference on Mechatronic Science, Electric Engineering and Computer, MEC 2011*: 146–149.

Zhao, D., Zhu, L., Jiang, D., Qian, M., Zhao, L. & Zhang, L. 2013. Modeling Comparison on Control System of Synchronous Generator between DlgSILENT Power Factory and PSASP. *International Journal of Computer and Electrical Engineering*, 5(2): 229–232.

## APPENDIX A

### DigSILENT PARAMETERS

- A1.1 Steam-turbine governing system settings for all synchronous generators used from generator 1 to generator 8

gov Common Model - Grid\G1\TGOV1.ElmDsl

Basic Data

Description

General Advanced 1 Advanced 2 Advanced 3

Name TGOV1

Model Definition ...odels\PSS/E compatible\gov\_TGOV1

Configuration Script

Out of Service  A-stable integration algorithm

	Parameter	
T3	Turbine Delay Time Constant [pu]	2.
T2	Turbine Derivative Time Constant [pu]	1.
At	Turbine power coefficient [pu]	1.11
Dt	Frictional Losses Factor [pu]	0.5
R	Controller Droop [pu]	0.1
T1	Governor Time Constant [s]	1.
PN	Turbine Rated Power(=0->PN=Pgnn) [Mw]	0.
Vmin	Minimum Gate Limit [pu]	0.
Vmax	Maximum Gate Limit [pu]	0.9

Export to Clipboard Set to default

OK Cancel Events Arrays/Matrices

- A1.2 IEET1 excitor settings used from generator 1 to generator 8.

avr Common Model - Grid\G1\IEEET1.ElmDsl

Basic Data

Description

General Advanced 1 Advanced 2 Advanced 3

Name IEEET1

Model Definition ...odels\PSS/E compatible\avr\_IEEET1

Configuration Script

Out of Service  A-stable integration algorithm

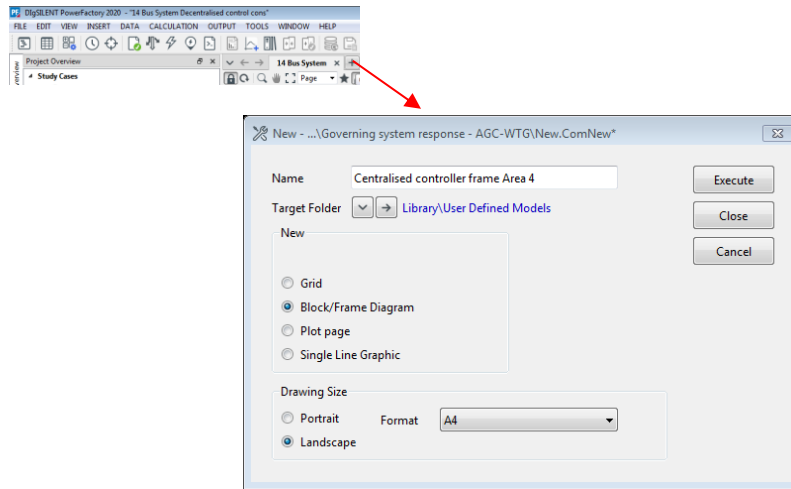
	Parameter	
Tr	Measurement Delay [s]	0.02
Ka	Controller Gain [pu]	200.
Ta	Controller Time Constant [s]	0.03
Ke	Exciter Constant [pu]	1.
Te	Exciter Time Constant [s]	0.2
Kf	Stabilization Path Gain [pu]	0.05
Tf	Stabilization Path Time Constant [s]	1.5
E1	Saturation Factor 1 [pu]	3.9
Se1	Saturation Factor 2 [pu]	0.1
E2	Saturation Factor 3 [pu]	5.2
Se2	Saturation Factor 4 [pu]	0.5
Vrmin	Controller Output Minimum [pu]	-5.
Vrmax	Controller Output Maximum [pu]	5.

Export to Clipboard Set to default

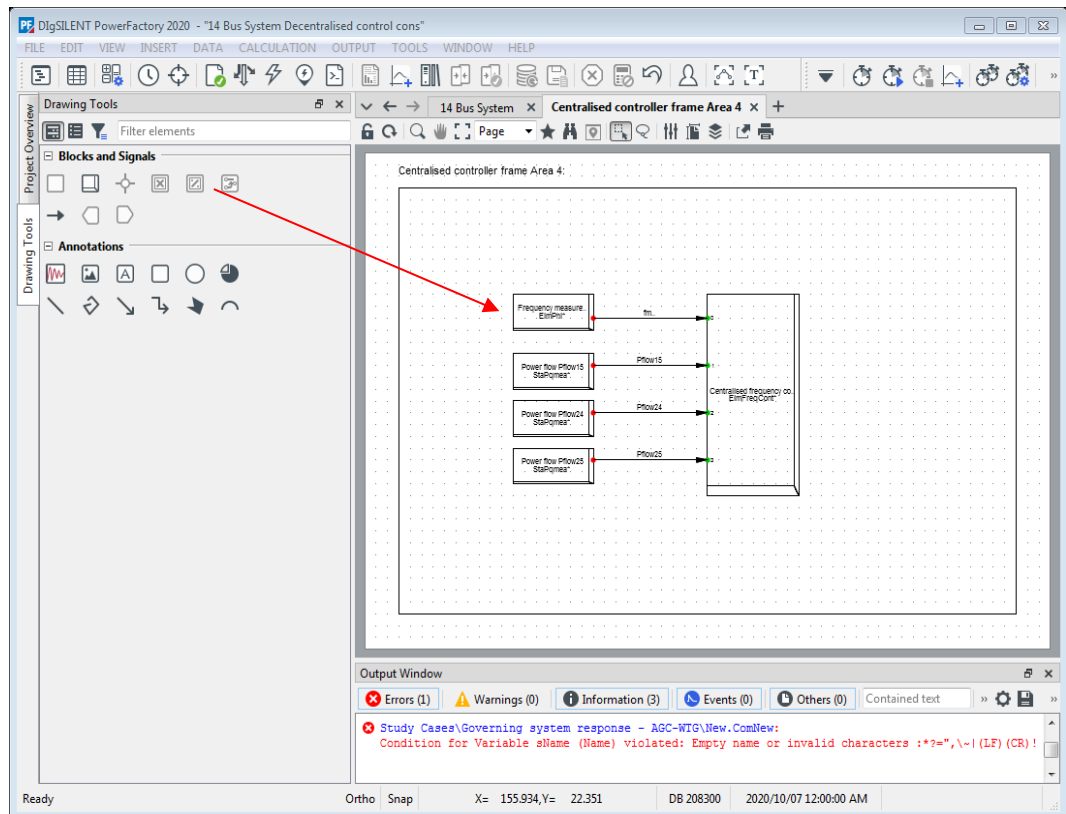
OK Cancel Events Arrays/Matrices

### A1.3 Frequency controller modeling on DigSILENT

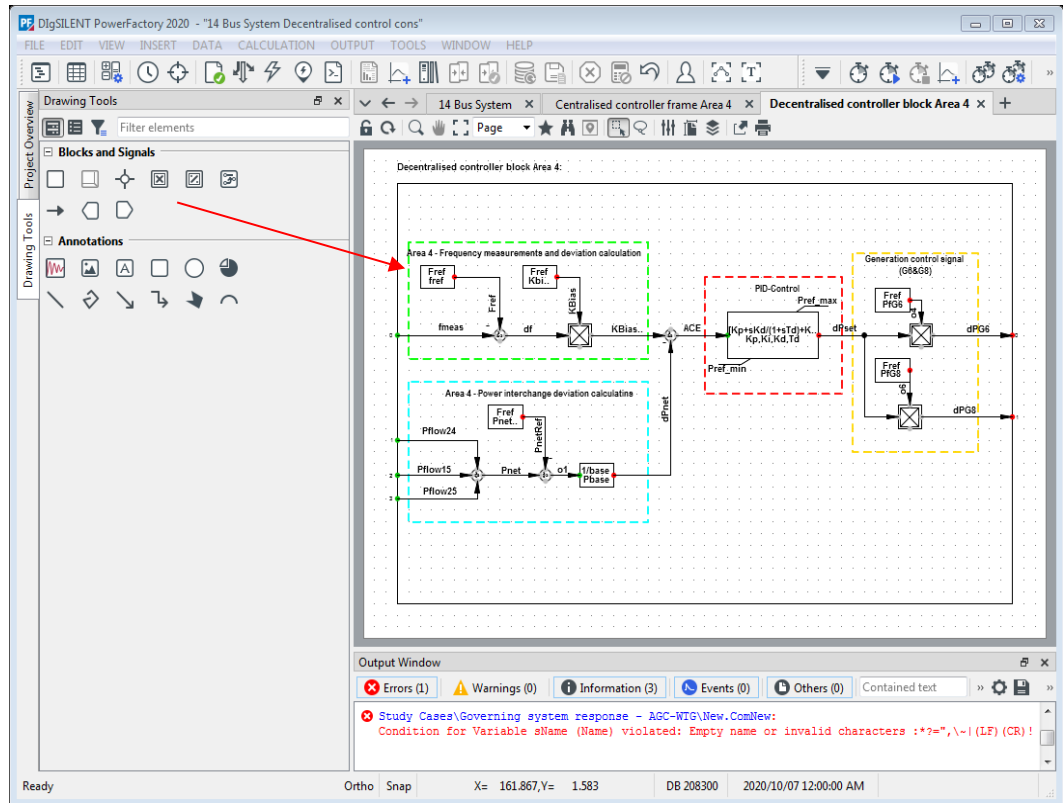
A1.3.1 Define the frame diagram by clicking on the plus icon, and a new window will open. Define the type as bloc/frame and click execute. A drawing grid will be populated



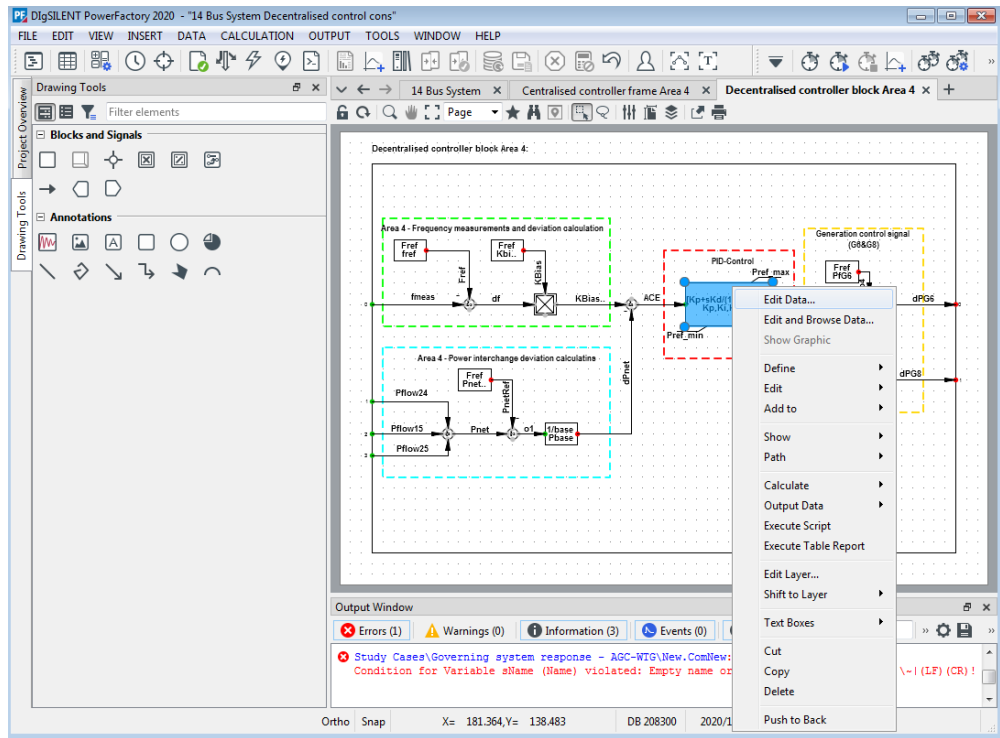
A1.3.2 Define the frame diagram by clicking on the plus icon, and a new window will open. Define the type as bloc/frame and click execute. A drawing grid will be populated. This is done to define and map the input signals to the controller



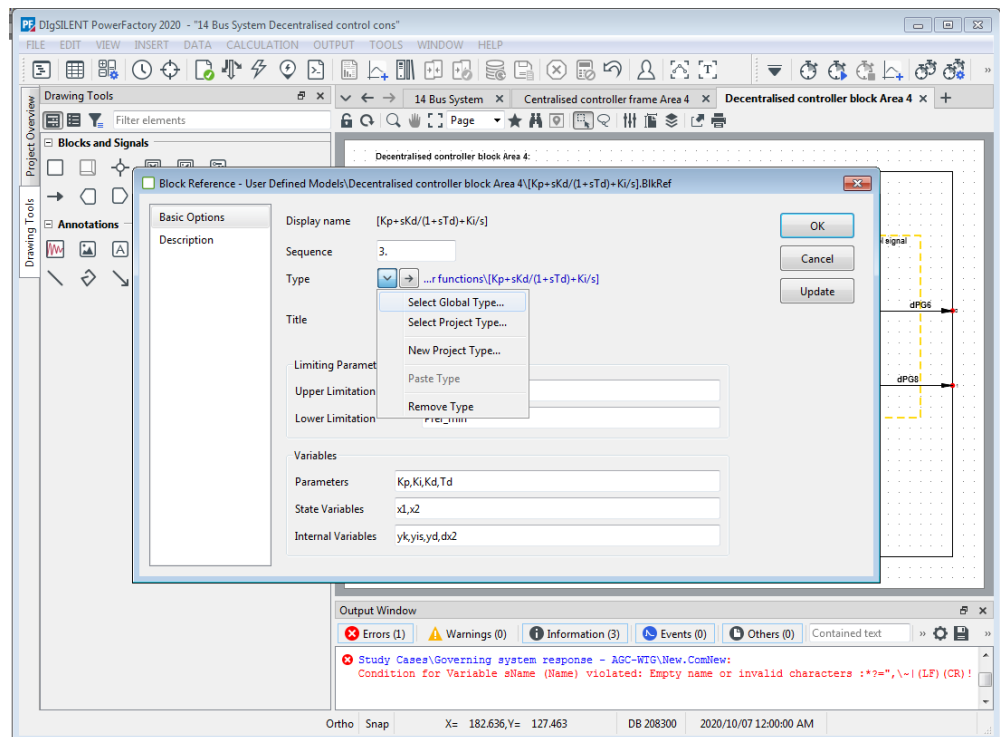
A1.3.3 Repeat the step in A1.3.1, and define the block diagram. The block diagram represents the internal controller. The input signals defined on the frame diagram are adequately mapped to the block diagram. The output signals to the governing system are also defined. The drawing tools to achieve the block diagram as shown on the left side of the window.



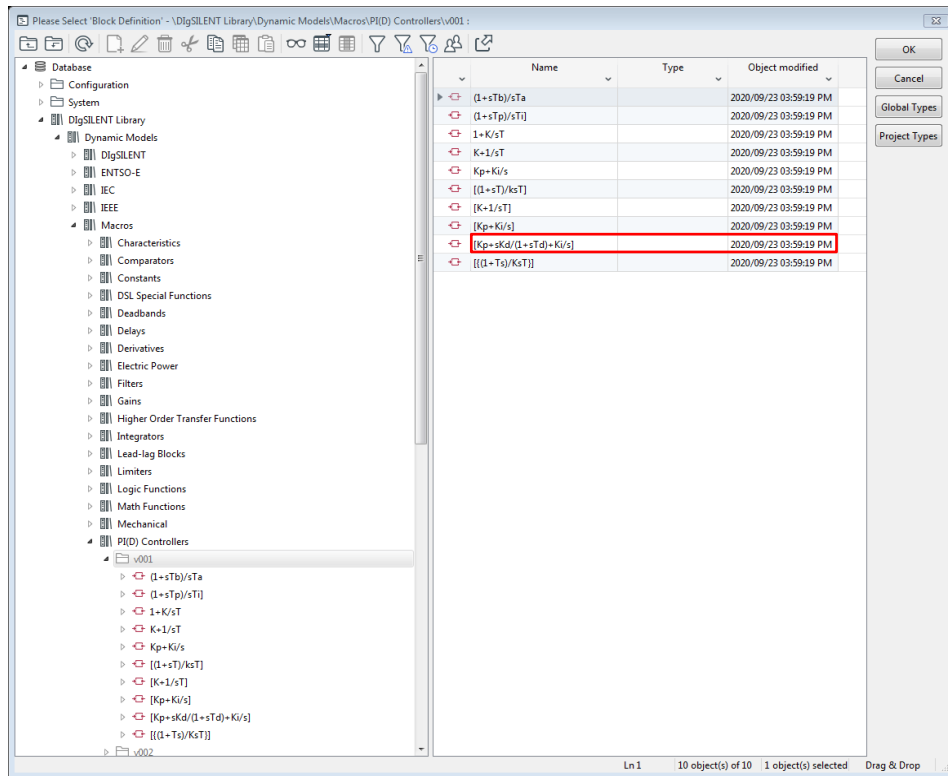
A1.3.4 Within the block diagram, to define a component within the DigSILENT library, right-click on the block and click “Edit Data,” as shown below, a new control window will open.



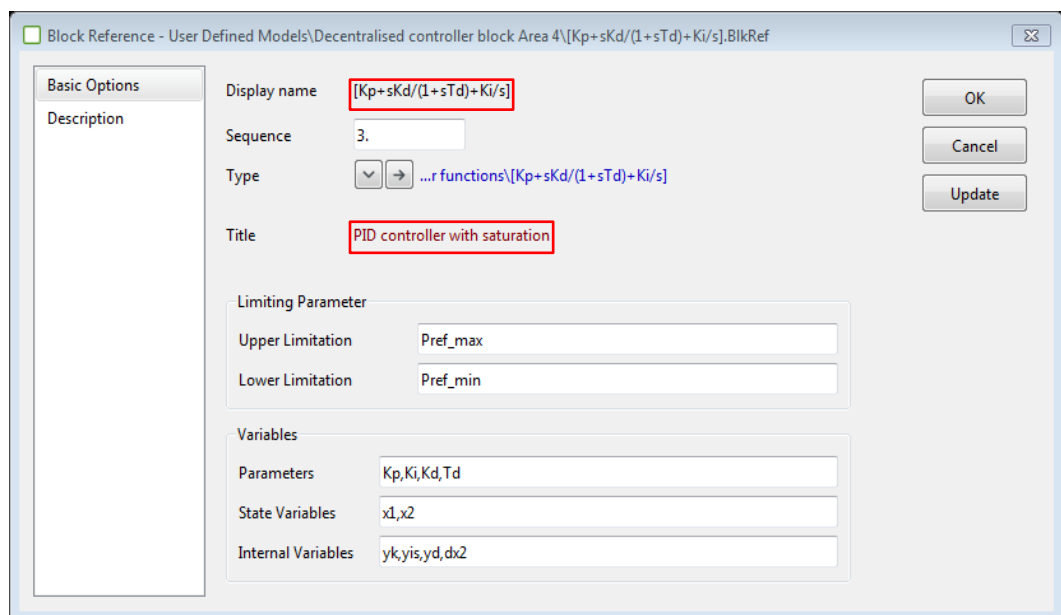
A1.3.5 Under type, the drop-down arrow click on “select global type,” and the global library of DigSILENT 2020 will open.



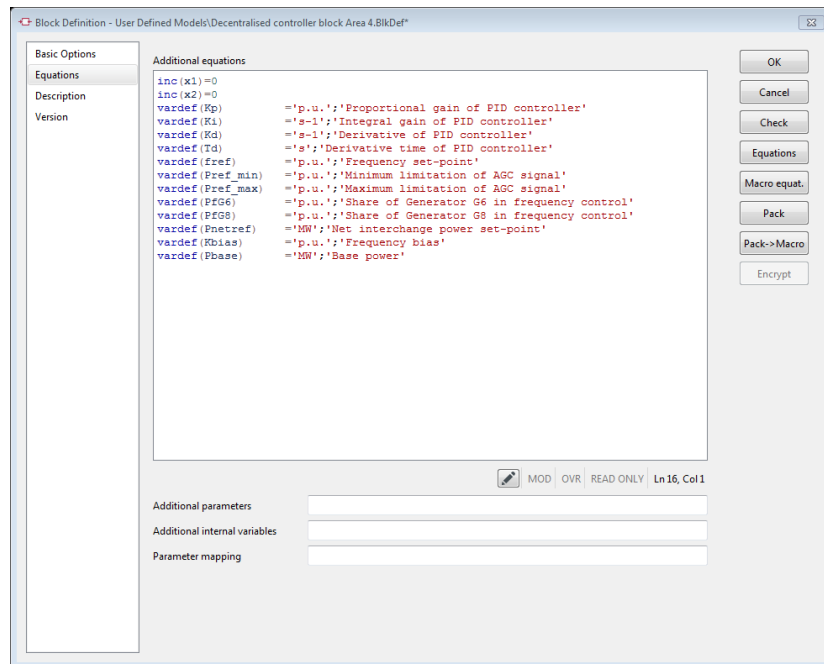
A1.3.6 Below is the DlgSILENT global library window. Select the component required, and in our application, it is the PID controller with saturation. This controller is found under Macros, and navigate PI(D) controller, and select v001.



A1.3.7 Once the component is selected, press OK, a new window with the selected component will appear as shown below.

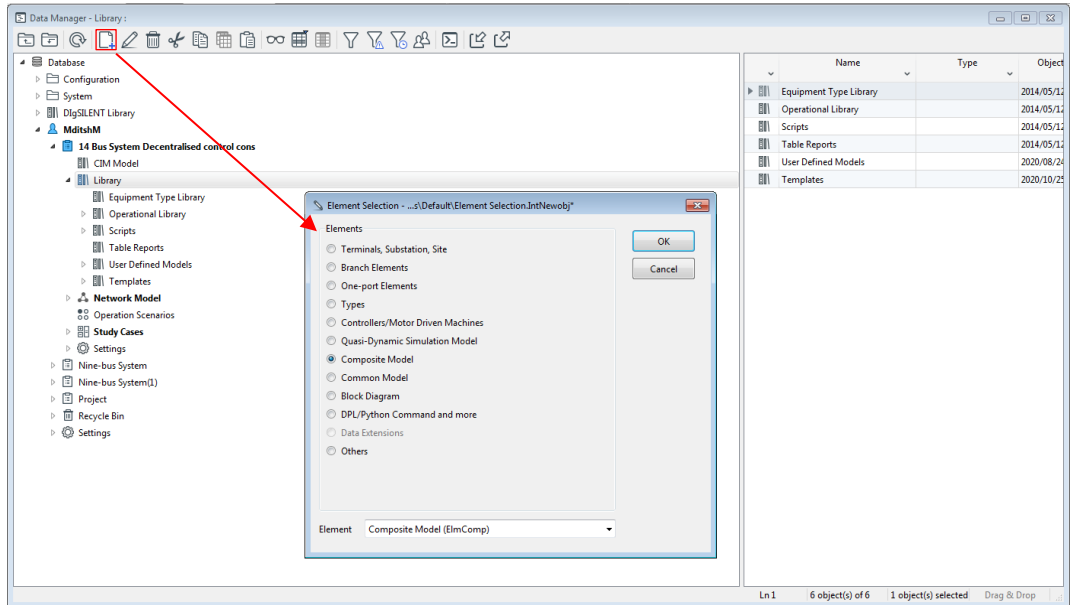


A1.3.8 The parameter description for the block diagram presented in A1.3.3 above is shown below clicking on the block definition grid, and the popup window will open and select equations. This description helps to corrected program the setting of the controller to the correct designation. In this parameter window, x1 and x2 are the initial setpoints of the controller state variables. If these state variables are not defined and reference zero, errors will be encountered on the controller's initialization. The description of the parameters also includes the units of the parameters.

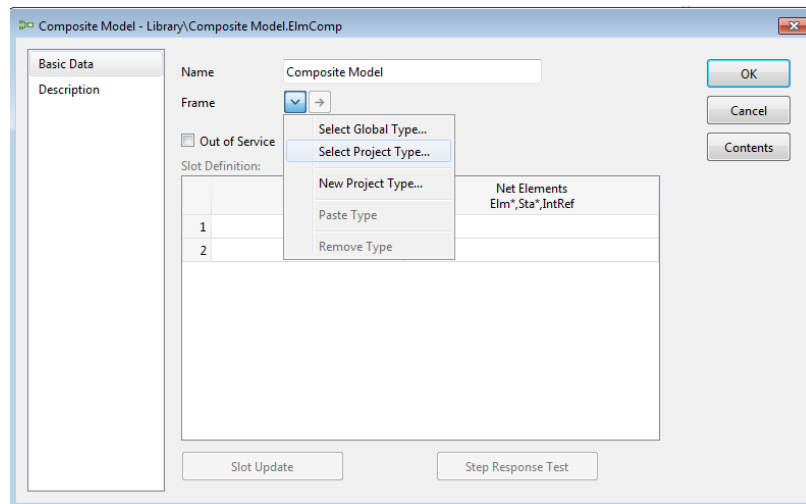




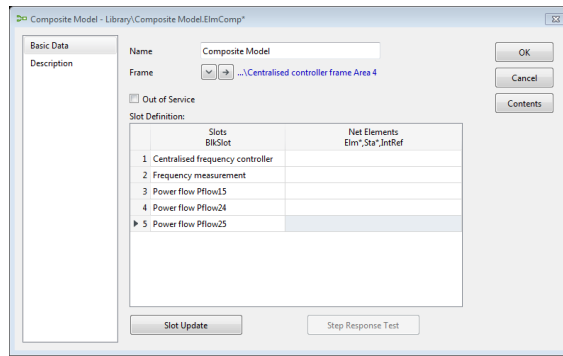
A1.3.9 The controller model is made complete by integrating the frame diagram and the block definition diagram. This is done by selecting Data Manager on the main window and click “new object.” The types of elements will be shown and selected the one is required. In this case, the composite model type is selected, and press OK



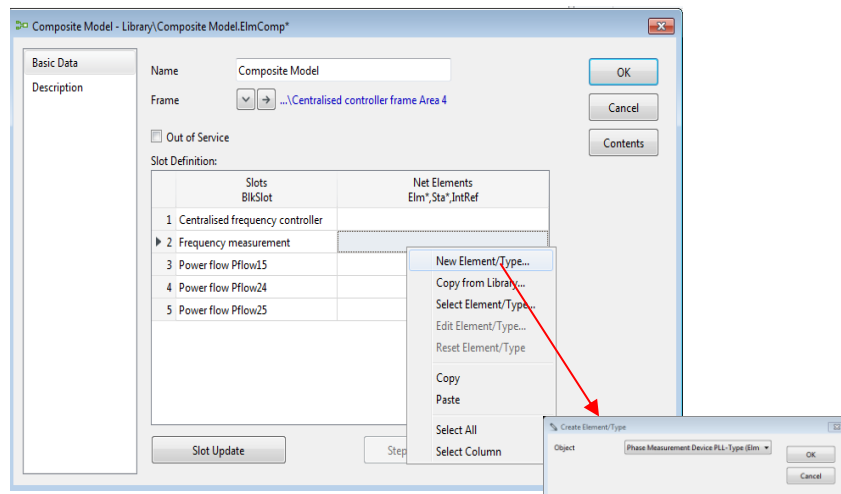
A1.3.10 The frame must be mapped to define an appropriate mapping of the input signals on the composite model. Under the frame, drop-down arrow click on “Select Project Type,” and navigate the frame to be used.



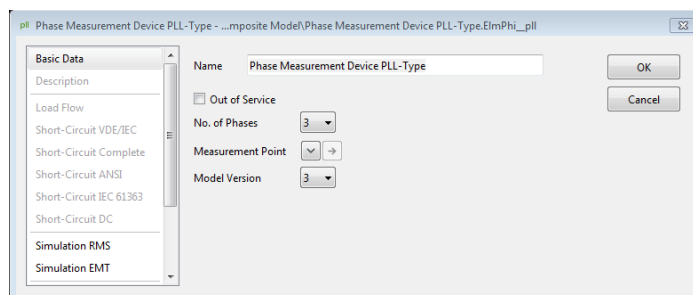
A1.3.11 The frame selected for this example is for the Centralised controller frame Area 4, as shown below. In addition, the controller input signal definitions are shown.



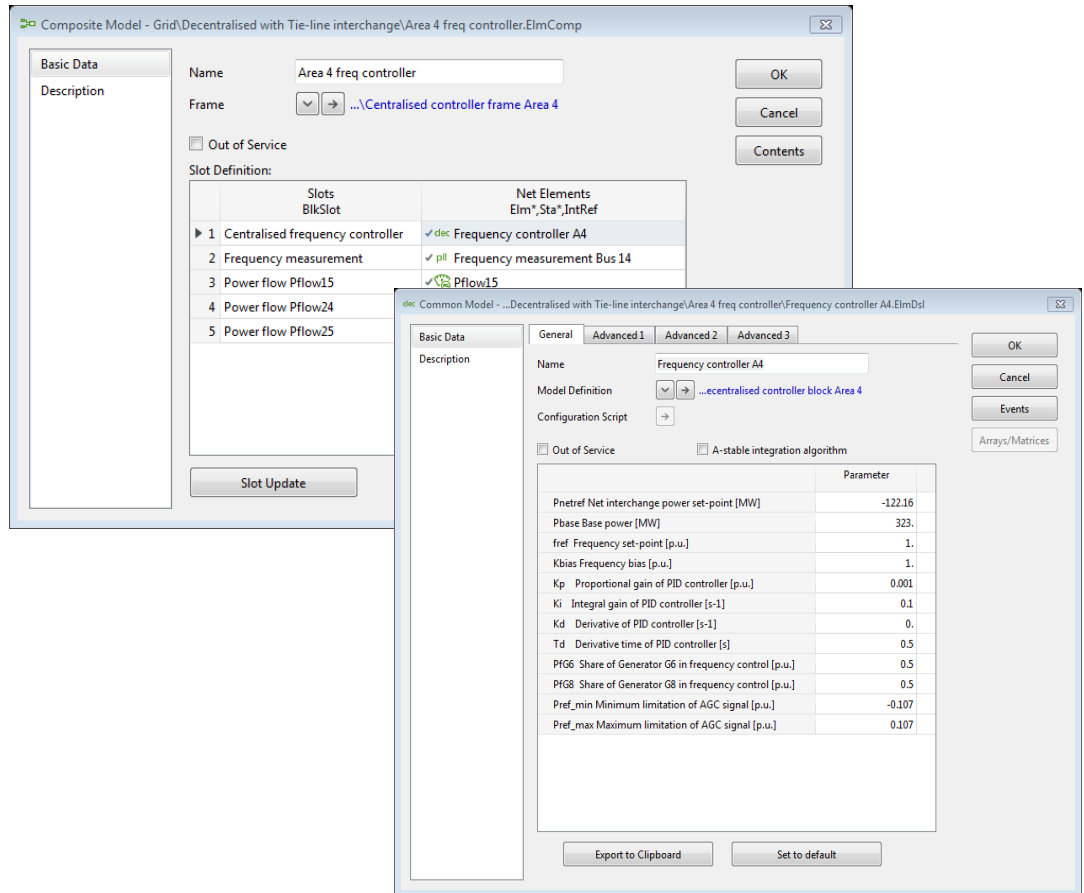
A1.3.12 Right-clicking on Net Elements blank space for each input signal row and select “New Element/Type.” A popup window will be shown to select the type of element to be created.



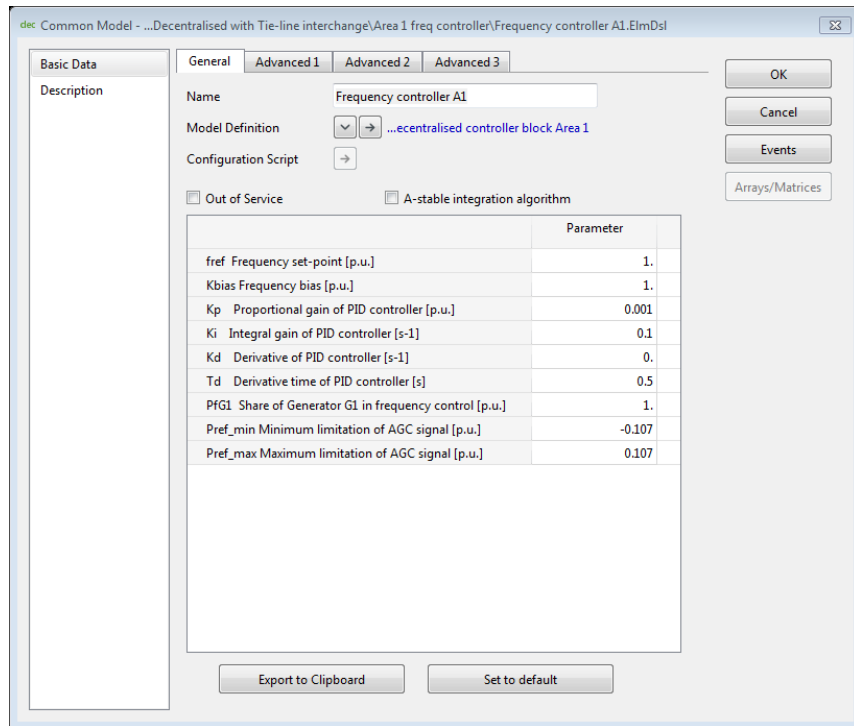
A1.3.13 Since we want to define the frequency measurement, therefore “Phase Measurement Device PLL-Type” is selected, and the node where the frequency will be measured (select appropriate bus bar)



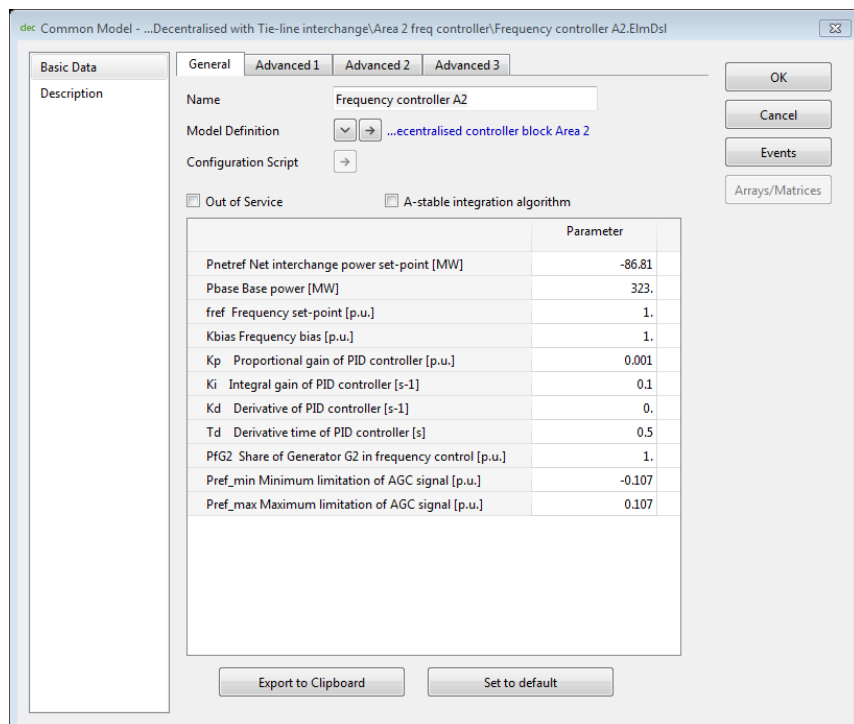
A1.3.14 To define the controller (common model) on the composite model, right-click on Net Elements/Type blank space on the Centralised frequency Controller tab. On the new popup window, browse the block definition diagram on the “Model Definition” drop-down arrow. The parameter section will be populated, and the settings can be correctly captured, then press Ok



A1.4 Parameters for area 1 automatic generation control (AGC) connected to generator 1 governing system



A1.5 Parameters for area 2 automatic generation control (AGC) connected to generator 2 governing system



A1.6 Parameters for area 3 automatic generation control (AGC) connected to generator 3 governing system

Common Model - ...Decentralised with Tie-line interchange\Area 3 freq controller\Frequency controller A3.ElmDsl

Basic Data Description

General Advanced 1 Advanced 2 Advanced 3

Name: Frequency controller A3

Model Definition: ...centralised controller block Area 3

Configuration Script: [ ]

Out of Service  A-stable integration algorithm

Parameter	Value
Pnetref Net interchange power set-point [MW]	-63.2
Pbase Base power [MW]	323.
fref Frequency set-point [p.u.]	1.
Kbias Frequency bias [p.u.]	1.
Kp Proportional gain of PID controller [p.u.]	0.001
Ki Integral gain of PID controller [s-1]	0.1
Kd Derivative of PID controller [s-1]	0.
Td Derivative time of PID controller [s]	0.5
PFG3 Share of Generator G3 in frequency control [p.u.]	1.
Pref_min Minimum limitation of AGC signal [p.u.]	-0.107
Pref_max Maximum limitation of AGC signal [p.u.]	0.107

Export to Clipboard Set to default

OK Cancel Events Arrays/Matrices

A1.7 Parameters for area 4 automatic generation control (AGC) connected to generator 6, and generator 8 governing system

Common Model - ...Decentralised with Tie-line interchange\Area 4 freq controller\Frequency controller A4.ElmDsl

Basic Data Description

General Advanced 1 Advanced 2 Advanced 3

Name: Frequency controller A4

Model Definition: ...centralised controller block Area 4

Configuration Script: [ ]

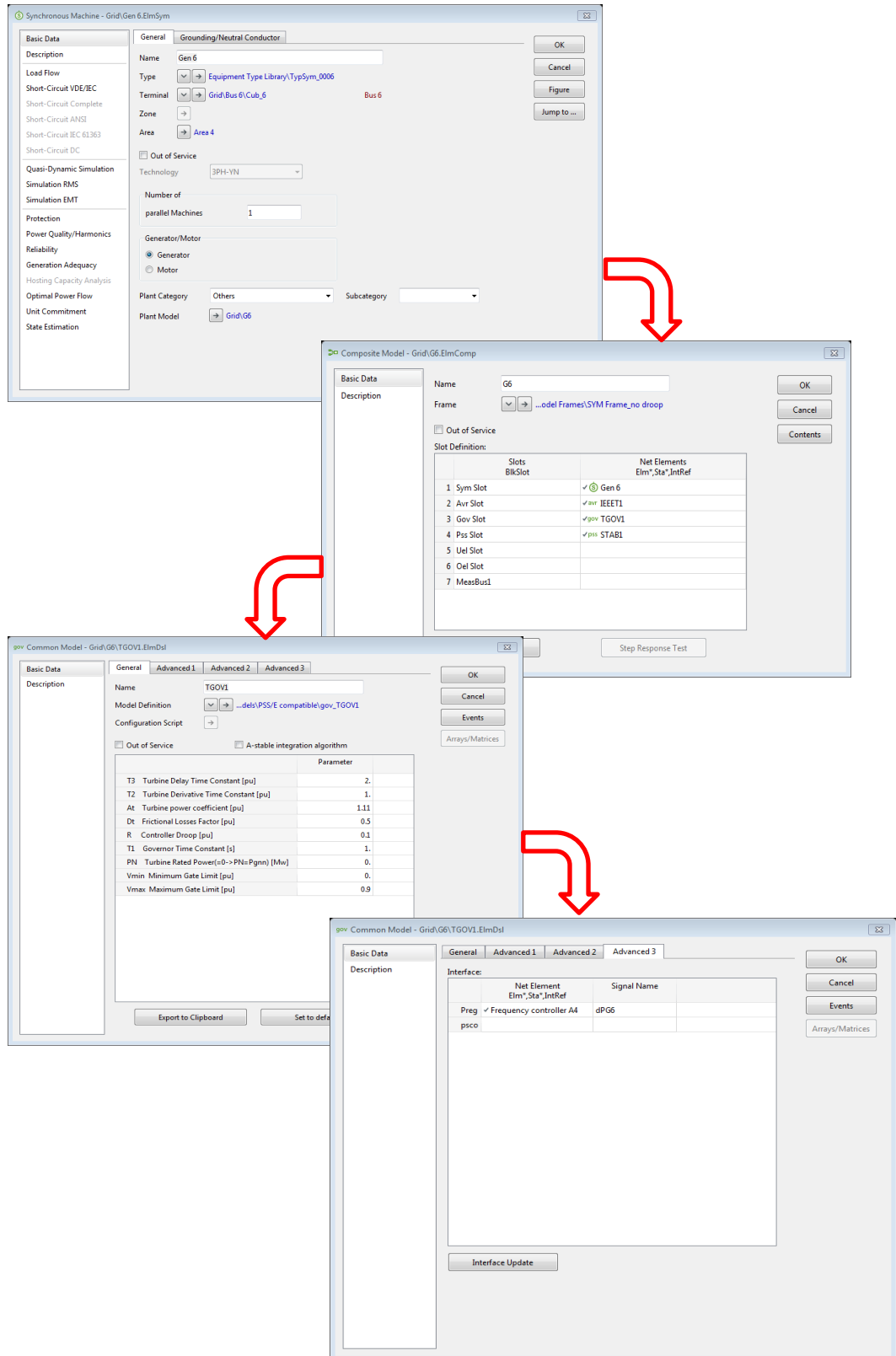
Out of Service  A-stable integration algorithm

Parameter	Value
Pnetref Net interchange power set-point [MW]	-122.16
Pbase Base power [MW]	323.
fref Frequency set-point [p.u.]	1.
Kbias Frequency bias [p.u.]	1.
Kp Proportional gain of PID controller [p.u.]	0.001
Ki Integral gain of PID controller [s-1]	0.1
Kd Derivative of PID controller [s-1]	0.
Td Derivative time of PID controller [s]	0.5
PFG6 Share of Generator G6 in frequency control [p.u.]	0.5
PFG8 Share of Generator G8 in frequency control [p.u.]	0.5
Pref_min Minimum limitation of AGC signal [p.u.]	-0.107
Pref_max Maximum limitation of AGC signal [p.u.]	0.107

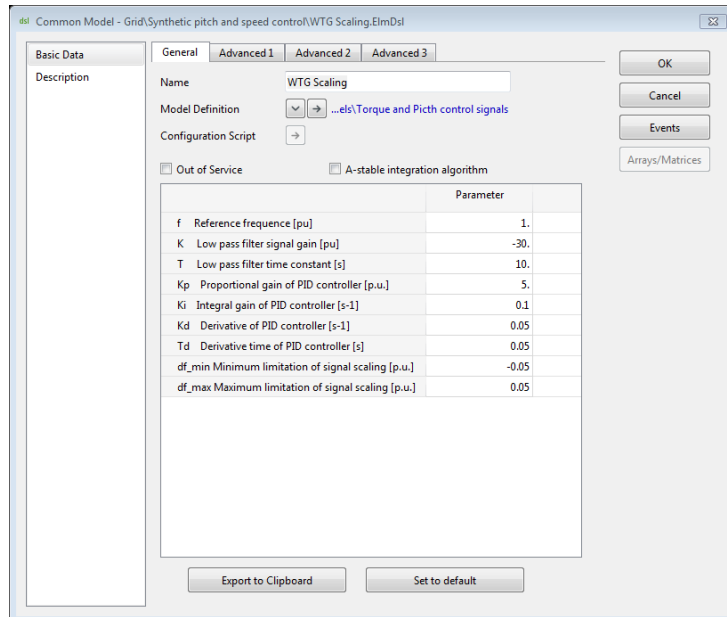
Export to Clipboard Set to default

OK Cancel Events Arrays/Matrices

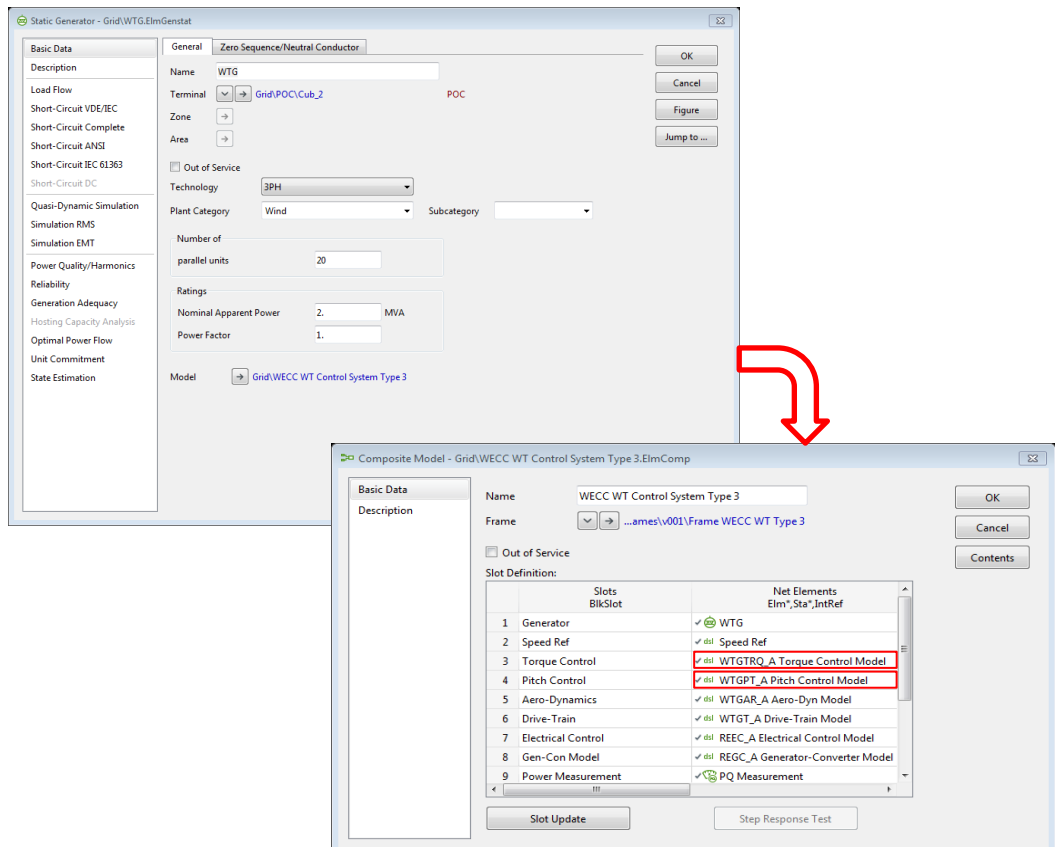
A1.8 To map the output signals of the defined controllers to their respective governing system, on the generator defined on the main grid, click on the plant model arrow, select the governing system used. On TGOV1 common model, select advanced 3 tab, and the mapping of the input signal from the frequency controller can be defined



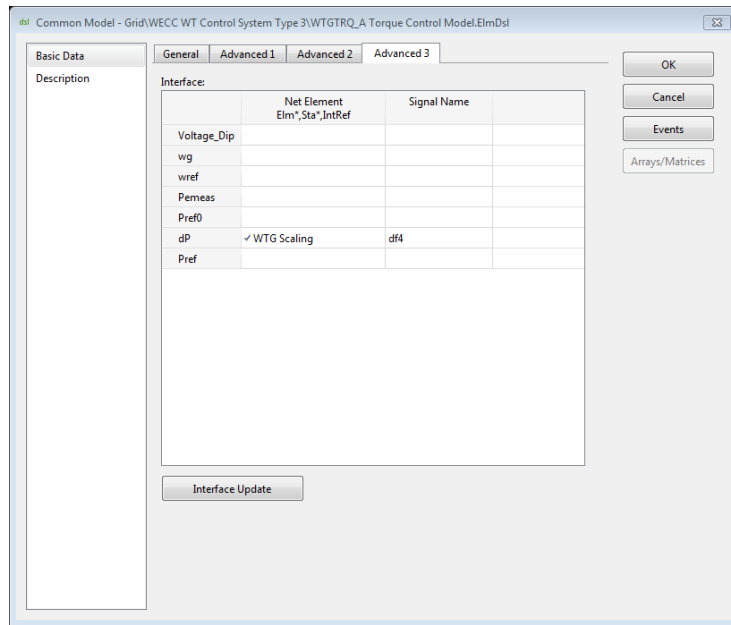
## A1.9 Wind turbine generator active power scaling parameters



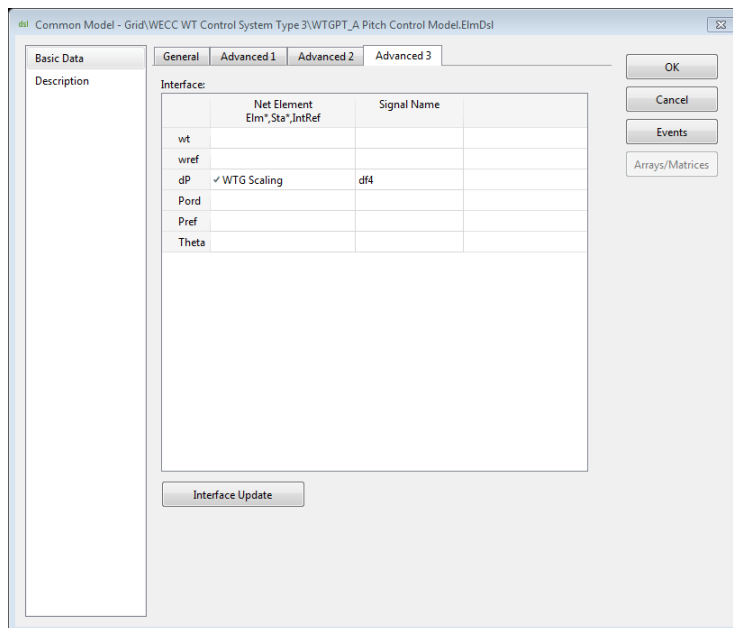
A1.10 To map the output signals of the defined wind turbine active power compensator to its respective control modules, double click on the wind turbine generator (WTG) defined on the main grid, and click on the model arrow, select the control model, which is the WECC WT Control System Type 3. The output signal of the WTG scaling logic is mapped as an input signal to the Torque controller and pitch controller



A1.11 Double click on the Torque control and click on the “Advanced 3” tab. The input signal can be mapped on dP element.



A1.12 Double click on the Pitch control model and click on the “Advanced 3” tab. The input signal can be mapped on dP element.





## APPENDIX B

### REAL-TIME DIGITAL SIMULATOR PARAMETERS AND CONFIGURATION

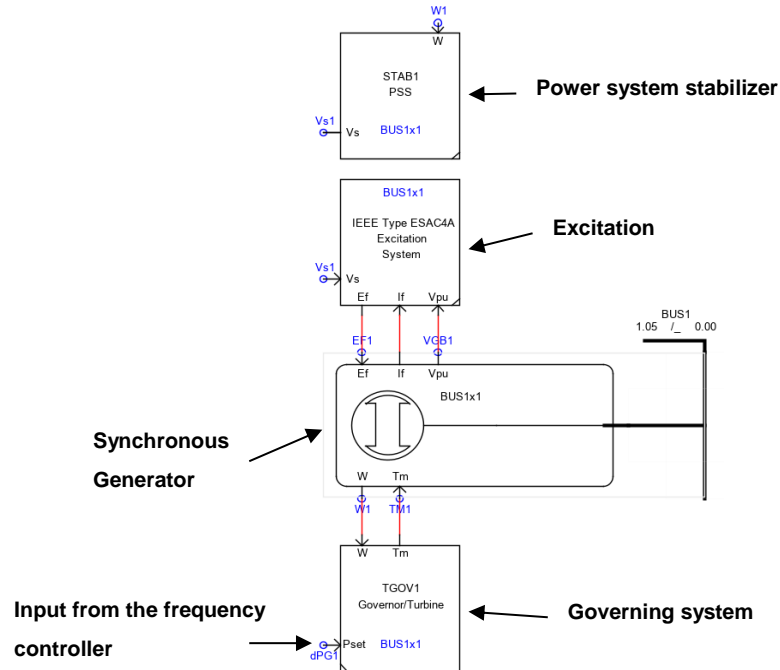
B1.1 Steam-turbine generator (TGOV1) governing system parameters for all synchronous generators used (G1 to G8)

_rtds_TGOV1.def					
CONFIGURATION		GOVERNOR/TURBINE PARAMETERS			
Name	Description	Value	Unit	Min	Max
R	Permanent droop	0.13	pu		
T1	Governor time constant	1	sec	1e-6	
Vmax	Maximum valve position	0.9	pu		
Vmin	Minimum valve position	0.0	pu		
T2	Time Constant of high-pressure fraction	2.0	sec		
T3	Reheater time constant	3	sec	1e-6	
Dt	Turbine damping coefficient	0.14	pu		

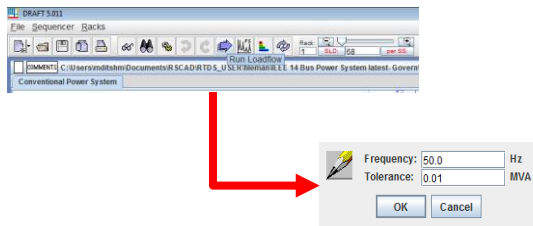
B1.2 IEEE type ESAC4A Excitation system parameters for all synchronous generators used (G1 to G8)

_rtds_ESAC4A.def					
CONFIGURATION		EXCITER PARAMETERS		SIGNAL NAMES	
Name	Description	Value	Unit	Min	Max
Tr	Voltage transducer time constant	0.000000	sec		
Tb	AVR Lead-Lag denominator time constant	0.000000	sec		
Tc	AVR Lead-Lag numerator time constant	0.000000	sec		
Ka	AVR amplifier gain	100.000000		1e-6	
Ta	AVR amplifier time constant	0.020000	sec	1e-6	
Kc	Rectifier regulation factor	0.000000			
Vrmax	Voltage regulator maximum output	7.000000	pu		
Vrmin	Voltage regulator minimum output	-7.000000	pu		
Vimax	Maximum regulator error limit	0.500000	pu		
Vimin	Minimum regulator error limit	-0.500000	pu		
Kvuel	Under Excitation Limiter Constant Value	0.0		-1.0e10	1e6

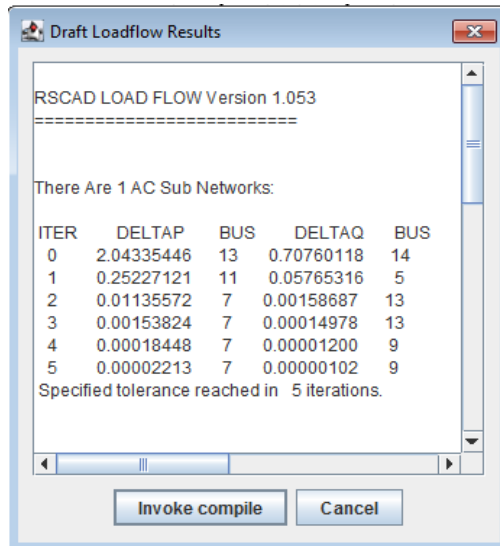
B1.3 Generation system configuration with its control system that includes power system stabilizer, excitation system, and the governing system. The configuration for all the other generation system within the model are the same as illustrated below



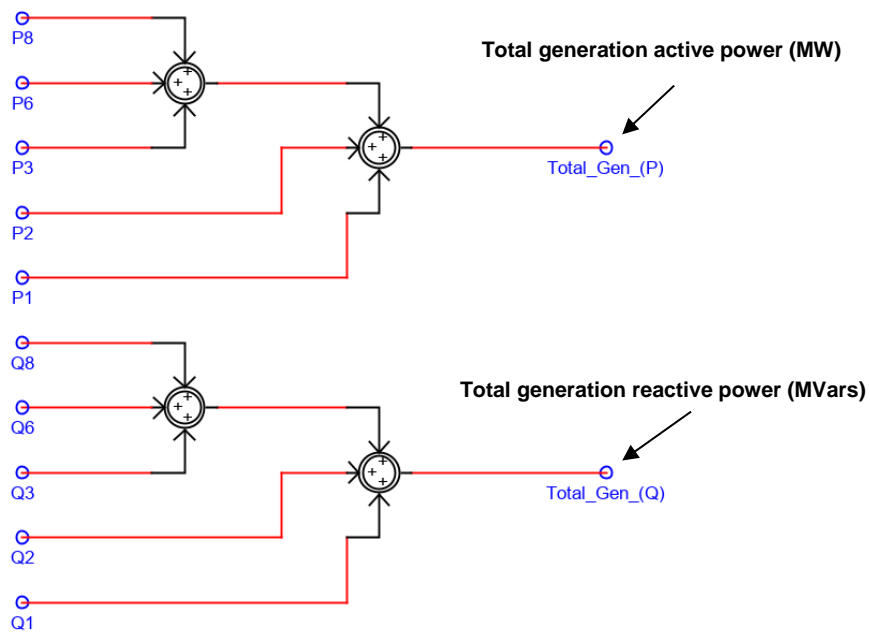
B1.4 To run load flow, select the purple arrow on RSCAD DRAFT. A popup box will appear, indicating at which frequency the load flow will be performed and the power tolerance. Once OK is pressed, the load flow calculation will commence.



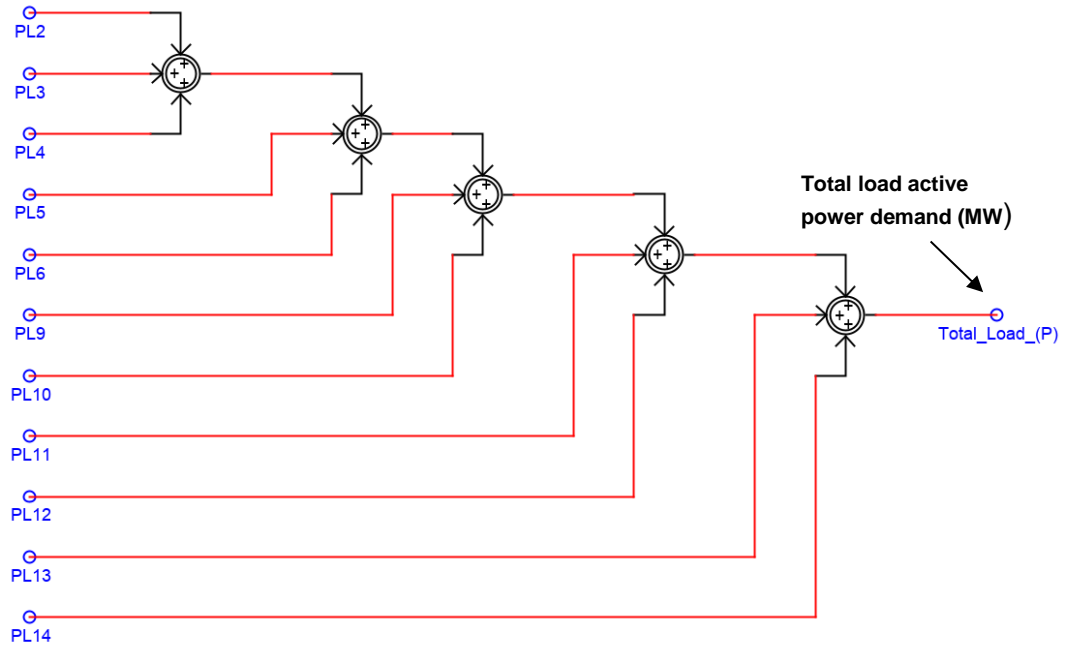
B1.5 Load flow results performed on RSCAD



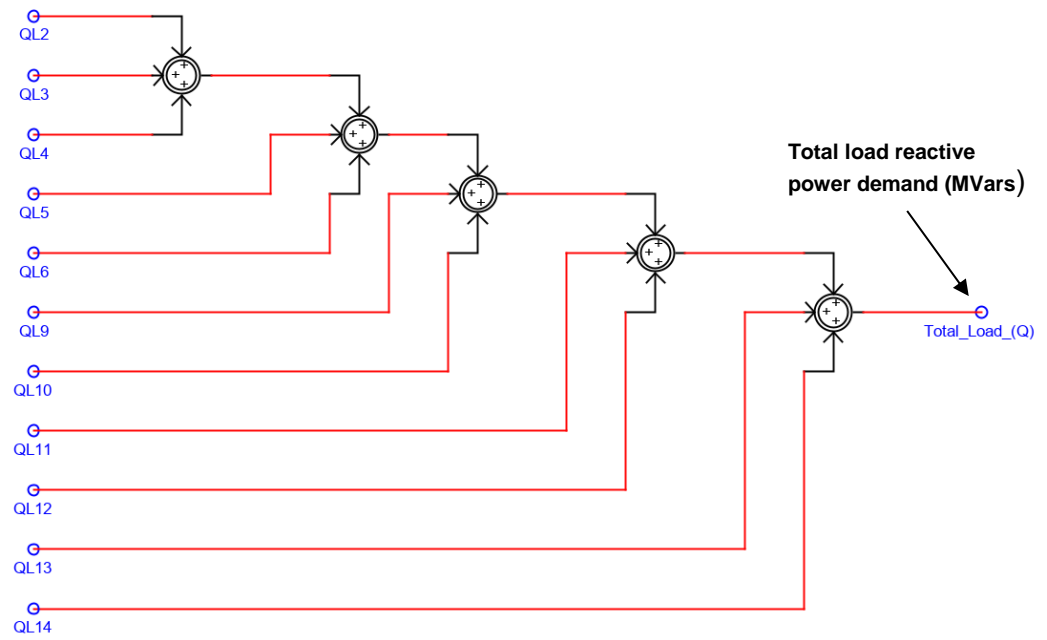
B1.6 Total generation active and reactive power summation logics developed on RSCAD in MW and MVars, respectively



B1.7 Total load demand active power summation logic



B1.8 Total load reactive power summation logic



B1.9 Load 2 active power scheduling. The highlighted part is the number of scheduling events and the initial active power for load 2. The scheduling configuration is the same for all the other loads.

rtds_sharc_ctl_SCHED					
CONFIGURATION		SCHEDULE (1-10)		SCHEDULE (10-20)	
Name	Description	Value	Unit	Min	Max
SDS	Schedule data source?	List			
NP	Number of Schedule items (if ...	15	1-30	1	30
Tu	Time entered as	sec			
RST	Reset time after	500		0.0	1e6
Y0	Initial Output	21.7			
YM	Output Values entered as	Yn*Y0			
EN	Include Start/Stop Input?	Yes		0	1
Proc	Assigned Controls Processor	1		1	36
Pri	Priority Level	18		1	

B1.10 Load 2 scheduling margin from 1% to 10% of the initial loan amount, Y1 to Y10 is the incremental steps by 1%, and T1 to T10 is the scheduled incremental period.

rtds_sharc_ctl_SCHED					
CONFIGURATION		SCHEDULE (1-10)		SCHEDULE (10-20)	
Name	Description	Value	Unit	Min	Max
note	Note: T1<T2<T3 ...				
T1	If time >=	1		0.0	1e6
Y1	Output=	1.01		-1e38	1e38
T2	If time >=	20		0.0	1e6
Y2	Output=	1.02		-1e38	1e38
T3	If time >=	40		0.0	1e6
Y3	Output=	1.03		-1e38	1e38
T4	If time >=	60		0.0	1e6
Y4	Output=	1.04		-1e38	1e38
T5	If time >=	80		0.0	1e6
Y5	Output=	1.05		-1e38	1e38
T6	If time >=	100		0.0	1e6
Y6	Output=	1.06		-1e38	1e38
T7	If time >=	120		0.0	1e6
Y7	Output=	1.07		-1e38	1e38
T8	If time >=	140		0.0	1e6
Y8	Output=	1.08		-1e38	1e38
T9	If time >=	160		0.0	1e6
Y9	Output=	1.09		-1e38	1e38
T10	If time >=	180		0.0	1e6
Y10	Output=	1.10		-1e38	1e38

B1.11 Load 2 scheduling margin from 11% to 15% of the initial load demand, Y11 to Y15 is the incremental steps by 1%, and T11 to T15 is the scheduled incremental period.

rtds_sharc_ctd_SCHED					
CONFIGURATION		SCHEDULE (1-10)		SCHEDULE (10-20)	
Name	Description	Value	Unit	Min	Max
T11	If time >=	200		0.0	1e6
Y11	Output=	1.11		-1e38	1e38
T12	If time >=	220		0.0	1e6
Y12	Output=	1.12		-1e38	1e38
T13	If time >=	240		0.0	1e6
Y13	Output=	1.13		-1e38	1e38
T14	If time >=	260		0.0	1e6
Y14	Output=	1.14		-1e38	1e38
T15	If time >=	280		0.0	1e6
Y15	Output=	1.15		-1e38	1e38
T16	If time >=	16.0		0.0	1e6
Y16	Output=	16.0		-1e38	1e38
T17	If time >=	17.0		0.0	1e6
Y17	Output=	17.0		-1e38	1e38
T18	If time >=	18.0		0.0	1e6
Y18	Output=	18.0		-1e38	1e38
T19	If time >=	19.0		0.0	1e6
Y19	Output=	19.0		-1e38	1e38
T20	If time >=	20.0		0.0	1e6
Y20	Output=	20.0		-1e38	1e38

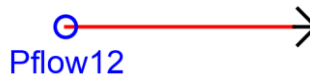
B1.12 The monitoring and measurement of the power interchange are done at the transmission line's receiving end. Considering T3 below are Area 2 and Area 3, the receiving-end is at area 3 according to the power flow direction. Therefore Pflow23 is on the receiving –end of T3. Double click on T3 at area 3, popup parameter box opens, and click on “NAMES FOR SIGNALS IN RUNTIME AND CC”

If rtds_sharc_sld_TLINE					
NAMES FOR SIGNALS IN RUNTIME AND CC			PROCESSOR ASSIGNMENT		
CONFIGURATION		OUTPUT OPTIONS		ENABLE MONITORING IN RUNTIME AND CC	
Name	Description	Value	Unit	Min	Max
nam1	Conductor #1 Current, kA, Name:	CRT1SE		0	1
nam2	Conductor #2 Current, kA, Name:	CRT2SE		0	1
nam3	Conductor #3 Current, kA, Name:	CRT3SE		0	1
nam4	Conductor #4 Current, kA, Name:	CRT4SE		0	1
nam5	Conductor #5 Current, kA, Name:	CRT5SE		0	1
nam6	Conductor #6 Current, kA, Name:	CRT6SE		0	1
nam11	Conductor #7 Current, kA, Name:	CRT7SE		0	1
nam12	Conductor #8 Current, kA, Name:	CRT8SE		0	1
nam13	Conductor #9 Current, kA, Name:	CRT9SE		0	1
nam14	Conductor #10 Current, kA, Name:	CRT10SE		0	1
nam15	Conductor #11 Current, kA, Name:	CRT11SE		0	1
nam16	Conductor #12 Current, kA, Name:	CRT12SE		0	1
nam21	Total A Ph Crt in 3 Ph sets, Name:	CRTASE		0	1
nam22	Total B Ph Crt in 3 Ph sets, Name:	CRTBSE		0	1
nam23	Total C Ph Crt in 3 Ph sets, Name:	CRTCSE		0	1
nam7	Cond #1 to #3 Real P, MW, Name:	Pflow23		0	1
nam8	Cond #1 to #3 React P, MVAR, Name:	QL1SE		0	1
nam9	Cond #4 to #6 Real P, MW, Name:	PL2SE		0	1
nam10	Cond #4 to #6 React P, MVAR, Name:	QL2SE		0	1
nam17	Cond #7 to #9 Real P, MW, Name:	PL3SE		0	1
nam18	Cond #7 to #9 React P, MVAR, Name:	QL3SE		0	1
nam19	Cond #10 to #12 Real P, MW, Name:	PL4SE		0	1
nam20	Cond #10 to #12 React P, MVAR, Name:	QL4SE		0	1
nam24	Total Real P in 3 Ph sets, Name:	PTSE		0	1
nam25	Total React P in 3 Ph sets, Name:	QTSE		0	1

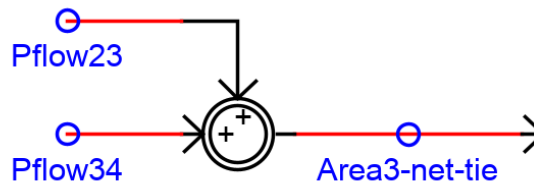
B1.13 To be able to monitor the active power, under enabled monitoring in runtime and CC, the real power needs to be enabled

If_rtds_sharc_sld_TLINE					
NAMES FOR SIGNALS IN RUNTIME AND CC			PROCESSOR ASSIGNMENT		
CONFIGURATION		ENABLE MONITORING IN RUNTIME AND CC			
Name	Description	Value	Unit	Min	Max
mon1	Monitor Conductor #1 Current, kA:	No		0	1
mon2	Monitor Conductor #2 Current, kA:	No		0	1
mon3	Monitor Conductor #3 Current, kA:	No		0	1
mon4	Monitor Conductor #4 Current, kA:	No		0	1
mon5	Monitor Conductor #5 Current, kA:	No		0	1
mon6	Monitor Conductor #6 Current, kA:	No		0	1
mon11	Monitor Conductor #7 Current, kA:	No		0	1
mon12	Monitor Conductor #8 Current, kA:	No		0	1
mon13	Monitor Conductor #9 Current, kA:	No		0	1
mon14	Monitor Conductor #10 Current, kA:	No		0	1
mon15	Monitor Conductor #11 Current, kA:	No		0	1
mon16	Monitor Conductor #12 Current, kA:	No		0	1
mon21	Monitor Total A Ph Crt in 3 Ph sets:	No		0	1
mon22	Monitor Total B Ph Crt in 3 Ph sets:	No		0	1
mon23	Monitor Total C Ph Crt in 3 Ph sets:	No		0	1
mon7	Monitor Cond 1 to 3 Real P, MW:	Yes		0	1
mon8	Monitor Cond 1 to 3 React P, MVAR:	No		0	1
mon9	Monitor Cond 4 to 6 Real P, MW:	No		0	1
mon10	Monitor Cond 4 to 6 React P, MVAR:	No		0	1
mon17	Monitor Cond 7 to 9 Real P, MW:	No		0	1
mon18	Monitor Cond 7 to 9 React P, MVAR:	No		0	1
mon19	Monitor Cond 10 to 12 Real P, MW:	No		0	1
mon20	Monitor Cond 10 to 12 React P, MVAR:	No		0	1
mon24	Monitor Total Real P in 3 Ph sets:	No		0	1
mon25	Monitor Total React P in 3 Ph sets:	No		0	1

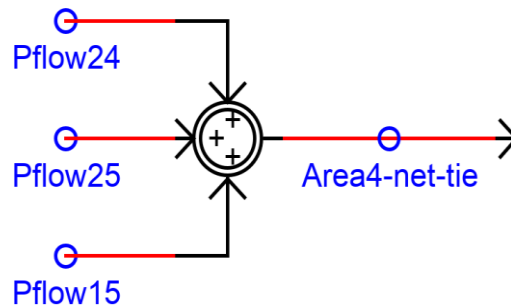
B1.14 Total Tie-line power interchange in area 2



B1.15 Total Tie-line power interchange in area 3



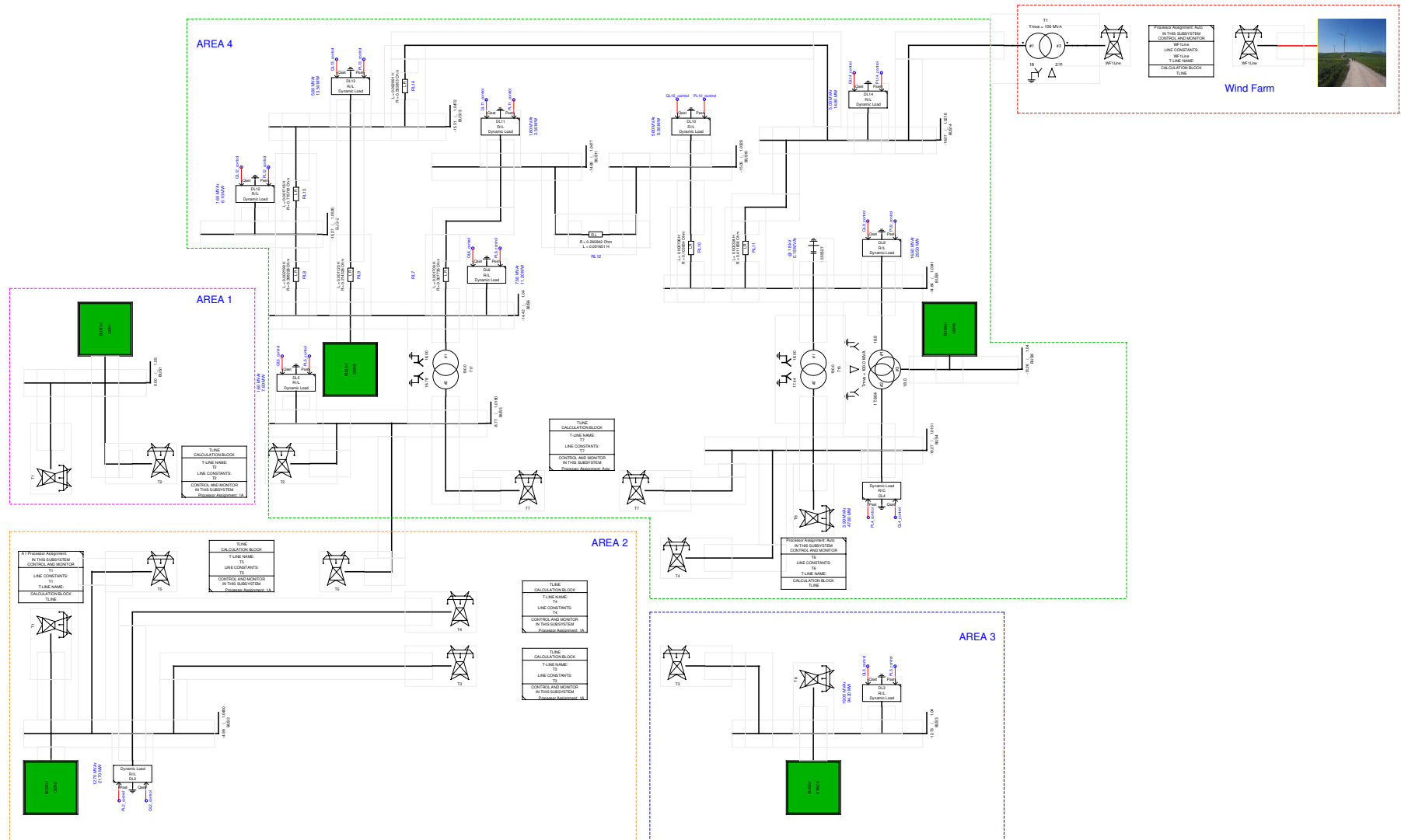
B1.16 Total Tie-line power interchange in area 4







B1.18 Modified IEEE 14 bus network integrated with Wind Farm model of RTDS - RSCAD



## APPENDIX C

### RTAC SEL-3555 DEVELOPED AGC AND WTG ACTIVE POWER COMPENSATION CONTROLLER

C1.1 Input control signals to the RTAC SEL-3555 published by RTDS GNET through GOOSE messaging system from area 1 to area 3

Expression	Type	Value	Comment
RSCAD_RTAC_CTRL_Gcb01.MV001	MV		
instMag	REAL	50.00382	← Bus 1-frequency
mag	REAL	0	
range	RANGE_T	normal	
q	quality_t		
t	timeStamp_t		
db	REAL	100	
zeroDb	REAL	2	
rangeC	rangeConfigReal_t		
RSCAD_RTAC_CTRL_Gcb01.MV002	MV		
instMag	REAL	50.00371	← Bus 2- frequency
mag	REAL	0	
range	RANGE_T	normal	
q	quality_t		
t	timeStamp_t		
db	REAL	100	
zeroDb	REAL	2	
rangeC	rangeConfigReal_t		
RSCAD_RTAC_CTRL_Gcb01.MV003	MV		
instMag	REAL	-97.27758	← Area 2 – Net power interchange
mag	REAL	-141.593353	
range	RANGE_T	normal	
q	quality_t		
t	timeStamp_t		
db	REAL	100	
zeroDb	REAL	2	
rangeC	rangeConfigReal_t		
RSCAD_RTAC_CTRL_Gcb01.MV004	MV		
instMag	REAL	50.0037155	← Bus 3- frequency
mag	REAL	0	
range	RANGE_T	normal	
q	quality_t		
t	timeStamp_t		
db	REAL	100	
zeroDb	REAL	2	
rangeC	rangeConfigReal_t		
RSCAD_RTAC_CTRL_Gcb01.MV005	MV		
instMag	REAL	-48.5744934	← Area 3 – Net power interchange
mag	REAL	0	
range	RANGE_T	normal	
q	quality_t		
t	timeStamp_t		
db	REAL	100	
zeroDb	REAL	2	
rangeC	rangeConfigReal_t		

C1.2 Input control signals to the RTAC SEL-3555 published by RTDS GNET through GOOSE messaging system for area 4 and WTG scaling

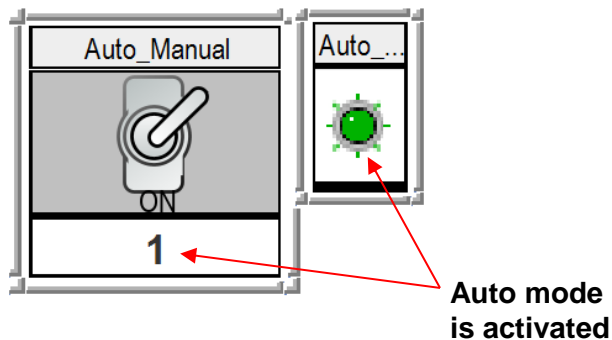
RSCAD\_RTAC\_CTRL\_Gcb01\_GRX

Project Properties: RSCAD\_RTAC\_CTRL\_Gcb01\_GRX

AGC Decentralised - IEC61850Device, Ethernet - Peer [GOOSE Receive Protocol]

Settings	Expression	Type	Value	Comment
Message	RSCAD_RTAC_CTRL_Gcb01.MV006	MV		
Message Data	instMag	REAL	50.00382	← Bus 14-frequency
	mag	REAL	0	
	range	RANGE_T	normal	
POU Pin Settings	q	quality_t		
Tags	t	timeStamp_t		
Controller	db	REAL	100	
	zeroDb	REAL	2	
	rangeC	rangeConfigReal_t		
	RSCAD_RTAC_CTRL_Gcb01.MV007	MV		
	instMag	REAL	-124.9277	← Area 4 – Net power interchange
	mag	REAL	-123.355835	
	range	RANGE_T	normal	
	q	quality_t		
	t	timeStamp_t		
	db	REAL	100	
	zeroDb	REAL	2	
	rangeC	rangeConfigReal_t		
	RSCAD_RTAC_CTRL_Gcb01.MV008	MV		
	instMag	REAL	50.0038223	← Bus 14 - frequency
	mag	REAL	0	
	range	RANGE_T	normal	
	q	quality_t		
	t	timeStamp_t		
	db	REAL	100	
	zeroDb	REAL	2	
	rangeC	rangeConfigReal_t		
	RSCAD_RTAC_CTRL_Gcb01.SPS001	SPS		
	stVal	BOOL	TRUE	← Control mode selection Status – true when its Auto
	q	quality_t		
	t	timeStamp_t		

C1.3 Control mode selector switch to change from manual to auto mode. The green LED indicates, and switch position 1 denotes that the control scheme is active



C1.4 Control signals to the respective governing system published by the RTAC SEL-3555 to RTDS GTNET card through GOOSE messaging system

The screenshot displays a configuration window for GOOSE messages. The table below represents the data visible in the 'Value' and 'Comment' columns of the configuration table.

Expression	Type	Value	Comment
GTXTags.NewDevice_GGI01_AnIn001	MV	0.0994000062	← dPG1
instMag	REAL	0	
mag	REAL	0	
range	RANGE_T	normal	
q	quality_t		
t	timeStamp_t		
db	REAL	100	
zeroDb	REAL	2	
rangeC	rangeConfigReal_t		
GTXTags.NewDevice_GGI01_AnIn002	MV	0.09943309	← dPG 2 signal
instMag	REAL	0	
mag	REAL	0	
range	RANGE_T	normal	
q	quality_t		
t	timeStamp_t		
db	REAL	100	
zeroDb	REAL	2	
rangeC	rangeConfigReal_t		
GTXTags.NewDevice_GGI01_AnIn003	MV	0.0994274	← dPG 3 signal
instMag	REAL	0	
mag	REAL	0	
range	RANGE_T	normal	
q	quality_t		
t	timeStamp_t		
db	REAL	100	
zeroDb	REAL	2	
rangeC	rangeConfigReal_t		
GTXTags.NewDevice_GGI01_AnIn004	MV	0.04986539	← dPG 6 signal
instMag	REAL	0	
mag	REAL	0	
range	RANGE_T	normal	
q	quality_t		
t	timeStamp_t		
db	REAL	100	
zeroDb	REAL	2	
rangeC	rangeConfigReal_t		
GTXTags.NewDevice_GGI01_AnIn005	MV	0.04986539	← dPG 8 signal
instMag	REAL	0	
mag	REAL	0	
range	RANGE_T	normal	
q	quality_t		
t	timeStamp_t		
db	REAL	100	
zeroDb	REAL	2	
rangeC	rangeConfigReal_t		

C1.5 WTG scaling control signal published by the RTAC SEL-3555 to RTDS GTNET card through GOOSE messaging system

The screenshot displays a configuration window for GOOSE messages. The table below represents the data visible in the 'Value' and 'Comment' columns of the configuration table.

Expression	Type	Value	Comment
GTXTags.NewDevice_GGI01_AnIn006	MV	-2.56329656	← WTG scaling
instMag	REAL	0	
mag	REAL	0	
range	RANGE_T	normal	
q	quality_t		
t	timeStamp_t		
db	REAL	100	
zeroDb	REAL	2	

C1.6 Lab-scale testbed developed for hardware in the loop power system frequency control scheme based on the IEC 61850 standard.

